frontiers | Research Topics

Plant reproduction under environmental stress

Edited by
Nico De Storme, Marta Adelina Mendes and Kevin Begcy

Published in
Frontiers in Plant Science

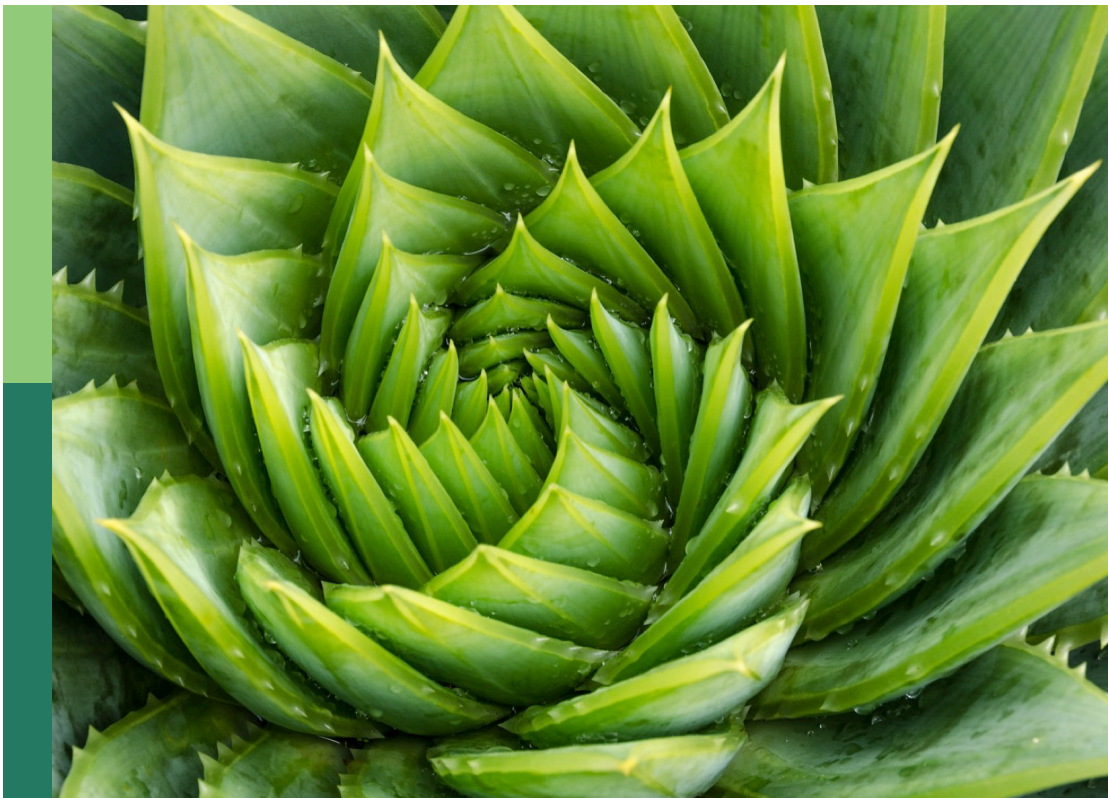

ISSN 1664-8714
ISBN 978-2-8325-4562-1
DOI 10.3389/978-2-8325-4562-1

About Frontiers

Frontiers is more than just an open access publisher of scholarly articles: it is a pioneering approach to the world of academia, radically improving the way scholarly research is managed. The grand vision of Frontiers is a world where all people have an equal opportunity to seek, share and generate knowledge. Frontiers provides immediate and permanent online open access to all its publications, but this alone is not enough to realize our grand goals.

Frontiers journal series

The Frontiers journal series is a multi-tier and interdisciplinary set of open-access, online journals, promising a paradigm shift from the current review, selection and dissemination processes in academic publishing. All Frontiers journals are driven by researchers for researchers; therefore, they constitute a service to the scholarly community. At the same time, the *Frontiers journal series* operates on a revolutionary invention, the tiered publishing system, initially addressing specific communities of scholars, and gradually climbing up to broader public understanding, thus serving the interests of the lay society, too.

Dedication to quality

Each Frontiers article is a landmark of the highest quality, thanks to genuinely collaborative interactions between authors and review editors, who include some of the world's best academicians. Research must be certified by peers before entering a stream of knowledge that may eventually reach the public - and shape society; therefore, Frontiers only applies the most rigorous and unbiased reviews. Frontiers revolutionizes research publishing by freely delivering the most outstanding research, evaluated with no bias from both the academic and social point of view. By applying the most advanced information technologies, Frontiers is catapulting scholarly publishing into a new generation.

What are Frontiers Research Topics?

Frontiers Research Topics are very popular trademarks of the *Frontiers journals series*: they are collections of at least ten articles, all centered on a particular subject. With their unique mix of varied contributions from Original Research to Review Articles, Frontiers Research Topics unify the most influential researchers, the latest key findings and historical advances in a hot research area.

Find out more on how to host your own Frontiers Research Topic or contribute to one as an author by contacting the Frontiers editorial office: frontiersin.org/about/contact

Plant reproduction under environmental stress

Topic editors
Nico De Storme — KU Leuven, Belgium
Marta Adelina Mendes — University of Milan, Italy
Kevin Begcy — University of Florida, United States

Citation
De Storme, N., Mendes, M. A., Begcy, K., eds. (2024). *Plant reproduction under environmental stress*. Lausanne: Frontiers Media SA.
doi: 10.3389/978-2-8325-4562-1

Table of contents

frontiers | Frontiers in Plant Science

TYPE Editorial
PUBLISHED 26 February 2024
DOI 10.3389/fpls.2024.1369070

OPEN ACCESS

EDITED BY
Manuel Nieves-Cordones,
Spanish National Research Council (CSIC), Spain

*CORRESPONDENCE
Kevin Begcy
kbegcy.padilla@ufl.edu

RECEIVED 11 January 2024
ACCEPTED 07 February 2024
PUBLISHED 26 February 2024

CITATION
Begcy K, Mendes MA and De Storme N (2024) Editorial: Plant reproduction under environmental stress.
Front. Plant Sci. 15:1369070.
doi: 10.3389/fpls.2024.1369070

Editorial: Plant reproduction under environmental stress

Kevin Begcy [1,2]*, Marta A. Mendes [3] and Nico De Storme [4]

[1]Environmental Horticulture Department, University of Florida, Gainesville, FL, United States, [2]Plant Molecular and Cellular Biology Graduate Program, University of Florida, Gainesville, FL, United States, [3]Dipartimento di Bioscienze, Università degli Studi di Milano, Milan, Italy, [4]Laboratory for Plant Genetics and Crop Improvement, Division of Crop Biotechnics, Department of Biosystems, Heverlee, KU Leuven, Belgium

KEYWORDS

flowering transition, ovule, pollen, seeds, stress responses, heat, cold, epigenetics

Editorial on the Research Topic
Plant reproduction under environmental stress

Reproductive development is an essential phase during the life cycle of flowering plants. It ensures preservation of karyotypic configuration and genomic stability, and additionally creates novel genetic variation in the offspring. In the current context of global warming and climate change, with plants being more intensively challenged by extreme environmental conditions, insights into the sensitivity of the molecular and physiological responses of the reproductive pathway to external stresses are highly relevant for both plant evolution and crop productivity. In this Research Topic, we present the impact of low and high temperatures as well as low light conditions on plant reproduction.

Impact of low temperatures on plant reproduction

For some crops, low temperatures are a serious threat that results in drastic yield decline. Using tomato (*Solanum lycopersicum*) as model plant, Yang et al. explored whether N6-methyladenosine (m^6A) regulates pollen development under low temperature stress and found that this condition affects pollen development at the tetrad stage, causing pollen sterility, characterized by changes in tapetum development and exine deposition. m^6A levels in anthers were decreased at both the tetrad and the uninucleate stages under low temperature stress compared to control conditions. Further transcriptome-wide detection of m^6A methylation levels in anthers at the tetrad stage under low temperature conditions showed that cold conditions affect m^6A levels in many predominantly downregulated mRNA transcripts. These differentially m^6A enriched transcripts under low temperature conditions were mainly related to ATP-binding pathways, adenosine triphosphatase activity, and lipid metabolism. Interestingly, *SlABCG31*, an ATP-binding transcript predominantly expressed in anthers, was proposed to participate in the regulation of abscisic acid (ABA), as its significant m^6A upregulation was correlated with higher ABA levels in anthers. These interesting findings suggest that the decrease in m^6A levels in response to low temperatures results in the altered transcription of many pollen development-related genes impacting anther ABA levels, leading to pollen sterility.

Another exciting story comes from a study in which the authors explored the impact of low temperatures on the transition from the vegetative to the reproductive phase (Nasim et al.). This critical developmental transition is primarily regulated by the expression of *FLOWERING LOCUS C* (*FLC*) and other clade-related genes controlled by Polymerase II-Associated Factor 1 Complex (PAF1C - *CELL DIVISION CYCLE73/PLANT HOMOLOGOUS TO PARAFIBROMIN*, *VERNALIZATION INDEPENDENCE2* (*VIP2*)/*EARLY FLOWERING7* (*ELF7*), *VIP3*, *VIP4*, *VIP5*, and *VIP6/ELF8*). In *Arabidopsis thaliana* T-DNA PAF1C-deficient mutant lines, strong early flowering was observed as temperature was decreased. Since changes in epigenetic status have been shown to be critical for the stress response during reproductive development (Begcy and Dresselhaus, 2018), Nasim et al. analyzed the levels of H3K27me3 and H3K4me3/H3K36me3 marks on *FLC* and the *FLC*-clade genes. Under low temperature stress, *FLC* and *FLC*-clade genes showed significantly increased enrichment of H3K27me3 and significantly reduced enrichment of H3K4me3 marks in PAF1C mutants, which is consistent with their transcriptional downregulation. These results show that PAF1C is required to maintain active histone H3K4me3 marks while preventing the deposition of H3K27me3 repressive marks at the *FLC* and *FLC*-clade genes, thereby maintaining their active transcription.

Another aspect covered in this Research Topic is the effect of low temperatures during the bloom period in grapes and their impact on fruit set. Keller et al. manipulated the inflorescence temperature of field-grown Cabernet Sauvignon grapevines during the bloom period. Low temperatures resulted in decreased fruit set, as indicated mainly by the lowest berry number per cluster, as well as seed and berry weight at harvest. At the biochemical level, low temperatures slightly decreased fruit soluble solids and pH, and increased titratable acidity, but did not affect color density. In summary, these results suggest that low temperatures not only decrease the proportion of flowers that set fruit but also limit the sink strength of the berries that do develop after fruit set.

Impact of heat stress on plant reproduction

High temperatures caused by climate change are negatively impacting reproductive success in many plant species (De Storme and Geelen, 2014; Chen et al., 2016; Begcy et al., 2019). An understanding of how plants try to overcome heat stress during their reproductive phase is fundamental to the effective design of strategies to improve agricultural productivity. In a well-considered review paper, Resentini et al. provided a general overview of the molecular mechanisms underlying heat stress resilience during reproductive development through comparison of a dicotyledonous and a monocotyledonous model system, *Arabidopsis* and *Oryza sativa*. The pollen and the ovule are two reproductive organs whose development is highly susceptible to heat stress. The authors describe four main strands of impact when temperatures are increased during normal development in these two organs: (1) morphological alteration of these tissues, including the anthers and pistils, impacting reproductive success; (2) inhibition of male and female gametophyte development; (3) inhibition of pollen development; and (4) limitation of pollen tube growth. These aspects highlight some of the weakest developmental organs during plant reproduction. Two important additional aspects, summarized by Resentini et al., are recent advances in understanding of the cellular responses to heat stress, represented by the induction of heat shock proteins and calcium signaling. A solid amount of data indicates that heat stress affects plant Ca^{2+} channels, inducing a transient increase in cytosolic Ca^{2+} concentration. Cytosolic Ca^{2+} ion acts as a second messenger that triggers specific cellular responses, including heat shock factors and heat shock proteins. These large groups of transcription factors and chaperones have been used to develop heat resilient crops (ul Haq et al., 2019; Kim et al., 2021).

In cucumber (*Cucumis sativus* L.), high temperature stress always results in sterility at the reproductive stage (Chen et al.). To elucidate the nature of this susceptibility, Chen et al. performed cross-section analysis of anther development in cucumber at high temperatures. The authors observed tapetum abnormality, abnormal microspore, and microspore degeneration in stressed anthers. A high rate of pollen grain abortion and a significant reduction in pollen fertility were also demonstrated. When antioxidant enzymatic activity was measured, including peroxidase, malondialdehyde, catalase, and superoxide dismutase, extremely high levels were found in heat-stressed anthers, which indicates a stressed physiological status. Interestingly, transcriptional analysis showed that carbohydrates and many saccharides and starch synthase-related genes, such as invertase, sucrose synthase, and starch-branching enzymes, were misregulated under exposure to increased temperatures, which represents a common stress response in many plant species, as shown in maize, cotton, and Arabidopsis (Begcy et al., 2019; Masoomi-Aladizgeh et al., 2021; Seydel et al., 2022).

Using a combination of invasive and non-invasive techniques to investigate floret development in barley (*Hordeum vulgare*), Callens et al. showed that while female reproductive organs are less susceptible to heat stress, male reproductive organs are severely impacted. A practical conclusion of this study was that the timing of stress relative to reproductive development has a significant impact on fertility in a cultivar-dependent manner. Immunolabelling of cell wall components in anthers and ovules of heat-stressed barley plants showed that anther cell wall components collapsed (including 1,3;1,4-β-glucan, de-esterified homogalacturonan, and cellulose). The immunolabelling of ovule sections showed that the embryo sac was present in all cases, but there seemed to be fewer cell layers between the embryo sac and the integument. However, no obvious irregularities in the morphology of the embryo sac were identified.

In tomato, the meiosis to early microspore stage of pollen development was found to be the most sensitive to heat stress, and only three days of heat exposure during this developmental window was sufficient to significantly reduce pollen viability at the flower anthesis stage. Cytological analysis showed that abnormalities in pollen development could first be observed after pollen mitosis I, while no deviations in tapetum development were observed. At the transcriptional and biochemical level, pollen development suffered from tapetal endoplasmic reticulum stress (Xu et al.).

Heat stress during seed development is a significant factor in reducing seed size and yield. Using *Camelina sativa*, Nadakuduti et al. explored the impact of high temperatures on fatty acids. Striking differences in the qualitative and quantitative levels of fatty acids were detected. A decrease in percentage polyunsaturated fatty acids and an increase in percentage monounsaturated accumulation of fatty acids was measured under heat stress conditions. The authors suggested that fatty acid biosynthesis shifted to monounsaturated fatty acid synthesis to protect cell function and embryo development by maintaining membrane stability and preventing fatty acid oxidation.

Jansma et al. used a *35S:nahG* tomato line, which has low levels of the stress response-associated hormone salicylic acid, to investigate whether this hormone improves pollen thermotolerance to high temperatures or negatively reduces the investment of resources in reproductive development. Low levels of salicylic acid were found to increase pollen viability under heat stress conditions by enhancing jasmonic acid signaling in developing anthers. These results open the door for alternative pathways within the current biotechnological and breeding strategies that are implemented to ameliorate stress responses.

Impact of low light on plant reproduction

Aiming to understand alfalfa (*Medicago sativa* L.) development during reproduction under shading conditions, Quin et al. studied flowering phenology, pollen viability, stigma receptivity, and seed quality. In general, low light conditions delayed flowering phenology, shortened the flowering stage, and significantly reduced pollen viability, stigma receptivity, number of flowers, and quantity and quality of seeds. Interestingly, since alfalfa is a forage crop used in intercropping or rotation ecosystems, low light conditions were beneficial in maintaining a high aboveground biomass (Qin et al.). This is likely due to the regulation of the accumulation and distribution of assimilates between the vegetative and reproductive organs.

Author contributions

KB: Conceptualization, Writing – original draft, Writing – review & editing. MM: Writing – review & editing. NS: Writing – review & editing.

Funding

The author(s) declare financial support was received for the research, authorship, and/or publication of this article. Experimental work on plant reproduction under environmental stresses in the laboratory of KB is funded by the USDA National Institute of Food and Agriculture NIFA-AFRI program (Grant 2023-67013-39412) and the Global Food Systems Institute.

Conflict of interest

The authors declare that the research was conducted in the absence of any commercial or financial relationships that could be construed as a potential conflict of interest.

Publisher's note

References

Begcy, K., and Dresselhaus, T. (2018). Epigenetic responses to abiotic stresses during reproductive development in cereals. *Plant Reprod.* 31, 343–355. doi: 10.1007/s00497-018-0343-4

Begcy, K., Nosenko, T., Zhou, L.-Z., Fragner, L., Weckwerth, W., and Dresselhaus, T. (2019). Male sterility in maize after transient heat stress during the tetrad stage of pollen development. *Plant Physiol.* 181, 683–700. doi: 10.1104/pp.19.00707

Chen, C., Begcy, K., Liu, K., Folsom, J. J., Wang, Z., Zhang, C., et al. (2016). Heat stress yields a unique MADS box transcription factor in determining seed size and thermal sensitivity. *Plant Physiol.* 171, 606–622. doi: 10.1104/pp.15.01992

De Storme, N., and Geelen, D. (2014). The impact of environmental stress on male reproductive development in plants: biological processes and molecular mechanisms. *Plant Cell Environ.* 37, 1–18. doi: 10.1111/pce.12142

Kim, T., Samraj, S., Jiménez, J., Gómez, C., Liu, T., and Begcy, K. (2021). Genome-wide identification of heat shock factors and heat shock proteins in response to UV and high intensity light stress in lettuce. *BMC Plant Biol.* 21, 185. doi: 10.1186/s12870-021-02959-x

Masoomi-Aladizgeh, F., Najeeb, U., Hamzelou, S., Pascovici, D., Amirkhani, A., Tan, D. K. Y., et al. (2021). Pollen development in cotton (*Gossypium hirsutum*) is highly sensitive to heat exposure during the tetrad stage. *Plant Cell Environ.* 44, 2150–2166. doi: 10.1111/pce.13908

Seydel, C., Kitashova, A., Fürtauer, L., and Nägele, T. (2022). Temperature-induced dynamics of plant carbohydrate metabolism. *Physiol. Plant* 174, e13602. doi: 10.1111/ppl.13602

ul Haq, S., Khan, A., Ali, M., Khattak, A. M., Gai, W.-X., Zhang, X.-H., et al. (2019). Heat shock proteins: dynamic biomolecules to counter plant biotic and abiotic stresses. *Int. J. Mol. Sci.* 20, 5321. doi: 10.3390/ijms20215321

frontiers in Plant Science

ORIGINAL RESEARCH
published: 04 June 2021
doi: 10.3389/fpls.2021.687826

RNA N6-Methyladenosine Responds to Low-Temperature Stress in Tomato Anthers

*Dandan Yang[1], Huachao Xu[1], Yue Liu[1], Mengzhuo Li[1], Muhammad Ali[1], Xiangyang Xu[2] and Gang Lu[1,3]**

[1] Department of Horticulture, Zhejiang University, Hangzhou, China, [2] College of Horticulture, Northeast Agricultural University, Harbin, China, [3] Key Laboratory of Horticultural Plant Growth, Development and Quality Improvement, Ministry of Agricultural, Zhejiang University, Hangzhou, China

Cold stress is a serious threat to subtropical crop pollen development and induces yield decline. N6-methyladenosine (m^6A) is the most frequent mRNA modification and plays multiple physiological functions in plant development. However, whether m^6A regulates pollen development is unclear, and its putative role in cold stress response remains unknown. Here, we observed that moderate low-temperature (MLT) stress induced pollen abortion in tomato. This phenotype was caused by disruption of tapetum development and pollen exine formation, accompanied by reduced m^6A levels in tomato anther. Analysis of m^6A-seq data revealed 1,805 transcripts displayed reduced m^6A levels and 978 transcripts showed elevated m^6A levels in MLT-stressed anthers compared with those in anthers under normal temperature. These differentially m^6A enriched transcripts under MLT stress were mainly related to lipid metabolism, adenosine triphosphatase (ATPase) activity, and ATP-binding pathways. An ATP-binding transcript, *SlABCG31*, had significantly upregulated m^6A modification levels, which was inversely correlated to the dramatically downregulated expression level. These changes correlated with higher abscisic acid (ABA) levels in anthers and disrupted pollen wall formation under low-temperature stress. Our findings characterized m^6A as a novel layer of complexity in gene expression regulation and established a molecular link between m^6A methylation and tomato anther development under low-temperature conditions.

Keywords: abscisic acid, m^6A, moderate low temperature, pollen development, tomato anther

OPEN ACCESS

Edited by:
Kevin Begcy, University of Florida, United States

Reviewed by:
Jing-Ke Weng, Whitehead Institute for Biomedical Research, United States
Michal Lieberman-Lazarovich, Agricultural Research Organization (ARO), Israel

***Correspondence:**
Gang Lu
glu@zju.edu.cn

Specialty section:
This article was submitted to Plant Abiotic Stress, a section of the journal Frontiers in Plant Science

Received: *30 March 2021*
Accepted: *12 May 2021*
Published: *04 June 2021*

Citation:
Yang D, Xu H, Liu Y, Li M, Ali M, Xu X and Lu G (2021) RNA N6-Methyladenosine Responds to Low-Temperature Stress in Tomato Anthers. Front. Plant Sci. 12:687826. doi: 10.3389/fpls.2021.687826

INTRODUCTION

In flowering plants, male reproductive development is vulnerable to abiotic stress (Al Mamun et al., 2010; De Storme and Geelen, 2014; Sharma and Nayyar, 2016; Kiran et al., 2019). Frequent temperature fluctuations cause male sterility in most crops, leading to lower fruit and seed set and final yield (Pacini and Dolferus, 2019). The male gametogenesis of plants depends on a series of complicated processes that lead to the development of premeiotic pollen mother cells into mature pollen grains. The male gametogenesis stage most sensitive to temperature stress is the transition from tetrad to uninucleate microspore (Kim et al., 2001; Oliver et al., 2005; Oda et al., 2010).

Increasing evidence indicates that male sterility induced by low- or high-temperature stresses is linked to tapetal dysfunction. The tapetum is the innermost sporophytic cell layer of the anther wall; it provides nutrients and precursors for microsporogenesis and pollen wall formation through programmed cell death (PCD)-triggered degradation (Ma, 2005; Ariizumi and Toriyama, 2011). The tapetum is the most susceptible to temperature fluctuations at the young microspore stage (Müller and Rieu, 2016). For instance, heat stress induces premature tapetum degeneration in *Arabidopsis thaliana* (Baron et al., 2012), rice (Ku et al., 2003), and wheat (Omidi et al., 2014). Conversely, cold stress disturbs tapetum development by delaying or inhibiting tapetal PCD (Liu et al., 2019). Various signaling pathways play pivotal roles in tapetum development and degeneration processes, including hormone and sugar signaling (Wang et al., 1999; Sun et al., 2019). Oliver et al. (2007) reported that in rice, male gametogenesis occurring under low-temperature stress, increased abscisic acid (ABA) levels and suppressed the expression of the tapetum-specific cell wall invertase (*CWIN*), *OsINV4*, and monosaccharide transporter genes, *OSMST8* and *OSMST7*. These expression changes interfere with tapetum PCD and lead to pollen abortion (Oliver et al., 2007).

As sessile organisms, plants have developed a variety of responses to tolerate environmental stress, including transcriptional, post-transcriptional, and post-translational regulatory processes (Barrero-Gil and Salinas, 2013; De Storme and Geelen, 2014; Guerra et al., 2015; Zhu, 2016). Post-transcriptional modifications based on RNA alternative splicing, processing, and modification shape the transcriptome in response to abiotic stress. While, N6-methyladenosine (m^{6}A), a methylation at the N6 position of adenosine, is the most abundant internal mRNA modification, which plays an important role in post-transcriptional gene expression regulation (Yue et al., 2015) by affecting RNA splicing (Liu et al., 2015; Xiao et al., 2016), stability (Wang et al., 2014; Du et al., 2016), translation (Zhou et al., 2015), and export (Roundtree et al., 2017). m^{6}A methylation is recognized by RNA-binding proteins (readers), and its levels are dynamically modified by RNA methyltransferases (Writers) and demethylases (Erasers) (Yue et al., 2019). Recent evidences demonstrated that m^{6}A also participates in plant responses to various abiotic stresses. In *Arabidopsis*, changed m^{6}A deposition affects RNA secondary structure under salt stress, resulting in increased stability of mRNA transcripts of abiotic stress response genes (Kramer et al., 2020). Additionally, *ALKBH6* (eraser) mutation results in increased salt, drought, and heat stress sensitivity during seed germination (Huong et al., 2020).

In *Arabidopsis*, m^{6}A levels vary across tissues, with a high m^{6}A/A ratio occurring in flowers (Zhong et al., 2008). MTA (one of the earliest discovered methyltransferases in *Arabidopsis*) disruption results in embryo development arrest at the globular stage (Zhong et al., 2008). Furthermore, the ALKBH10B demethylase (eraser) affects floral transition by regulating mRNA m^{6}A of key flowering genes (Duan et al., 2017). In rice, OsFIP (writer) regulates early microspore degeneration during male gametogenesis (Zhang et al., 2019). The tomato ALKBH2 participates in fruit ripening by affecting the stability of a DNA demethylase gene, *SlDML2*, *via* m^{6}A modification (Zhou et al., 2019). These findings suggest that m^{6}A plays essential roles in regulating reproductive developmental processes. However, whether and how m^{6}A participates in temperature stress response during the plant male reproductive stage remain elusive.

Tomato is one of the most widely cultivated subtropical vegetable crops in the world and its fruits and seeds are mainly derived from sexual reproduction. Because of its tropical origin, tomato is extremely sensitive to low temperature. In this study, we used m^{6}A sequencing to analyze changes in m^{6}A methylation in response to moderate low-temperature (MLT) stress during tomato anther development. We found that m^{6}A methylation was prevalent in tomato anther mRNA but that the levels declined upon MLT stress. Furthermore, MLT stress directly affected m^{6}A methylation abundance on a set of transcripts that regulate corresponding gene expression involved in anther development. Finally, we demonstrated that the decreased expression of an ATP-binding transcript, *SlABCG31*, was inversely correlated with its high m^{6}A deposition, which resulted in high ABA in MLT-stressed anthers. The decrease in *SlABCG31* expression may also participate in aberrant pollen coat formation after low temperature exposure. Overall, we demonstrated that mRNA m^{6}A modification was associated with anther development under low-temperature conditions.

MATERIALS AND METHODS

Plant Material and Growth Conditions

The tomato (*Solanum lycopersicum*) cultivar "Micro-Tom" provided by the Tomato Genetics Resource Center (University of California, Davis), was used in all experiments. Plants were grown in controlled chambers with 25°C ± 1/20 ± 1°C (normal temperature, NT), 16/8-h light/dark cycles, 300 μmol photons m^{-2} s^{-1} light intensity, and 60%–70% relative humidity. Six-week-old flowering plants were exposed to a 10°C/10°C (day/night) MLT treatment for 6 days and then moved back to NT for recovery.

Pollen Phenotypic Analysis and Light Microscopy

The development stages of the tomato anther are closely correlated to the flower bud size (Brukhin et al., 2003), which were roughly classified into six different stages (I–VI) according to semithin section observation as previously described (Peng et al., 2013; Chen et al., 2018). The anther at tetrad stage (stage II) were randomly marked with color strings before exposure to low temperature, because the tetrad stage is the most sensitive to ambient temperatures (Paupière et al., 2017; Begcy et al., 2019). The samples (anther at stages I–VI) harvested immediately after 6 days of MLT treatment were named MLT. Then the MLT-stressed plants were moved back to NT for recovery growth. The samples (anthers stages III–VI) developed from the marked tetrad anther at different time intervals that corresponded to time taken by tetrad anther to reach next different anther stages (stages III–VI) were named MLTR.

Mature pollen grain viability was determined using Alexander staining (Alexander, 1969). Scanning electron microscopy (SEM) was performed as previously described (Chen et al., 2018). Semithin section analysis was performed according to a previous report (Chen et al., 2018) with minor modifications. Briefly, the samples were fixed for 12 h at 4°C with 0.1 M phosphate-buffered saline (PBS) (pH 7.2) containing 2.5% glutaraldehyde (v/v). Subsequently, they were washed thrice with 0.1 M PBS, followed by soaking in 1% osmic acid (v/v) for 1–2 h. Specimens were rewashed thrice with 0.1 M PBS and then dehydrated through a gradient ethanol series. Further, we embedded and polymerized the specimens in Spurr's resin, and cut them into 2-μm-thick sections, which were stained with 1% methylene blue. Sections were observed and photographed under a Nikon Eclipse 90i microscope (Nikon, Japan). Terminal deoxynucleotidyl transferase-mediated dUTP nick-end labeling (TUNEL) assays were performed with the TUNEL Apoptosis Detection Kit (Roche, Switzerland) according to the manufacturer's protocol and using 10-μm paraffin sections of anthers at different stages. Furthermore, fluorescence signals were analyzed using Nikon's confocal laser scanning microscope, A1-SHS (Nikon, Japan).

RNA Isolation and qRT-PCR Analyses

Immediately after 6 days of MLT stress, anthers (about 0.5 g, >15 plants for each sample) at the six different stages (I–VI) were manually sampled and subjected to total RNA isolation using the Total RNA Kit II (OMEGA, United States). First-strand cDNA was synthesized using the PrimeScript^{TM} RT reagent kit (Takara, Japan). Quantitative RT-PCR reactions were performed using SYBR® Green Realtime PCR Master Mix (Toyobo, Japan). Reactions were run on Bio-Rad CFX96 (Bio-Rad, United States) in triplicate technical replicates and with *SlUbi3* as the endogenous control. Ct values were recorded and normalized with the $2^{-\Delta\Delta Ct}$ method (Livak and Schmittgen, 2001). The experiment was repeated as three independent biological replicates. Primers used for qRT-PCR analysis are listed in **Supplementary Table 1**.

Quantitative Analysis of m^{6}A in Total RNA

The total RNA m^{6}A levels were determined with the EpiQuik^{TM} m^{6}A RNA Methylation Quantification Kit (Colorimetric) (Epigentek, United States) following the manufacturer's instructions. Briefly, RNA was bound to strip wells using RNA high binding solution. RNA m^{6}A modification was captured and detected with capture and detection antibodies. Signals were enhanced and quantified colorimetrically by determining the absorbance at 450 nm using a microplate spectrophotometer with three technical replicates. Both negative and positive control RNA samples (m^{6}A 2 μg/mL) were provided with the kit. The standard curve was generated using the positive control sample. All experiments were performed three independent times.

High-Throughput m^{6}A Sequencing

m^{6}A-seq was performed as previously described (Dominissini et al., 2013). The anthers (about 0.5 g) at the tetrad stage from NT- and MLT-treated plants ($n > 15$ plants for each sample) were collected to extract the total RNAs. Three biological replicates of m6A RIP sequencing were performed. RNA quality was checked with the Agilent 2100 bioanalyzer (Agilent, United States) and using gel electrophoresis. Separation of mRNAs from total RNAs and sequencing of immunoprecipitated mRNA and pre-immunoprecipitated mRNA (input control) was performed at Novogene Biotech (Beijing, China) using an Illumina HiSeq 4000 system. Sequence data were deposited into the NCBI Sequence Read Archive under accession BioProject ID: PRJAN713408. A total of 23–29 million clean reads were produced from each library, and more than 95% of the reads were uniquely mapped to the tomato reference genome (Tomato Genome Consortium, 2012). The MACS software was used to identify m^{6}A peaks in immunoprecipitated samples using the corresponding input sample as the control. The strict cutoff criterion with assigned false discovery rate < 0.05 was applied to obtain high-confidence peaks (Zhang et al., 2008). Only peaks captured in all three biological samples were considered as confident peaks and used for further analysis. The *de novo* motif identification of the m6A peak data was carried out using the HOMER (hypergeometric optimization of motif enrichment) software (version 4.7[1]) to obtain their position and accurate motif regions. Visualization analysis of m^{6}A peaks was performed using the Integrated Genome Browser (Helt et al., 2009). All m^{6}A modification sites were assigned to different transcription regions covering transcription start site (TSS), 5′ untranslated region (UTR), coding sequence (CDS), 3′UTR, and intron. The gene expression level was calculated using RPKM method (Reads Per Kilobase per Million mapped reads). Differential m^{6}A peaks between NT and MLT anthers were determined using the m^{6}A site differential algorithm (Meng et al., 2013) with a P-value < 0.05. Gene Ontology (GO) and Kyoto Encyclopedia of Genes and Genomes (KEGG) enrichment analysis of were performed to identify the biological processes involving the differentially modified genes.

Quantification of Endogenous ABA Levels

Measurement of endogenous ABA was performed as previously reported (Chen et al., 2018) with minor modifications. Fresh anthers (about 0.5 g) at the tetrad stage were collected from NT and MLT plants (>15 plants for each sample) and ground into a powder in liquid nitrogen with a mortar and pestle. For each sample, 100 mg of powder was homogenized using 1 mL ethyl acetate spiked with d6-ABA (OlchemIm, Czechia). Samples were then agitated for 10 min and centrifuged at 13,000 *g* for 20 min at 4°C. The supernatant was collected and dried in N_2 gas. Dried samples were resuspended in 0.2 mL of 60% (v/v) methanol and then centrifuged at 13,000 *g* for 10 min at 4°C. The supernatant sample was filtered through a 0.22-μm nylon membrane and analyzed using HPLC/MS-MS on an Agilent 1290 Infinity HPLC system coupled with an Agilent 6460 Triple Quad LC/MS device (Agilent, United States). Agilent Zorbax XDB C18 columns (150 mm × 2.1 mm, 3.5 μm) were used to perform the HPLC analysis. Three independent biological replicates were performed for each sample.

[1]http://homer.ucsd.edu/homer/

Statistical Analysis

All experiments were conducted in randomized complete block design. Mean values were used to represent the data of at least three independent experiments. The statistical differences between treatments were verified using two-tailed Student's *t*-tests.

RESULTS

Impact of MLT Stress on Tomato Pollen Development

To investigate tomato pollen development response to low-temperature stress, flowering tomato plants were treated with MLT (10°C/10°C) for 6 days and then moved to normal growing conditions for recovery. Plants continuously grown under NT (25°C/20°C) were used as controls (**Supplementary Figure 1A**). Surprisingly, after 6 days of MLT treatment, pollen viability was similar in control and stressed plants, reaching 95.0% (**Figures 1A,B**). Tomato reproductive organ development nearly ceases when the ambient temperature is below 12°C (Criddle et al., 1997). Therefore, the anther development may be delayed and cease under MLT-stress. We determined the viability of mature pollen grains developed from marked anthers at the tetrad stage after MLTR. Strikingly, pollen viability decreased by 95.8% after MLTR (**Figures 1A,B**). We also examined pollen morphology using SEM. Under NT, pollen had an elliptical shape and grain surface was densely microperforated and granulated with three germination ditches (**Figure 1C**). Conversely, 97.9% of MLTR-stressed pollen grains were highly shriveled and aggregated. The pollen grain surface was smooth, lacking granulation and germination ditch (**Figures 1C,D**). To monitor the dynamic response to MLT stress, we generated transverse semithin sections of anthers at different developmental stages and assessed their morphology. Under NT, tapetal cells formed a regular layer surrounding the locules at tetrad stage, which subsequently underwent PCD, gradually degenerating until disappearing completely at binucleate stage (**Figure 1E**). Anther morphology did not differ between MLT and NT plants, except for few pollen grain abortions at mature pollen stage (**Figure 1E**). However, under MLTR-stress, at early uninucleate stage, anther chambers were irregular and harbored numerous shriveled microspores, and tapetal cells became vacuolated. More importantly, tapetal cell degeneration was incomplete even at the binucleate stage, contributing to pollen grain abortion at the mature stage (**Figure 1E**). To further investigate the timing of tapetal cell degeneration in pollen development, we performed TUNEL assays on different stage anthers from plants grown under NT or MLTR conditions. Under NT, TUNEL signals were first detected on tapetal cells at the tetrad stage. They gradually intensified from the early to late uninucleate stage and finally disappeared at the binucleate stage (**Supplementary Figure 1B**). However, under MLTR, TUNEL signals appeared at the uninucleate stage and became weaker at the binucleate stage, suggesting that tapetal cells PCD was delayed (**Supplementary Figure 1B**). Our data show that pollen development was sensitive to low temperature and that plants exposed to MLT stress had pollen sterility, characterized by changes in tapetum development and exine deposition.

MLT Stress Influences m^{6}A Levels and m^{6}A-Related Gene Expression in Tomato Anthers

To determine whether m^{6}A participates in tomato anther development and responds to suboptimal temperature stress, we performed colorimetric m^{6}A quantification assays in plants grown under NT and MLT. Under NT conditions, overall RNA m^{6}A levels were slightly lower at the tetrad stage than at the pollen mature cells (PMC) stage. m^{6}A increased mildly at the uninucleate stage and peaked at the binucleate stage (**Supplementary Figure 2A**). However, under MLT stress, anther m^{6}A levels were decreased at both the tetrad and uninucleate stages compared to that at NT (**Figure 2A**).

Next, we analyzed the spatial and temporal expression profiles of m^{6}A-related components (writers, erasers, and readers) in NT tomato plants using qRT-PCR. Among the 26 investigated genes (seven writers, ten erasers, and nine readers), 23 had altered expression among different tissues or anthers at different developmental stages. The exceptions were *SlMTB*, *SlALKBH9B*, and *SlALKBH10B*, which had low expression levels in all 11 tested organs/tissues. The writer genes, including *SlMTA*, *SlMTD*, and *SlHAKAI*, were mostly expressed in tomato anthers at the mature pollen stage (VI) and fruits (**Figure 2B**). Several erasers, including *SlALKBH2B* and *SlALKBH6B*, were preferentially expressed in mature anthers and young fruits, whereas *SlALKBH7B* and *SlALKBH8B* were rarely expressed in reproductive tissues (**Figure 2B**). Moreover, *SlECT1* and *SlECT2* reader genes were also preferentially expressed in mature anthers and young fruits; they had higher expression levels than other readers, including *SlECT3*, *SlECT4*, and *SlECT7*, which had low expression in anthers at all stages except stage VI (**Figure 2B**). The expression profiles of m^{6}A-related genes analyzed using qRT-PCR assay were consistent with the *in silico* data available from the tomato eFP Browser (**Supplementary Figures 2B–D**).

Since total RNA m^{6}A levels were lower in MLT anthers at stages II and III, we further analyzed the changes in m^{6}A-related gene expression profiles in MLT and NT anthers using qRT-PCR. *SlMTA*, *SlMTC*, and *SlMTD* expression significantly decreased at the microspore mother cell stage (I) under MLT stress compared with that at NT. At tetrad (II) and uninucleate (III and IV) stages, only *SlMTD* expression significantly decreased (**Figure 2C**), whereas *SlMTC* and *SlMTD* were significantly downregulated at the binucleate stage (V) under MLT stress. More importantly, all writer genes analyzed (*SlMTA*, *SlMTC*, *SlMTD*, *SlFIP37*, and *SlHAKAI*) were downregulated in MLT anthers at the mature pollen stage (VI) (**Figure 2C**). Furthermore, the *SlALKBH1B* eraser gene was significantly downregulated in anthers at the stages IV and VI. *SlALKBH2B* was significantly downregulated at stages II, III, and VI, and *SlALKBH4B* and *SlALKBH6B* were decreased at both stages V and VI (**Figure 2C**). However, the m^{6}A reader *SlECT1* was significantly upregulated in MLT at stage II (**Figure 2C**). These data indicate that m^{6}A modification

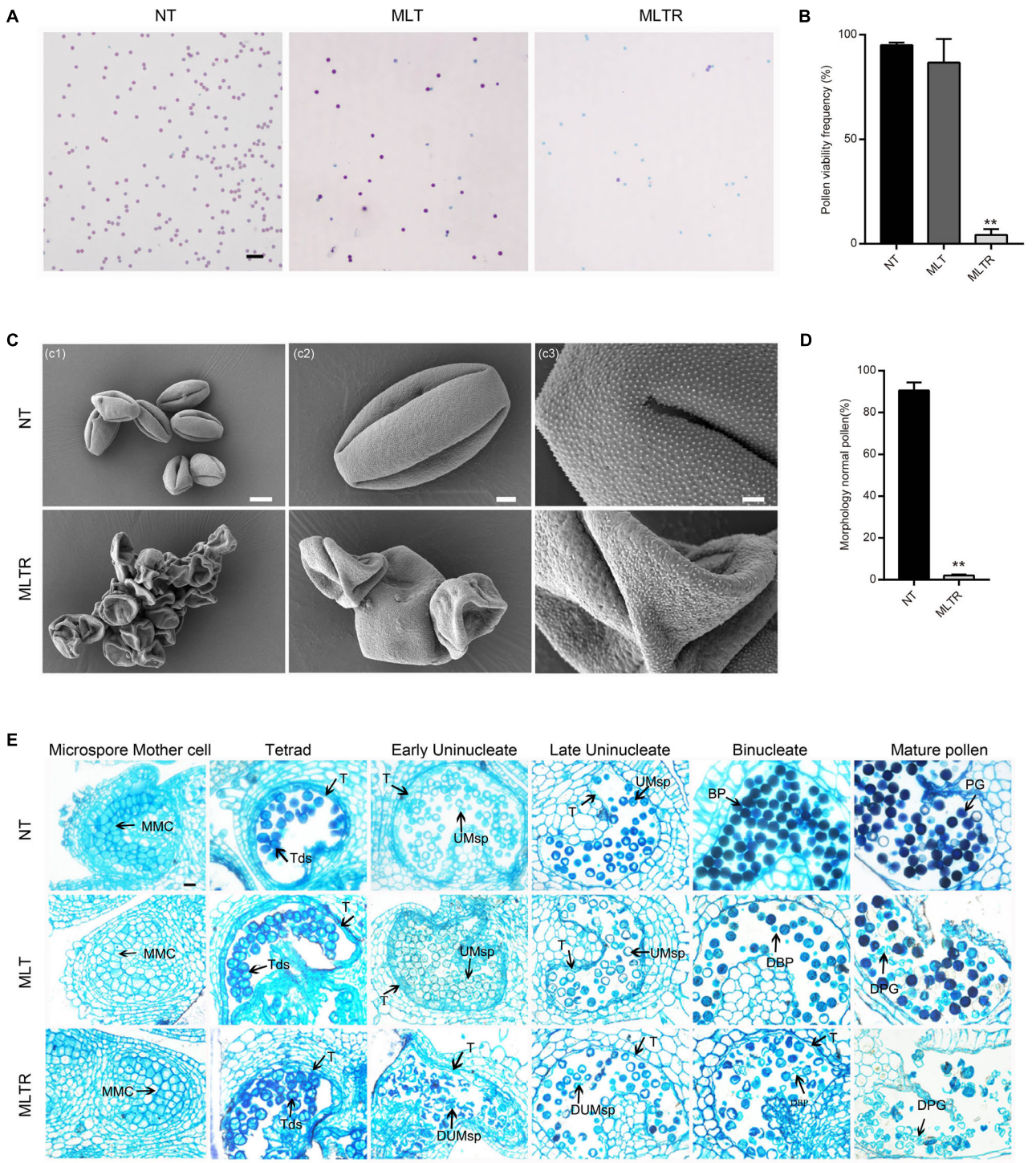

FIGURE 1 | Moderate low temperature (MTL) stress at the tetrad stage affects pollen development in tomato. **(A)** Alexander staining of mature pollen grains from the plants exposed to normal temperature (NT), MLT-stress and returned to normal growing temperature for recovery after moderate low temperature treatment (MLTR). Scale bars = 100 μm. **(C)** Scanning electron microscopy indicated that MLTR-stress pollen grains were seriously shrunk and collapsed, appearing aggregated. Scale bars c1 = 10 μm; c2 = 3 μm; c3 = 1 μm. **(B,D)** Quantification of viable mature pollen grains and morphology normal pollen from NT, MLT, and MLTR plants, respectively. Each value is the mean ± SD (n = at least three biological replicates with 15 plants each). *$P < 0.05$; **$P < 0.01$ (two-tailed Student's t- test). **(E)** Semithin cross sections of anthers in different stages under NT and MLT condition. The tapetum degeneration was postponed under MLTR compare to NT condition. MMC, microspore mother cell; Tds, tetrads; UMsp, uninucleate microspore; BP, binucleate pollen; PG, pollen grains; DUMsp, degenerated uninucleate microspore; DBP, degenerated binucleate pollen; DPG, degenerated pollen grains; T, tapetum. The experiment was repeated three times independently with consistent results. Scale bars = 20 μm.

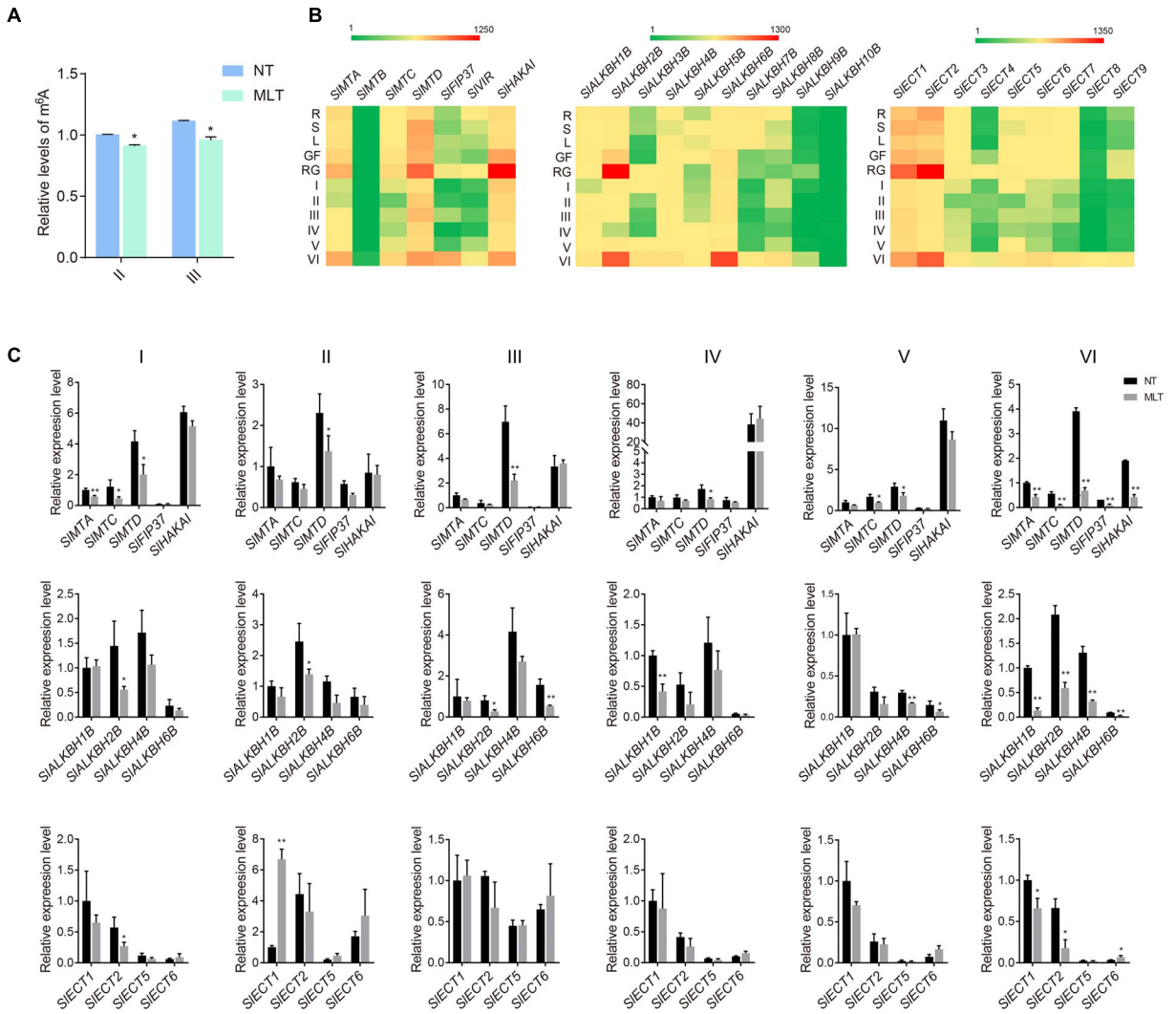

FIGURE 2 | The expression profiles of m^{6}A writers, erasers and readers under NT and MLT conditions. **(A)** The relative levels of m^{6}A in total RNA of anther at stage-II and III under NT and MLT conditions. The level of m^{6}A in stage-II under NT condition is set to 1. Each value is the mean ± SD (*n* = at least three biological replicates with 15 plants each). **P* < 0.05; ***P* < 0.01 (two-tailed Student's *t*- test). **(B)** Expression patterns of genes in various tissues of plants under NT condition, especially in anther of different stages. Green, weak expression; Red, strong expression. R, root; S, stem; L, leaf; GF, green fruit; RF, red fruit; I, anther at microspore mother cell stage; II, anther at tetrad stage; III, anther at early uninucleate stage; IV, anther at late uninucleate stage; V, anther at binucleate stage; VI, anther at mature pollen stage. **(C)** qRT-PCR analysis of writer, erasers and readers genes in anther at different stages under NT and MLT conditions. The levels of genes expression normalized to *Ubiquitin* expression are shown relative to *SlMTA*, *SlALKBH1B*, and *SlECT1* under NT condition set to 1, respectively. Each value is the mean ± SD (*n* = at least three biological replicates with 15 plants each). **P* < 0.05; ***P* < 0.01 (two-tailed Student's *t*- test).

levels and the expression pattern of its related genes were changed under low-temperature stress. We speculated that m^{6}A methylation plays a fundamental role in anther development and temperature stress responses.

Transcriptome-Wide Detection of m^{6}A Methylation in Tomato Anthers

To explore the molecular mechanisms behind m^{6}A regulation of anther development in tomato, we performed a transcriptome-wide detection of m^{6}A methylation through m^{6}A-seq using NT- and MLT- anthers at the tetrad stage. Six MeRIP libraries were analyzed (**Supplementary Figure 3A**) and high Pearson correlation coefficients were found between biological replicates, indicating a high reproducibility for the m^{6}A-seq data (**Supplementary Figure 3B**). m^{6}A modification sites, named m^{6}A peaks, were identified on the basis of the comparison of read distribution between the input and immunoprecipitation samples using exomePeak with an estimated *P*-value < 0.05. We used high-confidence m^{6}A peaks that were observed in all three biological replicates for subsequent analysis. A total of 10,235 and 9,911 high-confidence m^{6}A peaks, representing 8,541 and 8,743 gene transcripts, were detected in NT and MLT anthers, respectively (**Figure 3A** and **Supplementary Figure 3C**).

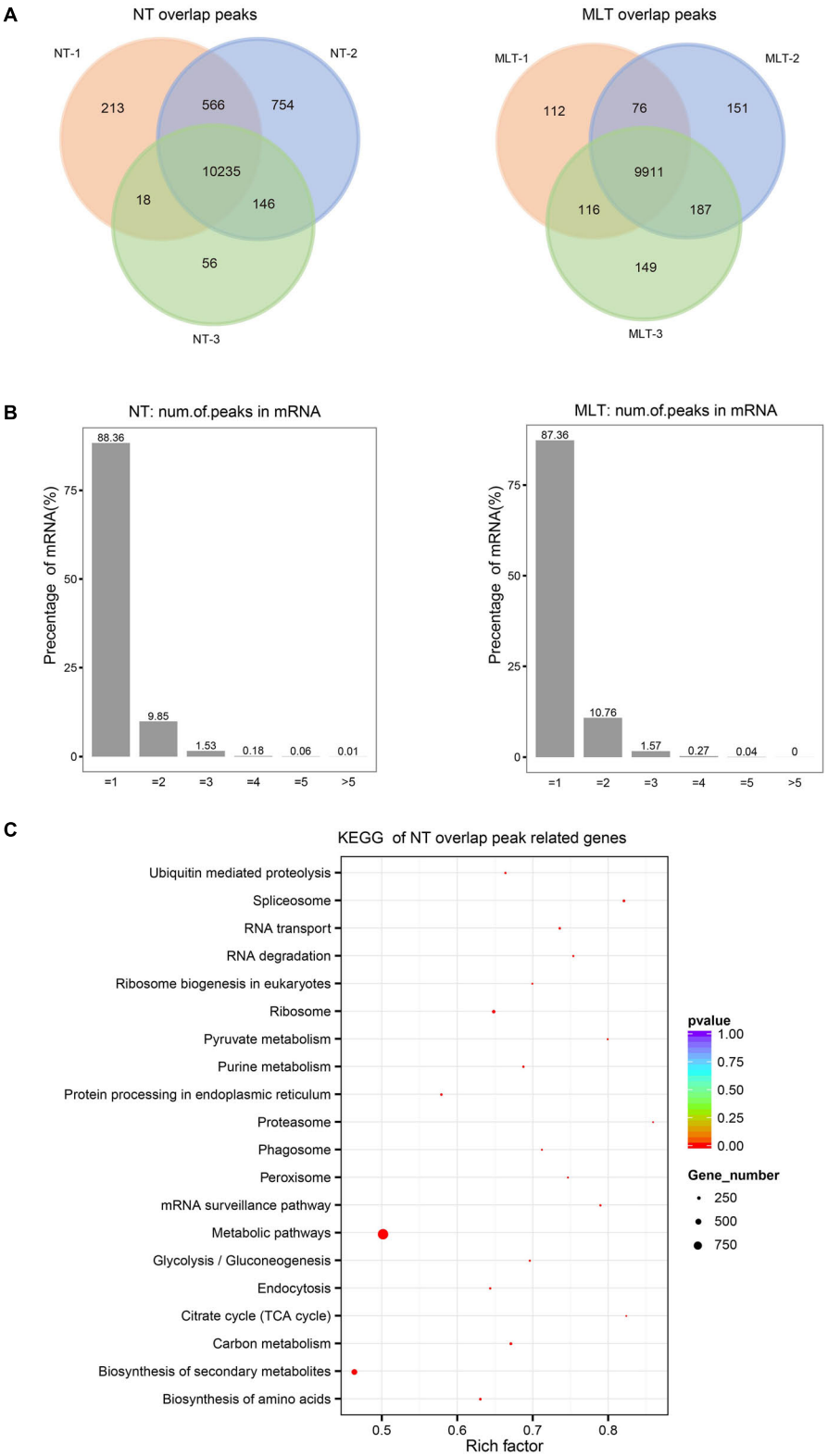

FIGURE 3 | Transcriptome-wide m^{6}A methylation profiles in tomato anther at stage-II. **(A)** The number of overlapped m^{6}A peaks identified in three biological replicates under NT and MLT conditions, respectively. The peaks identified in all three biological replicates were used for subsequent analysis. **(B)** Statistics on proportion of the m^{6}A-modifited transcripts containing different m^{6}A sites numbers in NT and MLT conditions. **(C)** KEGG enrichment analysis of all the transcripts with m^{6}A peaks in NT condition.

Among transcripts harboring m^{6}A modification, 88.36, 9.85, 1.53, and 0.26% contained one, two, three, and more than three peaks, respectively (**Figure 3B**). Enrichment analysis using the KEGG revealed that these m^{6}A-containing transcripts in NT condition were enriched in multiple conserved metabolic pathways, including tricarboxylic acid (TCA) cycle, spliceosome, proteasome, and pyruvate metabolism (**Figure 3C**).

The analyses of m^{6}A peak distribution across the tomato transcriptome in NT anthers showed that highly enriched m^{6}A modifications surrounded stop codon and 3′-UTRs (**Figure 4A**), as seen in tomato fruits (Zhou et al., 2019). Furthermore, we assigned each m^{6}A peak to one of five transcript segments based on their location: TSS, 5′-UTR, CDS, stop codon (a 100-nucleotide window centered on the stop codon), and 3′-UTR. These analyses revealed that m^{6}A peaks were abundant near stop codons (49.04%) and 3′-UTRs (40.34%), followed by CDS (9.12%) (**Figure 4B**). After segment normalization by the total length of each gene portion, we confirmed that m^{6}A peaks were predominantly enriched around the stop codon and 3′-UTR (**Figure 4B**). Homer was used to identify the sequence motifs enriched within the m^{6}A peaks in tomato anthers and it showed that UGUAYY (where Y represents A, G, U, or C) was the most statistically over-represented motif (**Figure 4C**). This phenomenon was observed previously in *Arabidopsis* and tomato fruits (Luo et al., 2014; Zhou et al., 2019), suggesting that m^{6}A methylation sequence motifs are conserved between *Arabidopsis* and tomato.

Comparison Between NT and MLT Anther m^{6}A Methylation Profiles

To systemically elucidate the m^{6}A methylome response to low temperature, we compared NT and MLT m^{6}A-seq data. There was no obvious difference in whole transcriptome m^{6}A distribution between NT and MLT anthers (**Figure 4A**). The analysis showed that 7,846 m^{6}A modified transcripts containing 9,396 m^{6}A peaks were shared by MLT and NT (**Figure 5A** and **Supplementary Figure 3D**). However, a total of 3,837 m^{6}A peaks harboring 3,434 gene transcripts differed between NT and MLT anthers in m^{6}A levels (P-value < 0.05) (**Supplementary Table 2**). Among them, the m^{6}A peaks of 2,783 transcripts appeared in stop codons or 3′-UTRs; the m^{6}A levels of 978 of these transcripts were higher in MLT than in NT, whereas the inverse was true for 1,805 transcripts (**Figure 5B** and **Supplementary Table 2**). These data suggested that MLT stress markedly affected m^{6}A levels in a large number of mRNA transcripts, which are predominantly downregulated.

To identify the potential correlation between m^{6}A levels and transcript abundance in tomato anthers, we investigated the transcript levels of genes under MLT stress and NT by RNA-seq. Among the 1,805 transcripts with lower m^{6}A levels in MLT anthers, 70.2% were upregulated under MLT stress, whereas 29.8% were downregulated. Accordingly, among 978 transcripts with higher m^{6}A levels in MLT anthers, 569 had lower expression levels in MLT-stressed anthers (**Figure 5B**). These results revealed that m^{6}A methylome in stop codon or 3′-UTR generally negatively correlated with the transcript levels. KEGG analysis showed that, under MLT stress, transcripts with increased m^{6}A methylation were significantly enriched in phenylalanine, tyrosine, and tryptophan metabolism and amino acid biosynthesis pathways. Furthermore, transcripts with decreased m^{6}A were significantly enriched in mRNAs for surveillance and carbon metabolism pathways (**Supplementary Figure 4**). These metabolic pathways may be associated with plant pollen development (Yang et al., 2001; Min et al., 2014; Fang et al., 2016).

MLT Stress Induces the m^{6}A Level Alteration in Anther-Related Transcripts

To further analyze m^{6}A response to MLT stress during anther development, we performed GO analysis of the transcripts that were significantly differentially modified by m^{6}A methylation ($|\log_2\text{FoldChange}| > 1$ and P-value < 0.05) between NT and MLT stress. In MLT anthers, transcripts with decreased m^{6}A methylation were significantly enriched in "cellular lipid metabolic process," "regulation of RNA biosynthetic process," and "adenosine triphosphatase (ATPase) activity-related function" categories (**Figure 5C**). Whereas the transcripts with increased m^{6}A methylation under MLT stress were significantly enriched in "carbohydrate derivative binding," "nucleoside phosphate binding," "anion binding," and "ATP-binding" categories (**Figure 5C**). These changed pathways play important roles in anther development (Lucca and León, 2012; Shi et al., 2015; Zhao et al., 2016).

We further analyzed the expression patterns of the significantly differentially modified transcripts in response to MLT stress. The transcripts of diacylglycerol acyltransferase 1 (*SlDGAT1*) and inositol-3-phosphate synthase 2 (*SlMIPS2*), which are involved in lipid metabolism, were significantly upregulated under MLT stress and had decreased m^{6}A levels (**Figure 6**). Conversely, calcium-transporting ATPase isoform 2 (*SlACA2*) expression was downregulated under MLT stress (**Figure 6C**). The transcript levels of factors with decreased m^{6}A modification, including WRKY DNA-binding protein 33 (*SlWRKY33*), auxin response factor 9B (*SlARF9B*), and ethylene response factor 3 (*SlESE3*), were significantly upregulated in MLT anthers (**Figure 6**). Additionally, the expression of the ATP-binding member of ATP-binding cassette G31 (*SlABCG31*), CTR1-like protein kinase (*SlCTR1*), and receptor-like kinase 1 (*SlRLK1*) genes, which had high m^{6}A methylation levels, was downregulated under MLT stress (**Figure 6C**). Overall, these data implied that MLT stress affected m^{6}A methylation of various transcripts, altering their expression levels to regulate pollen development.

MLT Stress Increases *SlABCG31* m^{6}A Levels and ABA Content

Because m^{6}A levels changed in transcripts that may be involved in pollen development under MLT stress, such as *SlDGAT1*, *SlMIPS2*, *SlACA2,* and *SlABCG31* (**Figures 5C**, **6**), we further examined the underlying mechanisms of pollen development regulation by m^{6}A methylation. Members of the ATP-binding cassette transporter (ABC) family, particularly ABC sub-family

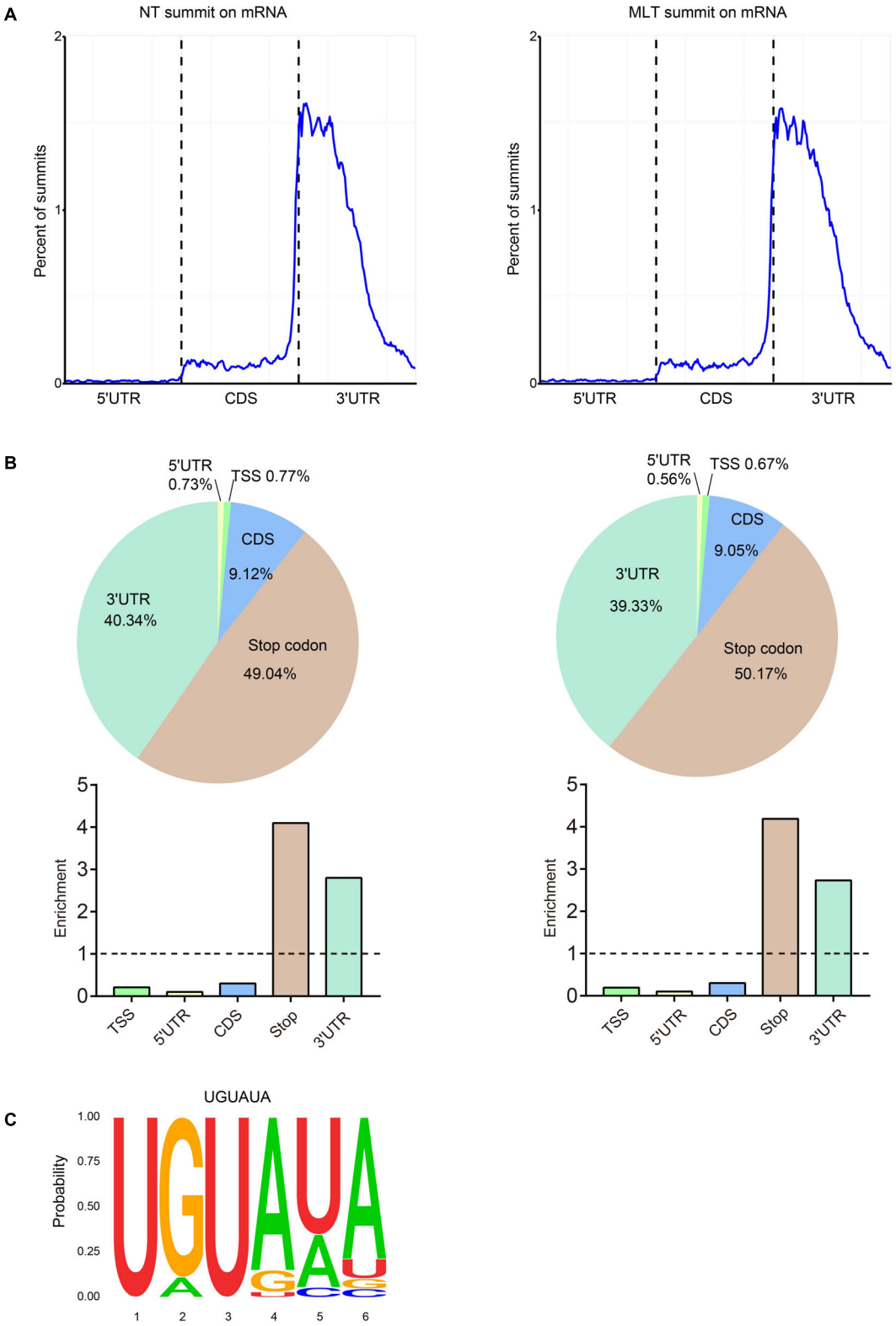

FIGURE 4 | Distribution pattern of m^{6}A peaks along the transcripts and the sequence motif in tomato anther. **(A)** m^{6}A peaks summits localization along the transcripts in NT and MLT conditions. Each transcript is divided into three parts: 5′-UTR, CDS and 3′ -UTR. UTR, untranslated region; CDS, coding sequence. **(B)** The m^{6}A peaks summits and relative enrichment in five non-overlapping transcripts segments in NT and MLT conditions. TSS, transcription start site. **(C)** The conserved sequence motif for m^{6}A peaks in NT and MLT conditions.

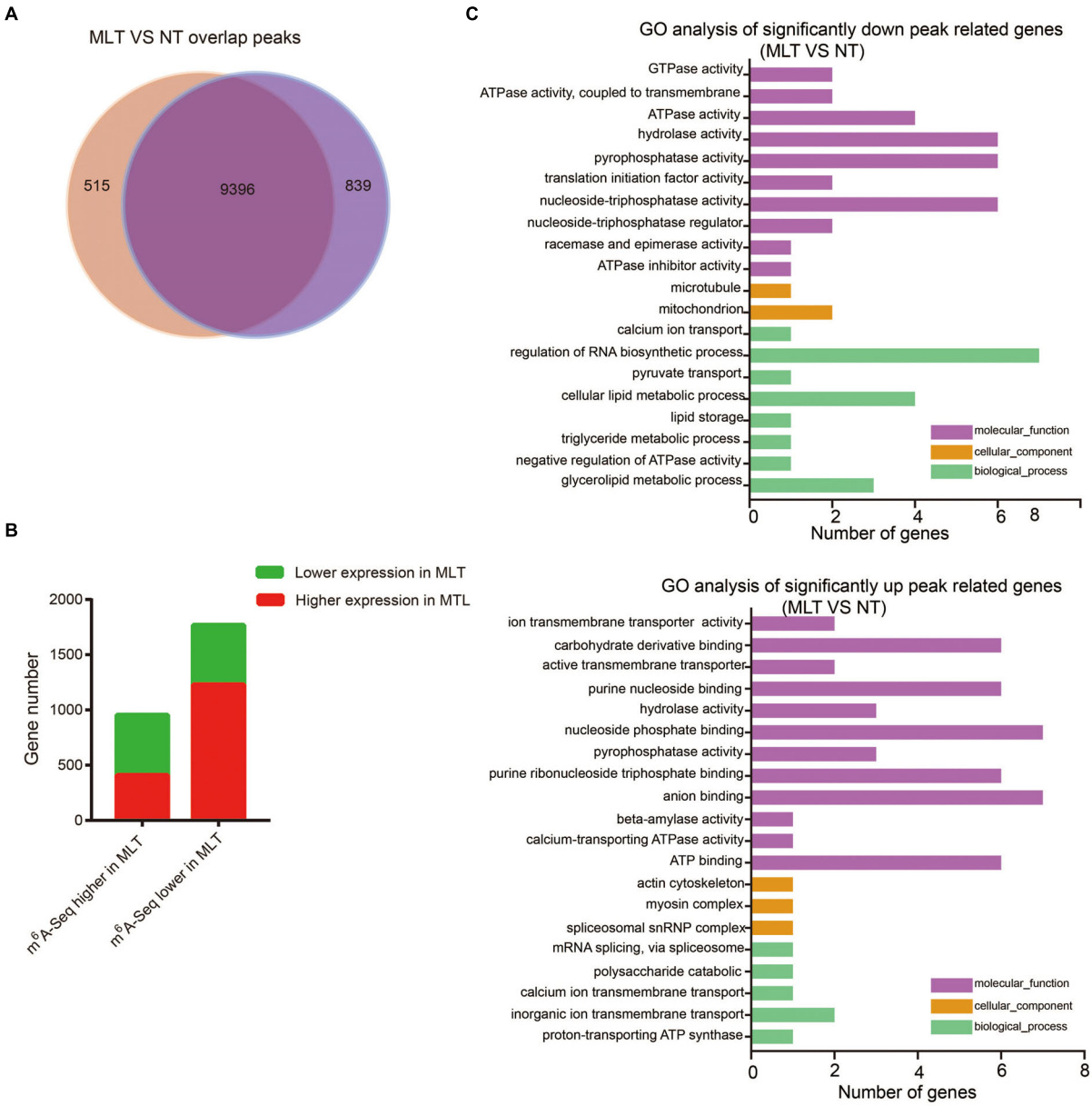

FIGURE 5 | Comparative analysis transcriptome-wide m^{6}A profiles between NT and MLT anthers at stage-II. **(A)** The number of overlapped m^{6}A peaks between NT and MLT anthers. **(B)** The gene number of transcripts with differential m^{6}A enrichment and differential transcript levels between NT and MLT anthers. **(C)** GO analysis significantly different enrichment peaks related genes between NT and MLT anthers.

G members, are involved in ABA transport. Accordingly, *AtABCG31* functions in exporting ABA from the endosperm to the embryo in *Arabidopsis* (Borghi et al., 2015; Kang et al., 2015). The tomato *SlABCG31* is highly homologous (71%) to *AtABCG31* (**Supplementary Figure 5**). To identify whether *SlABCG31* participates in pollen development under MLT stress, we analyzed its expression with qRT-PCR in different tomato tissues and anthers at different developmental stages. The data revealed that *SlABCG31* is predominantly accumulated in anthers and is rarely detected in other tissues and organs (**Figure 7A**). Because *SlABCG31* expression sharply decreased under MLT stress (**Figure 6B**), we investigated whether it affected ABA levels in MLT anthers. Surprisingly, endogenous ABA levels measured using HPLC–mass spectrometry were noticeably increased in MLT anthers than in NT anthers at the tetrad stage (**Figure 7B**). Furthermore, qRT-PCR data revealed that the expression of the ABA signaling-related genes, *SlPYLs* and *SlPP2Cs*, was significantly changed under MLT stress (**Supplementary Figure 6**). *SlPYL4*, which had the highest expression level at the tetrad stage, was significantly decreased in MLT anthers. *SlPP2C1* and *SlPP2C3* were significantly upregulated under MLT stress compared with those under NT condition.

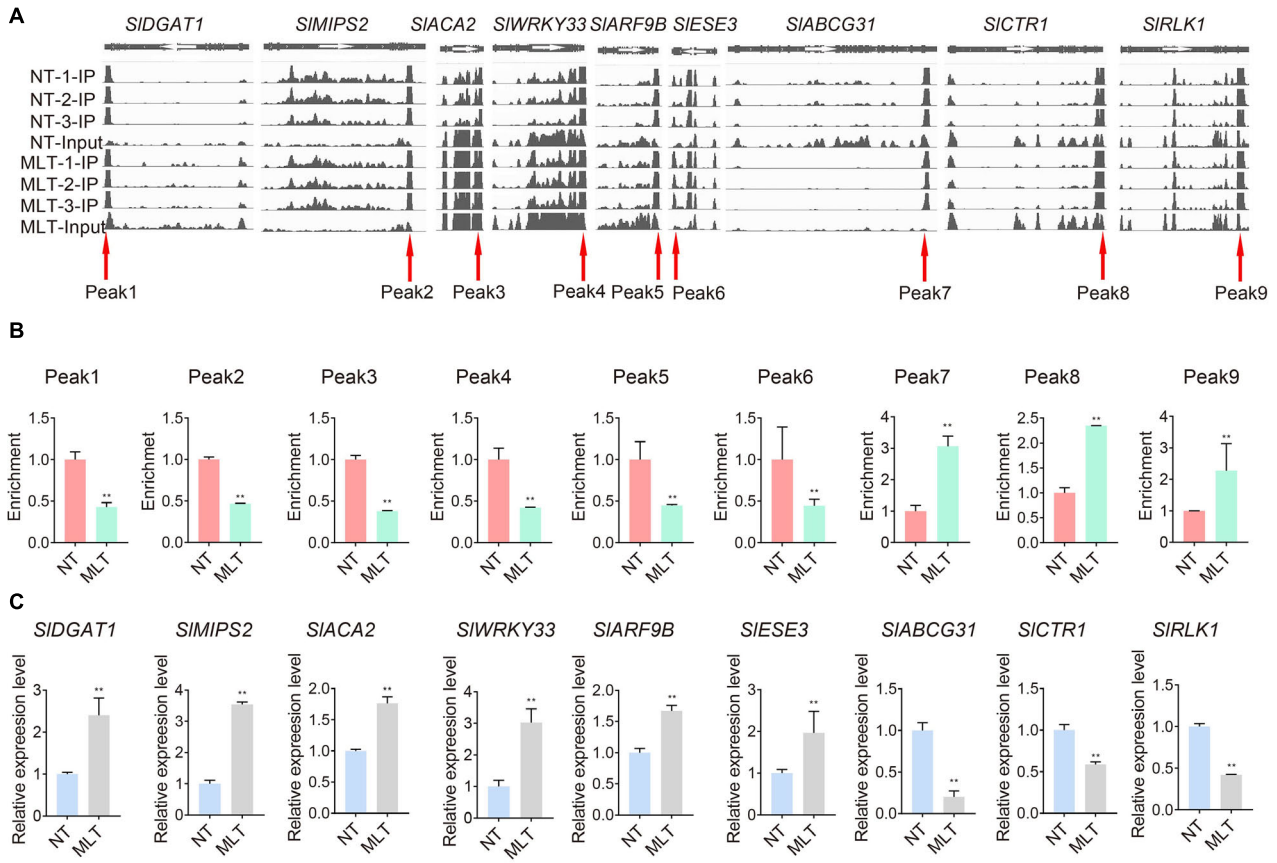

FIGURE 6 | Comparison on m^{6}A levels and expression levels of transcripts in NT and MLT anthers at stage-II. **(A)** Integrative Genome Browser (IGB) showing m^{6}A-seq read distributions in transcripts. The red arrowheads indicate the position of m^{6}A peaks with significantly changed m^{6}A enrichment in MLT-stress stage-II anther compared to NT. The white arrowheads represent the direction of gene. **(B)** The m^{6}A enrichment of transcripts involved in pollen development in NT and MLT anthers. The level of m^{6}A in stage-II under NT condition is set to 1. Each value is the mean ± SD (n = 3 biological replicates with 15 plants each). *P < 0.05; **P < 0.01 (two-tailed Student's t- test). **(C)** qRT-PCR analysis validates the different m^{6}A enrichment peak related genes expression levels between NT and MLT anthers. The levels of genes expression normalized to *Ubiquitin* expression are shown relative to genes expression under NT condition set to 1, Each value is the mean ± SD (n = at least three biological replicates with 15 plants each). *P < 0.05; **P < 0.01 (two-tailed Student's t- test).

Increased ABA levels lead to high pollen abortion through negative regulation of *CWIN* expression, which may distort the anther carbohydrate pool (Oliver et al., 2007). Our qRT-PCR analysis showed that *SlCWIN7* and *SlCWIN9* were strikingly downregulated at the uninucleate stage under MLT stress (**Figure 7C**). Overall, we speculate that MLT stress increased m^{6}A methylation in *SlABCG31*, resulting in its decreased expression, which in turn increased the ABA content in tomato anthers to suppress *SlCWINs* expression and cause pollen abortion (**Figure 8**).

DISCUSSION

N6-methyladenosine methylation is the most prevalent type of internal mRNA modification in eukaryotes. Previous studies revealed that m^{6}A modification plays essential roles in embryo development, shoot stem cell fate, root development, and floral transition in *Arabidopsis* (Vespa et al., 2004; Zhong et al., 2008; Bodi et al., 2012; Růžička et al., 2017). In tomato, m^{6}A methylation participates in fruit ripening regulation through *SlALKBH2*, which mediates the m^{6}A methylation of *SlDML2* transcripts (Zhou et al., 2019). Recent study revealed that the OsFIP methylase may regulate early microspore development in rice (Zhang et al., 2019). Although the roles of m^{6}A in plant growth and development have been demonstrated, mostly in *Arabidopsis*, its involvement and putative functions in the response to abiotic stress are still unknown. Here RNA methylome analysis revealed that mRNA m^{6}A methylation is widespread in tomato anthers and is disturbed in response to low-temperature stress. Changes in m^{6}A methylation may affect the expression of the genes involved in tapetum and microspore development through multiple pathways, at least partly through modifying ABA signaling genes (**Figure 8**).

Under normal growing conditions, anthers at the tetrad stage take about 6–7 days to reach the mature pollen stage. However, the reproductive development may slow down after exposure to low temperature stress. In our study, after

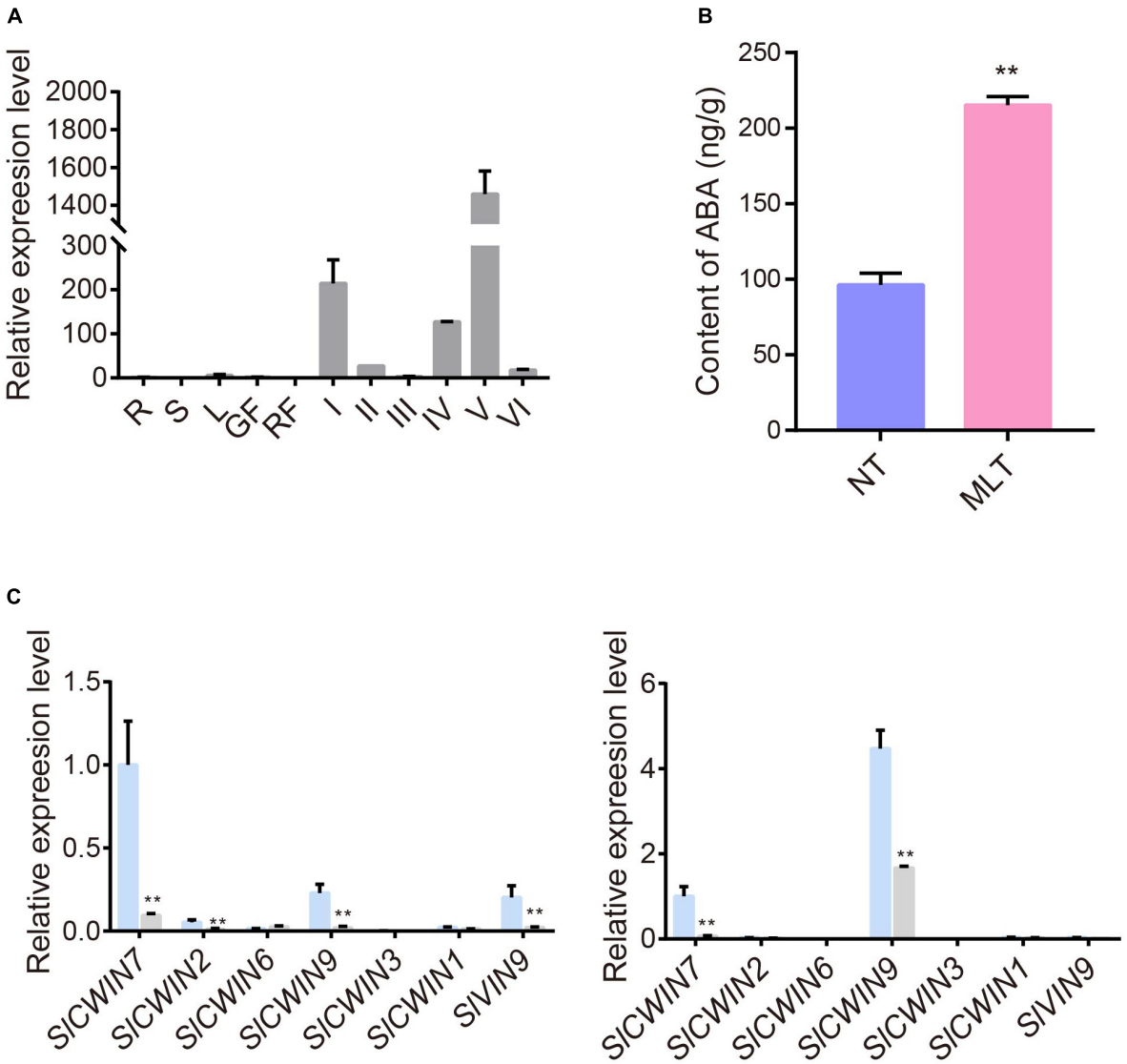

FIGURE 7 | The expression profiles of *SlABCG31* and ABA levels in anther under NT and MLT conditions. **(A)** qPCR analysis of *SlABCG31* in various tissues of tomato, especially in anther at different stages. The genes expression levels normalized to *Ubiquitin* expression are shown relative to root set to 1. R, root; S, stem; L, leaf; GF, green fruit; RF, red fruit; I, anther at microspore mother cell stage; II, anther at tetrad stage; III, anther at early uninucleate stage; IV, anther at late uninucleate stage; V, anther at binucleate stage; VI, anther at mature pollen stage. Each value is the mean ± SD (n = at least three biological replicates with 15 plants each). **(B)** ABA levels in anther at stage-II under MLT-stress were increased in comparison to NT condition. Each value is the mean ± SD (n = at least three biological replicates with 15 plants each). $^*P < 0.05$; $^{**}P < 0.01$ (two-tailed Student's t- test). **(C)** The expression levels of *SlCWINs* genes in anther at stage-II and III in NT and MLT conditions. The levels of genes expression normalized to *Ubiquitin* expression are shown relative to the expression of *SlCWIN7* in NT condition set to 1. Each value is the mean ± SD (n = at least three biological replicates with 15 plants each). $^*P < 0.05$; $^{**}P < 0.01$ (two-tailed Student's t- test).

6 days MLT-stress, the marked anthers were still at tetrad stage, suggesting that at 10°C cold stress, the tomato anthers development nearly ceases, which is consistent with previous study showing that tomato reproductive organ development ceases when the ambient temperature is below 12°C (Criddle et al., 1997). Therefore, it is not surprising that the viability of mature pollen grains harvested immediately after 6 days (MLT) was similar to that in NT conditions. However, when the plants were moved back to NT conditions for recovery after cold stress, the marked anthers need another 6–7 days to reach the mature pollen stage (MLTR), and the mature pollen grains exhibited highly aborted (**Figure 1E**). Our cytological observations showed that low-temperature-induced pollen abortion could be attributed to delayed tapetal cell degradation at tetrad and early uninucleate stages, resulting in impaired pollen wall formation and pollen abortion (**Figure 1**). Correspondingly, m^{6}A levels in total RNA were significantly decreased in anthers at both tetrad and uninucleate stages after MLT exposure (**Figure 2A**). Furthermore, *SlMTD* expression was significantly decreased at tetrad and early uninucleate stages,

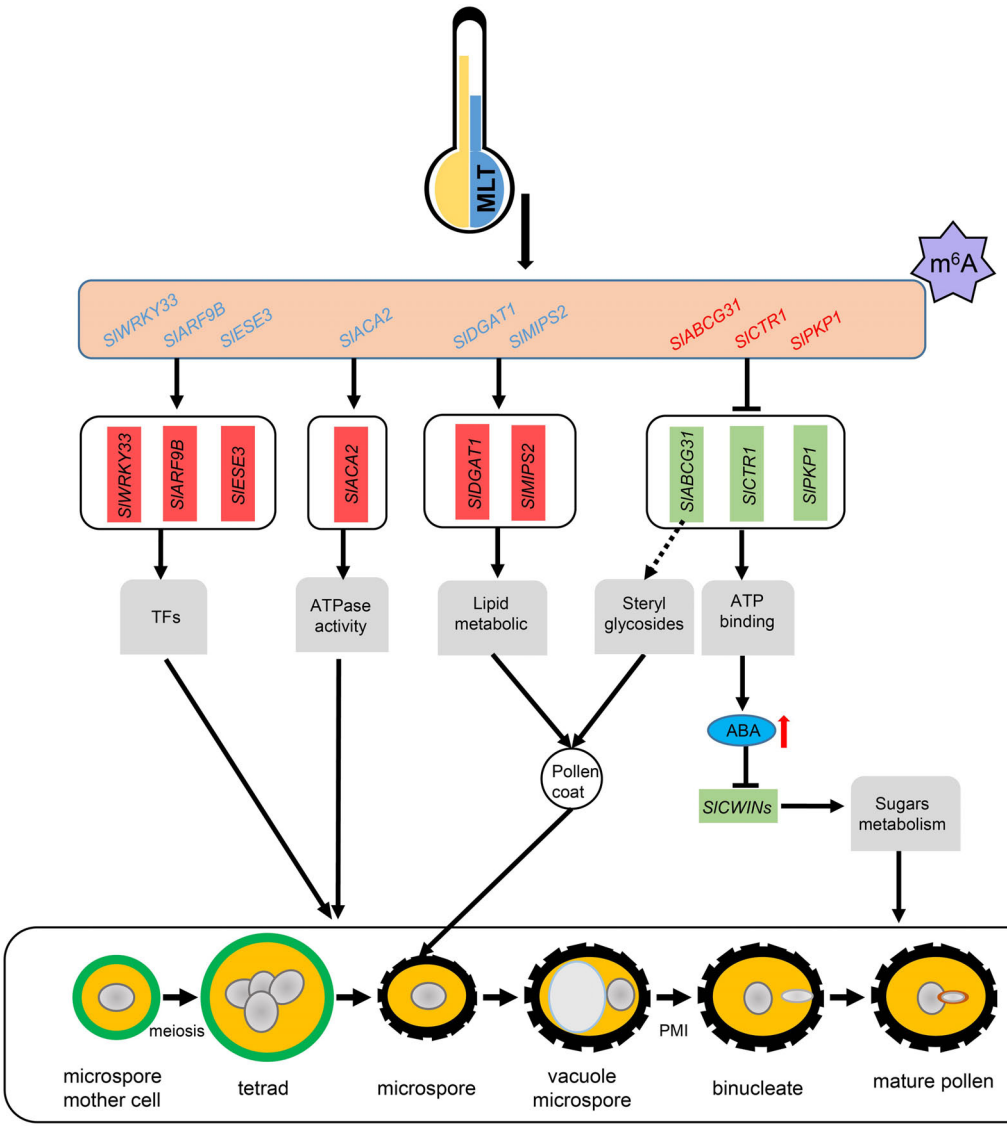

FIGURE 8 | A working model for m^{6}A methylation affects pollen development under MLT-stress. MLT, moderate low temperature; TFs, transcript factors; Blue letters means transcripts with lower m^{6}A levels, and red letters means transcripts with higher m^{6}A levels; Red and green boxes represent unregulated and downregulated genes expression levels, respectively; Red arrow, significant increase.

whereas *SlECT2* was dramatically overexpressed at the tetrad stage under MLT stress (**Figure 2C**). m^{6}A-seq analysis revealed that MLT treatments significantly altered the m^{6}A levels of 2,783 transcripts in tomato anthers at the tetrad stage, which may contribute to abnormal pollen development. These data indicated that m^{6}A modification might be involved in tomato anther development under MLT stress. Among the altered transcription, 65% were downregulated. Similarly, in rice, knockouts of the methylase genes, *OsFIP* or *OsMTA2*, dramatically reduced m^{6}A levels and resulted in microspore degeneration at the uninucleate stage and in a male sterility phenotype (Zhang et al., 2019). These results support the speculation that m^{6}A methylation participates in male developmental regulation. However, our findings firstly reveal that m^{6}A methylation may be involved in low-temperature stress responses during anther development.

Growing evidence suggests that diverse abiotic stresses can change transcript m^{6}A methylation levels (Hu et al., 2019; Huong et al., 2020; Liu et al., 2020). Moreover, m^{6}A levels usually negatively regulate gene expression by influencing mRNA stability and the subsequent protein synthesis process (Shen et al., 2016; Duan et al., 2017; Zhao et al., 2017). By combining MeRIP-seq and RNA-seq analyses on NT and MLT anthers at the tetrad stage, we revealed that, at the transcriptome-wide level, transcript m^{6}A enrichment was usually inversely correlated with gene expression levels under MLT stress (**Figure 5B**). Some of these transcripts are involved in lipid metabolism, ATPase activity, and ATP-binding processes and these pathways have been well

characterized in plant male organ reproduction (**Figures 5C**, **6**; Lucca and León, 2012; Shi et al., 2015; Zhao et al., 2016). These results suggest that changes in m^{6}A methylation under MLT stress may affect target mRNA abundance, ultimately leading to pollen abortion. Several studies revealed abiotic stress causes transcriptome-wide redistribution of the m^{6}A modification. For example, heat shock increases m^{6}A enrichment at 5′-UTRs, and it mainly mapped to regions surrounding stop codons in NT condition. The m^{6}A modification at 5′-UTR promotes mRNA cap-independent translation initiation (Meyer et al., 2015). It is noteworthy that in this study, the distribution of m^{6}A peaks in transcripts from tomato anthers were all enriched in stop codons and 3′-UTRs under NT and MLT conditions (**Figure 4**), suggesting that low temperature stress affects m6A levels of transcripts but not the m6A distribution regions on the transcripts.

ABA plays vital roles in developmental processes and mediates plant response to abiotic stress. Evidence supports that ABA signaling pathways involved in abiotic stress response differ between reproductive organs and vegetative tissues (Sharma and Nayyar, 2016). During vegetative development, increased ABA levels improve abiotic stress tolerance; exogenous ABA application enhances cold tolerance in citrus leaves, and up-regulation of ABA biosynthesis genes enhances drought resistance in petunia seedlings (Melgoza et al., 2014; Estrada-Melo et al., 2015). Previous studies revealed a negative relationship between ABA content in anthers and pollen fertility under cold stress (Sharma and Nayyar, 2016). Consistently, in our study, ABA levels were significantly increased in MLT anthers at the tetrad stage (**Figure 7B**). *SlPYLs* and *SlPP2Cs* gene families encode ABA signal transduction core components during tomato development and abiotic stress. ABA perception by the PYLs proteins suppressed PP2C-meidated dephosphorylation of the SnRKs and allows their activate ABA responsive genes (Raghavendra et al., 2017). Here, expression levels of ABA signal transduction core genes, *SlPYL4* was significantly downregulated and *SlPP2C1* and *SlPP2C3* were significantly upregulated by MLT stress (**Supplementary Figure 6**), suggesting that the ABA signal pathway regulates anther development under MLT stress. Numerous studies revealed that ABA accumulation in rice anthers under cold stress suppresses the expression of the tapetum-specific gene *OsINV4* and of sugar transport genes. It disturbs tapetum PCD, resulting in pollen abortion (Oliver et al., 2005; Ji et al., 2011). Previous studies have also reported that tomato anther carbohydrate levels were alerted responding to temperature stress (Pressman et al., 2002; Firon et al., 2006). Surprisingly, nearly all *SlCWINs* genes in our study were significantly downregulated under MLT stress. *SlCWIN7*, the rice homolog to *OsINV4*, was dramatically downregulated at both tetrad and early uninucleate stages (**Figure 7C**), which might distort anther sugar metabolism and, consequently, lead to pollen sterility in tomato (**Figure 1**).

Baron et al. (2012) reported that enhancing ABA biosynthetic gene expression or decreasing ABA transport gene expression leads to increased ABA content in *Arabidopsis* inflorescence meristems under cold stress (Baron et al., 2012). Moreover, the tomato gene, *SlABCG31*, may participate in ABA transport and is predominantly expressed in anthers (**Figure 7A**); however, it was significantly downregulated at the tetrad stage under MLT stress. In addition, we found an enhancement in its m^{6}A methylation under MLT stress, suggesting that the decrease in *SlABCG31* transcript levels might result from its high m^{6}A methylation (**Figure 6**). Down-regulation of *SlABCG31* results in high ABA content in tomato anthers and disturbs sugar metabolism, which may be associated with pollen abortion (**Figure 8**). Furthermore. in *Arabidopsis AtABCG31* also participates in the accumulation of sterol for pollen coat formation, and the *Atatabcg31* mutant displays collapsed or sticking pollen grains (Choi et al., 2014). Interestingly, in our study, tomato MLT-treated pollen grains also displayed severe collapse and aggregation phenotypes, with differences in pollen coat sculptured surfaces compared to that in NT conditions, which resembles the *Atatabcg31* mutant (**Figure 1B**).

In conclusion, this study reveals a unique property of anther growth under MLT stress. MLT-induced pollen abortion is the consequence of disrupted microgametogenesis, tapetum degeneration, and pollen wall formation, which may be related to differential m^{6}A modification of transcripts (**Figure 8**). m^{6}A modification is associated with ABA transport in anthers or sterol accumulation for pollen wall formation by targeting the ATP-binding cassette G gene, *SlABCG31*. Considering that pollen development and m^{6}A methylation are complex processes, the molecular mechanisms behind m^{6}A methylation function in pollen development under temperature stress should be further studied.

DATA AVAILABILITY STATEMENT

The datasets presented in this study can be found in online repositories. The names of the repository/repositories and accession number(s) can be found in the article/ **Supplementary Material**.

AUTHOR CONTRIBUTIONS

GL and DY conceived the study. DY, HX, YL, and ML carried out the experiment. DY, XX, and MA performed the data analysis. DY and GL wrote the article. All authors discussed and commented on the final manuscript.

FUNDING

This work was supported by grants from the National Key Research and Development Program of China (2018YFD1000800), the National Natural Science Foundation of China (31772316 and 31471878), and the Natural Science Foundation of Zhejiang Province, China (LZ17C150002).

ACKNOWLEDGMENTS

We would like to thank Jingquan Yu (Zhejiang University, China) for support during hormone analysis.

SUPPLEMENTARY MATERIAL

The Supplementary Material for this article can be found online at: https://www.frontiersin.org/articles/10.3389/fpls.2021.687826/full#supplementary-material

Supplementary Figure 1 | Schematic illustration of moderate low temperature (MLT, 10°C) stress and TUNEL assay of tapetum program cell death (PCD) in anthers. **(A)** Schematic illustration of moderate low temperature (MLT, 10°C) stress setup and sampling scheme in cultivar "Micro-Tom." Six-week-old flowering tomato plants were exposed to MLT-stress for 6 days then moved back to normal temperature for recovery growth. The sample harvested immediately after 6 days MLT-stress were named MLT and harvested from marked tetrad anthers after recovery were named MLTR. Green and yellow lines indicate MLT-stress and NT regimes, respectively. **(B)** TUNEL assay of tapetum program cell death (PCD) in anther at tetrad, early and late uninucleate and binucleate stages under NT and MLTR conditions. The red signal is propidium iodide staining, and the green fluorescence is TUNEL positive signal. The white arrows indicate TUNEL positive signals. Scale bars = 50 μm.

Supplementary Figure 2 | The expression profiles of writers, erasers and readers. **(A)** The relative levels of m^{6}A in total RNA of anthers at different stages in NT condition. The levels of m^{6}A in total RNA in stage-I is set to 1. I, anther at microspore mother cell stage; II, anther at tetrad stage; III, anther at early uninucleate stage; IV, anther at late uninucleate stage; V, anther at binucleate stage; VI, anther at mature pollen stage. Each value is the mean ± SD (n = at least 3 biological replicates with 15 plants each). **(B)** The expression of writers *in silico* data available from the tomato eFP Browser. RPKM, Reads Per Kilobase per Million mapped reads. **(C)** The expression of eraser *in silico* data available from the tomato eFP Browser. **(D)** The expression of readers *in silico* data available from the tomato eFP Browser.

Supplementary Figure 3 | m^{6}A-seq data analysis. **(A)** m^{6}A-seq reads and mapping status with tomato genome in anther at stage-II under NT and MLT conditions. **(B)** Pearson correlation analysis of m^{6}A-seq. R^2 means the square of Pearson correlation. **(C)** The number of overlapped m^{6}A peak-containing genes identified in three biological replicates in anthers under NT and MLT conditions, respectively. **(D)** The number of overlapped m^{6}A peak-containing genes between NT and MLT anthers.

Supplementary Figure 4 | KEGG analysis of different enrichment peaks related genes between NT and MLT anthers at stage-II.

Supplementary Figure 5 | Comparative analysis of genes expression levels in NT and MLT conditions. **(A,B)** The expression levels of *SlPYLs* and *SlPP2Cs* genes in anther at stage-II under NT and MLT conditions. The levels of genes expression normalized to *Ubiquitin* expression are shown relative to the expression of *SlPYL2* or *SlPP2C1* in NT condition set to 1. Each value is the mean ± SD (n = at least three biological replicates with 15 plants each). $^*P < 0.05$; $^{**}P < 0.01$ (two-tailed Student's t- test).

Supplementary Figure 6 | Alignment of AtABCG31 and SlABCG31 full-length proteins. The multiple sequence alignment was generated using Clustal Omega. Same amino acid residues were shading with black color.

Supplementary Table 1 | Primer sequences used in this study.

Supplementary Table 2 | Differential m^{6}A peaks and related transcripts between NT and MLT anthers.

REFERENCES

Al Mamun, E., Cantrill, L. C., Overall, R. L., and Sutton, B. G. (2010). Mechanism of low-temperature-induced pollen failure in rice. *Cell Biol. Int.* 34, 469–476. doi: 10.1042/CBI20090417

Alexander, M. P. (1969). Differential staining of aborted and nonaborted pollen. *Stain Technol.* 44, 117–122. doi: 10.3109/10520296909063335

Ariizumi, T., and Toriyama, K. (2011). Genetic regulation of sporopollenin synthesis and pollen exine development. *Annu. Rev. Plant Biol.* 62, 437–460. doi: 10.1146/annurev-arplant-042809-112312

Baron, K. N., Schroeder, D. F., and Stasolla, C. (2012). Transcriptional response of abscisic acid (ABA) metabolism and transport to cold and heat stress applied at the reproductive stage of development in *Arabidopsis thaliana*. *Plant Sci.* 188–189, 48–59. doi: 10.1016/j.plantsci.2012.03.001

Barrero-Gil, J., and Salinas, J. (2013). Post-translational regulation of cold acclimation response. *Plant Sci.* 205–206, 48–54. doi: 10.1016/j.plantsci.2013.01.008

Begcy, K., Nosenko, T., Zhou, L. Z., Fragner, L., Weckwerth, W., and Dresselhaus, T. (2019). Male sterility in maize after transient heat stress during the tetrad stage of pollen development. *Plant Physiol.* 181, 683–700. doi: 10.1104/pp.19.00707

Bodi, Z., Zhong, S., Mehra, S., Song, J., Graham, N., Li, H., et al. (2012). Adenosine methylation in *Arabidopsis* mRNA is associated with the 3'- end and reduced levels cause developmental defects. *Front. Plant Sci.* 3:48. doi: 10.3389/fpls.2012.00048

Borghi, L., Kang, J., Ko, D., Lee, Y., and Martinoia, E. (2015). The role of ABCG-type ABC transporters in phytohormone transport. *Biochem. Soc. Trans.* 43, 924–930. doi: 10.1042/BST20150106

Brukhin, V., Hernould, M., Gonzalez, N., Chevalier, C., and Mouras, A. (2003). Flower development schedule in tomato *Lycopersicon esculentum* cv. sweet cherry[J]. *Sex. Plant Reprod.* 15, 311–320. doi: 10.1007/s00497-003-0167-7

Chen, L., Yang, D., Zhang, Y., Wu, L., Zhang, Y., Ye, L., et al. (2018). Evidence for a specific and critical role of mitogen-activated protein kinase 20 in uni-to-binucleate transition of microgametogenesis in tomato. *New Phytol.* 219, 176–194. doi: 10.1111/nph.15150

Choi, H., Ohyama, K., Kim, Y. Y., Jin, J. Y., Lee, S. B., Yamaoka, Y., et al. (2014). The role of *Arabidopsis* ABCG9 and ABCG31 ATP binding cassette transporters in pollen fitness and the deposition of steryl glycosides on the pollen coat. *Plant Cell* 26, 310–324. doi: 10.1105/tpc.113.118935

Criddle, R., Smith, B., and Hansen, L. (1997). A respiration-based description of plant growth rate responses to temperature. *Planta* 201, 441–445. doi: 10.1007/s004250050087

De Storme, N., and Geelen, D. (2014). The impact of environmental stress on male reproductive development in plants: biological processes and molecular mechanisms. *Plant Cell Environ.* 37, 1–18. doi: 10.1111/pce.12142

Dominissini, D., Moshitch-Moshkovitz, S., Salmon-Divon, M., Amariglio, N., and Rechavi, G. (2013). Transcriptome-wide mapping of N(6)-methyladenosine by m6A-seq based on immunocapturing and massively parallel sequencing. *Nat. Protocols* 8, 176–189. doi: 10.1038/nprot.2012.148

Du, H., Zhao, Y., He, J., Zhang, Y., Xi, H., and Liu, M. (2016). YTHDF2 destabilizes m6A-containing RNA through direct recruitment of the CCR4-NOT deadenylase complex. *Nat. Commun.* 7, 1–11. doi: 10.1038/ncomms12626

Duan, H. C., Wei, L. H., Zhang, C., Wang, Y., Chen, L., Lu, Z., et al. (2017). ALKBH10B is an RNA N6-methyladenosine demethylase affecting *Arabidopsis* floral transition. *Plant Cell* 29, 2995–3011. doi: 10.1105/tpc.16.00912

Estrada-Melo, A. C., Ma, C., Reid, M. S., and Jiang, C. Z. (2015). Overexpression of an ABA biosynthesis gene using a stress-inducible promoter enhances drought resistance in petunia. *Hortic. Res.* 2, 1–9. doi: 10.1038/hortres.2015.13

Fang, X., Fu, H. F., Gong, Z. H., and Chai, W. G. (2016). Involvement of a universal amino acid synthesis impediment in cytoplasmic male sterility in pepper. *Sci. Rep.* 6, 1–15. doi: 10.1038/srep23357

Firon, N., Shaked, R., Peet, M. M., Pharr, D. M., Zamski, E., Rosenfeld, K., et al. (2006). Pollen grains of heat tolerant tomato cultivars retain higher carbohydrate concentration under heat stress conditions. *Sci. Hortic.* 109, 212–217. doi: 10.1016/j.scienta.2006.03.007

Guerra, D., Crosatti, C., Khoshro, H. H., Mastrangelo, A. M., Mica, E., and Mazzucotelli, E. (2015). Post-transcriptional and post-translational regulations of drought and heat response in plants: a spider's web of mechanisms. *Front. Plant Sci.* 6:57. doi: 10.3389/fpls.2015.00057

Helt, G. A., Nicol, J. W., Erwin, E., Blossom, E., Blanchard, S. G., Chervitz, S. A., et al. (2009). Genoviz software development kit: java tool kit for building

genomics visualization applications. *BMC Bioinformatics* 10:266. doi: 10.1186/1471-2105-10-266

Hu, J., Manduzio, S., and Kang, H. (2019). Epitranscriptomic RNA methylation in plant development and abiotic stress responses. *Front. Plant Sci.* 10:500. doi: 10.3389/fpls.2019.00500

Huong, T. T., Ngoc, L. N. T., and Kang, H. (2020). Functional characterization of a putative RNA demethylase alkbh6 in *Arabidopsis* growth and abiotic stress responses. *Int. J. Mol. Sci.* 21, 1–14. doi: 10.3390/ijms21186707

Ji, X., Dong, B., Shiran, B., Talbot, M. J., Edlington, J. E., Hughes, T., et al. (2011). Control of abscisic acid catabolism and abscisic acid homeostasis is important for reproductive stage stress tolerance in cereals. *Plant physiol.* 156, 647–662. doi: 10.1104/pp.111.176164

Kang, J., Yim, S., Choi, H., Kim, A., Lee, K. P., Lopez-Molina, L., et al. (2015). Abscisic acid transporters cooperate to control seed germination. *Nat. Commun.* 6, 1–10. doi: 10.1038/ncomms9113

Kim, S. Y., Hong, C. B., and Lee, I. (2001). Heat shock stress causes stage-specific male sterility in *Arabidopsis thaliana*. *J. Plant Res.* 114, 301–307. doi: 10.1007/PL00013991

Kiran, A., Kumar, S., Nayyar, H., and Sharma, K. D. (2019). Low temperature-induced aberrations in male and female reproductive organ development cause flower abortion in chickpea. *Plant Cell Environ.* 42, 2075–2089. doi: 10.1111/pce.13536

Kramer, M. C., Janssen, K. A., Palos, K., Nelson, A. D. L., Vandivier, L. E., Garcia, B. A., et al. (2020). N6-methyladenosine and RNA secondary structure affect transcript stability and protein abundance during systemic salt stress in *Arabidopsis*. *Plant Direct* 4, 1–22. doi: 10.1002/pld3.239

Ku, S., Yoon, H., Suh, H. S., and Chung, Y. Y. (2003). Male-sterility of thermosensitive genic male-sterile rice is associated with premature programmed cell death of the tapetum. *Planta* 217, 559–565. doi: 10.1007/s00425-003-1030-7

Liu, B., Mo, W. J., Zhang, D., De Storme, N., and Geelen, D. (2019). Cold influences male reproductive development in plants: a hazard to fertility, but a window for evolution. *Plant Cell Physiol.* 60, 7–18. doi: 10.1093/pcp/pcy209

Liu, G., Wang, J., and Hou, X. (2020). Transcriptome-wide N6-methyladenosine (m6A) methylome profiling of heat stress in pak-choi (*Brassica rapa* ssp. chinensis). *Plants* 9, 1–12. doi: 10.3390/plants9091080

Liu, N., Dai, Q., Zheng, G., He, C., Parisien, M., and Pan, T. (2015). N(6)-methyladenosine-dependent RNA structural switches regulate RNA-protein interactions. *Nature* 518, 560–564. doi: 10.1038/nature14234

Livak, K. J., and Schmittgen, T. D. (2001). Analysis of relative gene expression data using real-time quantitative PCR and the 2-ΔΔCT method. *Methods* 25, 402–408. doi: 10.1006/meth.2001.1262

Lucca, N., and León, G. (2012). Arabidopsis ACA7, encoding a putative auto-regulated Ca2+-ATPase, is required for normal pollen development. *Plant Cell Rep.* 31, 651–659. doi: 10.1007/s00299-011-1182-z

Luo, G. Z., Macqueen, A., Zheng, G., Duan, H., Dore, L. C., Lu, Z., et al. (2014). Unique features of the m6A methylome in *Arabidopsis thaliana*. *Nat. Commun.* 5, 1–8. doi: 10.1038/ncomms6630

Ma, H. (2005). Molecular genetic analyses of microsporogenesis and microgametogenesis in flowering plants. *Annu. Rev. Plant Biol.* 56, 393–434. doi: 10.1146/annurev.arplant.55.031903.141717

Melgoza, F. J., Kusakabe, A., Nelson, S. D., and Melgar, J. C. (2014). Exogenous applications of abscisic acid increase freeze tolerance in citrus trees. *Int. J. Fruit Sci.* 14, 376–387. doi: 10.1080/15538362.2014.899138

Meng, J., Cui, X., Liu, H., Zhang, L., Zhang, S., and Rao, M. K. (2013). "Unveiling the dynamics in RNA epigenetic regulations," in *IEEE International Conference on Bioinformatics and Biomedicine*, Shanghai, 139–144.

Meyer, K. D., Patil, D. P., Zhou, J., Zinoviev, A., Skabkin, M. A., Elemento, O., et al. (2015). 5' UTR m6A promotes cap-independent translation. *Cell* 163, 999–1010. doi: 10.1016/j.cell.2015.10.012

Min, L., Li, Y., Hu, Q., Zhu, L., Gao, W., Wu, Y., et al. (2014). Sugar and auxin signaling pathways respond to high-temperature stress during anther development as revealed by transcript profiling analysis in cotton. *Plant Physiol.* 164, 1293–1308. doi: 10.1104/pp.113.232314

Müller, F., and Rieu, I. (2016). Acclimation to high temperature during pollen development. *Plant Reprod.* 29, 107–118. doi: 10.1007/s00497-016-0282-x

Oda, S., Kaneko, F., Yano, K., Fujioka, T., Masuko, H., Park, J. I., et al. (2010). Morphological and gene expression analysis under cool temperature conditions in rice anther development. *Genes Genet. Syst.* 85, 107–120. doi: 10.1266/ggs.85.107

Oliver, S. N., Dennis, E. S., and Dolferus, R. (2007). ABA regulates apoplastic sugar transport and is a potential signal for cold-induced pollen sterility in rice. *Plant Cell Physiol.* 48, 1319–1330. doi: 10.1093/pcp/pcm100

Oliver, S. N., Van Dongen, J. T., Alfred, S. C., Mamun, E. A., Zhao, X., Saini, H. S., et al. (2005). Cold-induced repression of the rice anther-specific cell wall invertase gene OSINV4 is correlated with sucrose accumulation and pollen sterility. *Plant Cell Environ.* 28, 1534–1551. doi: 10.1111/j.1365-3040.2005.01390.x

Omidi, M., Siahpoosh, M. R., Mamghani, R., and Modarresi, M. (2014). The influence of terminal heat stress on meiosis abnormalities in pollen mother cells of wheat. *Cytologia* 79, 49–58. doi: 10.1508/cytologia.79.49

Pacini, E., and Dolferus, R. (2019). Pollen developmental arrest: maintaining pollen fertility in a world with a changing climate. *Front. Plant Sci.* 10:679. doi: 10.3389/fpls.2019.00679

Paupière, M. J., Müller, F., Li, H., Rieu, I., Tikunov, Y. M., Visser, R. G. F., et al. (2017). Untargeted metabolomic analysis of tomato pollen development and heat stress response. *Plant Reprod.* 30, 81–94. doi: 10.1007/s00497-017-0301-6

Peng, Z., Cheng, L., He, Y. J., Wang, J., Guan, X., Liu, S., et al. (2013). Cytological study on microsporogenesis of Solanum lycopersicum var. micro-tom under high temperature stress. *Acta Ecol. Sin.* 33, 2084–2092. doi: 10.5846/stxb201112261972

Pressman, E., Peet, M. M., and Pharr, D. M. (2002). The effect of heat stress on tomato pollen characteristics is associated with changes in carbohydrate concentration in the developing anthers. *Ann. Bot.* 90, 631–636. doi: 10.1093/aob/mcf240

Raghavendra, A. S., Gonugunta, V. K., Christmann, A., and Grill, E. (2017). ABA perception and signalling. *Trends Plant Sci.* 15, 395–401. doi: 10.1016/j.tplants.2010.04.006

Roundtree, I. A., Luo, G. Z., Zhang, Z., Wang, X., Zhou, T., Cui, Y., et al. (2017). YTHDC1 mediates nuclear export of N6-methyladenosine methylated mRNAs. *eLife* 6, 1–28. doi: 10.7554/eLife.31311

Růžička, K., Zhang, M., Campilho, A., Bodi, Z., Kashif, M., Saleh, M., et al. (2017). Identification of factors required for m6A mRNA methylation in *Arabidopsis* reveals a role for the conserved E3 ubiquitin ligase HAKAI. *New Phytol.* 215, 157–172. doi: 10.1111/nph.14586

Sharma, K. D., and Nayyar, H. (2016). Regulatory networks in pollen development under cold stress. *Front. Plant Sci.* 7:402. doi: 10.3389/fpls.2016.00402

Shen, L., Liang, Z., Gu, X., Chen, Y., Teo, Z. W., Hou, X., et al. (2016). N(6)-Methyladenosine RNA modification regulates shoot stem cell fate in *Arabidopsis*. *Dev. Cell* 38, 186–200. doi: 10.1016/j.devcel.2016.06.008

Shi, J., Cui, M., Yang, L., Kim, Y. J., and Zhang, D. (2015). Genetic and biochemical mechanisms of pollen wall development. *Trends Plant Sci.* 20, 741–753. doi: 10.1016/j.tplants.2015.07.010

Sun, L., Sui, X., Lucas, W. J., Li, Y., Feng, S., Ma, S., et al. (2019). Down-regulation of the sucrose transporter cssut1 causes male sterility by altering carbohydrate supply. *Plant Physiol.* 180, 986–997. doi: 10.1104/pp.19.00317

Tomato Genome Consortium (2012). The tomato genome sequence provides insights into fleshy fruit evolution. *Nature* 485, 635–641. doi: 10.1038/nature11119

Vespa, L., Vachon, G., Berger, F., Perazza, D., Faure, J. D., and Herzog, M. (2004). The immunophilin-interacting protein AtFIP37 from *Arabidopsis* is essential for plant development and is involved in trichome endoreduplication. *Plant Physiol.* 134, 1283–1292. doi: 10.1104/pp.103.028050

Wang, M., Hoekstra, S., van Bergen, S., Lamers, G. E., Oppedijk, B. J., van der Heijden, M. W., et al. (1999). Apoptosis in developing anthers and the role of ABA in this process during androgenesis in *Hordeum vulgare* L. *Plant Mol. Biol.* 39, 489–501. doi: 10.1023/a:1006198431596

Wang, X., Lu, Z., Gomez, A., Hon, G. C., Yue, Y. N., Han, D. L., et al. (2014). N6-methyladenosine-dependent regulation of messenger RNA stability. *Nature* 505, 117–120. doi: 10.1038/nature12730

Xiao, W., Adhikari, S., Dahal, U., Chen, Y. S., Hao, Y. J., Sun, B. F., et al. (2016). Nuclear m6A reader YTHDC1 regulates mRNA splicing. *Mol. Cell* 61, 507–519. doi: 10.1016/j.molcel.2016.01.012

Yang, S., Sweetman, J. P., Amirsadeghi, S., Barghchi, M., Huttly, A. K., Chung, W. I., et al. (2001). Novel anther-specific myb genes from tobacco as putative regulators of phenylalanine ammonia-lyase expression. *Plant Physiol.* 126, 1738–1753. doi: 10.1104/pp.126.4.1738

Yue, H., Nie, X., Yan, Z., and Weining, S. (2019). N6-methyladenosine regulatory machinery in plants: composition, function and evolution. *Plant Biotechnol. J.* 17, 1194–1208. doi: 10.1111/pbi.13149

Yue, Y., Liu, J., and He, C. (2015). RNA N6-methyladenosine methylation in post-transcriptional gene expression regulation. *Genes Dev.* 29, 1343–1355. doi: 10.1101/gad.262766.115

Zhang, F., Zhang, Y. C., Liao, J. Y., Yu, Y., Zhou, Y. F., Feng, Y. Z., et al. (2019). The subunit of RNA n6-methyladenosine methyltransferase OsFIP regulates early degeneration of microspores in rice. *PLoS Genet.* 15:e1008120. doi: 10.1371/journal.pgen.1008120

Zhang, Y., Liu, T., Meyer, C. A., Eeckhoute, J., Johnson, D. S., Bernstein, B. E., et al. (2008). Model-based analysis of ChIP-Seq (MACS). *Genome Biology* 9, R137. doi: 10.1186/gb-2008-9-9-r137

Zhao, B. S., Roundtree, I. A., and He, C. (2017). Post-transcriptional gene regulation by mRNA modifications. *Nat. Rev. Mol. Cell Biol.* 18, 31–42. doi: 10.1038/nrm.2016.132

Zhao, G., Shi, J., Liang, W., and Zhang, D. (2016). ATP binding cassette G transporters and plant male reproduction. *Plant Signal. Behav.* 11, 1–6. doi: 10.1080/15592324.2015.1136764

Zhong, S., Li, H., Bodi, Z., Button, J., Vespa, L., Herzog, M., et al. (2008). MTA is an *Arabidopsis* messenger RNA adenosine methylase and interacts with a homolog of a sex-specific splicing factor. *Plant Cell* 20, 1278–1288. doi: 10.1105/tpc.108.058883

Zhou, J., Wan, J., Gao, X., Zhang, X., Jaffrey, S. R., and Qian, S. B. (2015). Dynamic m6A mRNA methylation directs translational control of heat shock response. *Nature* 526, 591–594. doi: 10.1038/nature15377

Zhou, L., Tian, S., and Qin, G. (2019). RNA methylomes reveal the m6A-mediated regulation of DNA demethylase gene SlDML2 in tomato fruit ripening. *Genome Biol.* 20, 1–23. doi: 10.1186/s13059-019-1771-7

Zhu, J. K. (2016). Abiotic stress signaling and responses in plants. *Cell* 167, 313–324. doi: 10.1016/j.cell.2016.08.029

Conflict of Interest: The authors declare that the research was conducted in the absence of any commercial or financial relationships that could be construed as a potential conflict of interest.

frontiers in Plant Science

ORIGINAL RESEARCH
published: 22 October 2021
doi: 10.3389/fpls.2021.758976

Phenotypic Characteristics and Transcriptome of Cucumber Male Flower Development Under Heat Stress

*Lin Chen[1,2], Maomao Yun[1,2], Zhenqiang Cao[1,2], Zhaojun Liang[1,2], Wenrui Liu[1,2], Min Wang[1,2], Jinqiang Yan[1,2], Songguang Yang[1,2], Xiaoming He[1,2], Biao Jiang[1,2], Qingwu Peng[1,2] and Yu'e Lin[1,2]**

[1] Vegetable Research Institute, Guangdong Academy of Agricultural Sciences, Guangzhou, China, [2] Guangdong Key Laboratory for New Technology Research of Vegetables, Guangzhou, China

OPEN ACCESS

Edited by:
Kevin Begcy,
University of Florida, United States

Reviewed by:
Kazuo Nakashima,
Japan International Research Center for Agricultural Sciences (JIRCAS), Japan
Rong Zhou,
Aarhus University, Denmark

***Correspondence:**
Yu'e Lin
cucumber200@163.com

Specialty section:
This article was submitted to Plant Abiotic Stress, a section of the journal Frontiers in Plant Science

Received: 15 August 2021
Accepted: 13 September 2021
Published: 22 October 2021

Citation:
Chen L, Yun M, Cao Z, Liang Z, Liu W, Wang M, Yan J, Yang S, He X, Jiang B, Peng Q and Lin Y (2021) Phenotypic Characteristics and Transcriptome of Cucumber Male Flower Development Under Heat Stress. Front. Plant Sci. 12:758976. doi: 10.3389/fpls.2021.758976

Cucumber (*Cucumis sativus* L.) is an important vegetable crop, which is thermophilic not heat resistant. High-temperature stress always results in sterility at reproductive stage. In the present study, we evaluate the male flower developmental changes under normal (CK) and heat stress (HS) condition. After HS, the activities of peroxidase (POD) and superoxide dismutase (SOD) and the contents of malondialdehyde (MDA) were increased. In addition, the pollen fertility was significantly decreased; and abnormal tapetum and microspore were observed by paraffin section. Transcriptome analysis results presented that total of 5828 differentially expressed genes (DEGs) were identified after HS. Among these DEGs, 20 DEGs were found at four stages, including DNA binding transcription factor, glycosyltransferase, and wound-responsive family protein. The gene ontology term of carbohydrate metabolic process was significantly enriched in all anther stages, and many saccharides and starch synthase-related genes, such as invertase, sucrose synthase, and starch branching enzyme, were significantly different expressed in HS compared with CK. Furthermore, co-expression network analysis showed a module (midnightblue) strongly consistent with HS, and two hub genes (*CsaV3_6G004180* and *CsaV3_5G034860*) were found with a high degree of connectivity to other genes. Our results provide comprehensive understandings on male flower development in cucumber under HS.

Keywords: cucumber, heat stress, pollen fertility, carbohydrate metabolism, RNA-seq

INTRODUCTION

In recent years, global warming has resulted in climate changes, including extreme high temperatures, and these changes have caused devastating damage to crop production (Ray et al., 2015). High-temperature stress mainly affects plant seed germination, plant growth, photosynthesis, respiration, water relationship, membrane stability, crop yield, etc.

(Kotak et al., 2007; Sehgal et al., 2017; Janni et al., 2020). Nevertheless, plants have developed complex and diverse physiological changes to cope with HS, and many important factors involved in these physiological changes (Alsamir et al., 2021). For example, heat shock proteins, which function as molecular chaperones, will be synthesized in a short time to enhance the heat tolerance of plants and maintain the normal vitality of cells. In addition, antioxidant enzyme systems, including peroxidase (POD), catalase, and superoxide dismutase (SOD), are believed to be necessary for the detoxification of reactive oxygen species (ROS) overproduction under high-temperature stress, which is an important role for maintenance of cell membrane stability (Bita and Gerats, 2013).

In all the processes of plant growth and development, the plant reproductive development stage has the strictest requirements on temperature (Hedhly et al., 2009). The male flower is more sensitive to temperature than female flower (Peet et al., 1998). The damages caused by high temperature to male flowers include pollen abortion, reduce in pollen viability, keep of pollen in anthers and decline pollen germination, degradation of tapetum, formation of pollen wall, destruction of the plasma reticulum in the ribosome, abnormal shape of the vascular bundle cells, the incomplete degradation of the drug barrier, obstruction of the thickening of the inner wall, blocking of the division of anther cells, and so on (Porch and Jahn, 2001; Harsant et al., 2013; Rieu et al., 2017; Shi et al., 2018). In addition, high temperature also changes the carbohydrate metabolism of male flower, for instance, reducing starch accumulation during pollen development, and ultimately leading to pollen abortion (Jain et al., 2010; Cao et al., 2015).

Cucumber, which is one of the most important vegetable crops, is widely cultivated all over the world. The optimum growth temperature of cucumber is between 25 and 30℃, and heat damage will occur if the temperature exceeds 35℃. The cucumbers often encounter high-temperature stress in open-field cultivation or greenhouse cultivation on account of high temperatures in summer in China, which causes the physiological metabolism disorder, the inhibition of growth, abnormal fruit shape and quality, and yield loss (Meng et al., 2004; Sun et al., 2018). A growing number of studies have been reported to heat resistance of cucumber (Li et al., 2016; He et al., 2020; Wang et al., 2020). Ding et al. (2016) reported that exogenous glutathione can enhance cucumber seedling heat tolerance through regulation of antioxidant, osmolytes, and photosynthesis systems. A lot of work has been done on quantitative trait locus (QTL)/gene mapping of heat tolerance in cucumber, such as qHT3.1, qHT3.2, qHT3.3, qHT4.1, qHT4.2, and qHT6.1 (Dong et al., 2020). Liu et al. (2021) identified a heat tolerance QTL named qHT1.1 on chromosome 1 by recombinant inbred lines (RILs). Yu et al. (2018) reported that *CsCaM3* may improve heat tolerance and prevent photosynthetic and oxidative system by regulating the high-temperature responsive genes in cucumber. The male and female flowers of cucumber are most sensitive to high temperature, and the sensitivity of male flower to high temperature is higher than female flower (Miao and Li, 2001). The cucumber pollen showed partial pollen sterility and low pollen vigor when cucumber male flowers are subjected to high temperatures. Furthermore, the meiosis and single microspore stage are the most sensitive to high temperature (Miao, 2000). In addition, the putrescine, spermine, spermidine, and proline content were kept at higher levels in heat resistant varieties compared with heat-sensitive varieties (Miao and Cao, 2002).

Recently, the RNA sequencing (RNA-seq) and microarray technology are powerful and cost-effective tools to investigate the differently crucial genes involved in plant growth and development, abiotic stresses, and biotic stresses (Zhou and Pawlowski, 2014; Fu et al., 2017; Li et al., 2021). The RNA-seq was widely used to understand genes expression involving in abiotic stresses in plant, such as Arabidopsis (Huang et al., 2019), rice (Jin et al., 2013), maize (Guo et al., 2020), tomato (Zhou et al., 2019), wheat (Wang et al., 2019), and eggplant (Zhang et al., 2019). Furthermore, RNA-seq has also been widely applied to investigate the differently expressed genes in cucumber. For instance, transcriptome technique was applied in cucumber to study the floral sex determination (Guo et al., 2010; Wu et al., 2010), fruit curving (Li et al., 2020), fruit spine (Xie et al., 2018), salt stress (Jiang et al., 2020), and disease resistant (Yang et al., 2020). He et al. (2020) reported that cucumber respond to high-temperature stress by full transcriptomic analysis and integrated the potential ceRNA function of lncRNAs/circRNAs for the first time in response to high-temperature stress. However, until now, the differently expressed genes still lack in cucumber male flower after heat stress (HS).

Based on the hypothesis that male flower development is affected in cucumbers under HS, we used physiological and cellular observation and RNA-seq to study the change of male flower. In this study, we thus primarily aimed to evaluate morphological, physiological, and cellular changes in male flower development under normal-temperature and high-temperature stress. It is a comprehensive exploration of the cucumber male flower development under high-temperature stress. In addition, we detected differentially expressed genes (DEGs) in anthers between normal-temperature and high-temperature stress at four development stages by using RNA-seq, which offered insights into the molecular mechanism underlying normal- and high-temperature stress condition. It is a systematic and comprehensive exploration of the cucumber male flower development under high-temperature stress.

MATERIALS AND METHODS

Plant Material and Growth Conditions

A northern type of China cucumber material, B80, which is widely used for breeding in our group, was chosen for this study. Cucumber plants were grown under normal condition until four true leaves. Then, they were transferred to phytotron in normal (CK, 12 h light/12 h dark, 12 h 28℃/12 h 25℃, 70% relative humidity) and HS (12 h light/12 h dark, 12 h 38℃/12 h 30℃, 70% relative humidity) condition, and these states were remained until the end of sampling and investigation. Male flowers were divided into four classes based on male flowers length: 0–3, 3–6, 6–9, and >9 mm, representing S1, S2, S3, and S4, respectively. The anthers were dissected from male flowers at four stages and were collected for three biological replicates.

Determination of Peroxidase and Superoxide Dismutase Activity and Malondialdehyde Contents in Anther

The anther of CK and HS were collected according to S1, S2, S3, and S4. The activities of POD and SOD and the contents of malondialdehyde (MDA) were measured using kits (Suzhou Keming Bioengineer Company, China). Three biological replicates were performed for all measurements.

Cytological Observation

The male flowers were harvested between CK and HS, and fixed in Carnoy's solution (ethanol: acetic acid = 3:1) for 24 h, and they were kept in 70% ethanol after washing three times. The anther was removed from the inflorescences and placed in 1% iodine-potassium (I2-KI), and the normal and abnormal pollens were observed on a microscope (Motic BA200).

The anthers at different development stages were harvested and kept in formaldehyde-acetic acid-ethanol (FAA) (70% ethanol: acetic acid: methanol = 89:6:5), and then embedded in paraffin after dehydration by a series of ethanol concentration according to the protocol of manufacturers. The cross sections of 2 to 5 μm thickness were cut with the microtome (Leica RM2235). The cross sections were stained in 0.05% toluidine blue (m/v) and covered with a slide cover. The sections of anther were observed under a microscope (Motic BA200).

RNA Sequencing Experiments and Data Analysis

All samples of anther were collected and immediately moved to liquid nitrogen and kept at −80°C for RNA extraction. The RNAs of three biological samples were isolated by TRIzol Reagent (Life technologies, California, United States) according to manual instructions. The libraries were constructed by manual protocols, and transcriptome sequencing was performed on the Illumina Novaseq platform according to the recommended protocol of vendor. Clean reads were obtained by removing reads containing adapter, reads containing N base, and low-quality reads from raw reads. The mapped reads of each sample were assembled by StringTie (v1.3.3b) (Pertea et al., 2015) in a reference-based approach. And then fragments per kilobase of transcript per million fragments mapped reads (FPKM) of each gene were calculated by StringTie. The DEG was detected using the DESeq2 software (Love et al., 2014). The false discovery rate (FDR) was used to determine the threshold of the *P*-value in multiple tests. The DEG was used for subsequent analysis according to the following criteria: FDR ≤ 0.05 and the absolute value of $\log_2$ (fold change) > 1 or $\log_2$ (fold change) < -1. The sequencing raw data were also uploaded in National Center for Biotechnology Information (NCBI) (PRJNA748460).

The Stage-Specific Genes and Weighted Gene Co-expression Network Analysis

The stage-specific genes in anther at different development stages were identified according to the method described previously (Zhan et al., 2015; Garg et al., 2017). The stage specificity coefficient (SSC) score ≥ 0.5 was used to discover the genes specifically expressed at a special stage.

The weighted gene co-expression network analysis (WGCNA) is a system and comprehensive biology method used to describe gene association patterns between different samples. The co-expression networks analysis was used in WGCNA package in R (Langfelder and Horvath, 2008) according to log2 of the FPKM data of all expressed genes, and analysis is based on the default settings. The kME (eigengene connectivity) values were calculated, and the hub genes in a given module were defined by kME > 0.95, which measures the connectivity of a gene in the specific module (Gao et al., 2018).

Quantitative Real-Time Polymerase Chain Reaction Analysis

The quantitative real-time (qRT)-polymerase chain reaction (PCR) primers were designed by Primer Premier 5.0 software and checked specificity in the NCBI (**Supplementary Table 1**). The cDNA was from sequenced samples by PrimeScript^{TM} RT reagent Kit with gDNA Eraser (TAKARA), and qRT-PCR was implemented on TB Green Premix Ex Taq^{TM} II (TAKARA). The qRT-PCR reaction condition was similar with Chen et al. (2019), 30 s at 95°C, 40 cycles of 95°C denaturation for 5 s and 60°C annealing. The analysis method was $2^{-\Delta\Delta Ct}$ method to calculate gene-related expression (Livak and Schmittgen, 2001). All qRT-PCR reactions were performed in triplicate.

RESULTS

Effects of Heat Stress on Male Reproductive Development

To study the cucumber responses to HS at reproduction stage, the cucumber plants were moved to grow under CK (12 h light/12 h dark, 12 h 28℃/12 h 25℃) and HS (12 h light/12 h dark, 12 h 38℃/12 h 30℃) when seedlings were with four true leaves. There are no differences on male flower between HS and CK condition (**Figure 1A**). To investigate how pollen fertility was affected by HS, pollen viability was tested using I_2-IK staining. As shown in **Figures 1B–D**, many mature pollen grains were aborted on HS, and pollen fertility (55.92%) was significantly lower than CK. In addition, we investigated SOD enzyme activity, POD activity, and the contents of MDA at S1, S2, S3, and S4 (see detail in materials and methods section) (**Figures 1E–G**). In POD activity, there were extremely significant increase at S3 and S4 between HS and CK (**Figure 1E**). The MDA contents of HS were higher than CK, and there were significant or extremely significant differences between HS and CK at S1, S2, and S4 (**Figure 1F**). The results of SOD activity were significant or extremely significant differences at every anther development stage between HS and CK (**Figure 1G**).

The cross section assay was carried out to investigate anther development in CK and HS by paraffin section (**Figure 2**). Many abnormal phenomena were found since microspore stage to mature pollen stage underlying HS. At microspore stage, there were tapetum abnormality, abnormal microspore, and microspore degeneration in HS (**Figures 2G–I**). At mature pollen

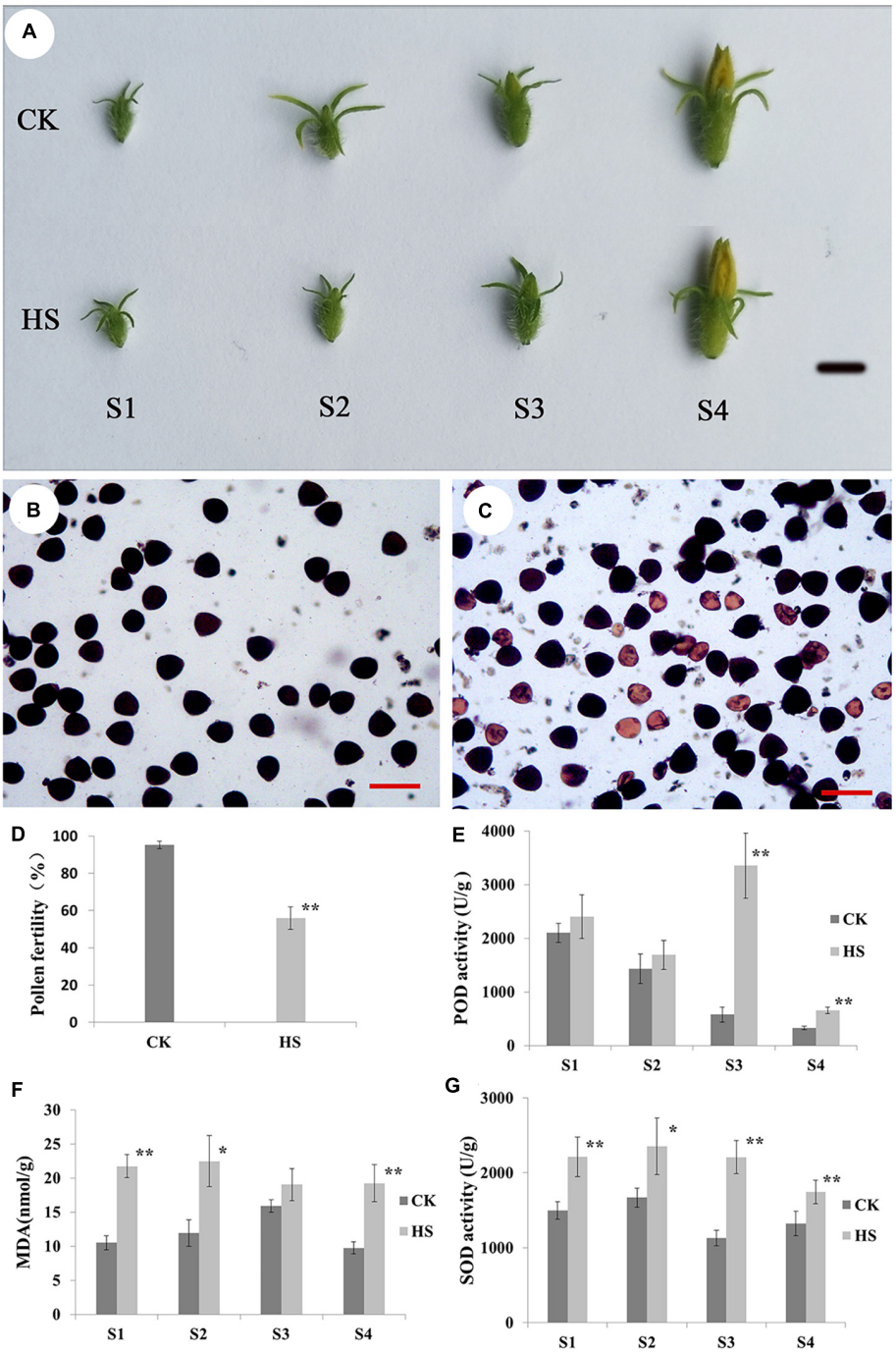

FIGURE 1 | Phenotype of male flower at different developmental stages between normal (CK) and heat stress (HS). **(A)** Phenotype of male flower at different developmental stages between CK and HS, bar = 1cm. Pollen grain of CK **(B)** and HS **(C)** observed by staining with 1% iodine-potassium (I_2-KI), pollen fertility **(D)**, bar = 100 μm. Peroxidase (POD) **(E)**, malondialdehyde (MDA) **(F)**, and superoxide dismutase (SOD) **(G)** in anther of CK and HS at male flower development stages.

stage, the pollen grains were filled with starch and tapetum was degenerated in CK. However, the pollen grains became sterile and tapetum did not degenerate in HS (**Figures 2J–L**). Taken together, these results showed that HS has a large impact on anther development.

Transcriptomic Profiles of Cucumber Anther Under Heat Stress

About 102 million clean reads were obtained after moving low quality read in different samples. We mapped the clean reads to cucumber reference genome (V3.0), and

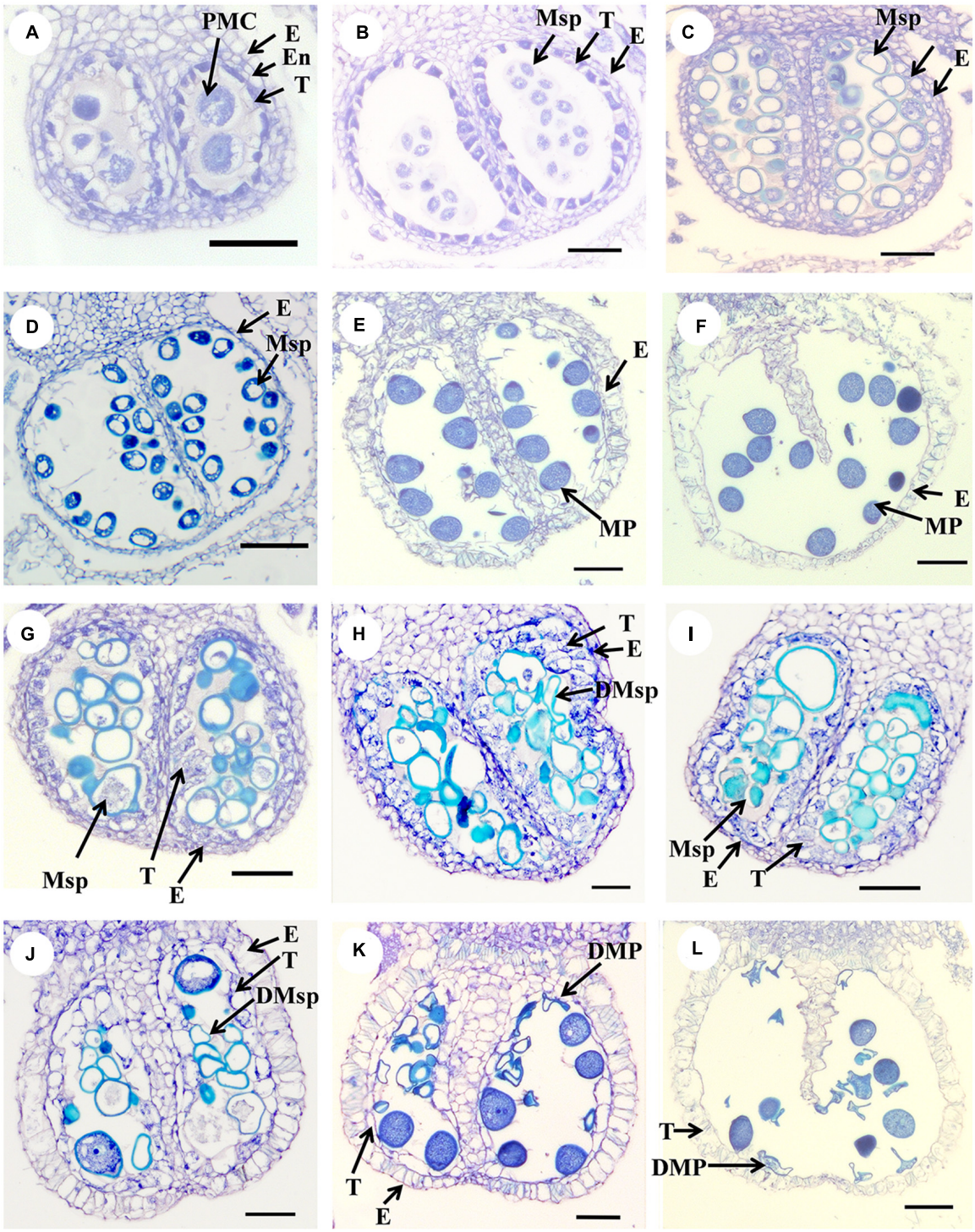

FIGURE 2 | The cross-section analysis of anther development in CK and HS. **(A–F)** Anther cross-sections of different developmental stages under CK, **(A–B)** meiosis stage, **(C–D)** microspore stage, **(E–F)** and mature stage. **(G–L)** Abnormal anther in HS. bar = 50 μm.

91.07% to 94.52% clean reads were uniquely mapped to the reference genome in different samples (**Supplementary Table 2**). The correlation coefficient of each sample was more than 0.9 (**Supplementary Figure 1**), and principal component analysis (PCA) showed that biological replicates were clustered together (**Supplementary Figure 1**) and sample of each stage was classed together. These results indicated that gene expression patterns have high similarity between

biological replications and sample of each stage have similar expression pattern.

Specifically Different Expression at Anther Development

To investigate the specifically different expression at different anther development stages under different growth conditions, we identified specifically expressed genes in different anther development stages by using SSC. Total of 1162 and 986 specifically expressed genes were discovered at a particular sample on normal and HS condition, respectively (**Figure 3A**). The stage-specific genes varied from 23 to 600 for CK and 10 to 574 for HS (**Figure 3A**). The S1 presented the largest number of stage-specific genes and the lowest number of stage-specific genes was detected in S3 in both growth conditions (**Figures 3A,B**). More stage-specific genes were found in S1 and S4 stages; this indicated these two stages are more active.

The gene ontology (GO) enrichment analyses showed that all the stage-specific genes were related to various transport, response, biosynthetic, and metabolic processes (**Supplementary Table 2**). These GO terms are well known to be related to the growth and development of plants. Total of 55, 87, and 51 GO terms were significantly enriched in CK, HS, and both growth conditions by enrichment stage-specific genes, respectively (**Figure 3C** and **Supplementary Figure 2**). In the biological processes, GO terms of response to oxidative stress and response to stress were significantly enriched in both growth conditions, and other GO terms are specifically significantly enriched in one growth condition. For example, signal transduction, glycolipid biosynthetic process, membrane lipid biosynthetic process, cell cycle process, transmembrane transport, glycolipid metabolic process, DNA integration, and liposaccharide metabolic process were specific to CK, whereas GO terms related to sulfate transport, sulfur compound transport, inorganic anion transport, alpha-amino acid biosynthetic process, cellulose metabolic process, and cellulose biosynthetic process were specific to HS. The GO terms, including defense response, response to biotic stimulus, carbohydrate metabolic process, polysaccharide metabolic process, cellular glucan metabolic process, glucan metabolic process, and cellular polysaccharide metabolic process, were identified enrichment in common stage-specific genes between both growth conditions (**Figure 3C**). These results indicate that a group of genes implement stage-specific functions during anther development stage between both growth conditions.

Differentially Expressed Genes in Male Reproductive Under Heat Stress

We detected DEGs with heat-induced expression change at anther development stage. We identified 1230, 1215, 1706, and 1677 DEGs in S1, S2, S3, and S4 in HS compared with CK (**Figure 4A**), respectively. Additionally, 20 DEGs were significantly expressed at every development stage in HS compared with CK (**Figure 4B**). These 20 DEGs were also selected for qRT-PCR analysis and confirmed this prediction outcome (**Figure 4C**). Totally, six and 10 DEGs were detected significantly downregulated and upregulated at all stages in HS compared with CK, and four DEGs differently significantly expressed in different stage. The six DEGs were detected significantly downregulated in HS, including chorismate mutase (*CsaV3_5G038370*), threonine aldolase (*CsaV3_2G003740*), pectate lyase (*CsaV3_2G025090*), hexosyltransferase (*CsaV3_6G000050*), xyloglucan endotransglucosylase (*CsaV3_1G020800*), and syntaxin (*CsaV3_6G021780*). The 10 DEGs were detected significantly upregulated in HS, including Reactive intermediate/imine deaminase (*CsaV3_3G005070*), (R)-mandelonitrile lyase (*CsaV3_2G008160*), protein NRT1 (*CsaV3_3G039930*), Beta-glucosidase (*CsaV3_1G042490*), sequence-specific DNA binding transcription factor (*CsaV3_3G036680*), fatty acid desaturase (*CsaV3_6G030990*), Glycosyltransferase (*CsaV3_3G008220*), and three unknown protein (*CsaV3_2G012830*, *novel.621*, and *novel.922*). The four DEGs differently expressed in different stages, including wound-responsive family protein (*CsaV3_1G011730*), dof zinc finger protein like (*CsaV3_3G006960*), glycine-rich protein-2 (*CsaV3_3G001620*), and unknown protein (*novel.8*). These genes may have key roles in anther development and pollen formation, and may be used as marker gene to distinguish HS and CK conditions.

Total of 416 DEGs belong to 58 transcription factors (TFs), and including 93, 119, 121, and 84 TFs were found in S1, S2, S3, and S4 in HS compared with CK (**Supplementary Figure 3A**), respectively. The TFs of MYB, ERF, ERF, and bHLH were mostly detected in S1, S2, S3, and S4 in HS compared with CK (**Supplementary Figure 3B**), respectively. We further analyzed heat shock transcription factors (HSFs) in different development stages and detected six HSFs (three upregulated and three downregulated) in S2, five HSFs (one upregulated and four downregulated) in S3, and one downregulated HSF in S4 (**Supplementary Table 4**). In particular, *CsaV3_2G002270* was downregulated in S2 and S3, and *CsaV3_7G027860* was downregulated in S2, S3, and S4. *CsaV3_3G036820* was upregulated in S2 and S3. In addition, 18 heat shock proteins (HSPs) were found significantly different expressed in different development stages, and 11 HSPs (four upregulated and seven downregulated) in S1, four HSPs (three upregulated and one downregulated) in S3, six HSPs (five upregulated and one downregulated) in S3, and two downregulated HSPs in S4 (**Supplementary Table 4**). Interestingly, the *CsaV3_1G035830* was downregulated in S1, S3, and S4.

The GO analysis presented that 42, 68, 51, and 80 GO terms were significantly enriched in S1, S2, S3, and S4, respectively (**Figure 5** and **Supplementary Table 4**). In the biological processes category, carbohydrate metabolic process was enriched at every stage. The GO terms of response to biotic stimulus, defense response, and response to oxidative stress were significantly enriched in S1, S2, and S3, and response to stress (response to biotic stimulus, defense response, and response to oxidative stress are subterm of response to stress) was significantly enriched in S1 and S2. A total of eight GO terms, such as heme binding, tetrapyrrole binding, iron ion binding, hydrolase activity, and acting on glycosyl bonds, were identified in molecular function category at every development stage. In cell component category, GO terms related to cell wall, external

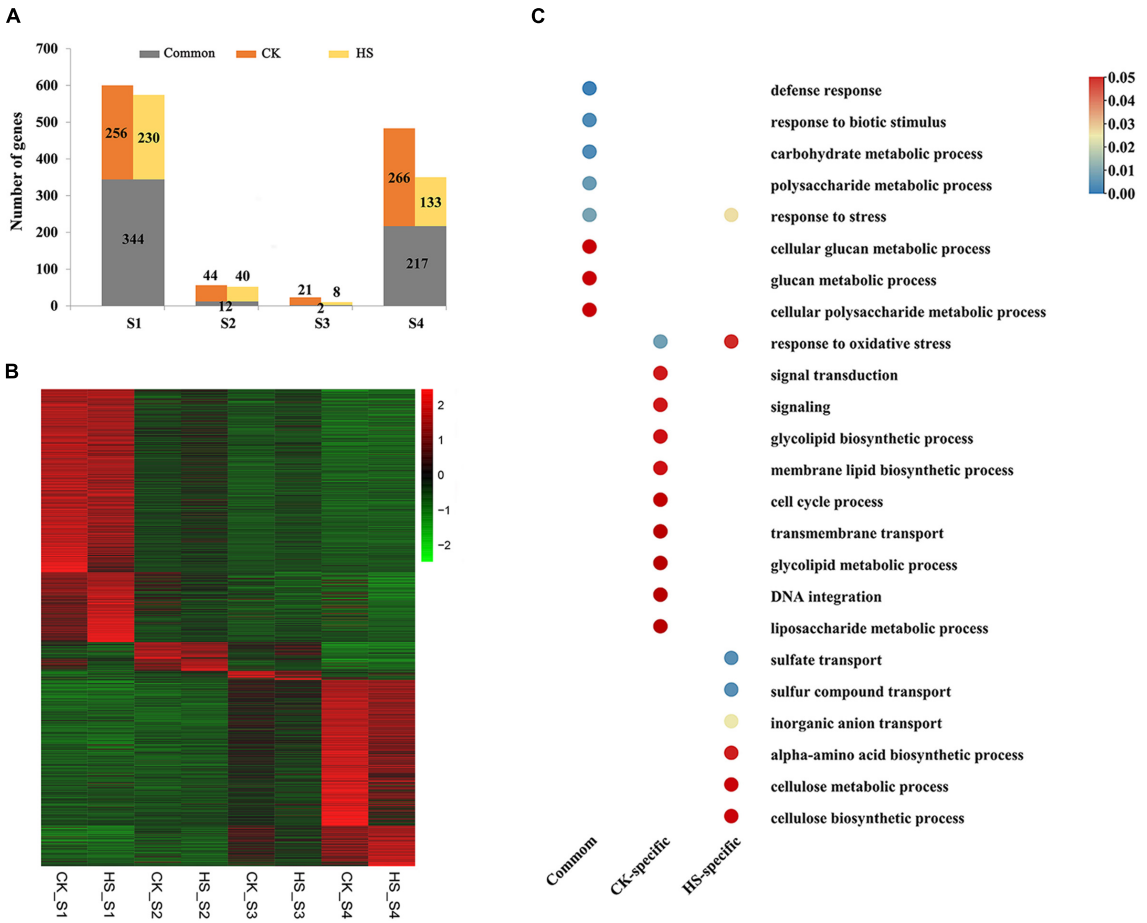

FIGURE 3 | Specifically expressed genes at male development stages in cucumber. **(A)** The number of specifically expressed genes specifically and commonly in CK and HS at each stage of anther development. **(B)** The expression profile of specifically expressed genes between in CK and HS. Color scale represents Z-score. **(C)** The significantly enriched gene ontology (GO) terms (biological process) of specifically expressed genes at anther development in CK and HS.

encapsulating structure, and apoplast at every development stage were identified (**Figure 5** and **Supplementary Table 4**).

Differently Expressed Genes Involved in Carbohydrate Metabolism

A total of 121 DEGs involved in carbohydrate metabolic process were differentially expressed on anther at four stages between CK and HS, including 75 DEGs are encode glycosyl hydrolase protein, and three DEGs are translated glycosyl transferase protein. There are 58 DEGs that were downregulated in HS, and 55 DEGs were upregulated in HS, and eight DEGs were differently expressed pattern between HS and CK. *CsaV3_1G036000*, *CsaV3_5G005550*, and *CsaV3_1G020800* were downregulated at S1, S2, and S3. *CsaV3_3G036070* was upregulated at S1, S3, and S4, and *CsaV3_7G021990*, *CsaV3_1G031460*, and *CsaV3_2G016560* were upregulated at S2, S3, and S4. In particular, *CsaV3_1G042490* was upregulated at all stages (**Supplementary Figure 4**). In addition, there are many DEGs that were involved in starch and sucrose metabolism and sucrose transporters (**Figure 6**). The three sucrose transporter genes (*CsaV3_2G010710*, *CsaV3_2G010690*, and *CsaV3_2G010720*) were detected as significantly different expressed HS compared with CK. The invertase (INV) (*CsaV3_3G037440*, *CsaV3_5G003970*, and *CsaV3_7G034730*), sucrose synthase (SUS) (*CsaV3_4G000970* and *CsaV3_1G041400*), and starch branching enzyme (*CsaV3_7G021990*) displayed different expression patterns between HS and CK (**Figure 6**).

Co-expression Network Analyses Different Anther Development Stage by Weighted Gene Co-expression Network Analysis

The WGCNA was constructed to understand the gene regulatory network in response to HS on anther at different development stages. A total of 12781 genes were used for WGCNA, and distributed to 17 modules (**Supplementary Figures 5A,B** and **Supplementary Table 6**). The number of genes in these modules varied from 15 (MEgrey) to 4931 (MEturquoise), and the

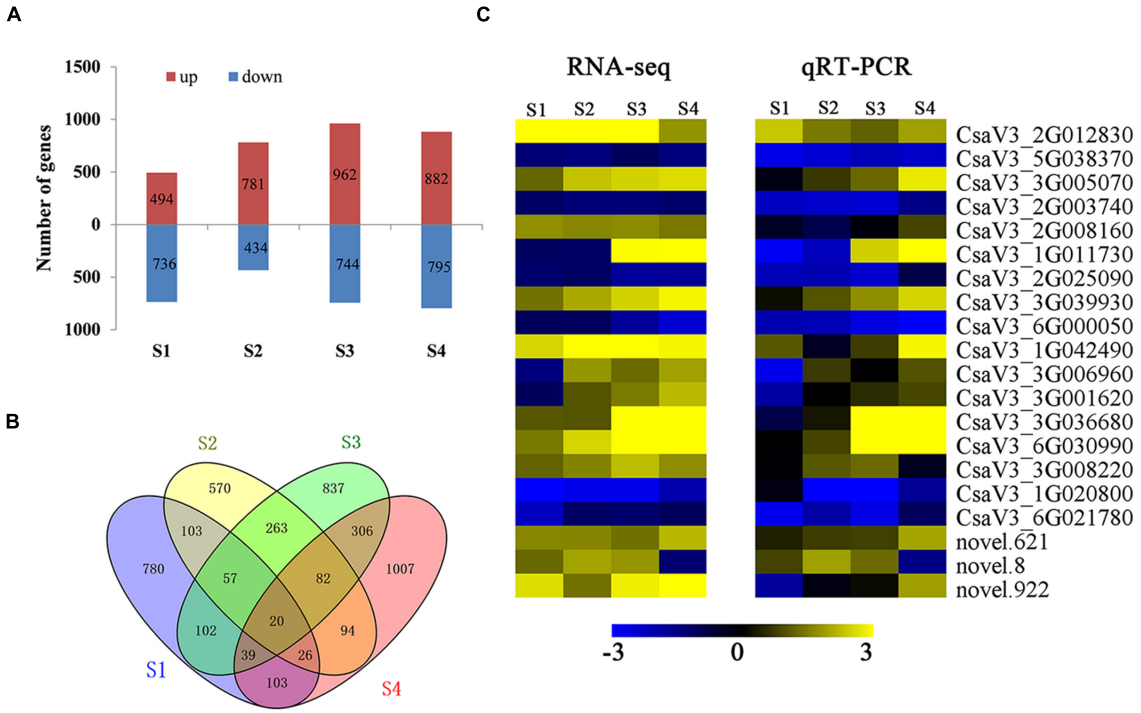

FIGURE 4 | Differentially expressed genes (DEGs) in HS compared with CK at anther development stages. **(A)** Number of up and downregulated DEGs in a HS compared with CK. **(B)** Venn diagram of DEGs in HS compared with CK. **(C)** Expression patterns of common DEGs by RNA-seq and qRT-PCR.

modules harbored TF genes varying 1 (MElightblue) to 319 (MEblue) (**Supplementary Figure 5C**).

Identification of Heat Response-Related Modules

We found that some modules showed different expression patterns between CK and HS at different development stages. For example, the tan module showed low expression in CK, but high expression in HS at S3 and S4 stages. The pink module showed low expression in CK, but high expression in HS at S1, S2, and S3 stages. Likewise, the black module showed low expression in HS, but high in CK at S3 stage. The red module showed low expression in HS, but high expression in CK at S4 stage. The green and lightcyan module showed low expression in HS, but high expression in CK at S4 stage. The magenta module showed low expression in HS, but high expression in CK at S2 and S3 stages (**Supplementary Figure 6**). Particularly, the midnightblue module was preferential expression in CK, and lower expression in HS at all anther development stages (**Figure 7A**).

The midnightblue modules, including 62 genes, may be related to HS in anther development, and we further analyzed the genes of midnightblue modules. The GO enrichment analysis revealed that the midnightblue module was enriched for many metabolic processes in biological processes, including isoprenoid metabolic process, carboxylic acid metabolic process, and organic acid metabolic process (**Figure 7B**). The hub genes, which can be deemed as representative of the gene expression profile of the module, were identified by kME value. The genes (kME > 0.95) were chosen as hub genes in each module. Two genes (*CsaV3_6G004180* and *CsaV3_5G034860*) were found as hub genes in midnightblue module (**Supplementary Table 7**). Functional annotations showed that *CsaV3_6G004180* encodes ACT (aspartokinase, chorismate mutase and TyrA) domain containing protein and *CsaV3_5G034860* might be repressor of RNA polymerase III transcription. We visualized genes with high correlation to *CsaV3_6G004180* and *CsaV3_5G034860* (**Figure 7C**). Notably, *CsaV3_6G004180* and *CsaV3_5G034860* shared 33 overlapped correlation genes, such as WRKY factor (*CsaV3_3G004410*) and zinc finger protein (*CsaV3_4G030470*) and calcium-dependent protein kinase (*CsaV3_3G017510*).

DISCUSSIONS

High Temperature Effects Pollen Fertility

Plants are sensitive to high temperature at reproductive development, which can cause male or female sterility (Hedhly et al., 2009). Furthermore, many studies found that male reproductive organs were more susceptible to HS than female reproductive organs (Peet et al., 1998). In cucumber, high temperature changed many physiological characteristics, including MDA content, catalase, glutathione reductase, guaiacol peroxidase (G-POD), and SOD activities (Ding et al., 2016). In the current study, we explored phenotype and physiology in cucumber anther development under HS. The results showed that the anthers are no obviously different feature, but the SOD,

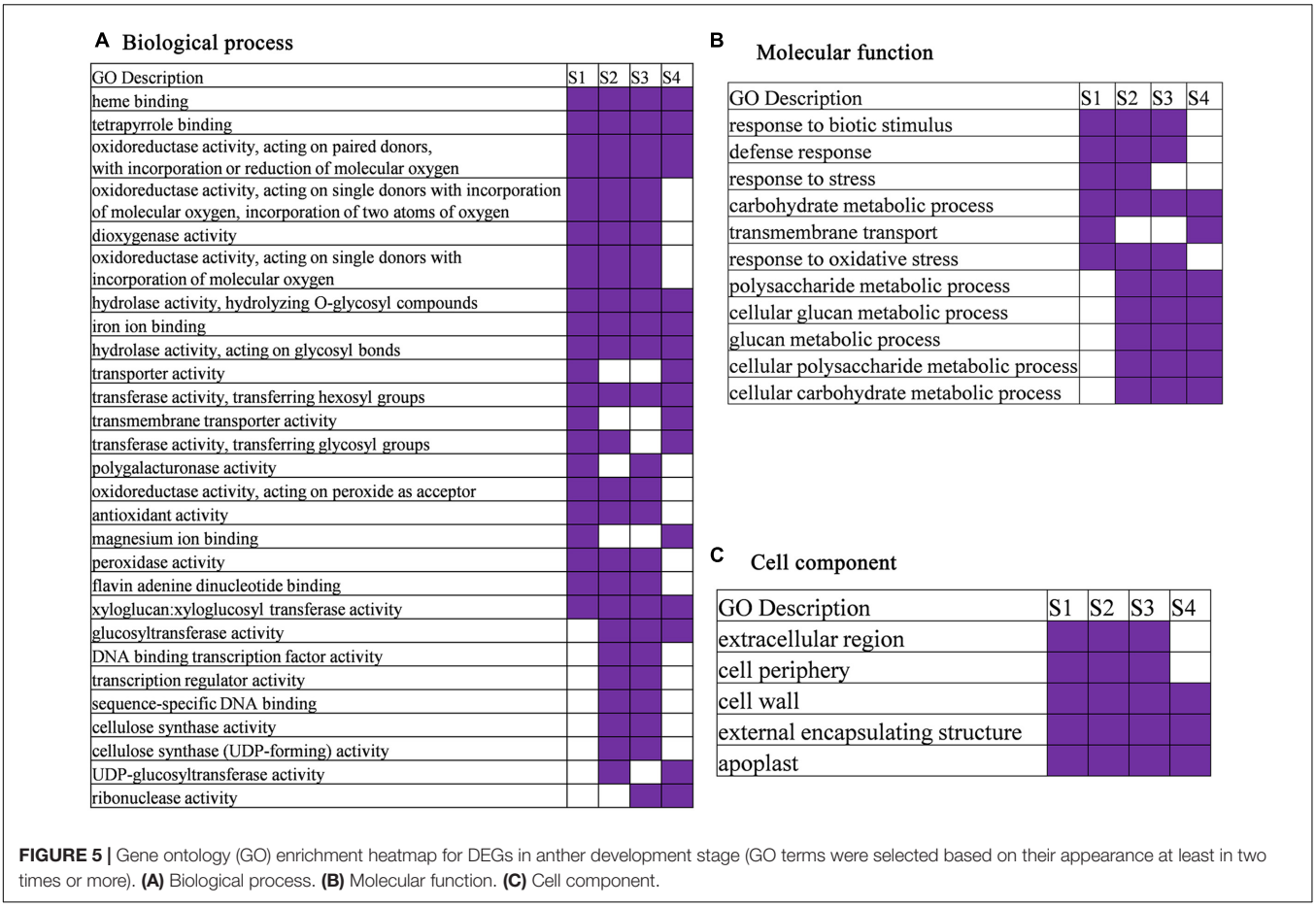

FIGURE 5 | Gene ontology (GO) enrichment heatmap for DEGs in anther development stage (GO terms were selected based on their appearance at least in two times or more). **(A)** Biological process. **(B)** Molecular function. **(C)** Cell component.

POD, and MDA present difference in anther between CK and HS. The physiological investigation results are consisted with other studies on high-temperature stress. In rice, the pollen fertility markedly reduced when rice experienced high temperature at pollen development stage, including reduced number of pollen grain, decreased pollen vitality, and abnormal pollen morphology (Endo et al., 2009; Shi et al., 2013; Kumar et al., 2019). Moreover, high temperatures also cause pollen sterility in cucumber (Miao, 2000). In this study, cytological results presented many abnormal anthers were found in HS, including tapetum swollen, tapetum delayed degradation, degraded microspore, and aborted pollen. Furthermore, the pollen fertility was significantly reduced in HS compared with CK. These results indicated that high temperature may harm the development of cucumber male flowers and causes partial sterility of pollen.

The Abrupt Expression of Saccharides and Starch Synthase-Related Genes May Cause Partial Pollen Sterility by Heat Stress

It is well known that carbohydrate metabolism is essential for plant growth and development. As the main nutrients, the carbohydrates supply energy for the development of pollen (Ruan et al., 2010). In addition, Chen et al. (2018) reported that abnormal saccharides distribution pattern and abrupt saccharides-related genes expression may decrease pollen fertility in autotetraploid rice. Moreover, the starch-related genes were mis-regulation in mature pollen after heat treatment in maize (Begcy et al., 2019), and many proteins of starch and sucrose metabolism were increased expression in pollen under heat treatment in cotton (Masoomi-Aladizgeh et al., 2021). Here, the genes expression profile analysis suggested that carbohydrate metabolic process was detected significantly enriched in DEG at each stage between CK and HS (**Figure 5**). The SUS and INV are two important enzymes involving sucrose degradation in plants (Ruan, 2012). Here, three SUSs and two INVs were identified to significantly express in HS and CK. There are three enzymes that catalyze the starch synthesis and metabolism in plants, including starch synthase, starch debranching, and starch branching enzyme (Zeeman et al., 2010). The starch branching enzyme (*CsaV3_7G021990*) genes was upregulated at S2, S3, and S4 in HS compared with CK. The endoglucanase is necessary for normal cellulose synthesis and has effects on plant cell growth (Read and Bacic, 2002). In our results, nine endoglucanase genes were detected significantly different expressed between HS and CK. The β-glucosidase is extensively involved biotic and abiotic stresses in plant (Xu et al., 2012; Zamioudis et al., 2014), and β-glucosidases gene takes part in the development of pollen in *Brassica species* (Dong et al., 2019).

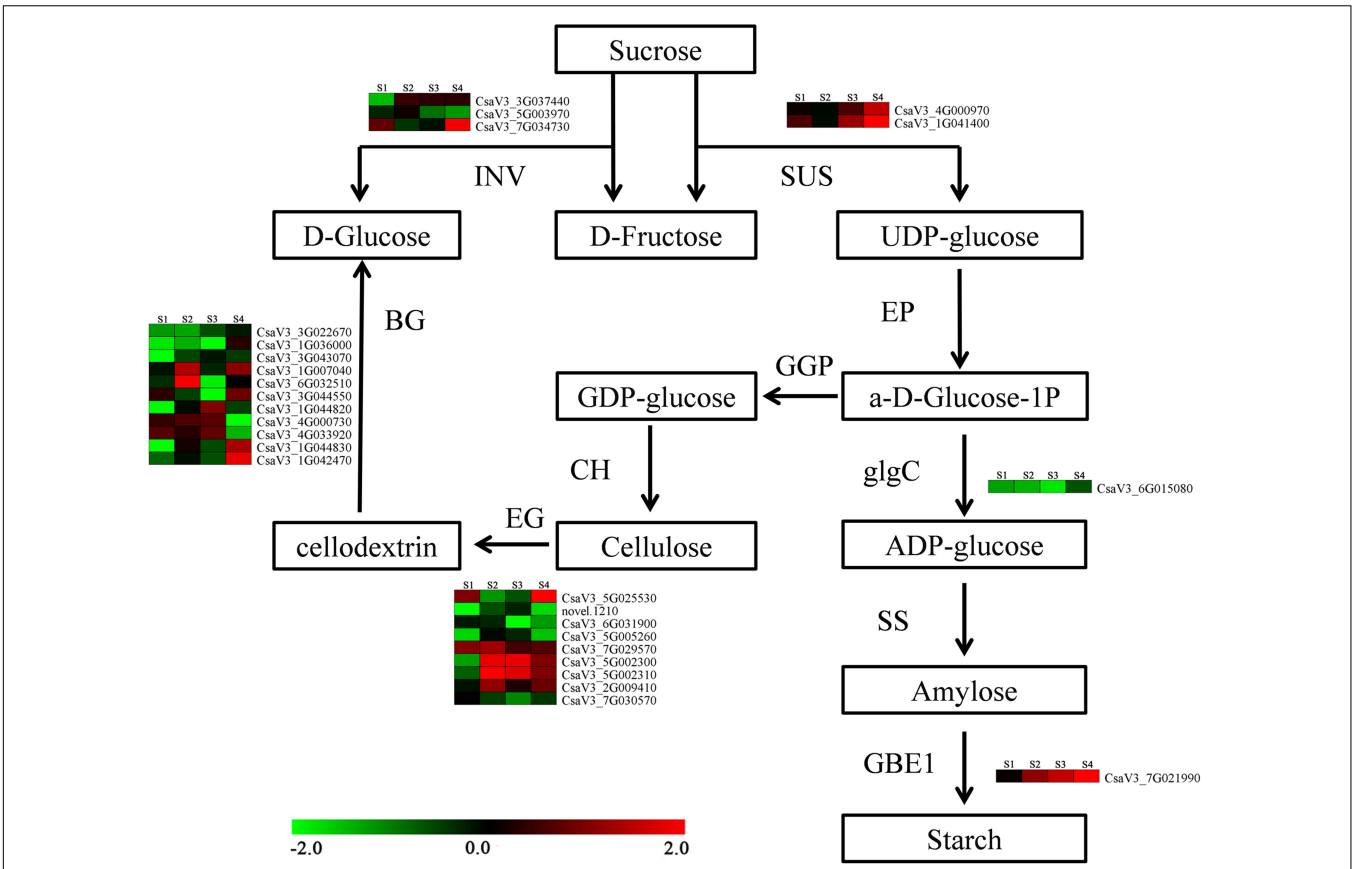

FIGURE 6 | Predicted carbohydrate metabolism pathways in different anther development under HS. INV: invertase; SUS: sucrose synthase; EP: ectonucleotide pyrophosphatase; glgC: glucose-1-phosphate adenylyltransferase; SS: starch synthase; GBE1: glucan branching enzyme; CH: cellulose synthase; EG: endoglucanase; BG: beta-glucosidase.

A total of 11 DEGs, which encode β-glucosidases, were found between HS and CK.

Sucrose transporters support translocation of sucrose from source to sink organs, and maintain connection between sucrose transport and pollen development (Srivastava et al., 2008; Hirose et al., 2010). *CsSUT1*, which is a sucrose transporter protein, was found to be important for male sterility (Sun et al., 2019). The *CsSUT1* was found upregulated at S4 in HS, and two sucrose transporters (*CsaV3_2G010710* and *CsaV3_2G010720*) were detected. These results showed that many saccharides metabolism, starch synthase, and sucrose transporter-related genes were significantly expressed in HS and CK, and consisted with maize (Begcy et al., 2019) and cotton (Masoomi-Aladizgeh et al., 2021). We conjectured that those abrupt expressions of saccharides metabolism and starch synthase-related genes may cause low pollen fertility in HS.

Heat Shock Protein and Heat Shock Transcription Factor Play an Important Role in Anther Responding to High Temperature

It has been reported that HSP and HSF play a crucial role for responding to HS. HSF is a transcription factor necessary to induce HS response, and HSFs are evolutionarily conserved in eukaryotes (Ohama et al., 2017). According to the characteristics of their flexible linkers and oligomerization domains, the HSFs are divided into three categories (A, B, and C) (Nover et al., 2001; Bharti et al., 2004). In Arabidopsis, *HsfA3* was high expression at later phase of the high-temperature response, and it is an important factor in thermotolerance network by forming complexes with other HSFs (Schramm et al., 2008). In current study, eight HSFs were significantly different expressed in CK and HS, including six, six, and one HSFs were detected at S2, S3, and S4, respectively. In particular, a HSF (*CsaV3_7G027860*) was significantly downregulated in HS at S2, S3, and S4. In addition, the HSP, such as HSP60, HSP70, HSP90, and HSP21, respond broadly to HS by regulating protein quality (Qu et al., 2013). In Arabidopsis, *HSP21* may regulate plastid encoded RNA polymerase transcription to maintain the normal development of chloroplasts under high-temperature stress (Zhong et al., 2013). The HSP appeared differently expressed in cotton pollen under high-temperature stress (Masoomi-Aladizgeh et al., 2021). Here, 18 HSPs were significantly different expressed in CK and HS, including 11, four, six, and two HSPs were detected at S1, S2, S3, and S4, respectively. There was a HSP (*CsaV3_1G035830*), which was significantly downregulated in HS at S1, S3, and S4. These results showed these HSFs and HSPs have essential roles

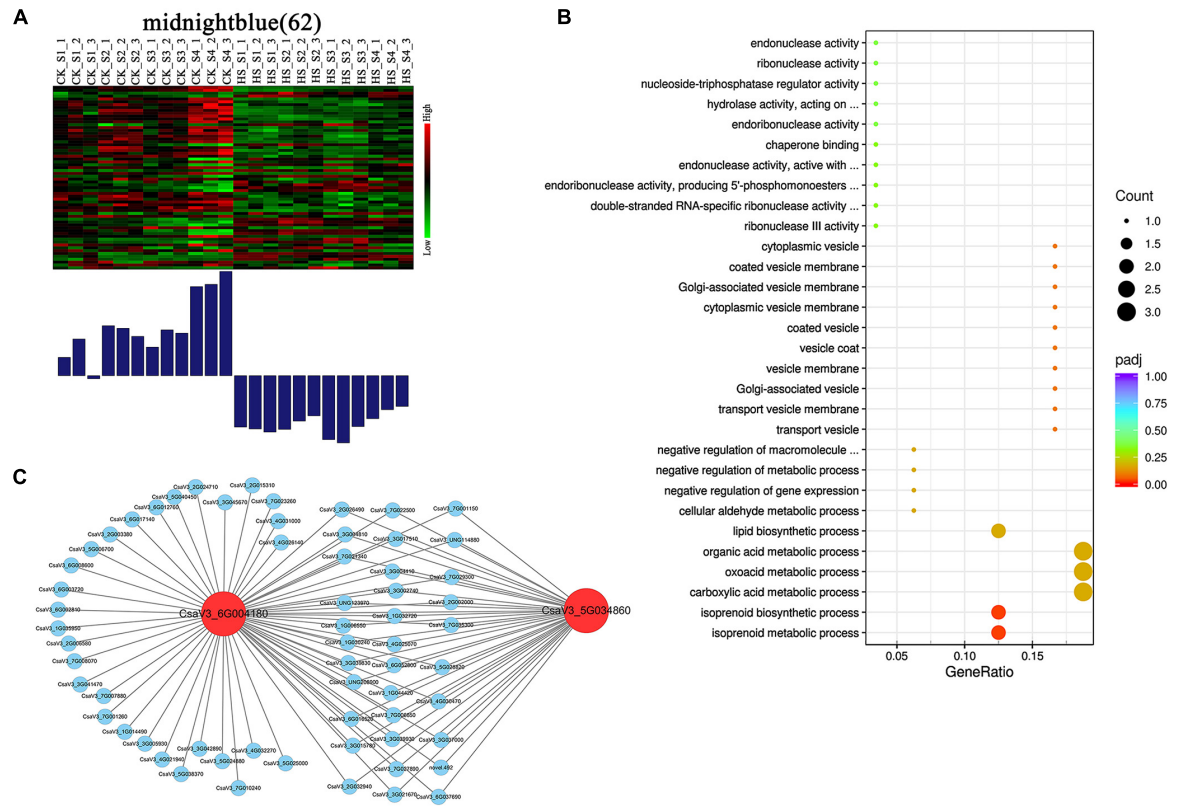

FIGURE 7 | Expression profile and transcriptional regulatory network of midnightblue module associated with opposite expression patterns in CK and HS. **(A)** The midnightblue modules showing opposite expression patterns in CK and HS. Heatmaps show the expression profile of all the co-expressed genes (number given on the top) in the midnightblue modules. The color scale represents Z-score. Bar graphs (below the heatmaps) show the consensus expression pattern of the co-expressed genes in midnightblue modules. The bars show opposite expression patterns in CK and HS. **(B)** The GO terms (biological process) of genes in midnightblue modules. **(C)** High co-expressed genes of two hub genes in midnightblue module.

under HS and may be important factors for cucumber anthers responding to HS at male flowering development stages.

Transcription Regulatory Modules Related to Heat Stress in Cucumber Anther Development

Weighted gene co-expression network analysis (WGCNA), which is a systems analysis tool, was used to identify large gene clusters and relationships of networks and phenotypes. The WGCNA is widely used in rice, tomatoes, chickpea, strawberry, and soybean. In the present study, WGCNA were used to detect that gene different expressed pattern between HS and CK. A module (midnightblue) was identified as oppositely expressed pattern between HS and CK at all anther development stages. In addition, WGCNA analysis found two hub (*CsaV3_6G004180* and *CsaV3_5G034860*) genes in midnightblue module (**Figure 7**). *CsaV3_6G004180* is ACT domain containing protein. ACT domain containing protein can interact with small heat stress protein (Hayakawa et al., 2006), and may regulate ROS and salicylic acid (SA) accumulation to modulate SA-associated defense responses and disease resistance in Arabidopsis (Singh et al., 2018). *CsaV3_5G034860* encoded repressor of RNA polymerase III transcription. The RNA polymerase III was essential for reproductive development (Onodera et al., 2008), and loss of RNA polymerase III will cause hybrid pollen sterility in rice (Nguyen et al., 2017). On further analysis, 33 genes were highly correlated with *CsaV3_6G004180* and *CsaV3_5G034860*. The *CsaV3_6G004180,* and *CsaV3_5G034860* play an important related role in adjusting HS in anther development.

Although it is well known that cucumber is sensitive to HS at male flower development stage, the molecular mechanisms are poorly understood in cucumber male flower development underlying HS. In this study, we analyzed physiological, cellular changes, and transcriptomes data in male flower between CK and HS. The results showed that physiological levels, including POD, SOD, and MDA, are affected by HS. The many HSPs and HSFs were observed to be abrupt and could affect flower development as well in HS. Moreover, the carbon utilization genes were found to change and might be the cause of partial pollen sterility in HS. These results revealed that multiple reasons jointly cause partial pollen abortion in cucumber under HS.

DATA AVAILABILITY STATEMENT

The datasets presented in this study can be found in online repositories. The names of the repository/repositories and

accession number(s) can be found below: NCBI SRA BioProject, accession no: PRJNA748460.

AUTHOR CONTRIBUTIONS

LC and YL designed the experiment. LC, MY, ZC, ZL, WL, MW, JY, XH, BJ, and QP performed most of the experiments. LC wrote the manuscript. SY edited the manuscript. All authors read and approved the final version of the manuscript.

FUNDING

This work was supported by the science and technology program of Guangdong (2020B020220001), special fund for scientific innovation strategy-construction of high level academy of agriculture science (R2019YJ-YB3004), Guangzhou science and technology planning project (202102020503), and key laboratory open fund project of vegetable institution of GAAS (201901).

ACKNOWLEDGMENTS

We thank Liu Xiangdong of South China Agricultural University for technological guidance and support.

SUPPLEMENTARY MATERIAL

The Supplementary Material for this article can be found online at: https://www.frontiersin.org/articles/10.3389/fpls.2021.758976/full#supplementary-material

REFERENCES

Alsamir, M., Mahmood, T., Trethowan, R., and Ahmad, N. (2021). An overview of heat stress in tomato (*Solanum lycopersicum* L.). *Saudi J. Biol. Sci.* 28, 1654–1663. doi: 10.1016/j.sjbs.2020.11.088

Begcy, K., Nosenko, T., Zhou, L. Z., Fragner, L., Weckwerth, W., and Dresselhaus, T. (2019). Male sterility in maize after transient heat stress during the tetrad stage of pollen development. *Plant Physiol.* 181, 683–700. doi: 10.1104/pp.19.00707

Bharti, K., Von Koskull-Doring, P., Bharti, S., Kumar, P., Tintschl-Korbitzer, A., Treuter, E., et al. (2004). Tomato heat stress transcription factor HsfB1 represents a novel type of general transcription coactivator with a histone-like motif interacting with the plant CREB binding protein ortholog HAC1. *Plant Cell* 16, 1521–1535. doi: 10.1105/tpc.019927

Bita, C. E., and Gerats, T. (2013). Plant tolerance to high temperature in a changing environment: scientific fundamentals and production of heat stress-tolerant crops. *Front. Plant Sci.* 4:273. doi: 10.3389/fpls.2013.00273

Cao, Z., Zhao, Q., Huang, F., Wei, K., Zaidi, S., Zhou, W.-J., et al. (2015). Effects of high temperature at anthesis on spikelet fertility and grain weight in relation to floral positions within a panicle of rice (*Oryza sativa* L.). *Crop Pasture Sci.* 66, 922–929.

Chen, L., Shahid, M. Q., Wu, J., Chen, Z., Wang, L., and Liu, X. (2018). Cytological and transcriptome analyses reveal abrupt gene expression for meiosis and saccharide metabolisms that associated with pollen abortion in autotetraploid rice. *Mol. Genet. Genomics* 293, 1407–1420. doi: 10.1007/s00438-018-1471-0

Chen, L., Yuan, Y., Wu, J., Chen, Z., Wang, L., Shahid, M. Q., et al. (2019). Carbohydrate metabolism and fertility related genes high expression levels promote heterosis in autotetraploid rice harboring double neutral genes. *Rice* 12:34. doi: 10.1186/s12284-019-0294-x

Ding, X., Jiang, Y., He, L., Zhou, Q., Yu, J., Hui, D., et al. (2016). Exogenous glutathione improves high root-zone temperature tolerance by modulating photosynthesis, antioxidant and osmolytes systems in cucumber seedlings. *Sci. Rep.* 6:35424. doi: 10.1038/srep35424

Dong, S., Zhang, S., Wei, S., Liu, Y., Li, C., Bo, K., et al. (2020). Identification of quantitative trait loci controlling high-temperature tolerance in cucumber (*Cucumis sativus* L.) seedlings. *Plants* 9:115. doi: 10.3390/plants9091155

Dong, X., Jiang, Y., and Hur, Y. (2019). Genome-Wide analysis of glycoside hydrolase family 1 beta-glucosidase genes in *Brassica rapa* and their potential role in pollen development. *Int. J. Mol. Sci.* 20:1663. doi: 10.3390/ijms20071663

Endo, M., Tsuchiya, T., Hamada, K., Kawamura, S., Yano, K., Ohshima, M., et al. (2009). High temperatures cause male sterility in rice plants with transcriptional alterations during pollen development. *Plant Cell Physiol.* 50, 1911–1922. doi: 10.1093/pcp/pcp135

Fu, C., Wang, F., Liu, W., Liu, D., Li, J., Zhu, M., et al. (2017). Transcriptomic analysis reveals new insights into high-temperature-dependent glume-unclosing in an elite rice male sterile line. *Front. Plant Sci.* 8:112. doi: 10.3389/fpls.2017.00112

Gao, H., Wang, Y., Li, W., Gu, Y., Lai, Y., Bi, Y., et al. (2018). Transcriptomic comparison reveals genetic variation potentially underlying seed developmental evolution of soybeans. *J. Exp. Bot.* 69, 5089–5104. doi: 10.1093/jxb/ery291

Garg, R., Singh, V. K., Rajkumar, M. S., Kumar, V., and Jain, M. (2017). Global transcriptome and coexpression network analyses reveal cultivar-specific molecular signatures associated with seed development and seed size/weight determination in chickpea. *Plant J.* 91, 1088–1107. doi: 10.1111/tpj.13621

Guo, J., Li, C., Zhang, X., Li, Y., Zhang, D., Shi, Y., et al. (2020). Transcriptome and GWAS analyses reveal candidate gene for seminal root length of maize seedlings under drought stress. *Plant Sci.* 292:110380. doi: 10.1016/j.plantsci.2019.110380

Guo, S., Zheng, Y., Joung, J., Liu, S., Zhang, Z., Crasta, O. R., et al. (2010). Transcriptome sequencing and comparative analysis of cucumber flowers with different sex types. *BMC Genomics* 11:384. doi: 10.1186/1471-2164-11-384

Harsant, J., Pavlovic, L., Chiu, G., Sultmanis, S., and Sage, T. L. (2013). High temperature stress and its effect on pollen development and morphological components of harvest index in the C3 model grass *Brachypodium distachyon*. *J. Exp. Bot.* 64, 2971–2983. doi: 10.1093/jxb/ert142

Hayakawa, T., Kudo, T., Ito, T., Takahashi, N., and Yamaya, T. (2006). ACT domain repeat protein 7, ACR7, interacts with a chaperone HSP18.0-CII in rice nuclei. *Plant Cell Physiol.* 47, 891–904. doi: 10.1093/pcp/pcj062

He, X., Guo, S., Wang, Y., Wang, L., Shu, S., and Sun, J. (2020). Systematic identification and analysis of heat-stress-responsive lncRNAs, circRNAs and miRNAs with associated co-expression and ceRNA networks in cucumber (*Cucumis sativus* L.). *Physiol. Plant.* 168, 736–754. doi: 10.1111/ppl.12997

Hedhly, A., Hormaza, J. I., and Herrero, M. (2009). Global warming and sexual plant reproduction. *Trends Plant Sci.* 14, 30–36. doi: 10.1016/j.tplants.2008.11.001

Hirose, T., Zhang, Z., Miyao, A., Hirochika, H., Ohsugi, R., and Terao, T. (2010). Disruption of a gene for rice sucrose transporter, OsSUT1, impairs pollen function but pollen maturation is unaffected. *J. Exp. Bot.* 61, 3639–3646. doi: 10.1093/jxb/erq175

Huang, J., Zhao, X., and Chory, J. (2019). The Arabidopsis transcriptome responds specifically and dynamically to high light stress. *Cell Rep.* 29, 4186–4199.e3. doi: 10.1016/j.celrep.2019.11.051

Jain, M., Chourey, P. S., Boote, K. J., and Allen, L. J. (2010). Short-term high temperature growth conditions during vegetative-to-reproductive phase transition irreversibly compromise cell wall invertase-mediated sucrose catalysis and microspore meiosis in grain sorghum (*Sorghum bicolor*). *J. Plant Physiol.* 167, 578–582. doi: 10.1016/j.jplph.2009.11.007

Janni, M., Gulli, M., Maestri, E., Marmiroli, M., Valliyodan, B., Nguyen, H. T., et al. (2020). Molecular and genetic bases of heat stress responses in crop plants and breeding for increased resilience and productivity. *J. Exp. Bot.* 71, 3780–3802. doi: 10.1093/jxb/eraa034

Jiang, J., Ren, X., Li, L., Hou, R., Sun, W., Jiao, C., et al. (2020). H2S Regulation of Metabolism in Cucumber in response to salt-stress through transcriptome and proteome analysis. *Front. Plant Sci.* 11:1283. doi: 10.3389/fpls.2020.01283

Jin, Y., Yang, H., Wei, Z., Ma, H., and Ge, X. (2013). Rice male development under drought stress: phenotypic changes and stage-dependent transcriptomic reprogramming. *Mol. Plant* 6, 1630–1645. doi: 10.1093/mp/sst067

Kotak, S., Larkindale, J., Lee, U., von Koskull-Doring, P., Vierling, E., and Scharf, K. D. (2007). Complexity of the heat stress response in plants. *Curr. Opin. Plant Biol.* 10, 310–316. doi: 10.1016/j.pbi.2007.04.011

Kumar, N., Jeena, N., and Singh, H. (2019). Elevated temperature modulates rice pollen structure: a Study from foothill of Himalayan agro-ecosystem in India. *3 Biotech* 9:175. doi: 10.1007/s13205-019-1700-1

Langfelder, P., and Horvath, S. (2008). WGCNA: an R package for weighted correlation network analysis. *BMC Bioinformatics* 9:559. doi: 10.1186/1471-2105-9-559

Li, H., Wang, Y., Wang, Z., Guo, X., Wang, F., Xia, X. J., et al. (2016). Microarray and genetic analysis reveals that csa-miR159b plays a critical role in abscisic acid-mediated heat tolerance in grafted cucumber plants. *Plant Cell Environ.* 39, 1790–1804. doi: 10.1111/pce.12745

Li, S., Wang, C., Zhou, X., Liu, D., Liu, C., Luan, J., et al. (2020). The curvature of cucumber fruits is associated with spatial variation in auxin accumulation and expression of a YUCCA biosynthesis gene. *Hortic. Res.* 7:135. doi: 10.1038/s41438-020-00354-5

Li, Z., Zhang, X., Zhao, K., Zhao, K., Qu, C., Gao, G., et al. (2021). Comprehensive transcriptome analyses reveal candidate genes for variation in seed size/weight during peanut (*Arachis hypogaea* L.) domestication. *Front. Plant Sci.* 12:666483. doi: 10.3389/fpls.2021.666483

Liu, Y., Dong, S., Wei, S., Wang, W., Miao, H., Bo, K., et al. (2021). QTL mapping of heat tolerance in cucumber (*Cucumis sativus* L.) at adult stage. *Plants* 10:324. doi: 10.3390/plants10020324

Livak, K. J., and Schmittgen, T. D. (2001). Analysis of relative gene expression data using real-time quantitative PCR and the 2-ΔΔCT method. *Methods* 25, 402–408. doi: 10.1006/meth.2001.1262

Love, M. I., Huber, W., and Anders, S. (2014). Moderated estimation of fold change and dispersion for RNA-seq data with DESeq2. *Genome Biol.* 15:550. doi: 10.1186/s13059-014-0550-8

Masoomi-Aladizgeh, F., Najeeb, U., Hamzelou, S., Pascovici, D., Amirkhani, A., Tan, D. K., et al. (2021). Pollen development in cotton (*Gossypium hirsutum*) is highly sensitive to heat exposure during the tetrad stage. *Plant Cell Environ.* 44, 2150–2166. doi: 10.1111/pce.13908

Meng, L., Qin, Z., Li, S., and Zhou, X. (2004). Effect of high temperature on yield and quality of different cucumber cultivars. *China Veg.* 5, 4–6.

Miao, M., and Cao, P. (2002). The relationship between heat injury and polyamines or proline contents during anther development and pollen germination in cucumber. *Acta Hortic. Sin.* 29, 233–237.

Miao, M., and Li, S. (2001). A primary study of the sensitive stage to high temperature in the development of male and female flower of cucumber. *J. Nanjing Agric. Univ.* 24, 120–122.

Miao, M. M. (2000). *Studies on the Mechanism of Heat Injury and Heat Adaptation and Summer Cultivation Techniques of Cucumber (Cucumis sativus L.)*. Ph.D. thesis. Nanjing: Nanjing Agricultural University.

Nguyen, G. N., Yamagata, Y., Shigematsu, Y., Watanabe, M., Miyazaki, Y., Doi, K., et al. (2017). Duplication and loss of function of genes encoding RNA polymerase III subunit c4 causes hybrid incompatibility in rice. *G3* 7, 2565–2575. doi: 10.1534/g3.117.043943

Nover, L., Bharti, K., Doring, P., Mishra, S. K., Ganguli, A., and Scharf, K. D. (2001). Arabidopsis and the heat stress transcription factor world: How many heat stress transcription factors do we need? *Cell Stress Chaperones* 6, 177–189.

Ohama, N., Sato, H., Shinozaki, K., and Yamaguchi-Shinozaki, K. (2017). Transcriptional regulatory network of plant heat stress response. *Trends Plant Sci.* 22, 53–65. doi: 10.1016/j.tplants.2016.08.015

Onodera, Y., Nakagawa, K., Haag, J. R., Pikaard, D., Mikami, T., Ream, T. S., et al. (2008). Sex-biased lethality or transmission of defective transcription machinery in Arabidopsis. *Genetics* 180, 207–218. doi: 10.1534/genetics.108.090621

Peet, M. M., Sato, S., and Gardner, R. G. (1998). Comparing heat stress effects on male-fertile and male-sterile tomatoes. *Plant Cell Environ.* 21, 225–231. doi: 10.1046/j.1365-3040.1998.00281.x

Pertea, M., Pertea, G. M., Antonescu, C. M., Chang, T. C., Mendell, J. T., and Salzberg, S. L. (2015). StringTie enables improved reconstruction of a transcriptome from RNA-seq reads. *Nat. Biotechnol.* 33, 290–295. doi: 10.1038/nbt.3122

Porch, T. G., and Jahn, M. (2001). Effects of high-temperature stress on microsporogenesis in heat-sensitive and heat-tolerant genotypes of Phaseolus vulgaris. *Plant Cell Environ.* 24, 723–731.

Qu, A. L., Ding, Y. F., Jiang, Q., and Zhu, C. (2013). Molecular mechanisms of the plant heat stress response. *Biochem. Biophys. Res. Commun.* 432, 203–207. doi: 10.1016/j.bbrc.2013.01.104

Ray, D. K., Gerber, J. S., MacDonald, G. K., and West, P. C. (2015). Climate variation explains a third of global crop yield variability. *Nat. Commun.* 6:5989.

Read, S. M., and Bacic, T. (2002). Plant biology. Prime time for cellulose. *Science* 295, 59–60. doi: 10.1126/science.1068155

Rieu, I., Twell, D., and Firon, N. (2017). Pollen development at high temperature: from acclimation to collapse. *Plant Physiol.* 173, 1967–1976. doi: 10.1104/pp.16.01644

Ruan, Y. L. (2012). Signaling role of sucrose metabolism in development. *Mol. Plant* 5, 763–765. doi: 10.1093/mp/sss046

Ruan, Y. L., Jin, Y., Yang, Y. J., Li, G. J., and Boyer, J. S. (2010). Sugar input, metabolism, and signaling mediated by invertase: roles in development, yield potential, and response to drought and heat. *Mol. Plant* 3, 942–955. doi: 10.1093/mp/ssq044

Schramm, F., Larkindale, J., Kiehlmann, E., Ganguli, A., Englich, G., Vierling, E., et al. (2008). A cascade of transcription factor DREB2A and heat stress transcription factor HsfA3 regulates the heat stress response of Arabidopsis. *Plant J.* 53, 264–274. doi: 10.1111/j.1365-313X.2007.03334.x

Sehgal, A., Sita, K., Kumar, J., Kumar, S., Singh, S., Siddique, K. H. M., et al. (2017). Effects of drought, heat and their interaction on the growth, yield and photosynthetic function of lentil (*Lens culinaris* medikus) genotypes varying in heat and drought sensitivity. *Front. Plant Sci.* 8:1776. doi: 10.3389/fpls.2017.01776

Shi, W., Li, X., Schmidt, R. C., Struik, P. C., Yin, X., and Jagadish, S. V. K. (2018). Pollen germination and *in vivo* fertilization in response to high-temperature during flowering in hybrid and inbred rice. *Plant Cell Environ.* 41, 1287–1297. doi: 10.1111/pce.13146

Shi, W., Muthurajan, R., Rahman, H., Selvam, J., Peng, S., Zou, Y., et al. (2013). Source-sink dynamics and proteomic reprogramming under elevated night temperature and their impact on rice yield and grain quality. *New Phytol.* 197, 825–837. doi: 10.1111/nph.12088

Singh, S. K., Sung, T. Y., Chung, T. Y., Lin, S. Y., Lin, S. C., Liao, J. C., et al. (2018). ACR11 modulates levels of reactive oxygen species and salicylic acid-associated defense response in Arabidopsis. *Sci. Rep.* 8:11851. doi: 10.1038/s41598-018-30304-0

Srivastava, A. C., Ganesan, S., Ismail, I. O., and Ayre, B. G. (2008). Functional characterization of the Arabidopsis AtSUC2 Sucrose/H+ symporter by tissue-specific complementation reveals an essential role in phloem loading but not in long-distance transport. *Plant Physiol.* 148, 200–211. doi: 10.1104/pp.108.124776

Sun, L., Sui, X., Lucas, W. J., Li, Y., Feng, S., Ma, S., et al. (2019). Down-regulation of the sucrose transporter CsSUT1 causes male sterility by altering carbohydrate supply. *Plant Physiol.* 180, 986–997. doi: 10.1104/pp.19.00317

Sun, Y., Zang, C., Yao, T., Li, X., and Yue, L. (2018). Research advances on heat tolerance of cucumber in China. *China Fruit Veg.* 38, 57–62. doi: 10.19590/j.cnki.1008-1038.2018.10.016

Wang, M., He, X., Peng, Q., Liang, Z., Peng, Q., Liu, W., et al. (2020). Understanding the heat resistance of cucumber through leaf transcriptomics. *Funct. Plant Biol.* 47, 704–715. doi: 10.1071/FP19209

Wang, X., Chen, S., Shi, X., Liu, D., Zhao, P., Lu, Y., et al. (2019). Hybrid sequencing reveals insight into heat sensing and signaling of bread wheat. *Plant J.* 98, 1015–1032. doi: 10.1111/tpj.14299

Wu, T., Qin, Z., Zhou, X., Feng, Z., and Du, Y. (2010). Transcriptome profile analysis of floral sex determination in cucumber. *J. Plant Physiol.* 167, 905–913. doi: 10.1016/j.jplph.2010.02.004

Xie, Q., Liu, P., Shi, L., Miao, H., Bo, K., Wang, Y., et al. (2018). Combined fine mapping, genetic diversity, and transcriptome profiling reveals that the auxin transporter gene ns plays an important role in cucumber fruit spine

development. *Theor. Appl. Genet.* 131, 1239–1252. doi: 10.1007/s00122-018-3074-x

Xu, Z., Lee, K., Dong, T., Jeong, J., Jin, J., Kanno, Y., et al. (2012). A vacuolar beta-glucosidase homolog that possesses glucose-conjugated abscisic acid hydrolyzing activity plays an important role in osmotic stress responses in Arabidopsis. *Plant Cell* 24, 2184–2199. doi: 10.1105/tpc.112.095935

Yang, Y., Wang, X., Chen, P., Zhou, K., Xue, W., Abid, K., et al. (2020). Redox status, JA et signaling pathway regulating responses to botrytis cinerea infection between the resistant cucumber genotype and Its susceptible mutant. *Front. Plant Sci.* 11:559070. doi: 10.3389/fpls.2020.559070

Yu, B., Yan, S., Zhou, H., Dong, R., Lei, J., Chen, C., et al. (2018). Overexpression of CsCaM3 improves high temperature tolerance in cucumber. *Front. Plant Sci.* 9:797. doi: 10.3389/fpls.2018.00797

Zamioudis, C., Hanson, J., and Pieterse, C. M. (2014). Beta-Glucosidase BGLU42 is a MYB72-dependent key regulator of rhizobacteria-induced systemic resistance and modulates iron deficiency responses in Arabidopsis roots. *New Phytol.* 204, 368–379. doi: 10.1111/nph.12980

Zeeman, S. C., Kossmann, J., and Smith, A. M. (2010). Starch: its metabolism, evolution, and biotechnological modification in plants. *Annu. Rev. Plant Biol.* 61, 209–234. doi: 10.1146/annurev-arplant-042809-112301

Zhan, J., Thakare, D., Ma, C., Lloyd, A., Nixon, N. M., Arakaki, A. M., et al. (2015). RNA sequencing of laser-capture microdissected compartments of the maize kernel identifies regulatory modules associated with endosperm cell differentiation. *Plant Cell* 27, 513–531. doi: 10.1105/tpc.114.135657

Zhang, S., Zhang, A., Wu, X., Zhu, Z., Yang, Z., Zhu, Y., et al. (2019). Transcriptome analysis revealed expression of genes related to anthocyanin biosynthesis in eggplant (*Solanum melongena* L.) under high-temperature stress. *BMC Plant Biol.* 19:387. doi: 10.1186/s12870-019-1960-2

Zhong, L., Zhou, W., Wang, H., Ding, S., Lu, Q., Wen, X., et al. (2013). Chloroplast small heat shock protein HSP21 interacts with plastid nucleoid protein pTAC5 and is essential for chloroplast development in Arabidopsis under heat stress. *Plant Cell* 25, 2925–2943. doi: 10.1105/tpc.113.111229

Zhou, A., and Pawlowski, W. P. (2014). Regulation of meiotic gene expression in plants. *Front. Plant Sci.* 5:413. doi: 10.3389/fpls.2014.00413

Zhou, R., Yu, X., Zhao, T., Ottosen, C., Rosenqvist, E., and Wu, Z. (2019). Physiological analysis and transcriptome sequencing reveal the effects of combined cold and drought on tomato leaf. *BMC Plant Biol.* 19:377. doi: 10.1186/s12870-019-1982-9

Conflict of Interest: The authors declare that the research was conducted in the absence of any commercial or financial relationships that could be construed as a potential conflict of interest.

Publisher's Note: All claims expressed in this article are solely those of the authors and do not necessarily represent those of their affiliated organizations, or those of the publisher, the editors and the reviewers. Any product that may be evaluated in this article, or claim that may be made by its manufacturer, is not guaranteed or endorsed by the publisher.

frontiers in Plant Science

ORIGINAL RESEARCH
published: 09 February 2022
doi: 10.3389/fpls.2022.817356

Polymerase II–Associated Factor 1 Complex-Regulated *FLOWERING LOCUS C*-Clade Genes Repress Flowering in Response to Chilling

Zeeshan Nasim, Hendry Susila, Suhyun Jin, Geummin Youn and Ji Hoon Ahn*

Department of Life Sciences, Korea University, Seoul, South Korea

RNA polymerase II–associated factor 1 complex (PAF1C) regulates the transition from the vegetative to the reproductive phase primarily by modulating the expression of *FLOWERING LOCUS C* (*FLC*) and *FLOWERING LOCUS M* [*FLM*, also known as *MADS AFFECTING FLOWERING1* (*MAF1*)] at standard growth temperatures. However, the role of PAF1C in the regulation of flowering time at chilling temperatures (i.e., cold temperatures that are above freezing) and whether PAF1C affects other *FLC*-clade genes (*MAF2–MAF5*) remains unknown. Here, we showed that *Arabidopsis thaliana* mutants of any of the six known genes that encode components of PAF1C [*CELL DIVISION CYCLE73/PLANT HOMOLOGOUS TO PARAFIBROMIN*, *VERNALIZATION INDEPENDENCE2* (*VIP2*)/*EARLY FLOWERING7* (*ELF7*), *VIP3*, *VIP4*, *VIP5*, and *VIP6/ELF8*] showed temperature-insensitive early flowering across a broad temperature range (10°C–27°C). Flowering of PAF1C-deficient mutants at 10°C was even earlier than that in *flc*, *flm*, and *flc flm* mutants, suggesting that PAF1C regulates additional factors. Indeed, RNA sequencing (RNA-Seq) of PAF1C-deficient mutants revealed downregulation of *MAF2–MAF5* in addition to *FLC* and *FLM* at both 10 and 23°C. Consistent with the reduced expression of *FLC* and the *FLC*-clade members *FLM/MAF1* and *MAF2–MAF5*, chromatin immunoprecipitation (ChIP)-quantitative PCR assays showed reduced levels of the permissive epigenetic modification H3K4me3/H3K36me3 and increased levels of the repressive modification H3K27me3 at their chromatin. Knocking down *MAF2–MAF5* using artificial microRNAs (amiRNAs) in the *flc flm* background (*35S::amiR-MAF2–5 flc flm*) resulted in significantly earlier flowering than *flc flm* mutants and even earlier than *short vegetative phase* (*svp*) mutants at 10°C. Wild-type seedlings showed higher accumulation of *FLC* and *FLC*-clade gene transcripts at 10°C compared to 23°C. Our yeast two-hybrid assays and *in vivo* co-immunoprecipitation (Co-IP) analyses revealed that MAF2–MAF5 directly interact with the prominent floral repressor SVP. Late flowering caused by *SVP* overexpression was almost completely suppressed by the *elf7* and *vip4* mutations, suggesting that SVP-mediated floral repression required a functional PAF1C. Taken together, our results showed that PAF1C regulates the transcription of *FLC* and *FLC*-clade genes to modulate temperature-responsive flowering at a broad range of temperatures and that the interaction between SVP and these FLC-clade proteins is important for floral repression.

Keywords: *Arabidopsis*, FLC, MAFs, PAF1C, flowering, epigenetics, temperature

OPEN ACCESS

Edited by:
Marta Adelina Mendes, University of Milan, Italy

Reviewed by:
Alice Pajoro, Max Planck Institute for Plant Breeding Research, Germany
Martina Cerise, Max Planck Institute for Plant Breeding Research, Germany

***Correspondence:**
Ji Hoon Ahn
jahn@korea.ac.kr

Specialty section:
This article was submitted to Plant Abiotic Stress, a section of the journal Frontiers in Plant Science

Received: *18 November 2021*
Accepted: *19 January 2022*
Published: *09 February 2022*

Citation:
Nasim Z, Susila H, Jin S, Youn G and Ahn JH (2022) Polymerase II–Associated Factor 1 Complex-Regulated FLOWERING LOCUS C-Clade Genes Repress Flowering in Response to Chilling. Front. Plant Sci. 13:817356. doi: 10.3389/fpls.2022.817356

INTRODUCTION

Plant survival and fitness depends on timely seed production through precise control of flowering time. Flowering time is modulated by a number of endogenous and environmental cues, such as daylength, age, and prolonged exposure to cold and ambient temperatures (Amasino, 2010; Srikanth and Schmid, 2011). To successfully survive a range of varying environmental conditions, plants have evolved a complex regulatory network that integrates these cues to control flowering time (Srikanth and Schmid, 2011). In Arabidopsis (*Arabidopsis thaliana*), nearly 400 flowering genes are known to regulate flowering time in genetically distinct pathways, e.g., the photoperiod, ambient temperature, aging, vernalization, hormonal, and sugar pathways (Bernier and Périlleux, 2005; Bouché et al., 2016). These pathways modulate flowering in response to different endogenous and environmental signals to optimize reproductive success.

Among the flowering time genes, *FLOWERING LOCUS C* (*FLC*), encoding a MADS-box transcription factor, is an important repressor of flowering in various plant species, including Arabidopsis (Michaels and Amasino, 1999; Sheldon et al., 1999; Ruelens et al., 2013). In Arabidopsis winter accessions, FRIGIDA (FRI) induces *FLC* transcription, whereas vernalization (prolonged exposure to cold) epigenetically represses *FLC* transcription (Johanson et al., 2000; Choi et al., 2011). By contrast, in rapid-cycling accessions lacking functional *FRI*, members of the autonomous pathway regulate *FLC* transcription (Amasino, 2010). FLC negatively regulates flowering by directly repressing the transcription of two important genes that promote flowering, *FLOWERING LOCUS T* (*FT*), and *SUPPRESSOR OF OVEREXPRESSION OF CO1* (*SOC1*; Helliwell et al., 2006; Searle et al., 2006; Li et al., 2008).

In addition to *FLC*, the Arabidopsis genome contains five more members of the *FLC* clade, e.g., *MADS AFFECTING FLOWERING1* [*MAF1*, also known as *FLOWERING LOCUS M* (*FLM*)] and *MAF2–MAF5* (Ratcliffe et al., 2001, 2003; Scortecci et al., 2001). The *MAF2–MAF5* genes occur in a tandem repeat within a 22-kb region. The role of *FLM* as a floral repressor has been well-studied (Scortecci et al., 2003; Balasubramanian et al., 2006), and its loss of function causes temperature-insensitive flowering (Lee et al., 2013). Like *FLM*, *MAF2* acts as a floral repressor, and the loss of *MAF2* function results in strong acceleration of flowering upon vernalization, whereas plants overexpressing *MAF2* flowered significantly later than wild-type plants (Ratcliffe et al., 2003). Similarly, MAF3 also represses flowering by directly binding to the promoter sequences of *FT* and *SOC1* and repressing their transcription. Interestingly, the effect of the loss of *MAF3* function was more evident at lower temperatures than at normal growth temperatures (Gu et al., 2013). Overexpression of *MAF3* produced a stronger floral delay in the Landsberg *erecta* (L*er*) accession compared to Columbia (Col-0; Ratcliffe et al., 2003). T-DNA mutants of *MAF4* exhibited accelerated flowering (Gu et al., 2009), and *MAF4* overexpression in L*er* resulted in a strong delay of flowering (Scortecci et al., 2003). Unlike *MAF1–MAF4*, the floral repressive effect of *MAF5* is not strong, and its overexpression only delayed flowering under non-inductive short-day conditions (Kim and Sung, 2010). These FLC-clade transcription factors physically interact with each other, and some of them interact with SHORT VEGETATIVE PHASE (SVP) to make repressor complexes for efficient floral repression (Gu et al., 2013).

Expression of *FLC*-clade genes is epigenetically regulated by a number of histone modifiers that are recruited to these loci by Polymerase II-Associated Factor 1 Complex (PAF1C; Zhang and Van Nocker, 2002; Zhang et al., 2003; Oh et al., 2004). In Arabidopsis, PAF1C components include CELL DIVISION CYCLE73 (CDC73)/PLANT HOMOLOGOUS TO PARAFIBROMIN (PHP), VERNALIZATION INDEPENDENCE2 (VIP2)/EARLY FLOWERING7 (ELF7), VIP3, VIP4, VIP5, and VIP6/ELF8 (Zhang and Van Nocker, 2002; Zhang et al., 2003; He, 2009; Yu and Michaels, 2010). Components of PAF1C interact with RNA Polymerase II (Betz et al., 2002) and recruit H3K4 methyltransferase to their target genes, primarily in the 5′ transcribed regions, thereby leading to the active expression of their target genes (Ng et al., 2003b). In addition to methyltransferases, PAF1C interacts with the splicing factor SKI-INTERACTING PROTEIN (SKIP) to modulate expression of *FLC* and *FLM* (Cao et al., 2015; Li et al., 2019).

Genetic studies revealed that lesions in these PAF1C components resulted in nearly identical early flowering phenotypes under standard growth conditions (He et al., 2004; Oh et al., 2004). PAF1C is required for the enrichment of active epigenetic marks, primarily H3K4me3, at the chromatin of *FLC* and its homologs to maintain their expression; PAF1C deficiency results in reduced expression of these floral repressors, which eventually accelerates flowering (Zhang et al., 2003; He et al., 2004; Yu and Michaels, 2010). For instance, loss of function of *ELF7* and *VIP6* results in the reduced expression of *FLC*, *FLM*/*MAF1*, and *MAF2* (He et al., 2004). Mutations in *VIP3* strongly reduced *FLC* expression and strongly accelerated flowering. In particular, *vip3* mutants flowered significantly earlier than *flc* mutants, suggesting that additional genes are involved in the early flowering of *vip3* mutants (Zhang et al., 2003). Loss of function of *VIP4* and *VIP5* also resulted in strong flowering acceleration that was comparable to that seen in *vip3* single mutants. However, after vernalization, the H3K27 methyltransferase complex Polycomb repressive complex 2 (PRC2) is involved in silencing *FLC* expression (and probably *MAF* expression) by depositing repressive H3K27me3 marks on the *FLC* chromatin (Wood et al., 2006; De Lucia et al., 2008). Although the regulation of *FLC* (and some *MAF* genes) is well-studied under standard growth temperature conditions, whether PAF1C-mediated regulation involves the entire *FLC* clade and the functional importance of this clade in regulating flowering at chilling temperatures remain unclear.

Here, we showed that PAF1C epigenetically regulates the entire set of *FLC*-clade genes. PAF1C-defective mutants showed ambient temperature-insensitive early flowering due to the downregulation of *FLC*-clade genes. The epigenetic status of the chromatin of *FLC* and *FLC*-clade genes was altered in PAF1C-defective mutants. Expression of *FLC* and *FLC*-clade genes was upregulated in response to low temperature in wild-type plants, and these genes play an important role in floral repression at chilling temperatures. Furthermore, MAF2–MAF5

physically interacted with SVP, and SVP-mediated floral repression requires PAF1C, suggesting the possibility that larger repressive complexes form to prevent precocious flowering, especially at chilling temperatures.

MATERIALS AND METHODS

Plant Materials and Growth Conditions

The *Arabidopsis thaliana* mutant lines for *ELF7* (*elf7-2*; SALK_046605 and SALK_070632; hereafter *elf7-4*), *CDC73* (*cdc73-1*; SALK_150644 and *cdc73-2*; SALK_008357), *VIP3* (*vip3-2*; SALK_083364 and *vip3-6*; SALK_060207), *VIP4* (*vip4-1*; SALK_122755 and *vip4-3*; SALK_006392), *VIP5* (*vip5-2*; SALK_062223 and SALK_055889; hereafter *vip5-3*), and *VIP6* (*vip6-2*; SALK_065364 and SALK_119910, hereafter *vip6-5*) were obtained from the ABRC. Genotyping of the mutant lines was performed using the primers described in **Supplementary Table 1**. The effect of the T-DNA insertion on gene expression was confirmed *via* RT-PCR for the uncharacterized mutant lines (*elf7-4*, *vip5-3*, and *vip6-5*). The *35S::SVP:HA* lines were previously generated (Cho et al., 2012). For expression analyses at different temperatures, seedlings from the identical developmental stage of 1.02 (8-day-old seedlings at 23°C and 22-day-old seedlings at 10°C; Boyes et al., 2001) grown under standard long-day (LD) conditions (16:8 h light:dark) were used. LED lights with a light intensity of 120 μmol m^{-2} s^{-1} were used in this study. Flowering time was measured as the total leaf number, and the data are presented as box plots generated using the "PlotsOfData" app in the R package shiny (Postma and Goedhart, 2019), with customized settings.

RNA Sequencing

RNA sequencing (RNA-Seq) was performed using 8-day-old seedlings grown at 23°C and 23-day-old seedlings grown at 10°C under standard LD conditions in two biological replicates for each sample. About 60–80 seedlings were harvested at Zeitgeber Time 16 (ZT16) and pooled for RNA extraction using Invitrogen's Plant RNA Purification Reagent. For RNA sequencing, library preparation was performed with an Illumina TruSeq Stranded Total RNA Sample Prep kit (Illumina), according to the manufacturer's protocols, and paired-end reads were produced using an Illumina HiSeq2000 sequencer. The raw RNA-seq data of PAF1C-deficient mutants generated in this study were deposited at the Gene Expression Omnibus (GEO) NCBI database and are available under the accession number GSE171778. Transcriptome data for *sdg8* mutants (GEO accession number GSE8528) were previously published (Pajoro et al., 2017).

RNA-Seq Data Analyses

The raw sequence reads were processed by adapter trimming, followed by qualitative analysis of raw reads using FastQC.[1] The resulting good quality reads were aligned to the TAIR10 reference genome using CLC Genomics Workbench v.11. Differentially expressed genes (DEGs) were defined as genes with at least a 1.5-fold change, unless mentioned otherwise. Heatmaps were generated using the built-in function of CLC Genomics Workbench. Gene Ontology (GO) analysis was performed with DAVID (Ashburner et al., 2000), and GO enrichment data plotting was performed using the R package ggplot2 (Wickham, 2011). For the identification of common targets, the intersection of the gene lists was identified using the R package UpSetR (Lex et al., 2014) and the Java-based program VennDis (Ignatchenko et al., 2015).

Reverse Transcription Quantitative PCR Analyses

Reverse transcription quantitative PCR (RT-qPCR) was used to validate the RNA-seq data obtained from the PAF1C-deficient mutants. Total RNA was extracted from seedlings at the identical developmental stage at ZT16 at different temperatures. Plant RNA purification reagent (Invitrogen) was used for RNA extraction. The DNase I–treated RNA (~2 μg) was reverse transcribed into cDNA using MMLV enzyme (ELPIS Biotech). qPCR analyses of cDNA or immunoprecipitated DNA (see below) were performed using ×2 A-Star Real Time PCR Master Mix (BioFACT) in a Thermo Fisher QuantStudio 5 real-time PCR machine. All qPCR experiments were conducted in three biological replicates, each with three technical replicates.

For RT-qPCR, data analyses were performed according to the previously published ΔΔCT method (Livak and Schmittgen, 2001), with the modification of using two reference genes, *PP2AA3* (*AT1G13320*) and a *SAND* family gene (*AT2G28390*) to normalize the data (Hong et al., 2010). Data normalization was performed using the geometric mean of the two reference genes. Sequences of primers used in RT-qPCR analyses are shown in **Supplementary Table 1**. The statistical significance of differences in gene expression levels among samples was assessed using one-way ANOVA with a 0.05 level of significance (95% CI).

Chromatin Immunoprecipitation Assays

Chromatin immunoprecipitation (ChIP) assays were performed using wild-type and *vip3* mutant seedlings, as described previously (Susila et al., 2021). Briefly, seedlings of each genotype were harvested at the 1.02 stage (Boyes et al., 2001) and crosslinked using fixation buffer (1% formaldehyde). Immunoprecipitation was performed with polyclonal anti-H3K4me3 (Millipore, 04-745) or anti-H3K27me3 (Millipore, 07-449) antibodies bound to Dynabead Protein A (Thermo Scientific). The ChIPed DNA was extracted using the ChIP DNA Clean & Concentrator kit (Zymo Research). Relative enrichment of histone modifications was analyzed using qPCR as described earlier (Susila et al., 2021). The primers used in ChIP-qPCR are shown in **Supplementary Table 1**. All ChIP experiments were performed with three biological replicates and three technical replicates for each genotype.

Designing and Cloning amiRNAs That Target *MAF* Genes

To posttranscriptionally knock down the *MAF2–MAF5* genes, artificial microRNAs (amiRNAs) were designed using the WMD3

[1]http://www.bioinformatics.babraham.ac.uk/projects/fastqc

webtool (Schwab et al., 2006). Predominantly expressed splice variants of *MAF2–MAF5* (*MAF2.3*, *MAF3.1*, *MAF4.3*, and *MAF5.2*) were selected from the Araport11 cDNA collection and used as target genes for subsequent studies. Two independent amiRNAs were selected and amplified using *pRS300* as a template with four amiRNA-specific primers (**Supplementary Table 1**), as previously described (Schwab et al., 2006). The amplified amiRNAs were cloned into the *pENTR2B* vector and subsequently into the *pEG100* vector containing the 35S promoter.

Protein–Protein Interaction Analyses Using Deep Learning Algorithms

To test whether MAF2–MAF5 interact with SVP, we used two recently developed artificial intelligence (AI)–based deep learning programs, D-SCRIPT (Sledzieski et al., 2021) and PPI-Detect (Romero-Molina et al., 2019). Protein sequences were provided in fasta format as an input for both programs. Protein phosphatase 2A A3 (PP2AA3) was used as a negative interactor control.

Yeast Two-Hybrid Assays

For confirmation of the physical interaction between MAF2–MAF5 and SVP, the full-length coding sequences of the predominantly expressed splice variants of MAF2–MAF5 (*MAF2.3*, *MAF3.1*, *MAF4.3*, and *MAF5.2*) were fused in-frame to the DNA binding domain (BD) in the *pGBKT7* vector. For the activation domain (AD)–fused SVP, full-length coding sequences of SVP were fused to the GAL4 AD in the *pGADT7* vector. The double transformation was performed by introducing a combination of *SVP* with the *MAF2–MAF5* vectors into the yeast strain AH109.

Co-immunoprecipitation Assays

Co-immunoprecipitation (Co-IP) experiments were performed in Arabidopsis mesophyll protoplasts as described earlier (Wu et al., 2009). The coding sequences of *MAF2–MAF5* were fused with GFP (*35S::MAF-GFP*) in the 326-GFP vector (Lee et al., 2001) and co-transfected with *35S::SVP-2HA* in the protoplasts isolated from wild-type plants. The transfected protoplasts were incubated at 23°C for 3 h to allow production of these proteins in sufficient quantities before overnight incubation at 10°C. After incubation, the protoplasts were pelleted and lysed with lysis buffer (10 mM Tris–HCl, pH 7.5, with .1% Triton X-100, and ×1 Roche Protease Inhibitor Cocktail). The lysate was then incubated overnight with GFP-Trap magnetic beads (Chromotek). Anti-GFP monoclonal antibodies (Roche) and anti-HA high-affinity monoclonal antibody clone 3F10 (Sigma-Aldrich) were used as primary antibodies for the western blots.

RESULTS

PAF1C-Deficient Mutants Flower Early at a Broad Range of Temperatures

To test the effect of a lesion in PAF1C on flowering time, we measured flowering time of PAF1C-deficient mutants at different temperatures ranging from chilling (i.e., cold but not freezing, 10°C) to high temperature (27°C). To show that any observed flowering time change was not specific to a single allele, we used two independent homozygous mutant lines for each PAF1C gene (*CDC73*, *ELF7*, *VIP3*, *VIP4*, *VIP5*, and *VIP6*; **Figures 1A,B**). For the previously uncharacterized T-DNA lines *elf7-4* (SALK_070632), *vip5-3* (SALK_055889), and *vip6-5* (SALK_119910), we performed conventional RT-PCR to examine their transcript levels; indeed, all three lines were found to be RNA-null alleles (**Supplementary Figure 1**).

Flowering time measurement showed that wild-type plants flowered with a mean total leaf number (TLN) of 36.3 ± 1.8, 32.0 ± 2.3, 15.6 ± 0.9, and 12.5 ± 0.5 at 10, 16, 23, and 27°C, respectively (**Figures 1A,B**; **Supplementary Table 2**). At all tested temperatures, the PAF1C-deficient mutants flowered significantly earlier than the wild-type plants, indicating that a lesion in PAF1C caused early flowering at a broad range of temperatures. In particular, PAF1C-deficient mutants showed very early flowering, compared with the wild type, as temperature decreased. We selected an allele that showed a strong early flowering phenotype from each gene (*cdc73-2*, *elf7-2*, *vip3-2*, *vip4-1*, *vip5-2*, and *vip6-2*) and used these mutants for further analyses.

To assess the temperature sensitivity of PAF1C-deficient mutants, we calculated the leaf number ratio (LNR) of *cdc73-2*, *elf7-2*, *vip3-2*, *vip4-1*, *vip5-2*, and *vip6-2* mutants, using the TLN values at different temperatures. A LNR close to 1 indicates that temperature has little effect on flowering. All PAF1C-deficient mutants showed significantly lower LNRs compared with wild-type plants (**Figure 1C**; **Supplementary Table 3**). These results indicated that a lesion in PAF1C caused ambient temperature-insensitive flowering, especially at lower temperatures.

We then compared flowering time of PAF1C mutants with that of *flc*, *flm*, and *flc flm* mutants at 10°C. The *flc*, *flm*, and *flc flm* mutants flowered with 27.0 ± 1.3, 24.8 ± 1.1, and 20.2 ± 1.6 leaves, respectively, at 10°C (**Figure 1D**). Interestingly, their flowering times (measured as TLN) were later than *elf7*, *vip3*, *vip4*, *vip5*, and *vip6* single mutants. This indicated that a lesion in both *FLC* and *FLM* was insufficient to phenocopy the early flowering time seen in PAF1C-deficient mutants. Therefore, considering that the PAF1C regulates *FLC* and *FLM* transcription (Zhang and Van Nocker, 2002; Zhang et al., 2003; Oh et al., 2004), these results suggested the possibility that PAF1C regulates other factors, in addition to *FLC* and *FLM*, in modulating flowering time at 10°C.

Transcriptome Analyses of PAF1C-Deficient Mutants

Mutants in all PAF1C components (except *CDC73*) flowered significantly earlier than *flc flm* double mutants at 10°C (**Figure 1D**), suggesting that additional factors are involved in this early flowering. To identify these factors, we performed RNA-seq using PAF1C-deficient mutants grown at 10 and 23°C. Euclidean distance clustering associated with complete linkage classified the transcriptome profiles into two major clades (**Figure 2A**): clade I, containing Col-0 and *cdc73* mutants grown at 23°C; and clade II, containing the remaining mutants

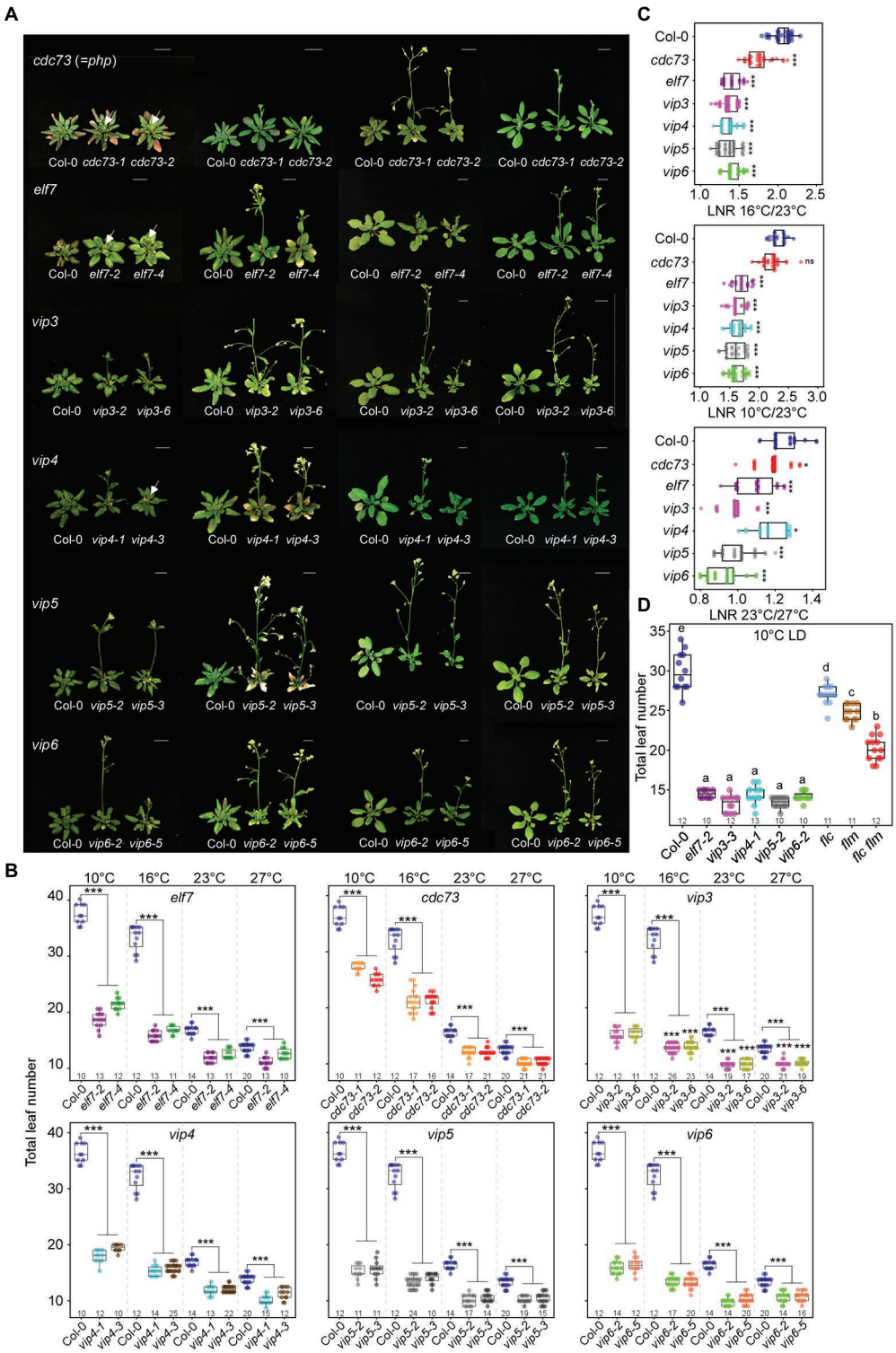

FIGURE 1 | Early flowering of polymerase II–associated factor 1 complex (PAF1C)-deficient mutants at all tested temperatures under long-day (LD) conditions. **(A,B)** Phenotype **(A)** and flowering time quantified as total leaf number **(B)** of PAF1C-deficient mutant lines at 10, 16, 23, and 27°C. Arrows indicate inflorescences. Note that the same leaf number data from Col-0 plants were used in each panel **(B)**. One-way ANOVA followed by Dunnett's multiple comparison tests were performed to test the statistical significance. Scale bar = 1 cm. **(C)** Leaf number ratio (LNR) of Col-0 and PAF1C-deficient mutants. **(D)** Flowering time comparison of PAF1C-deficient mutants with *flc*, *flm*, and *flc flm* mutants at 10°C. One-way ANOVA followed by Dunnett's multiple comparison tests were performed to test the statistical significance ($p < 0.05$). $^{*}p < 0.05$ and $^{***}p \leq 0.001$. Letters in **(D)** indicate significant difference by one-way ANOVA followed by Tukey's range tests Numbers above the *x*-axis represent *n*.

grown at 10 and 23°C. This indicates that the Col-0 plants and *cdc73* mutants grown at 23°C have similar transcriptome profiles. Clade II was further divided into plants grown at 23°C and plants grown at 10°C. Among plants grown at 10°C, Col-0 plants and *cdc73* mutants grouped together, whereas *elf7*, *vip3*, *vip4*, *vip5*, and *vip6* mutants grouped together. This expression profile-based classification was consistent with the flowering time changes of PAF1C-deficient mutants at low temperature. As both *cdc73* mutants flowered later than other PAF1C-deficient mutants (**Figure 1**) and *cdc73* mutants were grouped in the same clade with Col-0 plants based on RNA-seq data (**Figure 2A**), we excluded *CDC73* from further analyses.

We selected DEGs that showed increased or decreased transcript levels (>1.5-fold). Transcriptome analyses revealed large numbers of DEGs in PAF1C-deficient mutants at both 10 and 23°C (**Figure 2B**). We then analyzed DEGs that were commonly upregulated and downregulated in different mutants (**Figures 2C,D**). At 10°C, 1,519 genes were commonly downregulated in *elf7*, *vip3*, *vip4*, *vip5*, and *vip6* mutants, whereas 1,229 genes were commonly upregulated in these mutants (**Figure 2C**). At 23°C, 2,021 genes were commonly downregulated in *elf7*, *vip3*, *vip4*, *vip5*, and *vip6* mutants, and 1,352 genes were upregulated in these mutants (**Figure 2D**). These analyses indicated that the largest number of intersecting DEGs was in the set containing the *elf7*, *vip3*, *vip4*, *vip5*, and *vip6* mutants, suggesting that a large number of genes were commonly altered in these mutants at both temperatures. This observation was also consistent with the similar early flowering phenotypes of *elf7*, *vip3*, *vip4*, *vip5*, and *vip6* mutants at 10 and 23°C.

To understand the biological significance of the common DEGs in PAF1C-deficient mutants, we performed Gene Ontology (GO) analyses using the webtool DAVID (Ashburner et al., 2000). At 10°C, the downregulated genes showed significant enrichment for GO terms related to the response to transcription, microtubule-based movement, different metabolic processes, response to jasmonic acid, and stomatal complex development. The upregulated genes were enriched in GO terms related to different metabolic processes and response to different stimuli (**Supplementary Figure 2A**). At 23°C, the downregulated genes were enriched in GO terms related to response to Karrikin, different metabolic processes, MAPK cascade, and photosynthesis, whereas the upregulated genes were enriched with GO terms related to different metabolic processes, response to oxidative stress, and cell wall organization (**Supplementary Figure 2B**).

PAF1C Regulates the Expression of *FLC* and the Other *FLC*-Clade Genes

The Flowering Interactive Database (FLOR-ID; Bouché et al., 2016) contains known genes involved in regulating flowering time. To check whether PAF1C deficiency affects the expression of known flowering time genes, we analyzed which genes in FLOR-ID were included among the common DEGs in PAF1C-deficient mutants at 10 and 23°C (**Figures 2C,D**). As PAF1C is involved in maintaining the active transcription of its target genes (He et al., 2004; Oh et al., 2004; Yu and Michaels, 2010), we expect that the direct targets of PAF1C will be downregulated in the PAF1C-deficient plants. Interestingly, our analyses showed that 26 and 27 flowering time genes were downregulated at 10 and 23°C, respectively, and both sets included *FLC* and *MAF1*, *2*, *3*, *4*, and *5* (**Figures 3A,B**).

We performed RT-qPCR analyses to confirm the downregulation of *FLC* and *FLC*-clade genes in PAF1C-deficient mutants at 10°C. Among the alternatively spliced forms produced from the *FLM* locus, *FLM-ß* is the functional form (Scortecci et al., 2001; Pose et al., 2013); therefore, we measured *FLM-ß* transcript levels for *FLM*. The RT-qPCR showed that that *FLC*, *FLM*, and *MAF2–MAF5* showed significant downregulation in PAF1C-deficient mutants (**Figure 3C**). *FLC* showed 17.6-fold downregulation in *elf7-2* mutants, 18-fold in *vip3-2* mutants, 16-fold in *vip4-1* mutants, 20.1-fold in *vip5-2* mutants, and 18.3-fold in *vip6-2* mutants (**Figure 3C**), consistent with a previous study (Oh et al., 2004). Similarly, *FLM-ß* showed 15.6- to 18.2-fold downregulation in PAF1C-deficient mutants. *MAF2* showed 2.1-fold downregulation in *elf7-2* mutants, 2.9-fold in *vip3-2* mutants, 1.9-fold in *vip4-1* mutants, 2.7-fold in *vip5-2* mutants, and 2.6-fold in *vip6-2* mutants at 10°C. Similarly, *MAF3* was downregulated by 2.1- to 4.6-fold in the PAF1C-deficient mutants at 10°C. *MAF4* mRNA levels were downregulated by 4.1- to 7.1-fold and *MAF5* mRNA levels were downregulated 2.2- to 4.4-fold in the PAF1C-deficient mutants at 10°C.

We then measured the mRNA levels of *FT*, *TSF*, and *SOC1* by RT-qPCR and found that the mRNA levels of *FT*, *TSF*, and *SOC1* were significantly higher in the PAF1C-deficient mutants at 10 and 23°C compared with the wild type. *FT* mRNA levels were increased by 3.1- to 3.8-fold in the PAF1C-deficient mutants at 10°C (**Figure 3D**). At 23°C, *FT* was upregulated by 1.8- to 2.3-fold. *TSF* was also significantly upregulated in the PAF1C-deficient mutants at both temperatures. *SOC1* transcript levels showed a similar pattern, with a fold increase of 3.2–4.0 and 3.1–4.1 in PAF1C-deficient mutants at 10 and 23°C, respectively, consistent with the downregulation of *FLC* and *FLC*-clade genes in PAF1C-deficient mutants (**Figure 3C**). These results suggested that functional PAF1C is required for the expression of *FLC* and *FLC*-clade genes and that a lesion in one of its components results in the downregulation of *FLC* and *FLC*-clade genes, which leads to the derepression of *FT*, *TSF*, and *SOC1*, and early flowering. Furthermore, considering that the expression of all *MAF* genes was affected in PAF1C-deficient mutants and PAF1C-deficient mutants flowered significantly earlier than *flc flm* double mutants (**Figure 1D**), it is likely that the *MAF2–MAF5* genes play a significant role in floral repression at chilling temperatures. Although *FLC* and *FLC*-clade genes are known to undergo alternative splicing and their splice variants might have differential effects on flowering time (Caicedo et al., 2004; Lee et al., 2013; Pose et al., 2013; Rosloski et al., 2013), our RNA-seq data showed no significant difference in the levels of the splice variants of *FLC* and *FLC*-clade genes (**Supplementary Figure 3**), except for their overall downregulation, suggesting that the

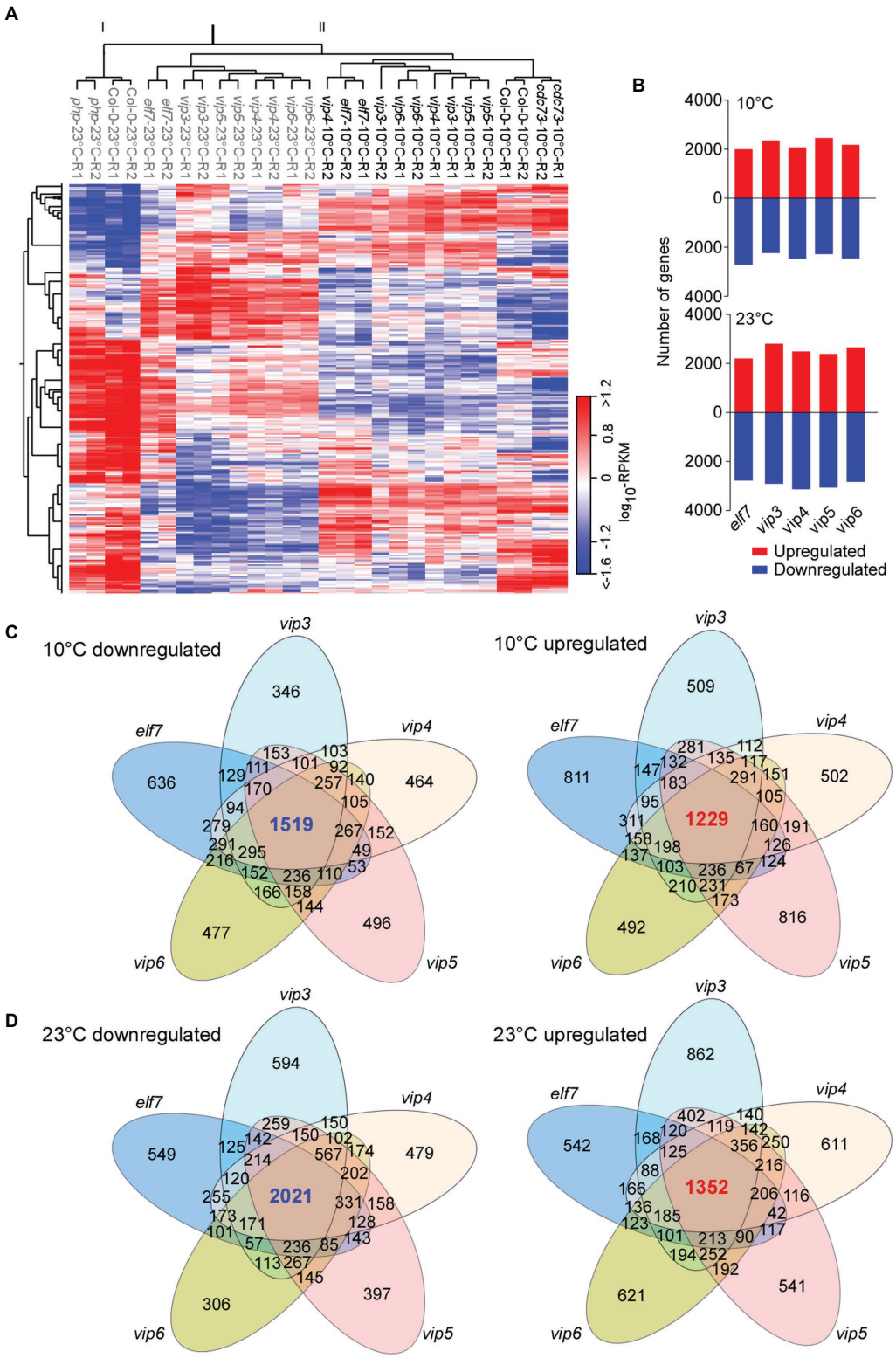

FIGURE 2 | Transcriptome analyses of PAF1C-deficient mutants. **(A)** Heatmap showing the global expression differences between the wild type (Col-0) and PAF1C-deficient mutants. The genotypes of plants grown at 23°C are shown in grey, whereas plants grown at 10°C are shown in black. **(B)** Differentially expressed genes (DEGs) in PAF1C-deficient mutants compared to wild-type (Col-0) seedlings at 10°C (upper panel) and 23°C (lower panel). **(C,D)** Venn diagrams representing the commonly downregulated and upregulated genes at 10°C **(C)** and 23°C **(D)** in PAF1C-deficient mutants.

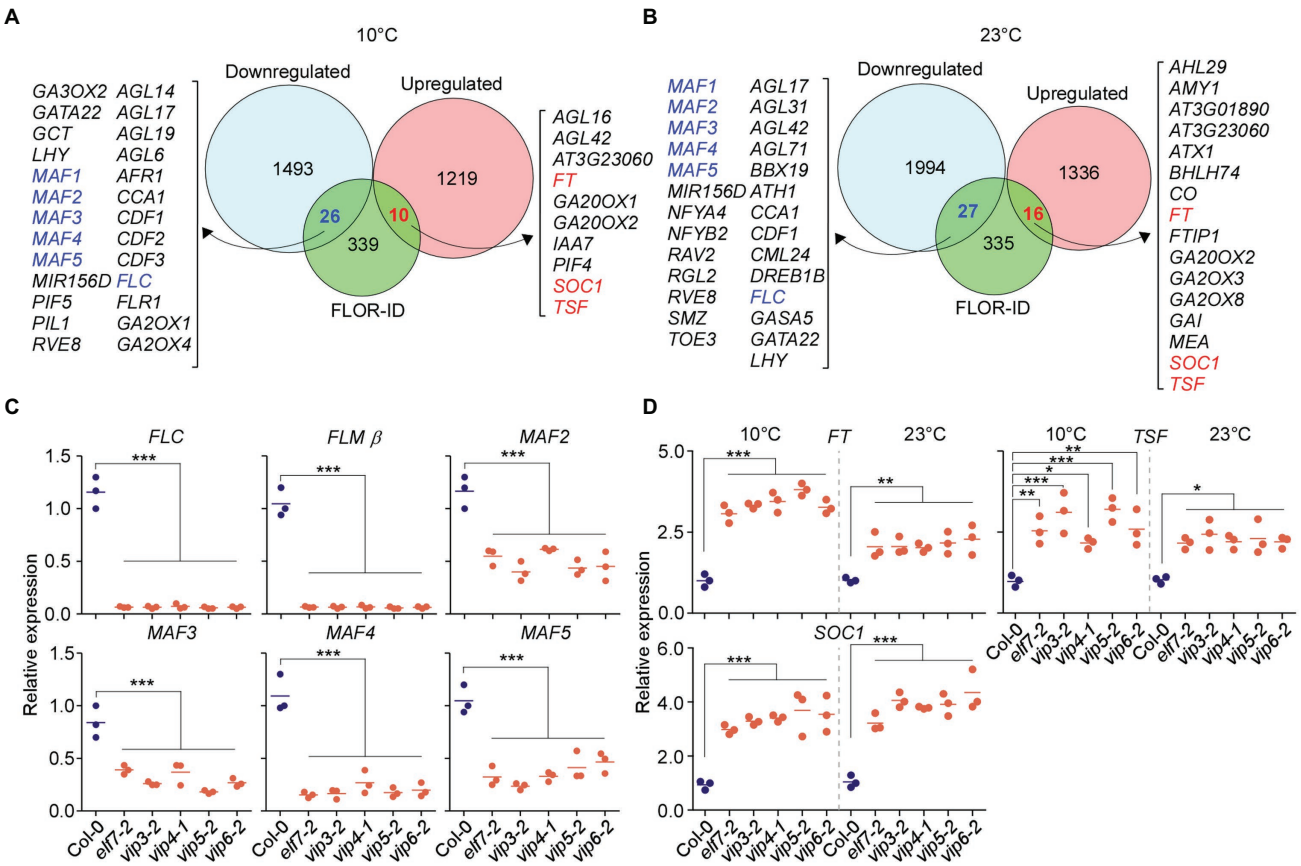

FIGURE 3 | Polymerase II–associated factor 1 complex regulates expression of *FLOWERING LOCUS C* (*FLC*) and the *FLC*-clade genes *MADS AFFECTING FLOWERING1* (*MAF1*)/*FLOWERING LOCUS M* (*FLM*) and *MAF2–MAF5*. **(A,B)** Commonly downregulated and upregulated flowering genes in PAF1C-deficient mutants at 10°C **(A)** and 23°C **(B)**. **(C)** qPCR confirmation of downregulation of *FLC* and *FLC*-clade genes in PAF1C-deficient mutants at 10°C. **(D)** mRNA levels of *FLOWERING LOCUS T* (*FT*), *TSF*, and *SUPPRESSOR OF OVEREXPRESSION OF CO1* (*SOC1*) in PAF1C-deficient mutants at 10 and 23°C. One-way ANOVA followed by Dunnett's multiple comparison tests were performed to test the statistical significance. $^{*}p < 0.05$; $^{**}p < 0.01$; and $^{***}p \leq 0.001$.

flowering time change seen in PAF1C-decificient mutants was not associated with the differential splicing patterns of *FLC* and *FLC*-clade genes.

PAF1C Deficiency Alters the Epigenetic Status of the *FLC*-Clade Genes

Our expression analyses showed that in addition to *FLC* and *FLM*, *MAF2–MAF5* were downregulated in PAF1C-deficient mutants (**Figure 3**), suggesting that this downregulation may be due to the altered epigenetic status at these loci in PAF1C-deficient mutants. To test this possibility, we analyzed the levels of the repressive H3K27me3 marks and permissive H3K4me3/H3K36me3 marks of *FLC* and the *FLC*-clade genes in *vip3-2* mutants (as a representative PAF1C-deficient mutant line) and wild-type plants grown at 10°C. Four different qPCR primer sets (P1–P4), spanning the entire gene bodies of the target genes, were used to assess the enrichment of the repressive/permissive marks (**Figure 4A**).

Consistent with their downregulation, the *FLC* and *FLC*-clade genes showed significantly increased enrichment of the repressive H3K27me3 marks throughout their gene bodies in *vip3* mutants (**Figure 4B**). In *FLC*, the highest enrichment (5.8-fold higher enrichment compared to wild-type plants) of repressive H3K27me3 marks was observed in the P2 region, which contains the transcription start site (**Figure 4B**), consistent with a previous finding (He et al., 2004). Significantly higher enrichment was also observed in the P1 (2.9-fold) and P3 (2.8-fold) regions of *FLC*. In *FLM* chromatin, the H3K27me3 enrichment was highest in the P1 region (5.8-fold) followed by P2 (3.1-fold) and P3 (2.0-fold) regions. *MAF2* and *MAF3* showed similar H3K27me3 patterns with the highest enrichment in the P1 region (3.7- and 5.3-fold, respectively), followed by P2 (3.6- and 4.4-fold, respectively) and P3 regions (2.4- and 2.7-fold, respectively). The enrichment of H3K27me3 in the *MAF5* chromatin was highest in the P3 and P2 regions (3.5- and 3.4-fold, respectively) followed by P1 with 2.4-fold higher enrichment of H3K27me3 in *vip3* mutants compared to wild-type plants at 10°C. H3K27me3 enrichment in the P4 regions of *FLC*, *FLM*, *MAF2*, and *MAF3* of *vip3* mutants was comparable with wild-type samples, whereas *MAF4* and *MAF5* showed

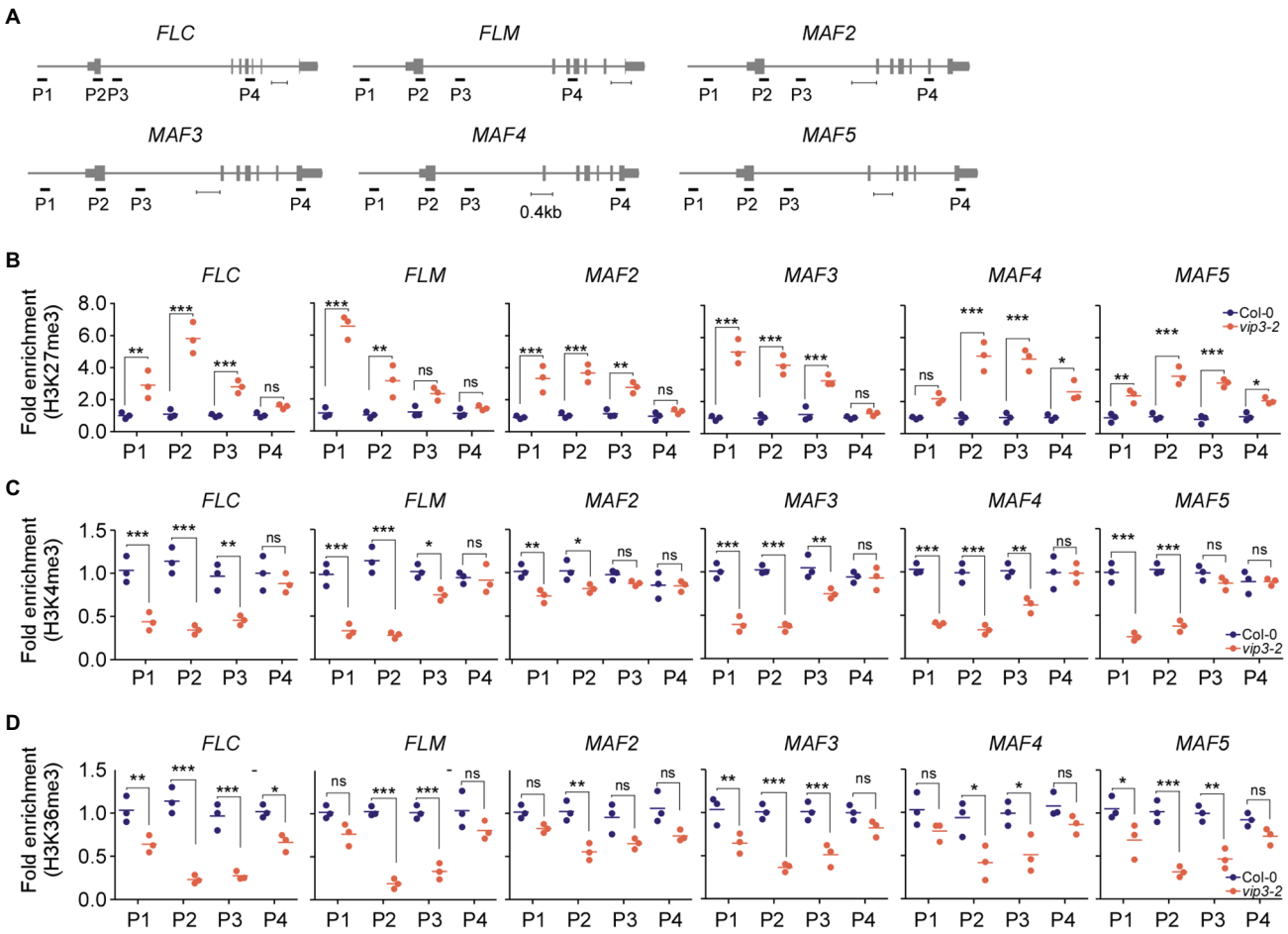

FIGURE 4 | Polymerase II–associated factor 1 complex deficiency alters the epigenetic status of chromatin of the *FLC* and the *FLC*-clade genes *MAF1/FLM* and *MAF2–MAF5*. **(A)** Schematic representation of the genomic regions of *FLC* and *FLC*-clade genes and the regions amplified for chromatin immunoprecipitation (ChIP) assays. Scale bar = 0.4 kb. Note that our P2 region in *FLC* partially overlaps with the region that was used in a previous study (He et al., 2004). In the case of *FLM*, our P2 region is included in a region that was previously shown to be affected (He et al., 2004). **(B–D)** Fold enrichment of the repressive epigenetic H3K27me3 marks **(B)**, permissive H3K4me3 marks **(C)**, and permissive H3K36me3 marks **(D)** at the genomic regions of *FLC* and *FLC*-clade genes in wild-type (Col-0) and PAF1C-deficient *vip3* mutant seedlings. For each primer pair, the enrichment was normalized to the wild-type control (Col-0). One-way ANOVA followed by Dunnett's multiple comparison tests were performed to test the statistical significance. $^{*}p < 0.05$; $^{**}p < 0.01$; $^{***}p \leq 0.001$; and ns: not significant.

slightly higher enrichment in the P4 regions (1.3- and 2.5-fold, respectively) in *vip3* mutants (**Figure 4B**).

By contrast, enrichment of the permissive H3K4me3 marks was significantly reduced in the chromatin of *FLC* and *FLC*-clade genes in *vip3* mutants, primarily in the P1 and P2 regions (**Figure 4C**). Enrichment of H3K4me3 in the *FLC* chromatin in *vip3* mutants was reduced 3.3-fold in the P2 region, 2.4-fold in P1, and 2.1-fold in P3 compared to wild-type plants. *FLM* also showed reduced enrichment of H3K4me3 marks in the P2 (4.1-fold) and P1 (2.9-fold) regions. In the *MAF2* chromatin, reduced H3K4me3 enrichment was seen in the P1 (1.4-fold) and P2 (1.3-fold) regions. In addition, in the *MAF3-5* chromatin, H3K4me3 enrichment was significantly lower in the P2 region (2.8-, 3.0-, and 2.7-fold, respectively) and the P1 region (2.6-, 2.5-, and 3.9-fold, respectively) in *vip3* mutants (**Figure 4C**). Similar reduction patterns were found for the H3K36me3 mark at the gene bodies of these genes, with significantly reduced enrichment at the P2 and P3 regions (**Figure 4D**). Taken together, these results suggest that PAF1C is required to maintain permissive epigenetic marks and prevent deposition of repressive marks at the *FLC* and *FLC*-clade genes, thereby maintaining their active transcription.

FLC-Clade Genes Are Upregulated in Wild-Type Plants at 10°C

The early flowering of PAF1C-deficient mutants at 10°C is likely due to the combinatorial effect of FLC, FLM, and the other MAFs, suggesting the functional importance of MAF2–MAF5 at low temperature (10°C). To test whether expression of these genes is upregulated in wild-type plants at 10°C, we compared the transcript levels of these genes in wild-type plants at 10 and 23°C using our RNA-seq data. This analysis revealed upregulation of *FLC*, *FLM*, and *MAF2–MAF5*

in wild-type plants at 10°C compared to 23°C by at least 1.5-fold (**Figure 5A**). RT-qPCR analyses also showed statistically significant induction of *FLC*, *FLM*, and *MAF2–MAF5* in wild-type plants at 10°C compared to 23°C (**Figure 5B**). Consistent with the upregulation of *FLC* and *FLC*-clade genes, transcript levels of *FT* and *TSF*, their downstream targets, were significantly reduced (>3-fold) in wild-type plants at 10°C in comparison to 23°C (**Figure 5C**). This suggests that these MAFs might play important roles in modulating flowering time at chilling temperatures by regulating *FT* and *TSF*.

FLC-Clade Genes Are Important for Floral Repression at Chilling Temperatures

Polymerase II–associated factor 1 complex modulates the expression of downstream genes by recruiting a number of histone modifiers, including SET DOMAIN GROUP8 (SDG8; Wood et al., 2003; Ng et al., 2003a; Kim et al., 2005). SDG8 recruited by PAF1C then regulates the expression of *FLC* and *FLM*; therefore, a mutation in *SDG8* causes early flowering at normal temperatures (Kim et al., 2005). Because the flowering response of *sdg8* mutants under chilling-stress temperatures is not known, we analyzed the flowering time of *sdg8* mutants at 10 and 23°C. We found that the *sdg8* mutants flowered significantly earlier than *flc*, *flm*, and *flc flm* mutants at 10°C (**Figures 6A,B**). The *sdg8* mutants flowered with 18.1 ± 1.0 leaves, which was significantly earlier than *flc* mutants (32.6 ± 1.6 leaves), *flm* mutants (26.5 ± 1.7 leaves), and *flc flm* double mutants (23.0 ± 1.1 leaves) at 10°C. However, at 23°C, the flowering time of *sdg8* mutants (8.5 ± .6 leaves) was only slightly earlier than *flc* and *flm* mutants (10.0 ± 0.7 and 9.7 ± 0.7 leaves, respectively) and was comparable to *flc flm* double mutants (8.4 ± .5 leaves; **Figure 6B**). LNR analyses revealed significantly decreased LNR values of *sdg8* mutants to low temperature (**Figure 6C**), indicating that the temperature responsiveness of *sdg8* mutants was reduced.

To determine whether *MAF* genes play a role in the regulation of flowering time in *sdg8* mutants, we first analyzed publicly

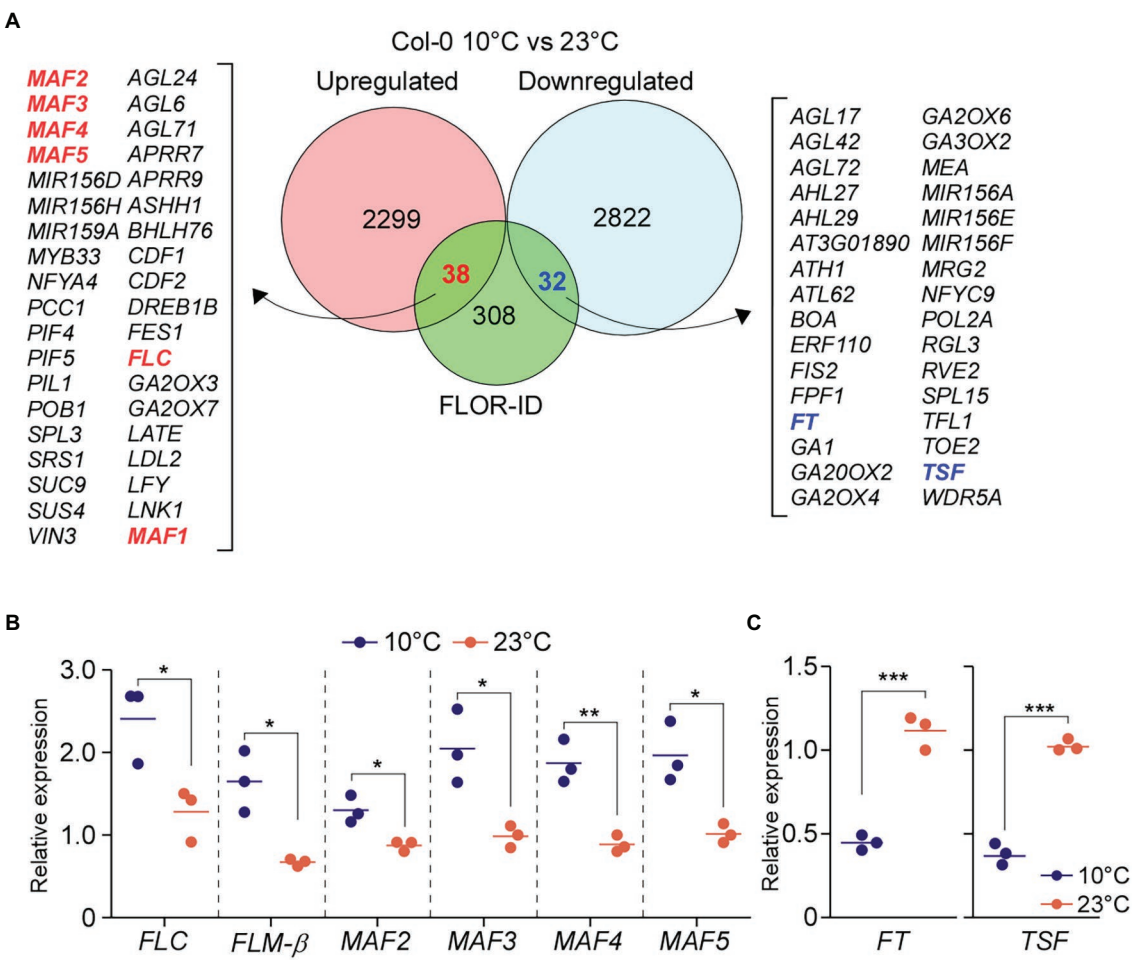

FIGURE 5 | Low temperature induces the expression of *FLC* and *FLC*-clade genes. **(A)** Differentially expressed genes (DEGs) between wild-type (Col-0) seedlings grown at 10 and 23°C under LD conditions. **(B,C)** Relative mRNA levels of *FLC* and *FLC*-clade genes **(B)** and *FT* **(C)** at 10°C under LD conditions. One-way ANOVA followed by Dunnett's multiple comparison tests were performed to test the statistical significance. $^{*}p < 0.05$; $^{**}p < 0.01$; and $^{***}p \leq 0.001$.

available RNA-seq data for *sdg8* mutants grown at 16°C with or without shifting to 25°C (GSE85282; Pajoro et al., 2017) and then found the intersection of (1) the set of DEGs in *sdg8* mutants, (2) the genes that were commonly downregulated in PAF1C-deficient mutants at 10°C (**Figure 2C**) and 23°C (**Figure 2D**), and (3) the list of flowering time genes from FLOR-ID (Bouché et al., 2016). From this comparison, we found that *FLC*, *FLM*, and *MAF3–MAF5* were commonly downregulated in *sdg8* mutants (**Figure 6D**; **Supplementary Figure 4**), like in PAF1C-deficient mutants (**Figure 3**). *MAF2*, which showed 1.8-fold downregulation in *sdg8* mutants, was not identified here, due to the criteria for selecting DEGs (2-fold change).

We then performed RT-qPCR to confirm the downregulation of these genes at 10°C. The RT-qPCR results showed statistically significant downregulation of *FLC*, *FLM-ß*, and *MAF2–MAF5* mRNA levels in *sdg8* mutants at 10°C (**Figure 6E**). *FLC* mRNA levels were decreased by 13.2-fold, whereas *FLM-ß* showed 15.9-fold downregulation in *sdg8* mutants at 10°C. In addition, expression of *MAF2–MAF5* was downregulated by 2.0-, 1.7-, 7.3-, and 1.9-fold, respectively, in *sdg8* mutants at 10°C (**Figure 6E**). Taken together, these results suggested that the early flowering phenotype of *sdg8* mutants at chilling temperature is mediated by the downregulation of *FLC* and *MAF* genes. However, it should be noted that *sdg8* mutants flowered slightly later than PAF1C-dificient mutants at 10°C (**Supplementary Figure 5**), suggesting a possibility that the PAF1C recruits an additional histone modifier(s), besides SDG8, to regulate the expression of the *FLC*-clade genes.

Knockout/Knockdown of *FLC* and *FLC*-Clade Genes Results in Extremely Early Flowering at 10°C

To genetically confirm the importance of *MAF* genes in repressing flowering at chilling temperatures, we used amiRNAs to repress the *MAF* genes. To this end, we designed two amiRNAs that simultaneously target *MAF2–MAF5* (**Figure 7A**) and overexpressed these amiRNAs in *flc flm* double mutants. Two independent transgenic lines overexpressing amiRNAs against *MAF2–MAF5* (*35S::amiR-MAF2-5 flc flm #1* and *#2*) flowered significantly earlier than *flc flm* double mutants (**Figures 7B,C**). At 10°C, The *35S::amiR-MAF2-5 flc flm #1* and *#2* plants flowered with an average TLN of 12.1 to 12.9 leaves (c.f., wild-type plants: 32.8 ± 3.8), indicating that knockout/down of *FLC* and all five *FLC*-clade genes caused extremely early flowering at 10°C. Furthermore, these transgenic lines flowered earlier than *flc flm* double mutants (21.6 ± 1.6 leaves; **Figure 7C**). Interestingly, both *35S::amiR-MAF2-5 flc flm* lines flowered

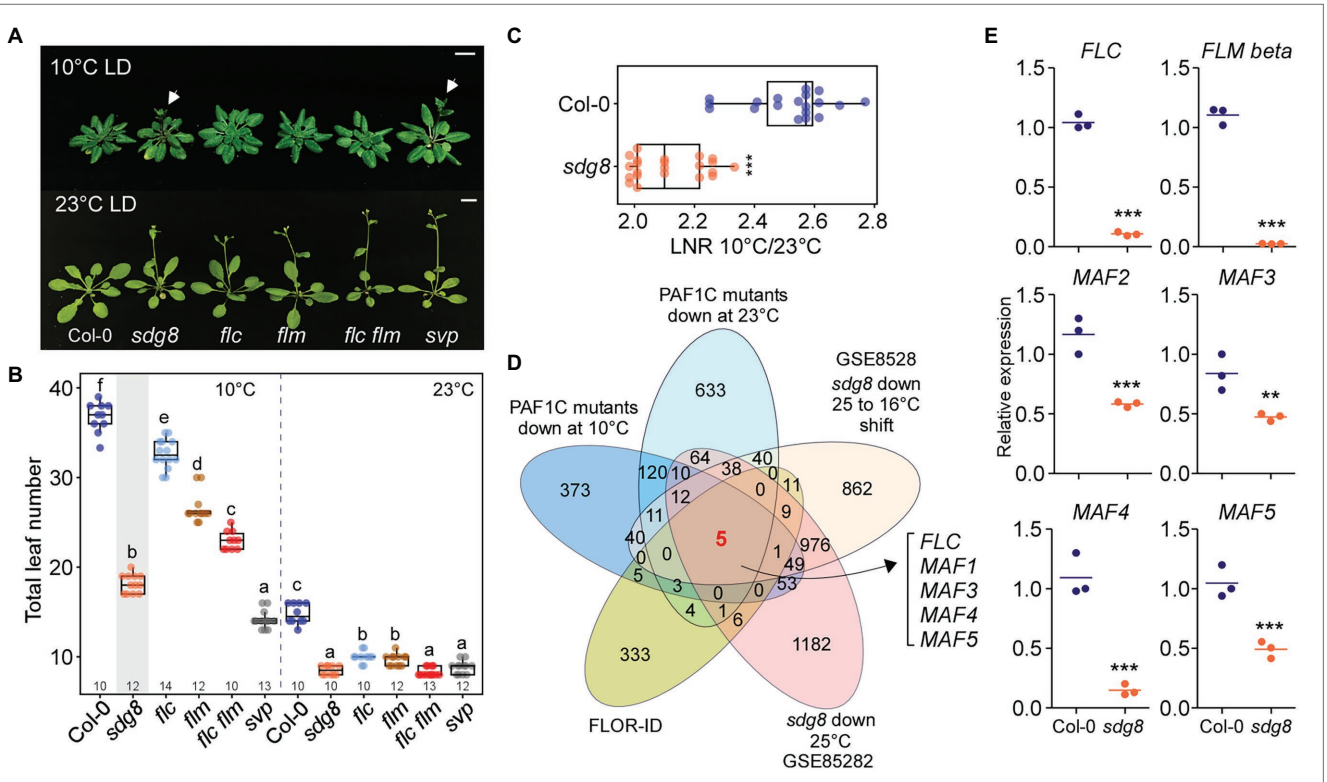

FIGURE 6 | *MAF* genes are important for floral repression at low temperature. **(A,B)** Flowering phenotype **(A)** and flowering time **(B)** of *sdg8*, *flc*, *flm*, *flc flm*, and *short vegetative phase* (*svp*) mutants at 10 and 23°C under LD conditions. Arrows indicate inflorescences. **(C)** Leaf number ratio (LNR; 10°C/23°C) of *sdg8* mutants. **(D)** Venn diagram of the genes that were commonly downregulated in *sdg8* mutants and PAF1C-deficient mutants at different temperatures. **(E)** Reverse transcription quantitative PCR (RT-qPCR) of *FLC* and *FLC*-clade genes in the wild type (Col-0) and *sdg8* mutants at 10°C under LD conditions. One-way ANOVA followed by Dunnett's multiple comparison tests were performed to test the statistical significance. $*p < 0.05$; $**p < 0.01$; $***p \leq 0.001$; and ns: not significant. Letters indicate significant differences by one-way ANOVA followed by Tukey's range tests ($p < 0.05$). Numbers above the *x*-axis in **(B)** represent *n*. Scale bar = 1 cm.

earlier than *svp* mutants (14.6 ± 1.4 leaves). However, at 23°C, The *35S::amiR-MAF2-5 flc flm #1* and *#2* plants flowered with an average TLN of 11.1–11.4 leaves (c.f., wild-type plants: 16.0 ± 1.1), which was similar to the TLN of *flc flm* double (11.7 ± 0.6 leaves) and *svp* single mutants (11.1 ± 0.7 leaves; **Figure 7C**). These results highlighted the importance of the MAF2–MAF5 transcription factors in repressing flowering at chilling temperatures.

To confirm that this early flowering of *35S::amiR-MAF2-5 flc flm #1* (1–1 and 13–3) and *#2* (1–4 and 2–2) plants was indeed due to the downregulation of *MAF2–MAF5*, we performed RT-qPCR analyses. These analyses confirmed the transgenic seedlings showed significantly lower *MAF* mRNA levels compared with the wild-type plants and *flc flm* double mutants (**Figure 7D**). Furthermore, *MAF2–MAF5* mRNA levels were significantly lower in *35S::amiR-MAF2-5 flc flm #1* plants than in *35S::amiR-MAF2-5 flc flm #2* plants, except *MAF4*. The stronger reduction of *MAF* transcript levels in the *35S::amiR-MAF2-5 flc flm #1* plants was consistent with their earlier flowering time phenotype compared with *35S::amiR-MAF2-5 flc flm #2* plants (**Figure 7C**). Taken together, these data suggest that ablation of function of *FLC* and all *FLC*-clade members resulted in earlier flowering than *flc flm* mutants at chilling temperatures; therefore, MAF2–MAF5 also play a role in repressing flowering at chilling temperatures.

MAFs Physically Interact With SVP to Form Repressor Complexes

Loss of *SVP* function results in early flowering across a broad range of temperatures (10°C–27°C; Lee et al., 2013). SVP interacts with FLC (Fujiwara et al., 2008; Li et al., 2008) and with FLM (Lee et al., 2013; Pose et al., 2013). *In vivo* and yeast two-hybrid (Y2H) analyses showed that SVP interacts with MAF2 and MAF4 (Gu et al., 2013). Since the *35S::amiR-MAF2-5 flc flm* (*#1* and *#2*) plants showed significantly earlier flowering at 10°C compared with *svp* mutants (**Figure 7C**), one possible scenario is that SVP alone is insufficient to repress flowering at 10°C and may require FLC-clade proteins to repress flowering.

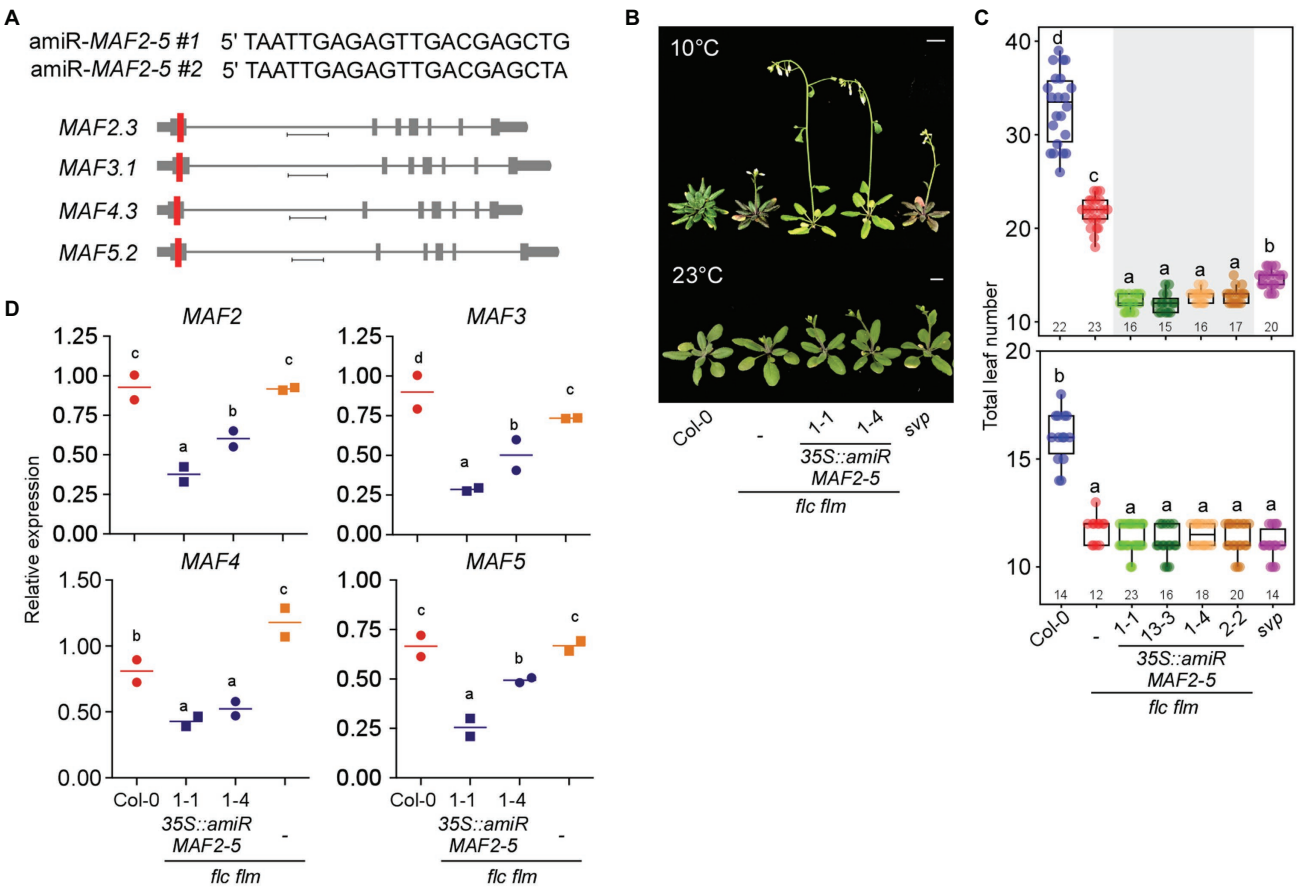

FIGURE 7 | Knockout/down of *FLC* and *MAFs* together results in precocious flowering at chilling temperatures. **(A)** Sequences of artificial microRNAs (amiRNAs) designed to knock down *MAF2–MAF5* genes (top) and schematic representation of their location (red vertical line) in a predominantly expressed spliced variant of *MAF2–MAF5* genes (bottom). Scale bar: 0.4 kb **(B,C)** Flowering phenotype **(B)** and flowering time **(C)** of *35S::amiR-MAF2-5 flc flm* transgenic seedlings at 10 and 23°C under LD conditions. Scale bar = 1 cm. **(D)** RT-qPCR confirmation of knockdown of *MAF2–MAF5* in *35S::amiR-MAF2-5 flc flm* transgenic lines. Letters indicate significant differences by one-way ANOVA followed by Tukey's range tests ($p < 0.05$). Numbers above the *x*-axis in **(C)** represent *n*.

To test whether FLC-clade proteins physically interact with SVP, we first used two recently developed artificial intelligence (AI)–based deep learning programs that were designed to predict protein–protein interactions: D-SCRIPT (Sledzieski et al., 2021) and PPI-Detect (Romero-Molina et al., 2019). These programs produce an interaction score between 0 (no interaction predicted) and 1 (interaction strongly predicted). In these analyses, FLC was used as a known interacting partner of SVP (Li et al., 2008), and PP2AA3 was used a negative control. The FLC–SVP interaction scores were 0.977 (D-SCRIPT) and 0.705 (PPI-Detect), whereas the PP2AA3–SVP interaction scores were 0.004 (D-SCRIPT) and 0.278 (PPI-Detect; **Figure 8A**). From D-SCRIPT analyses, the MAF2–SVP, MAF3–SVP, MAF4–SVP, and MAF5–SVP interaction scores were 0.789, 0.740, 0.586, and 0.779, respectively. From PPI-Detect analyses, the MAF2–SVP, MAF3–SVP, MAF4–SVP, and MAF5–SVP interaction scores were 0.584, 0.512, 0.915, and 0.822, respectively. All of these interaction scores were above the cut-off value of 0.5, suggesting that SVP interacts with MAF2–MAF5 *in vivo*.

We then performed Y2H analyses to experimentally validate the predicted interactions. Indeed, Y2H analyses showed that SVP interacts with MAF2–MAF5 in yeast cells (**Figure 8B**). To further test these interactions *in vivo*, we performed Co-IP experiments using Arabidopsis mesophyll protoplasts. To this end, *35S::2×HA:SVP* and *35S::GFP:MAF* vectors were transiently co-expressed in protoplasts to produce HA-tagged SVP and GFP-tagged MAF2–MAF5 proteins and then the transfected protoplasts were shifted to 10°C to test the protein–protein interaction at 10°C. We precipitated protein extracts using GFP-Trap and probed the resulting precipitates with anti-HA antibodies. SVP-2×HA successfully co-immunoprecipitated with each MAF transcription factor (**Figure 8C**; asterisk), confirming the interactions between SVP and MAFs. Taken together, these results suggest that MAF2–MAF5, like FLC and FLM, physically interact with SVP, further implying that SVP forms a repressor complex including FLC and MAFs. It is therefore likely that the formation of the complex leads to efficient floral repression, thus allowing the plant to acclimate to chilling temperatures.

SVP-Mediated Floral Repression Likely Requires *FLC* and *FLC*-Clade Genes

Since the PAF1C-deficient mutants showed strong early flowering at 10°C (**Figure 1**), we tested whether *SVP* transcript levels were affected in PAF1C-deficient mutants, as *svp* mutants flower early across a range of temperatures (10°C–27°C; Lee et al., 2013). RT-qPCR analyses showed that *SVP* mRNA levels in PAF1C-deficient mutants were similar to those of Col-0 plants at both 10 and 23°C (**Figure 9A**; He et al., 2004). This suggested that the flowering time change seen in PAF1C-deficient mutants at both 10 and 23°C was independent of *SVP* transcript levels.

We then tested whether SVP requires PAF1C to delay flowering time. For this experiment, we used *elf7-2* and *vip4-1* mutants as representative PAF1C-deficient mutants and crossed them with *35S::SVP:HA* plants. The *35S::SVP:HA* plants showed delayed flowering (23.3 ± 1.7 leaves) at 23°C, but the *35S::SVP:HA elf7-2* plants flowered with 10.4 ± .7 leaves (**Figures 9B,C**). Considering that *elf7-2* mutants flowered with 9.6 ± 0.9 leaves at 23°C, this genetic interaction study showed that the late flowering caused by *SVP* overexpression was almost completely suppressed by *elf7-2* mutation. Similarly, the late flowering of *35S::SVP:HA* plants was strongly suppressed by *vip4-1* mutation (**Supplementary Figure 6**). These results suggested that *SVP* overexpression was unable to delay flowering in the absence of a functional PAF1C.

Short vegetative phase was unable to repress flowering in *elf7-2* mutants, which have dramatically decreased mRNA levels of *FLC* and *FLC*-clade genes (**Figure 3B**), suggesting the possibility that SVP binding to its targets requires functional FLC and FLC-clade transcription factors. To test this hypothesis, we took advantage of a publicly available ChIP-seq dataset (GSE54881) for SVP-GFP in the presence/absence of *FLC* (*FRI FLC* and *FRI flc*; Mateos et al., 2015). Consistent with a previous study (Mateos et al., 2015), the number of targets bound by SVP-GFP was substantially reduced in plants without functional FLC (*FRI flc*), compared to the plants with functional FLC (*FRI FLC*; **Supplementary Figure 7**). In terms of the number of bound targets, SVP-GFP was only able to bind to 39.2% of its target genes in the absence of functional FLC (the number of targets bound by SVP-GFP in *FRI FLC* was set to 100%; **Supplementary Figure 7**A). Furthermore, SVP-GFP was able to bind to 553 additional target genes in the presence of FLC (**Supplementary Figure 7B**; Mateos et al., 2015), indicating the importance of FLC for SVP binding ability. Since other FLC-clade transcription factors also interact with SVP (**Figure 8**), these results suggest that the FLC-clade transcription factors play a similar role, especially at low temperatures.

DISCUSSION

In Arabidopsis, PAF1C regulates flowering primarily through epigenetic modulation of *FLC* and *FLM* expression under standard growth conditions (Kim et al., 2005; Yu and Michaels, 2010). However, the role of PAF1C in regulating flowering time at chilling temperatures remains unknown. In this study, we show that PAF1C not only regulates *FLC* and *FLM*, but also regulates the entire *FLC* clade of genes (*FLM/MAF1* and *MAF2–MAF5*), which play important roles in repressing flowering at low temperatures.

Several environmental factors, including temperature, affect flowering. At lower temperatures, Arabidopsis plants flower late compared to plants at elevated temperatures (Lee et al., 2013). Several MADS-box transcription factors, including FLC, FLM, and SVP, play an important role in delaying flowering (Lee et al., 2007, 2013). *FLC* and *FLM* are well-known to be epigenetically regulated by a number of histone modifiers, including SET domain-containing histone methyltransferases (He et al., 2003; Zhang et al., 2003; Oh et al., 2004; Nasim et al., 2021). PAF1C recruits these histone modifiers to modulate expression of its target genes, including *FLC*, *FLM*, and *MAF2* (Zhang and Van Nocker, 2002; He et al., 2003; Zhang et al., 2003; Oh et al., 2004).

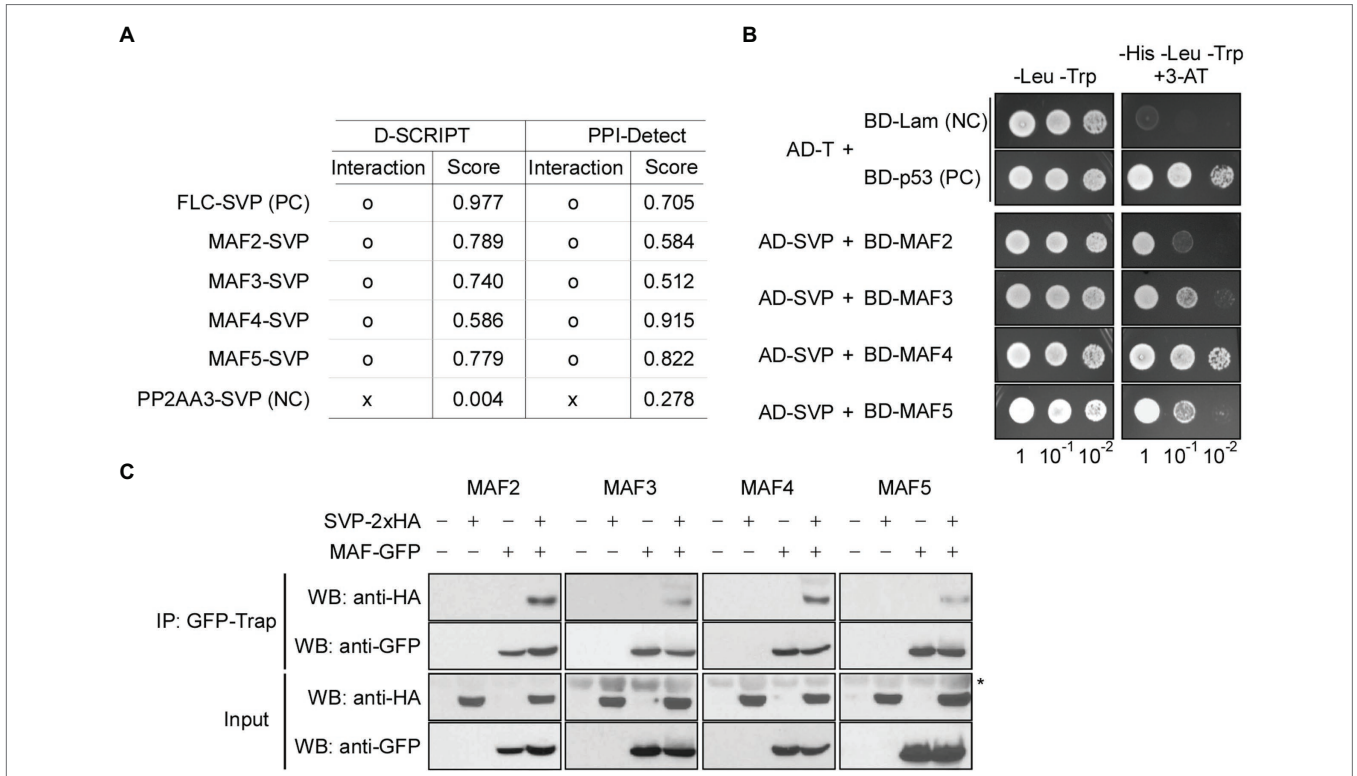

FIGURE 8 | MAFs physically interact with SVP. **(A)** Artificial intelligence (AI)–based prediction of interaction between MAFs and SVP. o: interaction, x: no interaction. Score (ranging from 0 to 1) represents the likelihood of interaction between two input proteins, where 0 represents no predicted interaction and 1 represents a high-confidence prediction that the proteins interact. **(B)** Yeast two-hybrid assays showing the interaction between MAFs and SVP. Positive control (PC): AD-T (SV40 large T-antigen) and BD-p53 (murine p53); negative control (NC): AD-T and BD-Lam (Lamin). **(C)** *In vivo* confirmation of MAF–SVP interactions *via* co-immunoprecipitation assays using Arabidopsis protoplasts at 10°C. PC; positive control, NC; negative control. The asterisk (*) represents a nonspecific signal on the anti-HA blot.

Polymerase II–associated factor 1 complex function is critical for proper plant growth and development, as lesions in PAF1C components result in strong defects in the vegetative and reproductive stages, such as severely stunted growth, stem cell maintenance defects, floral structure defects, and male sterility (Zhang et al., 2003; He et al., 2004; Oh et al., 2004; Fal et al., 2019). Flowering time analyses across a range of ambient temperatures showed that all PAF1C mutants flowered early in a temperature-independent manner with reduced expression of *FLC* and *FLC*-clade genes (**Figures 1**, **3**). This observation validates the previous findings that mutations in *VIP3*, *VIP5*, and *VIP6* result in reduced *FLC* and *FLM* expression and, hence, accelerated flowering (Zhang et al., 2003; Oh et al., 2004). However, flowering of *flc*, *flm*, and *flc flm* mutants was delayed at a chilling temperature of 10°C, indicating that these mutants showed temperature-sensitive flowering at 10°C. This further indicated that *FLC* and *FLM* function primarily from 16 to 27°C (Lee et al., 2013), suggesting that other genes may play important roles at lower temperatures. In this study, we observed that PAF1C-deficient mutants had lower transcript levels of *FLC* and the other *FLC*-clade genes at 10°C (**Figure 3**), indicating that *FLC*-clade genes are involved in repressing flowering at 10°C. Our ChIP-qPCR assays showed that downregulation of *FLC* and *FLC*-clade genes in PAF1C-deficient mutants is associated with higher enrichment of the repressive mark H3K27me3 and reduced levels of the permissive marks H3K4me3 and H3K36me3 in the chromatin of these genes (**Figure 4**). This is consistent with previous findings that PAF1C-deficient mutants had reduced *FLC* and *FLM* expression due to the reduced H3K4me3 levels at these loci (He et al., 2004; Oh et al., 2004; Xu et al., 2008). Moreover, we showed that PAF1C-mediated epigenetic regulation is not limited to *FLC* and *FLM*, but also affects the entire *FLC* clade.

A previous study showed that *MAF3* function is more important at lower temperatures than higher temperatures, as the *flc flm maf3* triple mutants flowered earlier than *flc flm* double mutants at 16°C, compared to 23°C (Gu et al., 2013). This supports our hypothesis that *FLC*-clade genes are important to repress flowering at low temperatures, as the *35S::amiR-MAF2-5 flc flm* plants flowered significantly earlier than the *flc flm* double mutants. Furthermore, we observed induction of *FLC* and *FLC*-clade genes in wild-type plants at 10°C (**Figure 5**), supporting previous findings that the mRNA levels of *FLC* and *FLM-ß* increased at low temperatures (16°C compared to 23°C; Lee et al., 2007; Pose et al., 2013). This might mean that plants increase transcription of these *FLC* family genes in response to low temperatures to ensure efficient floral

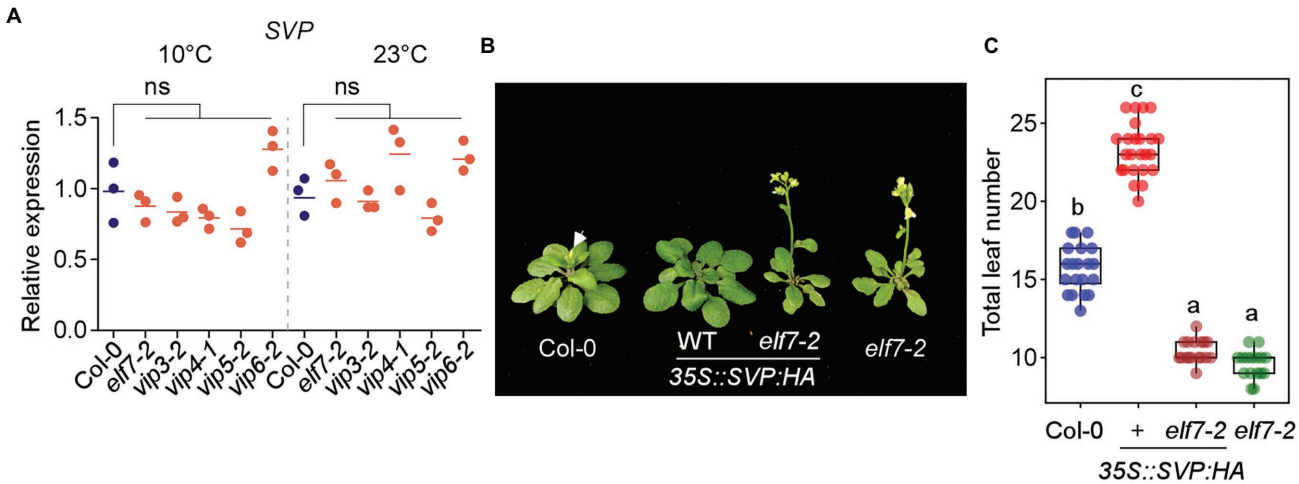

FIGURE 9 | SVP-mediated floral repression is dependent on *FLC* and *FLC*-clade genes. **(A)** *SVP* mRNA levels in PAF1C-deficient mutants at 10 and 23°C under LD conditions. ns; not significant. **(B,C)** Phenotype **(B)** and total leaf number **(C)** of *35S::SVP-HA* and *35S::SVP-HA elf7* plants. Note that these plants were first grown on medium containing phosphinothricin for 6 days at 23°C, transferred to soil, and then grown at 16°C. Letters indicate significant differences by one-way ANOVA followed by Tukey's range tests ($p < 0.05$).

repression, and this increase in transcription likely requires PAF1C. Since PAF1C components and functions are conserved from unicellular yeast to complex eukaryotic organisms (Tomson and Arndt, 2013), this regulatory mechanism might be conserved and have important functions in other plant species.

One important question raised by our observations is how these MAFs play such a critical role in floral repression at 10°C. One possible answer is their effect on SVP function. MADS-box transcription factors physically interact to form larger complexes that synergistically enhance their abilities to regulate transcription. Consistent with this, the MADS-box transcription factors FLC (Fujiwara et al., 2008; Li et al., 2008) and FLM (Lee et al., 2013) form floral repressor complexes with SVP and enhance their repression of flowering. Our data revealed that SVP interacts with all five MAF transcription factors *in vitro* and *in vivo* (**Figure 8**). This finding is consistent with our observation that in plants that lack (or have downregulated expression of) *FLC* and *FLC*-clade transcription factor genes, such as the PAF1C-deficient mutants and *35S::amiR-MAF2-5 flc flm* plants, SVP alone is not sufficient to repress flowering, especially at lower temperatures. Consistent with this notion, SVP overexpression was unable to delay flowering in PAF1C-deficient *elf7* and *vip4* mutants (**Figure 9**; **Supplementary Figure 6**), with significantly low levels of *FLC* and *FLC*-clade transcripts, suggesting that SVP function depends on FLC and FLC-clade transcription factors, and thus providing novel insight into SVP protein function at low temperatures. However, it should be noted that further genetic interaction analyses, such as analyses of plants overexpressing *SVP* in the *35S::amiR-MAF2-5 flc flm* background, will provide more direct genetic evidence.

Furthermore, our analysis of a previously published ChIP-seq dataset suggested that the presence/absence of FLC influences SVP binding to its targets, as the number of SVP-bound targets nearly doubled in the presence of functional FLC, implying that SVP function depends on FLC, as previously reported (Mateos et al., 2015). It is likely that FLC-clade transcription factors play similar roles, enhancing SVP binding to its targets and/or enhancing its ability to repress transcription; however, further experiments are required to confirm this hypothesis. It would be interesting to perform a genome-wide analysis of whether SVP can bind and repress its target genes in plants with reduced expression of *FLC* and *FLC*-clade genes, such as PAF1-deficient mutants or the *35S::amiR-MAF2-5 flc flm* plants.

In conclusion, our findings showed that PAF1C epigenetically regulates all the *FLC*-clade genes and that these genes play an important role in repressing flowering at chilling temperatures by forming floral repressor complexes with SVP. Wild-type plants accumulate higher levels of *FLC*-clade transcripts in response to chilling temperature to prevent precocious flowering. Our work uncovers the functional importance of MAF transcription factors in repressing flowering at chilling temperatures and increases the current understanding of how flowering is regulated in response to temperature.

DATA AVAILABILITY STATEMENT

The datasets presented in this study can be found in online repositories. The names of the repository/repositories and accession number(s) can be found at: https://www.ncbi.nlm.nih.gov/geo/, under the accession number GSE171778.

AUTHOR CONTRIBUTIONS

ZN and JA designed the research. ZN performed the bioinformatic analyses and conducted experimental work. HS helped with ChIP-qPCR experiments. SJ and GY provided technical assistance.

JA supervised the study. All authors contributed to the article and approved the submitted version.

FUNDING

This work was supported by a National Research Foundation (NRF) of Korea grant funded by the Korean government (NRF-2017R1A2B3009624 to JA) and Samsung Science and Technology Foundation under Project Number SSTF-BA1602-12.

ACKNOWLEDGMENTS

We thank Elizabeth S. Haswell for providing research materials, and Y. J. Kim for her technical assistance.

SUPPLEMENTARY MATERIAL

The Supplementary Material for this article can be found online at: https://www.frontiersin.org/articles/10.3389/fpls.2022.817356/full#supplementary-material

REFERENCES

Amasino, R. (2010). Seasonal and developmental timing of flowering. *Plant J.* 61, 1001–1013. doi: 10.1111/j.1365-313X.2010.04148.x

Ashburner, M., Ball, C. A., Blake, J. A., Botstein, D., Butler, H., Cherry, J. M., et al. (2000). Gene ontology: tool for the unification of biology. *Nat. Genet.* 25, 25–29. doi: 10.1038/75556

Balasubramanian, S., Sureshkumar, S., Lempe, J., and Weigel, D. (2006). Potent induction of *Arabidopsis thaliana* flowering by elevated growth temperature. *PLoS Genet.* 2:e106. doi: 10.1371/journal.pgen.0020106

Bernier, G., and Périlleux, C. (2005). A physiological overview of the genetics of flowering time control. *Plant Biotechnol. J.* 3, 3–16. doi: 10.1111/j.1467-7652.2004.00114.x

Betz, J., Chang, M., Washburn, T., Porter, S., Mueller, C., and Jaehning, J. (2002). Phenotypic analysis of Paf1/RNA polymerase II complex mutations reveals connections to cell cycle regulation, protein synthesis, and lipid and nucleic acid metabolism. *Mol. Gen. Genomics.* 268, 272–285. doi: 10.1007/s00438-002-0752-8

Bouché, F., Lobet, G., Tocquin, P., and Périlleux, C. (2016). FLOR-ID: an interactive database of flowering-time gene networks in *Arabidopsis thaliana*. *Nucleic Acids Res.* 44, D1167–D1171. doi: 10.1093/nar/gkv1054

Boyes, D. C., Zayed, A. M., Ascenzi, R., McCaskill, A. J., Hoffman, N. E., Davis, K. R., et al. (2001). Growth stage–based phenotypic analysis of *Arabidopsis*: a model for high throughput functional genomics in plants. *Plant Cell* 13, 1499–1510. doi: 10.1105/TPC.010011

Caicedo, A. L., Stinchcombe, J. R., Olsen, K. M., Schmitt, J., and Purugganan, M. D. (2004). Epistatic interaction between *Arabidopsis* FRI and FLC flowering time genes generates a latitudinal cline in a life history trait. *Proc. Natl. Acad. Sci.* 101, 15670–15675. doi: 10.1073/pnas.0406232101

Cao, Y., Wen, L., Wang, Z., and Ma, L. (2015). SKIP interacts with the Paf1 complex to regulate flowering via the activation of FLC transcription in *Arabidopsis*. *Mol. Plant* 8, 1816–1819. doi: 10.1016/j.molp.2015.09.004

Cho, H. J., Kim, J. J., Lee, J. H., Kim, W., Jung, J.-H., Park, C.-M., et al. (2012). SHORT VEGETATIVE PHASE (SVP) protein negatively regulates miR172 transcription via direct binding to the pri-miR172a promoter in *Arabidopsis*. *FEBS Lett.* 586, 2332–2337. doi: 10.1016/j.febslet.2012.05.035

Choi, K., Kim, J., Hwang, H.-J., Kim, S., Park, C., Kim, S. Y., et al. (2011). The FRIGIDA complex activates transcription of FLC, a strong flowering repressor in *Arabidopsis*, by recruiting chromatin modification factors. *Plant Cell* 23, 289–303. doi: 10.1105/tpc.110.075911

De Lucia, F., Crevillen, P., Jones, A. M., Greb, T., and Dean, C. (2008). A PHD-polycomb repressive complex 2 triggers the epigenetic silencing of FLC during vernalization. *Proc. Natl. Acad. Sci.* 105, 16831–16836. doi: 10.1073/pnas.0808687105

Fal, K., Cortes, M., Liu, M., Collaudin, S., Das, P., Hamant, O., et al. (2019). Paf1c defects challenge the robustness of flower meristem termination in *Arabidopsis thaliana*. *Development* 146:dev173377. doi: 10.1242/dev.173377

Fujiwara, S., Oda, A., Yoshida, R., Niinuma, K., Miyata, K., Tomozoe, Y., et al. (2008). Circadian clock proteins LHY and CCA1 regulate SVP protein accumulation to control flowering in *Arabidopsis*. *Plant Cell* 20, 2960–2971. doi: 10.1105/tpc.108.061531

Gu, X., Jiang, D., Wang, Y., Bachmair, A., and He, Y. (2009). Repression of the floral transition via histone H2B monoubiquitination. *Plant J.* 57, 522–533. doi: 10.1111/j.1365-313X.2008.03709.x

Gu, X., Le, C., Wang, Y., Li, Z., Jiang, D., Wang, Y., et al. (2013). *Arabidopsis* FLC clade members form flowering-repressor complexes coordinating responses to endogenous and environmental cues. *Nat. Commun.* 4:1947. doi: 10.1038/ncomms2947

He, Y. (2009). Control of the transition to flowering by chromatin modifications. *Mol. Plant* 2, 554–564. doi: 10.1093/mp/ssp005

He, Y., Doyle, M. R., and Amasino, R. M. (2004). PAF1-complex-mediated histone methylation of FLOWERING LOCUS C chromatin is required for the vernalization-responsive, winter-annual habit in *Arabidopsis*. *Genes Dev.* 18, 2774–2784. doi: 10.1101/gad.1244504

He, Y., Michaels, S. D., and Amasino, R. M. (2003). Regulation of flowering time by histone acetylation in *Arabidopsis*. *Science* 302, 1751–1754. doi: 10.1126/science.1091109

Heberle, H., Meirelles, G. V., da Silva, F. R., Telles, G. P., and Minghim, R. (2015). InteractiVenn: a web-based tool for the analysis of sets through Venn diagrams. *BMC Bioinform.* 16:169. doi: 10.1186/s12859-015-0611-3

Helliwell, C. A., Wood, C. C., Robertson, M., James Peacock, W., and Dennis, E. S. (2006). The *Arabidopsis* FLC protein interacts directly in vivo with SOC1 and FT chromatin and is part of a high-molecular-weight protein complex. *Plant J.* 46, 183–192. doi: 10.1111/j.1365-313X.2006.02686.x

Hong, S. M., Bahn, S. C., Lyu, A., Jung, H. S., and Ahn, J. H. (2010). Identification and testing of superior reference genes for a starting pool of transcript normalization in *Arabidopsis*. *Plant Cell Physiol.* 51, 1694–1706. doi: 10.1093/pcp/pcq128

Ignatchenko, V., Ignatchenko, A., Sinha, A., Boutros, P. C., and Kislinger, T. (2015). VennDIS: A JavaFX-based Venn and Euler diagram software to generate publication quality figures. *Proteomics* 15, 1239–1244. doi: 10.1002/pmic.201400320

Johanson, U., West, J., Lister, C., Michaels, S., Amasino, R., and Dean, C. (2000). Molecular analysis of FRIGIDA, a major determinant of natural variation in *Arabidopsis* flowering time. *Science* 290, 344–347. doi: 10.1126/science.290.5490.344

Kim, S. Y., He, Y., Jacob, Y., Noh, Y.-S., Michaels, S., and Amasino, R. (2005). Establishment of the vernalization-responsive, winter-annual habit in *Arabidopsis* requires a putative histone H3 methyl transferase. *Plant Cell* 17, 3301–3310. doi: 10.1105/tpc.105.034645

Kim, D.-H., and Sung, S. (2010). The plant Homeo domain finger protein, VIN3-LIKE 2, is necessary for photoperiod-mediated epigenetic regulation of the floral repressor, MAF5. *Proc. Natl. Acad. Sci.* 107, 17029–17034. doi: 10.1073/pnas.1010834107

Lee, Y. J., Kim, D. H., Kim, Y.-W., and Hwang, I. (2001). Identification of a signal that distinguishes between the chloroplast outer envelope membrane and the endomembrane system in vivo. *Plant Cell* 13, 2175–2190. doi: 10.1105/tpc.010232

Lee, J. H., Ryu, H.-S., Chung, K. S., Posé, D., Kim, S., Schmid, M., et al. (2013). Regulation of temperature-responsive flowering by MADS-box transcription factor repressors. *Science* 342, 628–632. doi: 10.1126/science.1241097

Lee, J. H., Yoo, S. J., Park, S. H., Hwang, I., Lee, J. S., and Ahn, J. H. (2007). Role of SVP in the control of flowering time by ambient temperature in *Arabidopsis*. *Genes Dev.* 21, 397–402. doi: 10.1101/gad.1518407

Lex, A., Gehlenborg, N., Strobelt, H., Vuillemot, R., and Pfister, H. (2014). UpSet: visualization of intersecting sets. *IEEE Trans. Vis. Comput. Graph.* 20, 1983–1992. doi: 10.1109/TVCG.2014.2346248

Li, D., Liu, C., Shen, L., Wu, Y., Chen, H., Robertson, M., et al. (2008). A repressor complex governs the integration of flowering signals in *Arabidopsis*. *Dev. Cell* 15, 110–120. doi: 10.1016/j.devcel.2008.05.002

Li, Y., Yang, J., Shang, X., Lv, W., Xia, C., Wang, C., et al. (2019). SKIP regulates environmental fitness and floral transition by forming two distinct complexes in *Arabidopsis*. *New Phytol.* 224, 321–335. doi: 10.1111/nph.15990

Livak, K. J., and Schmittgen, T. D. (2001). Analysis of relative gene expression data using real-time quantitative PCR and the $2-\Delta\Delta CT$ method. *Methods* 25, 402–408. doi: 10.1006/meth.2001.1262

Mateos, J. L., Madrigal, P., Tsuda, K., Rawat, V., Richter, R., Romera-Branchat, M., et al. (2015). Combinatorial activities of SHORT VEGETATIVE PHASE and FLOWERING LOCUS C define distinct modes of flowering regulation in *Arabidopsis*. *Genome Biol.* 16:31. doi: 10.1186/s13059-015-0597-1

Michaels, S. D., and Amasino, R. M. (1999). FLOWERING LOCUS C encodes a novel MADS domain protein that acts as a repressor of flowering. *Plant Cell* 11, 949–956. doi: 10.1105/tpc.11.5.949

Nasim, Z., Fahim, M., Hwang, H., Susila, H., Jin, S., Youn, G., et al. (2021). Nonsense-mediated mRNA decay modulates *Arabidopsis* flowering time via the SET DOMAIN GROUP 40–FLOWERING LOCUS C module. *J. Exp. Bot.* 72, 7049–7066. doi: 10.1093/jxb/erab331

Ng, H. H., Dole, S., and Struhl, K. (2003a). The Rtf1 component of the Paf1 transcriptional elongation complex is required for ubiquitination of histone H2B. *J. Biol. Chem.* 278, 33625–33628. doi: 10.1074/jbc.C300270200

Ng, H. H., Robert, F., Young, R. A., and Struhl, K. (2003b). Targeted recruitment of Set1 histone methylase by elongating pol II provides a localized mark and memory of recent transcriptional activity. *Mol. Cell* 11, 709–719. doi: 10.1016/S1097-2765(03)00092-3

Oh, S., Zhang, H., Ludwig, P., and van Nocker, S. (2004). A mechanism related to the yeast transcriptional regulator Paf1c is required for expression of the *Arabidopsis* FLC/MAF MADS box gene family. *Plant Cell* 16, 2940–2953. doi: 10.1105/tpc.104.026062

Pajoro, A., Severing, E., Angenent, G., and Immink, R. (2017). Histone H3 lysine 36 methylation affects temperature-induced alternative splicing and flowering in plants. *Genome Biol.* 18:102. doi: 10.1186/s13059-017-1235-x

Pose, D., Verhage, L., Ott, F., Yant, L., Mathieu, J., Angenent, G. C., et al. (2013). Temperature-dependent regulation of flowering by antagonistic FLM variants. *Nature* 503, 414–417. doi: 10.1038/nature12633

Postma, M., and Goedhart, J. (2019). PlotsOfData—A web app for visualizing data together with their summaries. *PLoS Biol.* 17:e3000202. doi: 10.1371/journal.pbio.3000202

Ratcliffe, O. J., Kumimoto, R. W., Wong, B. J., and Riechmann, J. L. (2003). Analysis of the *Arabidopsis* MADS AFFECTING FLOWERING gene family: MAF2 prevents vernalization by short periods of cold. *Plant Cell* 15, 1159–1169. doi: 10.1105/tpc.009506

Ratcliffe, O. J., Nadzan, G. C., Reuber, T. L., and Riechmann, J. L. (2001). Regulation of flowering in *Arabidopsis* by an FLCHomologue. *Plant Physiol.* 126, 122–132. doi: 10.1104/pp.126.1.122

Romero-Molina, S., Ruiz-Blanco, Y. B., Harms, M., Münch, J., and Sanchez-Garcia, E. (2019). PPI-detect: a support vector machine model for sequence-based prediction of protein–protein interactions. *J. Comput. Chem.* 40, 1233–1242. doi: 10.1002/jcc.25780

Rosloski, S. M., Singh, A., Jali, S. S., Balasubramanian, S., Weigel, D., and Grbic, V. (2013). Functional analysis of splice variant expression of MADS AFFECTING FLOWERING 2 of *Arabidopsis thaliana*. *Plant Mol. Biol.* 81, 57–69. doi: 10.1007/s11103-012-9982-2

Ruelens, P., De Maagd, R. A., Proost, S., Theißen, G., Geuten, K., and Kaufmann, K. (2013). FLOWERING LOCUS C in monocots and the tandem origin of angiosperm-specific MADS-box genes. *Nat. Commun.* 4:2280. doi: 10.1038/ncomms3280

Schwab, R., Ossowski, S., Riester, M., Warthmann, N., and Weigel, D. (2006). Highly specific gene silencing by artificial microRNAs in *Arabidopsis*. *Plant Cell* 18, 1121–1133. doi: 10.1105/tpc.105.039834

Scortecci, K. C., Michaels, S. D., and Amasino, R. M. (2001). Identification of a MADS-box gene, FLOWERING LOCUS M that represses flowering. *Plant J.* 26, 229–236. doi: 10.1046/j.1365-313x.2001.01024.x

Scortecci, K., Michaels, S. D., and Amasino, R. M. (2003). Genetic interactions between FLM and other flowering-time genes in *Arabidopsis thaliana*. *Plant Mol. Biol.* 52, 915–922. doi: 10.1023/A:1025426920923

Searle, I., He, Y., Turck, F., Vincent, C., Fornara, F., Kröber, S., et al. (2006). The transcription factor FLC confers a flowering response to vernalization by repressing meristem competence and systemic signaling in *Arabidopsis*. *Genes Dev.* 20, 898–912. doi: 10.1101/gad.373506

Sheldon, C. C., Burn, J. E., Perez, P. P., Metzger, J., Edwards, J. A., Peacock, W. J., et al. (1999). The FLF MADS box gene: a repressor of flowering in *Arabidopsis* regulated by vernalization and methylation. *Plant Cell* 11, 445–458. doi: 10.1105/tpc.11.3.445

Sledzieski, S., Singh, R., Cowen, L., and Berger, B. (2021). Sequence-based prediction of protein-protein interactions: a structure-aware interpretable deep learning model. bioRxiv [Preprint]. doi: 10.1101/2021.01.22.427866

Srikanth, A., and Schmid, M. (2011). Regulation of flowering time: all roads lead to Rome. *Cell. Mol. Life Sci.* 68, 2013–2037. doi: 10.1007/s00018-011-0673-y

Susila, H., Nasim, Z., Jin, S., Youn, G., Jeong, H., Jung, J.-Y., et al. (2021). "Profiling protein–DNA interactions by chromatin immunoprecipitation in *Arabidopsis*," in *Proteomic Profiling*. ed. A. Posch (New York City, US: Springer), 345–356.

Tomson, B. N., and Arndt, K. M. (2013). The many roles of the conserved eukaryotic Paf1 complex in regulating transcription, histone modifications, and disease states. *Biochim. Biophys. Acta* 1829, 116–126. doi: 10.1016/j.bbagrm.2012.08.011

Wickham, H. (2011). ggplot2. *Wiley Interdiscip. Rev. Comput. Stat.* 3, 180–185. doi: 10.1002/wics.147

Wood, C. C., Robertson, M., Tanner, G., Peacock, W. J., Dennis, E. S., and Helliwell, C. A. (2006). The *Arabidopsis thaliana* vernalization response requires a polycomb-like protein complex that also includes VERNALIZATION INSENSITIVE 3. *Proc. Natl. Acad. Sci.* 103, 14631–14636. doi: 10.1073/pnas.0606385103

Wood, A., Schneider, J., Dover, J., Johnston, M., and Shilatifard, A. (2003). The Paf1 complex is essential for histone monoubiquitination by the Rad6-Bre1 complex, which signals for histone methylation by COMPASS and Dot1p. *J. Biol. Chem.* 278, 34739–34742. doi: 10.1074/jbc.C300269200

Wu, F.-H., Shen, S.-C., Lee, L.-Y., Lee, S.-H., Chan, M.-T., and Lin, C.-S. (2009). Tape-*Arabidopsis* sandwich-a simpler *Arabidopsis* protoplast isolation method. *Plant Methods* 5:16. doi: 10.1186/1746-4811-5-16

Xu, L., Zhao, Z., Dong, A., Soubigou-Taconnat, L., Renou, J.-P., Steinmetz, A., et al. (2008). Di-and tri-but not monomethylation on histone H3 lysine 36 marks active transcription of genes involved in flowering time regulation and other processes in *Arabidopsis thaliana*. *Mol. Cell. Biol.* 28, 1348–1360. doi: 10.1128/MCB.01607-07

Yu, X., and Michaels, S. D. (2010). The *Arabidopsis* Paf1c complex component CDC73 participates in the modification of FLOWERING LOCUS C chromatin. *Plant Physiol.* 153, 1074–1084. doi: 10.1104/pp.110.158386

Zhang, H., Ransom, C., Ludwig, P., and Van Nocker, S. (2003). Genetic analysis of early flowering mutants in *Arabidopsis* defines a class of pleiotropic developmental regulator required for expression of the flowering-time switch flowering locus C. *Genetics* 164, 347–358. doi: 10.1093/genetics/164.1.347

Zhang, H., and Van Nocker, S. (2002). The VERNALIZATION INDEPENDENCE 4 gene encodes a novel regulator of *FLOWERING LOCUS C*. *Plant J.* 31, 663–673. doi: 10.1046/j.1365-313X.2002.01380.x

Conflict of Interest: The authors declare that the research was conducted in the absence of any commercial or financial relationships that could be construed as a potential conflict of interest.

Publisher's Note: All claims expressed in this article are solely those of the authors and do not necessarily represent those of their affiliated organizations, or those of the publisher, the editors and the reviewers. Any product that may be evaluated in this article, or claim that may be made by its manufacturer, is not guaranteed or endorsed by the publisher.

frontiers | Frontiers in Plant Science

ORIGINAL RESEARCH
published: 11 April 2022
doi: 10.3389/fpls.2022.828743

Low Salicylic Acid Level Improves Pollen Development Under Long-Term Mild Heat Conditions in Tomato

*Stuart Y. Jansma[1], Lidiya I. Sergeeva[2], Yury M. Tikunov[3], Wouter Kohlen[4], Wilco Ligterink[2†] and Ivo Rieu[1]**

[1] Plant Systems Physiology, Radboud Institute for Biological and Environmental Sciences, Radboud University, Nijmegen, Netherlands, [2] Laboratory of Plant Physiology, Wageningen University and Research, Wageningen, Netherlands, [3] Plant Breeding, Wageningen University and Research, Wageningen, Netherlands, [4] Laboratory of Molecular Biology, Wageningen University and Research, Wageningen, Netherlands

Exposure to high temperatures leads to failure in pollen development, which may have significant implications for food security with ongoing climate change. We hypothesized that the stress response-associated hormone salicylic acid (SA) affects pollen tolerance to long-term mild heat (LTMH) (≥14 days exposure to day-/nighttime temperature of 30–34/24–28°C, depending on the genotype), either positively, by inducing acclimation, or negatively, by reducing investment in reproductive development. Here, we investigated these hypotheses assessing the pollen thermotolerance of a *35S:nahG* tomato line, which has low SA levels. We found that reducing the SA level resulted in increased pollen viability of plants grown in LTMH and further characterized this line by transcriptome, carbohydrate, and hormone analyses. Low expression of *JAZ* genes in *35S:nahG* and LTMH hypersensitivity of low-jasmonic acid (JA) genotypes together suggest that the increased pollen thermotolerance in the low-SA line involves enhanced JA signal in developing anthers in LTMH. These findings have potential application in the development of more thermotolerant crops.

Keywords: plant reproduction, *Solanum lycopersicum* (tomato), pollen development, salicylic acid, jasmonic acid, high temperature stress, transcriptome analysis (RNAseq), male fertility

OPEN ACCESS

Edited by:
Kevin Begcy,
University of Florida, United States

Reviewed by:
Naser A. Anjum,
Aligarh Muslim University, India
Fengde Wang,
Vegetables and Flowers Research Institute of Shandong Academy of Agricultural Sciences, China

****Correspondence:***
Ivo Rieu
i.rieu@science.ru.nl

†Present address:
Wilco Ligterink,
Keygene N.V., Wageningen, Netherlands

Specialty section:
This article was submitted to Plant Abiotic Stress, a section of the journal Frontiers in Plant Science

Received: *03 December 2021*
Accepted: *22 February 2022*
Published: *11 April 2022*

Citation:
Jansma SY, Sergeeva LI, Tikunov YM, Kohlen W, Ligterink W and Rieu I (2022) Low Salicylic Acid Level Improves Pollen Development Under Long-Term Mild Heat Conditions in Tomato. Front. Plant Sci. 13:828743. doi: 10.3389/fpls.2022.828743

INTRODUCTION

Higher temperatures caused by climate change result in a significantly lower crop yield (Lobell and Field, 2007; Battisti and Naylor, 2009). In the second decade of the 21st century, the average global surface temperature has already increased by 1.09°C, relative to the estimated average global surface temperature during 1850–1900, and it is expected to increase further in the coming decades (Masson-Delmotte et al., 2021). This higher temperature results in an increase in the frequency, duration, and intensity of heatwaves (Masson-Delmotte et al., 2021).

Heat wave-type high-temperature stress ["long-term mild heat" (LTMH)] during flower development has been associated with a reduction in yield in many crop species (Charles and Harris, 1972; Munakata, 1976; Herrero and Johnson, 1980; Saini and Aspinall, 1982; Gibson and Paulsen, 1999; Angadi et al., 2000; Sato et al., 2002; Wang et al., 2006). In particular, a strong correlation has been found between fruit-set or crop yield and pollen viability (PV) (Sakata et al., 2000; Peng et al., 2004; Prasad et al., 2006; Farooq et al., 2011; Song et al., 2015; Xu et al., 2017; Driedonks et al., 2018; Wu et al., 2021).

Previous studies have identified thermosensitive stages of pollen development and provided some hypotheses for the mechanisms behind LTMH-induced pollen abortion, including altered phytohormone signaling (De Storme and Geelen, 2014), loss of tapetum identity in the anthers (Parish and Li, 2010; Müller et al., 2016), desynchronization of tapetum and pollen development (Suzuki et al., 2001; Ku et al., 2003; Endo et al., 2009; Parish et al., 2012; Meng et al., 2016; Yu et al., 2016), and disturbance of carbohydrate metabolism (Pressman et al., 2002). It remains to be elucidated whether acclimation responses take place in the anther to protect pollen development against LTMH and whether LTMH-induced pollen failure is the passive result of heat injury, or the result of an active cell physiological response to heat stress (Müller and Rieu, 2016).

Salicylic acid (SA) is involved in a range of acclimation responses, also in those to high temperatures, especially in case of heat shock. This type of heat stress has been shown to lead to the accumulation of SA in *Arabidopsis* seedlings (Clarke et al., 2009) and seedlings with reduced SA levels or signaling are more sensitive to heat shock (Larkindale and Knight, 2002; Clarke et al., 2004). Conversely, treatment with SA preceding heat exposure improved basal thermotolerance of Arabidopsis seedlings (Clarke et al., 2009). SA treatment has also been shown to have a positive effect on the thermotolerance of vegetative tissues in wheat (Khan et al., 2013). Furthermore, a single treatment with SA, prior to the onset of long-term exposure to 40°C, improved pollen thermotolerance in rice and this was linked to an increase in reactive oxygen species (ROS) scavenging, attenuation of Caspase 3 activity, and timely tapetum degradation (Zhang et al., 2017; Feng et al., 2018).

Acclimation responses are costly, meaning that trade-offs with growth and developmental processes are to be expected. A well-studied example is a trade-off between growth/development and defense (Herms and Mattson, 1992; Huot et al., 2014). Reducing the biotic stress response allows for more allocation of resources to growth and development (Simms and Rausher, 1987; Campos et al., 2016) and hormone signals that regulate growth and development, such as auxin (IAA), brassinosteroids, and gibberellin, may be inhibited by stress hormone signaling, such as from SA (Huot et al., 2014; Verma et al., 2016). We hypothesized that SA plays a role in tomato pollen LTMH tolerance, either in a positive sense by inducing a protective acclimation response, or in a negative sense, by reducing investment in pollen development under heat stress. To this end, we examined the effects of reduced SA level on tomato pollen thermotolerance and physiology and further characterized the pollen LTMH tolerance of the *35S:nahG* low-SA genotype.

MATERIALS AND METHODS

Plant Material and Cultivation

Solanum lycopersicum 35S:nahG has been described before (Brading et al., 2000) and was introgressed into cv. Micro-Tom (Carvalho et al., 2011). *def1* and *acx1* were in the Castlemart background (Howe et al., 1996; Li et al., 2005). Plants were grown on potting soil (No. 4, Horticoop, Lentse Potgrond, Slingerland Potgrond) with 4 g/L Osmocote Exact Standard 3–4 M (Everris). Plants were grown in climate-controlled cabinets with a 12/12 h photoperiod (Philips Green Power LED DR/B/FR 120, ∼250 μmol $m^{-2}s^{-1}$ at plant height) at 25°C during the daytime and 19°C during the nighttime and 50% relative humidity (RH). For LTMH treatment, plants were moved into LTMH conditions upon flowering. LTMH consisted of daytime temperature of 30–34°C and a corresponding 6°C lower night temperature, dependent on the experiment. RH in LTMH was adjusted to maintain equal vapor pressure deficit (VPD) as compared to control temperature (CT) conditions.

Pollen Viability Measurements

Flowers at the anthesis stage were sampled in CT conditions or after 10–21 days in LTMH conditions, on at least 3 different days. PV was determined through impedance flow cytometry, using Ampha^{TM} Z30 with D-chip, AF6 buffer, and other settings as recommended for tomato by the manufacturer (Amphasys AG, Root, Switzerland) (Heidmann et al., 2016). On each sampling day, 1–4 flowers at the stage of anthesis of each plant were pooled into a sample, and viability was determined for ∼20.000 pollen per sample.

Sampling and RNA Extraction for RNA-Seq

Anthers with polarized stage microspores (4.6–4.8 mm), as determined by DAPI staining of the pollen, were collected from CT and after 8 days of exposure to LTMH conditions. Samples were taken approximately 5 h into the light period. Six anthers were pooled per replicate and 4 biological replicates were generated for both the conditions and genotypes. RNA was isolated *via* TRI Reagent (Sigma-Aldrich, MA, United States) extraction with cleanup on the Qiagen Plant RNeasy (catalog no. 74104) columns. All the RNAs were treated with DNaseI using the Plant RNeasy Kit. RNA degradation and contamination were monitored on 1.5% agarose gels. RNA purity was checked using the NanoPhotometer® spectrophotometer (IMPLEN, CA, United States). RNA integrity and quantitation were assessed using the RNA Nano 6000 Assay Kit of the Bioanalyzer 2100 System (Agilent Technologies, CA, United States).

Ribonucleic Acid Sequencing

A total amount of 1 μg RNA per sample was used as input material for the RNA sample preparations. Sequencing libraries were generated using the NEBNext® Ultra^{TM} RNA Library Prep Kit for Illumina® (NEB, United States) following the manufacturer's recommendations and index codes were added to attribute sequences to each sample. Briefly, messenger RNA (mRNA) was purified from total RNA using poly-T oligo-attached magnetic beads. Fragmentation was carried out using divalent cations under elevated temperature in NEBNext First Strand Synthesis Reaction Buffer (5X). First-strand cDNA was synthesized using random hexamer primer and MMuLV Reverse Transcriptase (RNase H-). Second strand cDNA synthesis was subsequently performed using DNA polymerase I and RNase H. Remaining overhangs were converted into blunt ends *via*

exonuclease/polymerase activities. After adenylation of 3′ ends of DNA fragments, NEBNext Adaptor with hairpin loop structure was ligated to prepare for hybridization. To select cDNA fragments of preferentially 150–200 bp in length, the library fragments were purified with the AMPure XP system (Beckman Coulter, Beverly, MA, United States). Then, 3 μl USER Enzyme (NEB, United States) was used with size-selected, adaptor-ligated cDNA at 37°C for 15 min followed by 5 min at 95°C before PCR. Then PCR was performed with Phusion High-Fidelity DNA polymerase, Universal PCR primers, and Index (X) Primer. At last, PCR products were purified (AMPure XP system) and library quality was assessed on the Agilent Bioanalyzer 2100 System.

The clustering of the index-coded samples was performed on a cBot Cluster Generation System using PE Cluster Kit cBot-HS (Illumina) according to the manufacturer's instructions. After cluster generation, the library preparations were sequenced on an Illumina platform and 125/150 bp paired-end reads were generated. Raw reads of fastq format were filtered to remove reads containing adapters or reads of low quality, i.e., when uncertain nucleotides constitute more than 10% of either read and when low-quality nucleotides constitute more than 50% of the read. All the downstream analyses were based on clean data. Index of the reference genome (ITAG3.2) was built using Bowtie version 2.2.3 and paired-end clean reads were aligned to the reference genome using hisat2 version 2.0.5, using the following parameters: –dta –phred33. In total, 94.7% of the reads were uniquely mapped, of which for each sample at least 90% were exon-mapped reads. FeatureCounts v1.5.0-p3 software was used to count the reads numbers mapped to each gene, using default parameters. Fragments per kilobase of exon per million mapped fragments (FPKM) of each gene was calculated based on the length of the gene and reads count mapped to this gene, using a threshold FPKM of 0.1. Differential expression analysis of two conditions/groups was performed using the DESeq R package (1.18.0). The resulting *P*-values were adjusted using Benjamini and Hochberg's approach for controlling the false discovery rate (FDR). Genes with an FDR adjusted *P*-value < 0.05 found by DESeq and $|\text{foldchange}| \geq 1.5$ were assigned as differentially expressed.

Transcriptome Analyses

Principal component analysis (PCA) was performed using the online tool ClustVis[1] with all the standard settings (i.e., row centering on, row scaling with unit variance, and singular value decomposition with imputation). Genes were included if at least one sample had an FPKM value of at least 1. Unit variance scaling was applied. Prediction ellipses are such that with a probability of 0.95, a new observation from the same group will fall inside the ellipse. $n = 3$ or 4 samples (PC1, principal component 1; PC2, principal component 2).

A transcriptome-wide gene set enrichment analysis (FDR $q < 0.05$) for gene ontology (GO)-slim biological process annotations was performed on ranked fold-changes using the online software tool Panther (version 16.0[2]) with FDR correction (Mi et al., 2021). Over-representation of GO-slim biological process annotations among up- or downregulated genes was also determined using Panther, with Fisher's exact test and FDR correction. Targeted overrepresentation analyses were performed by calculating the statistical significance of the overlap between differentially expressed genes (DEGs) within a gene set and all DEGs among the whole genome using a Chi-square test with Yates' correction. The gene sets for pollen development and carbohydrate metabolism and transport were generated based on homology to annotated Arabidopsis genes, the gene set for heat shock response (HSR) was based on Fragkostefanakis et al. (2015) and Keller et al. (2018), and the gene sets for hormone metabolism, signaling, and response were derived from the annotation of the tomato genome version SL3.0 ITAG3.2 by Biobam using Omicsbox (Biobam, Valencia, Spain) (**Supplementary Table 1**).

Sampling for Carbohydrate and Hormone Measurements

Pollen stage was linked to flower length by categorizing 4′,6-diamidino-2-phenylindole (DAPI)-stained pollen and stages were selected based on their synchronized states when grown at different temperature regimes (**Supplementary Table 2**). Anthers were immediately frozen in liquid nitrogen upon isolation, and stored at –80°C.

Extraction and Quantification of Carbohydrates

Soluble carbohydrates were extracted by homogenizing 100 mg frozen anther material in 300 μl MeOH. The sample was diluted with 330 μl methanol and 300 μl water to 1 ml 70% methanol. After shaking for 30′ at RT, the sample was centrifuged at max speed. In total, 500 μl supernatants was transferred to a new Eppendorf tube, and 450 μl water and 250 μl chloroform were added. After vortexing for 5′, the sample was centrifuged at max speed. In total, 200 μL supernatant was transferred to a new Eppendorf tube and dried in a speed-vac. Samples were then analyzed using a Dionex HPLC system (Dionex, Sunnyvale, CA, United States), and analyzed using a CarboPac PA100 4 mm × 250 mm column followed by a guard column (CarboPac PA100, 4 mm × 50 mm), a gradient pump module (model GP40) and an ED40-pulsed electrochemical detector. Mono-, di-, and trisaccharides were separated by elution in an increasing concentration of NaOH (50–200 mM) with a flow rate of 1 ml min^{-1}. Peaks were identified by the co-elution of standards. The final sugar quantity was corrected *via* the internal standard (IS) and transformed to micrograms of sugar per milligram of fresh weight.

Extraction of ABA, SA, IAA, JA-ile, and CKs (iP, tZ, and cZ)

For extraction of salicylic acid (SA), abscisic acid (ABA), auxin (IAA), jasmonic acid-isoleucine (JA-ile), and cytokinins (CKs: iP, isopentyladenine; tZ, *trans*-zeatin; cZ, *cis*-zeatin), 70 mg of snap-frozen anther tissue was used per sample. The tissue was ground to a fine powder at –80°C using 3-mm stainless steel beads at

[1]https://biit.cs.ut.ee/clustvis_large/

[2]http://www.pantherdb.org

50 Hz for 1 min in a TissueLyser LT (Qiagen, Germantown, MD, United States). Ground samples were extracted with 1 ml of 100% methanol (MeOH) containing stable isotope-labeled IS (**Supplementary Table 3**). IS were used at an end concentration of 100 nM per compound per sample. Samples were extracted as previously described (Schiessl et al., 2019; Gühl et al., 2021) with the addition that, prior to the elution of CKs, acid phytohormones were eluted with 1 ml of 100% MeOH. All solvents were evaporated in a speed vacuum system (SPD121P, ThermoSavant, Hastings, United Kingdom) at room temperature and the residue stored at –20°C until further analysis.

Detection and Quantification of IAA, JA-ile, iP, tZ, and cZ by LC-MS/MS

Sample residues were dissolved in 100 μL of acetonitrile/water (acid hormones) or MeOH/water (CKs) (0.1% formic acid) (20:80, v/v), and filtered through a 0.45 mm Minisart SRP4 filter (Sartorius, Goettingen, Germany). Analyses of plant growth regulators were performed by comparing retention times and mass transitions with those of unlabeled standards (**Supplementary Table 3**) using a Waters XevoTQs mass spectrometer equipped with an electrospray ionization source coupled to an Acquity UPLC system (Waters, Milford, CT, United States). Chromatographic separations were conducted on an Acquity UPLC BEH C18 column (100 mm, 2.1 mm, 1.7 mm; Waters, United States) by applying an acetonitrile/water (0.1% formic acid) or methanol/water (0.1% formic acid) gradient. The column was operated at 50°C with a flow rate of 0.5 ml min^{-1}. The column was equilibrated for 30 min using either solvent composition at the start of a run. The acetonitrile/water (0.1% formic acid) gradient started from 20% (v/v) acetonitrile, increasing to 70% (v/v) acetonitrile in 17 min. To wash the column, the water/acetonitrile gradient was increased to 100% (v/v) acetonitrile in a 1.0 min gradient, which was maintained for 1.0 min before going back to 20% acetonitrile using a 1.0 min gradient, prior to the next run. The methanol/water (0.1% formic acid) gradient started from 5% (v/v) methanol, increasing to 70% (v/v) methanol in 17 min. To wash the column, the water/methanol gradient was increased to 100% (v/v) methanol in a 1.0 min gradient, which was maintained for 1.0 min before going back to 5% methanol using a 1.0 min gradient, prior to the next run. The sample injection volume was 3/5 μl (acids/CK, respectively). The mass spectrometer was operated in positive and negative electrospray ionization mode when required. Cone and desolvation gas flows were set to 150 and 1,000/800 l h^{-1}, respectively. The capillary voltage was set at 3.5/3.0 kV, the source temperature at 150°C, and the desolvation temperature at 550°C. The cone voltage was optimized for each standard compound using the IntelliStart MS Console (Waters, Milford, CT, United States). Argon was used for fragmentation by collision-induced dissociation. Multiple reaction monitoring (MRM) was used for quantification (Gühl et al., 2021). Parent–daughter transitions for the different (stable isotope-labeled) compounds were set using the IntelliStart MS Console. MRM transitions, cone voltage, and collision energy selected for compound identification and quantification are shown in **Supplementary Table 3**. To determine sample concentrations, a 10-point calibration curve was constructed for each compound ranging from 1 μM to 190 pM and each dilution also contained a known amount of an appropriate deuterium-labeled IS.

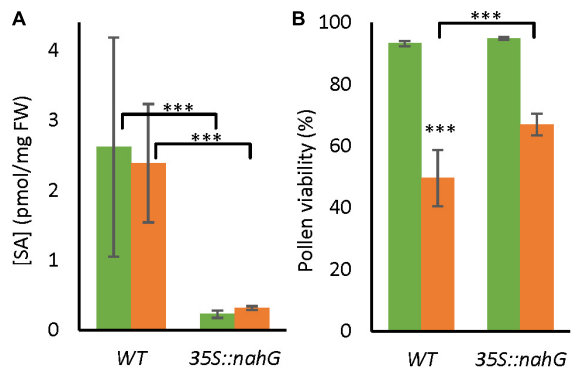

FIGURE 1 | Endogenous salicylic acid (SA) levels and pollen long-term mild heat (LTMH) tolerance of WT and *35S:nahG*. Green bars represent control temperature (CT), orange bars LTMH. **(A)** SA levels in bicellular pollen stage anthers of wild type (WT) and *35S:nahG* after exposure to LTMH. LTMH consisted of repeated exposure to 34°C (day) and 28°C (night). Hormone concentrations were measured after 7 days of exposure to the treatment. Values indicate the mean ± SD (n = 6 samples, with pools of 20 anther cones per sample). Two-way ANOVA main effects: temperature ns; genotype $P < 0.001$; interaction ns. **(B)** Pollen viability of WT and *35S:nahG* after exposure to LTMH. LTMH consisted of repeated exposure to (33.5°C day and 27.5°C night). Pollen viability was measured 14–20 days after the onset of the treatment. Values indicate the mean ± SD ($n \geq 4$ plants, with multiple pools of 3 anther cones per plant). Two-way ANOVA main effects: temperature $P < 0.001$; genotype $P < 0.001$; interaction $P < 0.05$. *Significantly different between LTMH and CT in WT or between mutant and WT within temperature treatment (brackets), one-way ANOVA with LSD *post hoc*, $P < 0.05$; $^{**}P < 0.01$; $^{***}P < 0.001$.

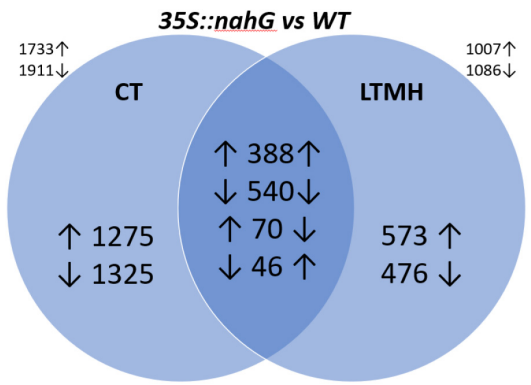

FIGURE 2 | Differentially expressed genes (DEGs) between polarized stage anthers of WT and *35S:nahG* in CT and LTMH. LTMH consisted of repeated exposure to 34°C (day) and 28°C (night). Values indicate the number of DEGs, and up and down arrows indicate higher or lower expression, respectively, in *35S:nahG*. An arrow left to the value indicates the direction of response in CT; on the right, in LTMH. The values outside the diagram indicate the total number of upregulated and downregulated DEGs for the concerning temperature condition.

Statistics

Pollen viability was averaged for each plant and logit transformed using the formula PV* = LN [(PV + 1)/(101 − PV)] for statistical analysis. Carbohydrate and phytohormone concentrations were log10 transformed for statistical analysis. Statistical significance was tested by means of a one-way ANOVA with LSD or Games–Howell *post hoc* analysis, as appropriate, using IBM SPSS Statistics version 25.

RESULTS

Endogenous Salicylic Acid Reduces Pollen Long-Term Mild Heat Tolerance

To test whether the endogenous SA signal affects the tolerance of pollen development to LTMH, we analyzed a transgenic line with constitutive expression of a bacterial gene that leads to SA degradation, *35S:nahG*, grown in LTMH conditions from the start of flowering. SA level of bicellular-stage anthers did not significantly change after exposure to LTMH in wild type (WT) or *35S:nahG*, but, as expected, the *35S:nahG* line contained significantly less SA than the WT (**Figure 1A**). Pollen from wild-type flowers that had fully developed in LTMH had significantly lower viability than those from the CT treatment (**Figure 1B** and **Supplementary Figure 1**). In the low-SA line, PV was not different from WT in CT, but significantly higher than WT in LTMH (**Figure 1B**).

Transcriptome Changes in the Long-Term Mild Heat Tolerant Low-Salicylic Acid Line

To get insight into the physiology behind pollen LTMH tolerance, we compared gene expression levels of developing anthers of *35S:nahG* and the wild type (**Supplementary Table 4**). Principle component analysis of the gene expression levels showed that the LTMH treatment had the biggest influence on gene expression, followed by genotype (**Supplementary Figure 2**). Two-thirds of the genes that responded to LTMH in WT ($|FC| > 1.5$; FDR $q < 0.05$), responded similarly in *35S:nahG*, but in the latter, the response was more extensive with about 50% more genes responding in total (**Supplementary Figure 3**). In total, 1,007 genes were found to be higher and 1,086 genes were found to be lower expressed in the low-SA line than in WT in LTMH (**Figure 2**).

To obtain a broad overview of processes modified in the *35S:nahG* line in LTMH, a transcriptome-wide gene set enrichment analysis (FDR $q < 0.05$) for GO-slim biological process annotations was performed. This showed a bias toward a higher expression of genes related to photosynthesis, response to ABA, generation of precursor metabolites, and energy and glucose metabolism (**Supplementary Table 5**). This was largely mirrored in the overrepresentation analysis among upregulated genes, with photosynthesis-related GO terms as the most upregulated sets, in addition to the response to abiotic stress and glucose and fructose metabolism (**Figure 3A** and **Supplementary Table 6**). Enrichment and overrepresentation analyses revealed lower expression of genes related to mitosis, ribosomal RNA/translation, response to endoplasmic reticulum (ER) stress, response to unfolded protein, as well as response to wounding/regulation of defense response (**Figure 3B** and **Supplementary Tables 5, 7**). Notably, the downward trend of response to wounding and regulation of defense response was mostly caused by genes encoding JAZ proteins, repressors in the JA signal transduction pathway, being less upregulated by LTMH, while no change was observed in the expression of the COI1 JA receptor gene (**Supplementary Figure 4**).

To better understand the differences between *35S:nahG* and WT in the expression of genes related to pollen development, the heat shock response, carbohydrate metabolism and transport, and hormone physiology, we performed targeted overrepresentation analyses with corresponding gene sets (**Supplementary Table 8**). A number of pollen development-related genes was expressed either higher or lower in the low-SA

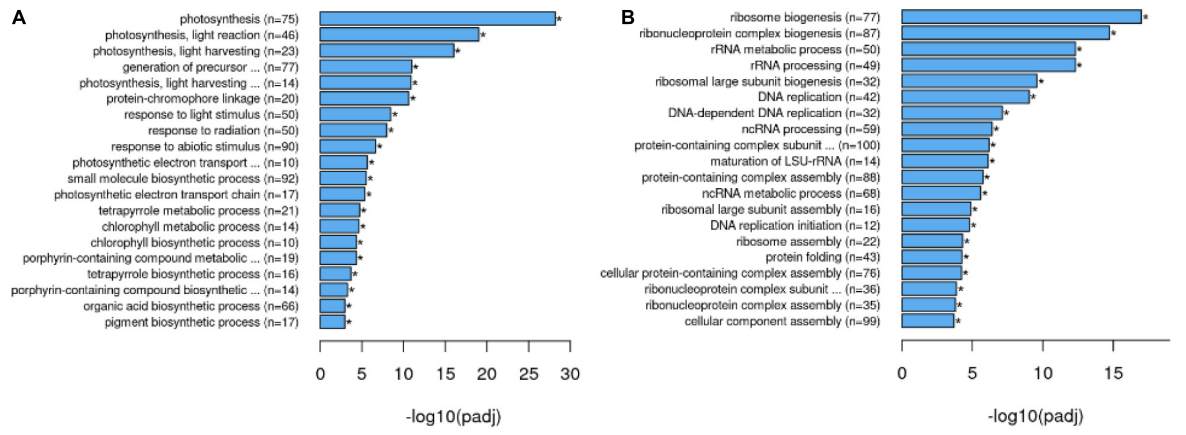

FIGURE 3 | Overrepresentation analysis of GO biological processes among genes differentially expressed between *35S:nahG* and WT in LTMH. Top categories are indicated among **(A)** DEGs that are higher expressed in *35S:nahG* than in WT (**Supplementary Table 6**) and **(B)** DEGs that are lower expressed in *35S:nahG* than in WT (**Supplementary Table 7**).

line in LTMH, although not more than expected. In particular, *MPK3* and *CALS5* homologs were expressed much higher in the low-SA line in LTMH (i.e., around 4–5-fold), whereas *WBC27*, *TDF1*, *CYP704B1*, and *CYP703A2* were expressed much lower (10–37-fold; **Supplementary Table 9**). The lower expression of *TDF1* was already seen in CT. Similarly, a number of HSR genes was expressed differentially between *35S:nahG* and WT in LTMH, but the total did not deviate significantly from what was expected. HSR-related differences included 2.5–3.5-fold higher expression of three HSF genes (two *HSFA6b* and *HSF9*) and a mitochondrial HSP40 gene, and strongly lower expression (40- to 225-fold) of genes for two small-HSPs and an HSP40. Most of these differences were already observed in CT conditions (**Supplementary Table 10**). Concerning carbohydrate-related genes, the amplitude of the higher expressed metabolic genes was limited (around twofold) and included a variety of enzymes. Three genes were more clearly lower expressed (3- to 9-fold) and included two types of invertases (vacuolar and cell wall) as well as an invertase inhibitor (**Supplementary Table 11**). Among the carbohydrate transport genes, the hexose transporters *SlSTP6* and *SlSWEET5a* were expressed much higher in the low-SA line in LTMH (around 15-fold). Several other SWEET transporter genes were lower expressed (2- to 4-fold; **Supplementary Table 12**). Finally, we analyzed genes related to metabolism, signaling, and response of several hormones (**Supplementary Table 13**). A significant number of ABA response, auxin signaling, and ethylene metabolism genes were overrepresented among genes that were expressed higher in *35S:nahG*. This included the orthologs of ABA-responsive *AtLTI65* and an LEA protein (6- to 37-fold), both involved in the regulation of water balance, an ACC-synthase, and two ACC-oxidases (2- to 3-fold) and several AUX/IAA-like repressors of auxin signaling (1.5 to 3-fold). There was, however, no clear overall pattern in expression changes of the TIR and AUX/IAA signaling component genes between *35S:nahG* and WT in LTMH, with both upregulated and downregulated members (**Supplementary Figure 5**).

Carbohydrate Content in the Long-Term Mild Heat-Tolerant Low-Salicylic Acid Line

Given the observed differences in carbohydrate-associated gene expression between the low-SA line and the wild type in LTMH, we investigated potential changes in carbohydrate levels in developing anthers when exposed to LTMH. In the WT at the polarized micropore stage, an opposite LTMH trend was seen for sucrose (up) and the hexoses (down). At the bicellular pollen stage, there was a downward trend for all sugars, and this LTMH response became statistically significant at the mature pollen stage. Differences between *35S:nahG* and WT were rather limited in either condition. In LTMH, there was a trend toward lower hexose content in polarized microspore stage anthers, slightly higher glucose levels at bicellular stage anthers, as well as slightly higher sucrose and glucose levels at mature pollen stage anthers (**Figure 4**).

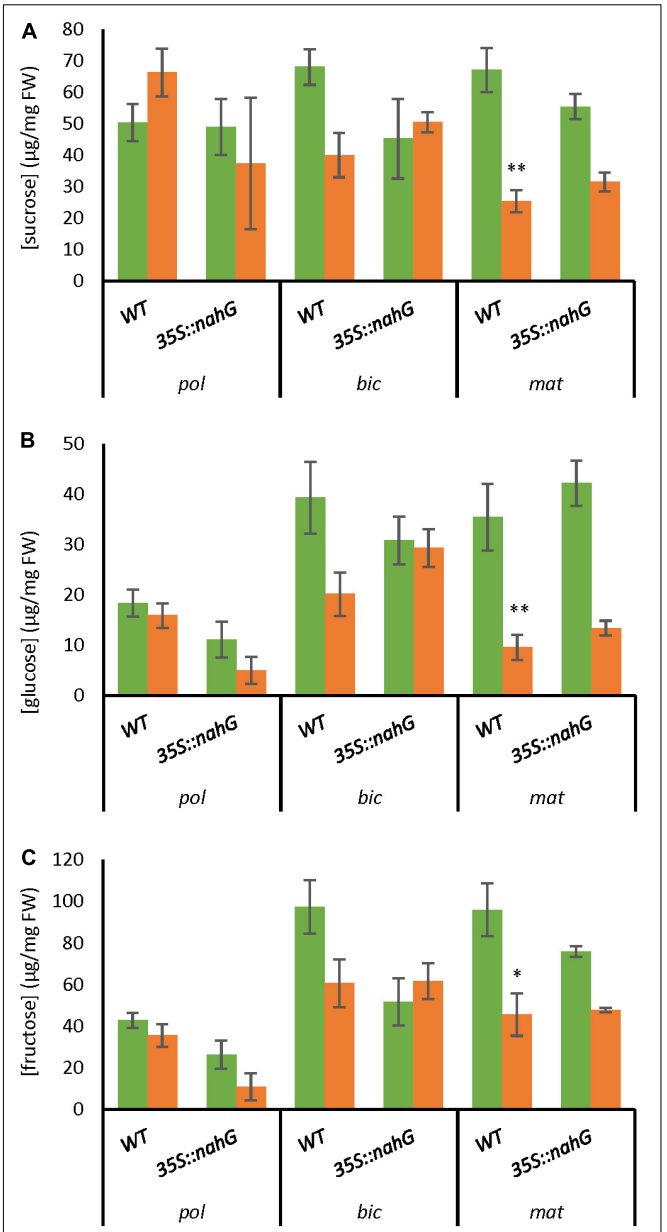

FIGURE 4 | Simple carbohydrate levels in developing anthers of WT and *35S:nahG* in CT and LTMH. LTMH consisted of repeated exposure to 34°C (day) and 28°C (night). Carbohydrate concentrations were measured after 4, 7, and 10 days of exposure to the treatment, respectively, for polarized microspore (pol), bicellular pollen (bic), and mature pollen (mat) stage anthers. Green bars represent CT, orange bars LTMH. Values indicate the mean ± SD (n = 6 samples, with pools of 20 (pol), 15 (bic), or 10 (mat) anther cones per sample). **(A)** Sucrose levels. Two-way ANOVA main effects in pol/bic/mat: temperature $P < 0.05/ < 0.01/ < 0.001$; genotype ns/$P < 0.05$/ns; interaction ns/$P < 0.05/ < 0.01$. **(B)** Glucose levels. Two-way ANOVA main effects in pol/bic/mat: temperature ns/$P < 0.01/ < 0.001$; genotype $P < 0.01$/ns/$P < 0.05$; interaction ns/$P < 0.01$/ns. **(C)** Fructose levels. Two-way ANOVA main effects in pol/bic/mat: temperature ns/ns/$P < 0.01$; genotype $P < 0.01/P < 0.01$/ns; interaction ns/$P < 0.01$/ns. *Significantly different within stage between LTMH and CT in WT or between mutant and WT within temperature treatment (brackets), one-way ANOVA with Games–Howell *post hoc*, $P < 0.05$; **$P < 0.01$; ***$P < 0.001$.

Hormone Levels in the Long-Term Mild Heat-Tolerant Low-Salicylic Acid Line

To further investigate potential interactions between SA and other plant hormones, we measured the level of ABA, JA-ile, IAA, and various CKs in bicellular-stage anthers of *35S:nahG* and the wild type (**Figure 5**). There was a trend toward lower ABA content in anthers of the wild type when exposed to LTMH, and this reduction was significant for IAA, JA-ile, and iP, while the concentration of cZ was increased. In CT, *35S:nahG* had lower levels of ABA, IAA, and JA-Ile than WT, and a higher level of iP. The only difference between *35S:nahG* and WT in LTMH was a slight increase in IAA level (**Figure 5B**).

Jasmonic Acid Is Required for Pollen Long-Term Mild Heat Tolerance

Although the level of JA-ile was equally low in the wild type and low-SA line in LTMH, the lower expression of multiple JAZ repressor genes suggested that the transgenic line was more sensitive to JA. To evaluate the role of JA in the pollen LTMH phenotype, we assessed the JA biosynthesis mutants *defenseless1* (*def1*) and *acyl-CoA oxidase A1* (*acx1*), in which the JA level is reduced (Howe et al., 1996; Li et al., 2005). While both lines performed as well as the WT in CT, they had a significantly lower PV than WT already in very mild LTMH conditions (**Figure 6**). The hypersensitive response in LTMH suggests that a low JA signal may indeed limit pollen development in this condition.

DISCUSSION

In this study, we have shown that endogenous levels of SA, which is often associated with biotic and abiotic stress responses, negatively affect pollen LTMH tolerance. We found that reducing SA levels had distinct effects on anther and pollen physiology under LTMH, and found evidence for a role of JA signaling in the mechanism behind pollen thermotolerance of the low-SA line.

Pollen Long-Term Mild Heat Tolerance Through Low Salicylic Acid Level

A high PV was observed in a *35S:nahG* low-SA tomato line compared to wild type when plants were subjected to LTMH. This result contrasts with the findings that SA has a positive effect on the basal and acquired thermotolerance of Arabidopsis seedlings exposed to heat shock (Larkindale et al., 2005; Clarke et al., 2009). Similarly, SA treatment reduced the effects of

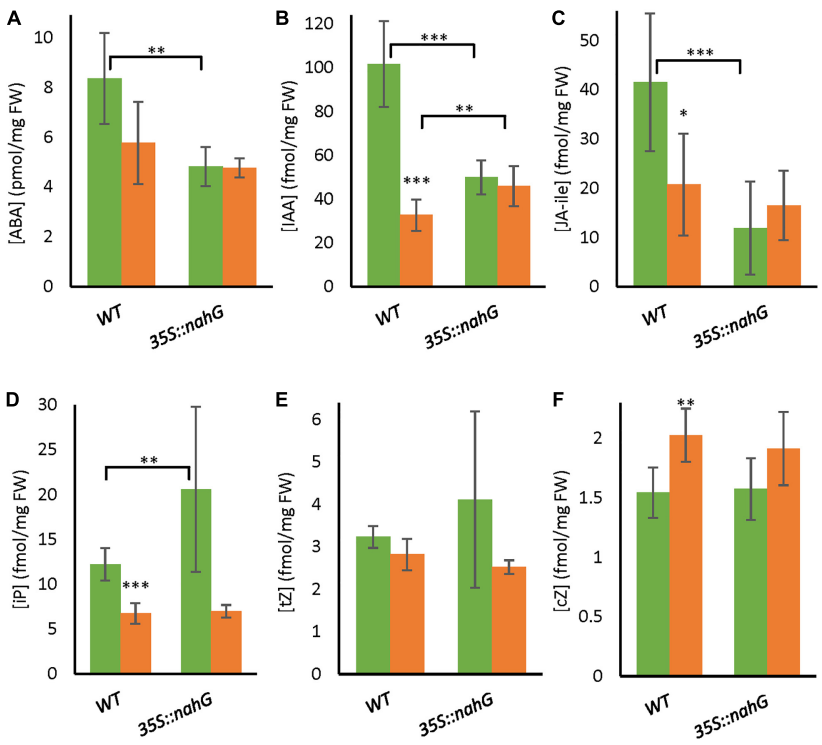

FIGURE 5 | Hormone levels in bicellular pollen stage anthers of WT and *35S:nahG* after exposure to LTMH. LTMH consisted of repeated exposure to 34°C (day) and 28°C (night). Hormone concentrations were measured after 7 days of exposure to the treatment. Green bars represent CT, orange bars LTMH. Values indicate the mean ± SD (n = 6 samples, with pools of 20 anther cones per sample). **(A)** Abscisic acid (ABA) levels. Two-way ANOVA main effects: temperature $P < 0.05$; genotype ns; interaction $P < 0.05$. **(B)** IAA levels. Two-way ANOVA main effects: temperature $P < 0.001$; genotype $P < 0.05$; interaction $P < 0.001$. **(C)** Jasmonic acid-isoleucine (JA-ile) levels. Two-way ANOVA main effects: temperature ns; genotype $P < 0.01$; interaction $P < 0.01$. **(D)** iP levels. Two-way ANOVA main effects: temperature $P < 0.001$; genotype $P < 0.05$; interaction $P < 0.05$. **(E)** tZ levels. Two-way ANOVA main effects: temperature $P < 0.01$; genotype ns; interaction ns. **(F)** cZ levels. Two-way ANOVA main effects: temperature $P < 0.01$; genotype ns; interaction ns. *Significantly different between LTMH and CT in WT or between mutant and WT within temperature treatment (brackets), one-way ANOVA with Games–Howell or LSD *post hoc*, $P < 0.05$; **$P < 0.01$; ***$P < 0.001$.

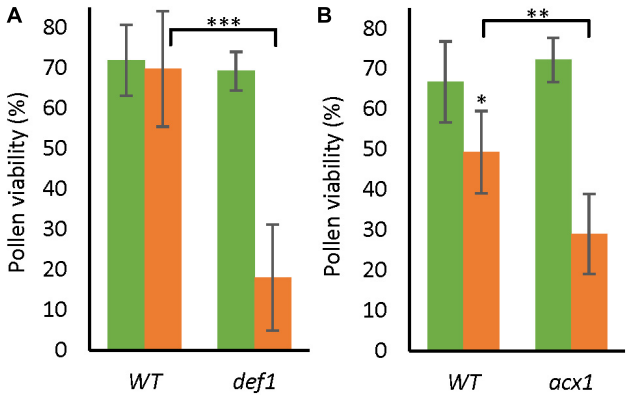

FIGURE 6 | Pollen viability of low-JA genotypes in CT and LTMH conditions. Pollen viability was measured 14–20 days after the onset of the treatment. Green bars represent CT, and orange bars LTMH treatment. **(A)** PV of *def1*. LTMH consisted of repeated exposure to 30°C (day) and 24°C (night). Values indicate the mean ± SD (n = 5 plants, with multiple pools of 3 anther cones per plant). Two-way ANOVA main effects: temperature $P < 0.01$; genotype $P < 0.001$; interaction $P < 0.01$. **(B)** PV of *acx1*. LTMH consisted of repeated exposure to 31°C (day) and 25°C (night). Values indicate the mean ± SD (n = 5 plants, with multiple pools of 3 anther cones per plant). Two-way ANOVA main effects: temperature $P < 0.001$; genotype ns; interaction $P < 0.05$. *Significantly different between LTMH and CT in WT or between mutant and WT within temperature treatment (brackets), one-way ANOVA with LSD *post hoc*, $P < 0.05$; **$P < 0.01$; ***$P < 0.001$.

heat stress on the vegetative tissues of wheat (Khan et al., 2013), and rice spikelets (Zhang et al., 2017; Feng et al., 2018). A possible explanation is a difference in the degree of heat injury experienced by the plants. Formation of ROS has been reported at an absolute high temperature, while milder heat regimes, such as in LTMH conditions, do not lead to detectable ROS damage (Djanaguiraman et al., 2014, 2018; Zhao et al., 2018). Indeed, it has been proposed before that the positive effect of SA on thermotolerance is associated with increased ROS scavenging activity (Larkindale and Knight, 2002; Herrera-Vásquez et al., 2015; Feng et al., 2018). Furthermore, the positive effects shown by increasing the signal of SA are mostly derived from experiments on vegetative tissues. Increased levels of SA may cause a shift of resource allocation from growth and development to a stress acclimation response (Huot et al., 2014; Karasov et al., 2017; Bechtold and Field, 2018). While existing vegetative tissue may be able to endure a period of scarcity by entering into a state of metabolic quiescence, the highly dynamic process of pollen development may not be able to do so. Thus, there is the possibility that in LTMH conditions, the temperature itself may not be detrimental to pollen development, but rather the investment in stress tolerance pathways, which prepares the plant for more severe temperature conditions, is. Accordingly, SA treatment in non-stressed conditions may reduce PV (Praba and Thangaraj, 2005). From an evolutionary viewpoint, a strong early acclimation to be able to withstand further temperature increases at the organismal level may be a beneficial trade-off against a temporary reduction of PV. However, from an agricultural perspective, the same can be an undesirable trait as stress levels do not always become unsustainable.

Low-Salicylic Acid Effects on Anther and Pollen Physiology in Long-Term Mild Heat

Based on transcriptomic and physiological analyses, several hypotheses for the mechanism behind higher pollen LTMH tolerance of the *35S:nahG* line might be posed. We found higher expression of photosynthesis-related gene expression in anthers of the low-SL line, counteracting the strong downregulation of these genes by LTMH in the wild type. Young anthers do contain chloroplasts for photosynthesis, which might be hypothesized to then function better in the low-SA line. However, it has been reported before that LTMH-type temperatures hardly affect photosynthesis rates (Camejo et al., 2005). Moreover, excluding light from developing flower buds did not compromise pollen development (data not shown). Thus, photosynthesis-related gene expression differences are not likely to be the reason for the pollen LTMH hypertolerance of the low-SA line.

There was a lower expression of mitosis-related genes in the low-SA anthers compared to wild type in LTMH specifically, indicating that certain cells in the low-SA anthers were less progressed toward mitosis, putatively the microspores. However, this process was not upregulated by LTMH in the wild type, suggesting it is not involved in the pollen LTMH phenotype. At the same time, there was decreased transcript accumulation of *TDF1*, *WBC27,* and *CYP703A2*, which are all expressed in the tapetum at early microspore stages (Xu et al., 2010; Xiong et al., 2016), and strongly repressed during further microspore development, suggesting advanced progression of certain tapetal developmental programs. Furthermore, we found that *MPK3* was expressed higher in the low-SA line. Knockout of *MPK3* in *Arabidopsis* results in smaller anthers, and in a double mutant with its closest homolog, *MPK6*, pollen development is severely impaired (Hord et al., 2008). The tomato orthologs of both, *MPK3* and *MPK6* (Solyc12g019460), were significantly downregulated by LTMH in the wild type; higher expression of *MPK3* in *35S:nahG* may thus prevent damage through this pathway. Taken together, various anther developmental pathways are differentially affected by *35S:nahG* in LTMH.

In addition, we found higher expression of *HSF6b* in LTMH and *HSF9* in CT and LTMH. It remains to be determined whether this constitutes an *HSFA2*-independent branch of the HSR that protects against LTMH. Enrichment analysis indicated that the responses to unfolded proteins and ER stress as a whole were reduced in *35S:nahG* in LTMH, which could be a result of constitutively better protection to protein unfolding. Carbohydrate-related gene annotations were overrepresented in the tolerant line. This was mainly caused by highly diverse expression changes of several *FBA*, *BAM*, *SWEET,* and *STP* genes, without a clear overall pattern. *35S:nahG* had a slightly increased sucrose and glucose level in bicellular and mature pollen stage anthers in LTMH, but overall carbohydrate levels were rather similar to wild type. Sucrose and hexose levels thus seem not to be predictive of pollen performance, either because they are

not limiting at these observed levels, or because they do not sufficiently capture underlying metabolic fluxes.

Enhanced Jasmonic Acid Signal May Mediate the Low-Salicylic Acid Effect on Pollen Long-Term Mild Heat Tolerance

Long-term mild heat had negative effects on the level of IAA, JA-ile, and iP in the wild type. When comparing the low-SA and wild-type plants, only the drop in IAA level seemed to be mitigated to some extent, raising the possibility that this contributed to improved LTMH tolerance. Indeed, indications that low IAA levels are causal for pollen failure have been reported for barley (Sakata et al., 2010). An absence of JA signal also causes severe anther and pollen developmental defects in Arabidopsis and reduced PV in tomatoes (Xie et al., 1998; Li et al., 2004). The severe pollen phenotype in two low-JA genotypes at mildly elevated temperature shows that there is a temperature-dependent requirement for this hormone in the process of pollen development. Interestingly, *35S:nahG* dampened the upregulation by LTMH of several JAZ genes, encoding repressors of the JA response (Chini et al., 2017), raising the possibility that low JA signaling is causal to pollen LTMH damage and that increased JA signaling strength in *35S:nahG* contributes to better pollen performance of this line. Indeed, Arabidopsis seedlings require JA signaling for heat tolerance, and heat-induced male sterility has been linked to reduced JA signal (Clarke et al., 2009; Khan et al., 2020; He et al., 2021). It is likely, however, that both, the LTMH pollen phenotype in the wild type and the increased tolerance in the low-SA line involve interaction between multiple hormones. In addition to JA, SA, auxin, and ABA have all been implicated in pollen development (Cardarelli and Cecchetti, 2014; Feng et al., 2018; Yao et al., 2018; Rezaul et al., 2019; Terceros et al., 2020). Furthermore, multiple hormones are associated with cell division (Shimotohno et al., 2021), carbohydrate metabolism (Eveland and Jackson, 2012), and the heat shock response (Snyman and Cronjé, 2008; Carranco et al., 2010; Huang et al., 2016; Tian et al., 2020; Li et al., 2021). Analysis of the role of single hormones as well as their interaction will be needed to be able to model and forecast the effects of hormone modifications on pollen heat tolerance.

Taken together, we have shown that low endogenous SA level promotes pollen development under LTMH conditions and found a number of plausible mechanisms for the tolerant phenotype. Future studies might investigate the involvement of specific genes, such as *MPK3* and *HSF*s, and the hormones IAA and JA, e.g., through analysis of lines with reduced JAZ gene activity. For potential future applications, it will be important to test whether anther-specific reduction of SA is sufficient to obtain the desired tolerance.

DATA AVAILABILITY STATEMENT

The datasets presented in this study can be found in online repositories. The names of the repository/repositories and accession number(s) can be found below: https://www.ncbi.nlm.nih.gov/geo/, GSE185583.

AUTHOR CONTRIBUTIONS

SJ and IR conceived and designed the study and wrote the manuscript. SJ, LS, YT, and WK performed the research. SJ, WL, and IR analyzed and interpreted the data. All authors contributed to the article and approved the submitted version.

FUNDING

This study was supported by the Dutch Organization for Scientific Research (NWO, Grant Number 867.15.011 to IR).

ACKNOWLEDGMENTS

We would like to thank Lázaro Peres (University of São Paulo, Brazil) for providing us with the *35S:nahG* transgenic line in the Micro-Tom background, Jan Henk Venema (University of Groningen, Netherlands) for the *def1* mutant, and Fiona Gogin (University of Arkansas, United States) for the *acx1* mutant. We would also like to express our gratitude to our greenhouse staff for their assistance in plant cultivation.

SUPPLEMENTARY MATERIAL

The Supplementary Material for this article can be found online at: https://www.frontiersin.org/articles/10.3389/fpls.2022.828743/full#supplementary-material

REFERENCES

Angadi, S., Cutforth, H., Miller, P., McConkey, B., Entz, M., Brandt, S., et al. (2000). Response of three Brassica species to high temperature stress during reproductive growth. *Can. J. Plant Sci.* 80, 693–701. doi: 10.4141/p99-152

Battisti, D. S., and Naylor, R. L. (2009). Historical warnings of future food insecurity with unprecedented seasonal heat. *Science* 323, 240–244. doi: 10.1126/science.1164363

Bechtold, U., and Field, B. (2018). *Molecular Mechanisms Controlling Plant Growth During Abiotic Stress*. Oxford: Oxford University Press.

Brading, P. A., Hammond-Kosack, K. E., Parr, A., and Jones, J. D. (2000). Salicylic acid is not required for Cf-2-and Cf-9-dependent resistance of tomato to Cladosporium fulvum. *Plant J.* 23, 305–318. doi: 10.1046/j.1365-313x.2000.00778.x

Camejo, D., Rodríguez, P., Morales, M. A., Dell'Amico, J. M., Torrecillas, A., and Alarcón, J. J. (2005). High temperature effects on photosynthetic activity of two tomato cultivars with different heat susceptibility. *J. Plant Physiol.* 162, 281–289. doi: 10.1016/j.jplph.2004.07.014

Campos, M. L., Yoshida, Y., Major, I. T., de Oliveira Ferreira, D., Weraduwage, S. M., Froehlich, J. E., et al. (2016). Rewiring of jasmonate and phytochrome B signalling uncouples plant growth-defense tradeoffs. *Nat. Commun.* 7, 1–10. doi: 10.1038/ncomms12570

Cardarelli, M., and Cecchetti, V. (2014). Auxin polar transport in stamen formation and development: how many actors? *Front. Plant Sci.* 5:333. doi: 10.3389/fpls.2014.00333

Carranco, R., Espinosa, J. M., Prieto-Dapena, P., Almoguera, C., and Jordano, J. (2010). Repression by an auxin/indole acetic acid protein connects auxin signaling with heat shock factor-mediated seed longevity. *Proc. Natl. Acad. Sci.* 107, 21908–21913. doi: 10.1073/pnas.1014856107

Carvalho, R. F., Campos, M. L., Pino, L. E., Crestana, S. L., Zsögön, A., Lima, J. E., et al. (2011). Convergence of developmental mutants into a single tomato model system:'Micro-Tom'as an effective toolkit for plant development research. *Plant Methods* 7, 1–14. doi: 10.1186/1746-4811-7-18

Charles, W., and Harris, R. (1972). Tomato fruit-set at high and low temperatures. *Can. J. Plant Sci.* 52, 497–506. doi: 10.4141/cjps72-080

Chini, A., Ben-Romdhane, W., Hassairi, A., and Aboul-Soud, M. A. (2017). Identification of TIFY/JAZ family genes in Solanum lycopersicum and their regulation in response to abiotic stresses. *PLoS One* 12:e0177381. doi: 10.1371/journal.pone.0177381

Clarke, S. M., Cristescu, S. M., Miersch, O., Harren, F. J., Wasternack, C., and Mur, L. A. (2009). Jasmonates act with salicylic acid to confer basal thermotolerance in Arabidopsis thaliana. *New Phytol.* 182, 175–187. doi: 10.1111/j.1469-8137.2008.02735.x

Clarke, S. M., Mur, L. A., Wood, J. E., and Scott, I. M. (2004). Salicylic acid dependent signaling promotes basal thermotolerance but is not essential for acquired thermotolerance in Arabidopsis thaliana. *Plant J.* 38, 432–447. doi: 10.1111/j.1365-313X.2004.02054.x

De Storme, N., and Geelen, D. (2014). The impact of environmental stress on male reproductive development in plants: biological processes and molecular mechanisms. *Plant Cell Environ.* 37, 1–18. doi: 10.1111/pce.12142

Djanaguiraman, M., Perumal, R., Ciampitti, I., Gupta, S., and Prasad, P. (2018). Quantifying pearl millet response to high temperature stress: thresholds, sensitive stages, genetic variability and relative sensitivity of pollen and pistil. *Plant Cell Environ.* 41, 993–1007. doi: 10.1111/pce.12931

Djanaguiraman, M., Prasad, P. V., Murugan, M., Perumal, R., and Reddy, U. K. (2014). Physiological differences among sorghum (Sorghum bicolor L. Moench) genotypes under high temperature stress. *Environ. Exp. Bot.* 100, 43–54. doi: 10.1016/j.envexpbot.2013.11.013

Driedonks, N., Wolters-Arts, M., Huber, H., de Boer, G.-J., Vriezen, W., Mariani, C., et al. (2018). Exploring the natural variation for reproductive thermotolerance in wild tomato species. *Euphytica* 214:67. doi: 10.1007/s10681-018-2150-2

Endo, M., Tsuchiya, T., Hamada, K., Kawamura, S., Yano, K., Ohshima, M., et al. (2009). High temperatures cause male sterility in rice plants with transcriptional alterations during pollen development. *Plant Cell Physiol.* 50, 1911–1922. doi: 10.1093/pcp/pcp135

Eveland, A. L., and Jackson, D. P. (2012). Sugars, signalling, and plant development. *J. Exp. Bot.* 63, 3367–3377. doi: 10.1093/jxb/err379

Farooq, M., Bramley, H., Palta, J. A., and Siddique, K. H. (2011). Heat stress in wheat during reproductive and grain-filling phases. *Crit. Rev. Plant Sci.* 30, 491–507. doi: 10.1080/07352689.2011.615687

Feng, B., Zhang, C., Chen, T., Zhang, X., Tao, L., and Fu, G. (2018). Salicylic acid reverses pollen abortion of rice caused by heat stress. *BMC Plant Biol.* 18:5. doi: 10.1186/s12870-018-1472-5

Fragkostefanakis, S., Simm, S., Paul, P., Bublak, D., Scharf, K.-D., and Schleiff, E. (2015). The chaperone network of tomato. *Plant Cell Environ.* 38, 693–709. doi: 10.1111/pce.12426

Gibson, L., and Paulsen, G. (1999). Yield components of wheat grown under high temperature stress during reproductive growth. *Crop Sci.* 39, 1841–1846. doi: 10.2135/cropsci1999.3961841x

Gühl, K., Holmer, R., Xiao, T. T., Shen, D., Wardhani, T. A., Geurts, R., et al. (2021). The effect of exogenous nitrate on LCO signalling, cytokinin accumulation, and nodule initiation in Medicago truncatula. *Genes* 12:988. doi: 10.3390/genes12070988

He, Y., Liu, C., Zhu, L., Fu, M., Sun, Y., and Zeng, H. (2021). Jasmonic Acid Plays a Pivotal Role in Pollen Development and Fertility Regulation in Different Types of P (T) GMS Rice Lines. *Int. J. Mol. Sci.* 22:7926. doi: 10.3390/ijms22157926

Heidmann, I., Schade-Kampmann, G., Lambalk, J., Ottiger, M., and Di Berardino, M. (2016). Impedance flow cytometry: a novel technique in pollen analysis. *PLoS One* 11:e0165531. doi: 10.1371/journal.pone.0165531

Herms, D. A., and Mattson, W. J. (1992). The dilemma of plants: to grow or defend. *Quart. Rev. Biol.* 67, 283–335. doi: 10.1086/417659

Herrera-Vásquez, A., Salinas, P., and Holuigue, L. (2015). Salicylic acid and reactive oxygen species interplay in the transcriptional control of defense genes expression. *Front. Plant Sci.* 6:171. doi: 10.3389/fpls.2015.00171

Herrero, M. P., and Johnson, R. (1980). High temperature stress and pollen viability of maize 1. *Crop Sci.* 20, 796–800. doi: 10.2135/cropsci1980.0011183x002000060030x

Hord, C. L., Sun, Y.-J., Pillitteri, L. J., Torii, K. U., Wang, H., Zhang, S., et al. (2008). Regulation of Arabidopsis early anther development by the mitogen-activated protein kinases, MPK3 and MPK6, and the ERECTA and related receptor-like kinases. *Mol. Plant* 1, 645–658. doi: 10.1093/mp/ssn029

Howe, G. A., Lightner, J., Browse, J., and Ryan, C. A. (1996). An octadecanoid pathway mutant (JL5) of tomato is compromised in signaling for defense against insect attack. *Plant Cell* 8, 2067–2077. doi: 10.1105/tpc.8.11.2067

Huang, Y.-C., Niu, C.-Y., Yang, C.-R., and Jinn, T.-L. (2016). The heat stress factor HSFA6b connects ABA signaling and ABA-mediated heat responses. *Plant Physiol.* 172, 1182–1199. doi: 10.1104/pp.16.00860

Huot, B., Yao, J., Montgomery, B. L., and He, S. Y. (2014). Growth–defense tradeoffs in plants: a balancing act to optimize fitness. *Mol. Plant* 7, 1267–1287. doi: 10.1093/mp/ssu049

Karasov, T. L., Chae, E., Herman, J. J., and Bergelson, J. (2017). Mechanisms to mitigate the trade-off between growth and defense. *Plant Cell* 29, 666–680. doi: 10.1105/tpc.16.00931

Keller, M., SPOT-ITN Consortium, and Simm, S. (2018). The coupling of transcriptome and proteome adaptation during development and heat stress response of tomato pollen. *BMC Genomics* 19:447. doi: 10.1186/s12864-018-4824-5

Khan, A. H., Min, L., Ma, Y., Wu, Y., Ding, Y., Li, Y., et al. (2020). High day and night temperatures distinctively disrupt fatty acid and jasmonic acid metabolism, inducing male sterility in cotton. *J. Exp. Bot.* 71, 6128–6141. doi: 10.1093/jxb/eraa319

Khan, M. I. R., Iqbal, N., Masood, A., Per, T. S., and Khan, N. A. (2013). Salicylic acid alleviates adverse effects of heat stress on photosynthesis through changes in proline production and ethylene formation. *Plant Signal. Behav.* 8:e26374. doi: 10.4161/psb.26374

Ku, S., Yoon, H., Suh, H. S., and Chung, Y.-Y. (2003). Male-sterility of thermosensitive genic male-sterile rice is associated with premature programmed cell death of the tapetum. *Planta* 217, 559–565. doi: 10.1007/s00425-003-1030-7

Larkindale, J., and Knight, M. R. (2002). Protection against heat stress-induced oxidative damage in Arabidopsis involves calcium, abscisic acid, ethylene, and salicylic acid. *Plant Physiol.* 128, 682–695. doi: 10.1104/pp.010320

Larkindale, J., Hall, J. D., Knight, M. R., and Vierling, E. (2005). Heat stress phenotypes of Arabidopsis mutants implicate multiple signaling pathways in the acquisition of thermotolerance. *Plant Physiol.* 138, 882–897. doi: 10.1104/pp.105.062257

Li, C., Schilmiller, A. L., Liu, G., Lee, G. I., Jayanty, S., Sageman, C., et al. (2005). Role of β-oxidation in jasmonate biosynthesis and systemic wound signaling in tomato. *Plant Cell* 17, 971–986. doi: 10.1105/tpc.104.029108

Li, L., Zhao, Y., McCaig, B. C., Wingerd, B. A., Wang, J., Whalon, M. E., et al. (2004). The tomato homolog of CORONATINE-INSENSITIVE1 is required for the maternal control of seed maturation, jasmonate-signaled defense responses, and glandular trichome development. *Plant Cell* 16, 126–143. doi: 10.1105/tpc.017954

Li, N., Euring, D., Cha, J. Y., Lin, Z., Lu, M., Huang, L.-J., et al. (2021). Plant hormone-mediated regulation of heat tolerance in response to global climate change. *Front. Plant Sci.* 11:2318. doi: 10.3389/fpls.2020.627969

Lobell, D. B., and Field, C. B. (2007). Global scale climate–crop yield relationships and the impacts of recent warming. *Environ. Res. Lett.* 2:014002. doi: 10.1088/1748-9326/2/1/014002

Masson-Delmotte, V., Zhai, P., Pirani, A., Connors, S. L., Péan, C., Berger, S., et al. (2021). "IPCC, 2021: climate change 2021: The physical science basis," in *Contribution of Working Group I to the Sixth Assessment Report of the Intergovernmental Panel on Climate Change*, (Cambridge: Cambridge University Press). doi: 10.1007/s10584-021-03233-7

Meng, L., Liu, Z., Zhang, L., Hu, G., and Song, X. (2016). Cytological characterization of a thermo-sensitive cytoplasmic male-sterile wheat line having K-type cytoplasm of Aegilops kotschyi. *Breed. Sci.* 2016:16039. doi: 10.1270/jsbbs.16039

Mi, H., Ebert, D., Muruganujan, A., Mills, C., Albou, L.-P., Mushayamaha, T., et al. (2021). PANTHER version 16: a revised family classification, tree-based classification tool, enhancer regions and extensive API. *Nucleic Acids Res.* 49, D394–D403. doi: 10.1093/nar/gkaa1106

Müller, F., and Rieu, I. (2016). Acclimation to high temperature during pollen development. *Plant Reprod.* 29, 107–118. doi: 10.1007/s00497-016-0282-x

Müller, F., Xu, J., Kristensen, L., Wolters-Arts, M., de Groot, P. F., Jansma, S. Y., et al. (2016). High-temperature-induced defects in tomato (Solanum lycopersicum) anther and pollen development are associated with reduced expression of B-class floral patterning genes. *PLoS One* 11:e0167614. doi: 10.1371/journal.pone.0167614

Munakata, K. (1976). Effects of temperature and light on the reproductive growth and ripening of rice. *Clim. Rice* 1976, 187–210.

Parish, R. W., and Li, S. F. (2010). Death of a tapetum: a programme of developmental altruism. *Plant Sci.* 178, 73–89. doi: 10.1016/j.plantsci.2009.11.001

Parish, R. W., Phan, H. A., Iacuone, S., and Li, S. F. (2012). Tapetal development and abiotic stress: a centre of vulnerability. *Funct. Plant Biol.* 39, 553–559. doi: 10.1071/FP12090

Peng, S., Huang, J., Sheehy, J. E., Laza, R. C., Visperas, R. M., Zhong, X., et al. (2004). Rice yields decline with higher night temperature from global warming. *Proc. Natl. Acad. Sci.* 101, 9971–9975. doi: 10.1073/pnas.0403720101

Praba, M. L., and Thangaraj, M. (2005). Effect of growth regulators and chemicals on pollen sterility in TGMS lines of rice. *Plant Growth Regul.* 46, 117–124. doi: 10.1007/s10725-005-7362-5

Prasad, P. V., Boote, K. J., and Allen, L. H. Jr. (2006). Adverse high temperature effects on pollen viability, seed-set, seed yield and harvest index of grain-sorghum [Sorghum bicolor (L.) Moench] are more severe at elevated carbon dioxide due to higher tissue temperatures. *Agricult. For. Meteorol.* 139, 237–251. doi: 10.1016/j.agrformet.2006.07.003

Pressman, E., Peet, M. M., and Pharr, D. M. (2002). The effect of heat stress on tomato pollen characteristics is associated with changes in carbohydrate concentration in the developing anthers. *Ann. Bot.* 90, 631–636. doi: 10.1093/aob/mcf240

Rezaul, I. M., Baohua, F., Tingting, C., Weimeng, F., Caixia, Z., Longxing, T., et al. (2019). Abscisic acid prevents pollen abortion under high-temperature stress by mediating sugar metabolism in rice spikelets. *Physiol. Plant.* 165, 644–663. doi: 10.1111/ppl.12759

Saini, H., and Aspinall, D. (1982). Abnormal sporogenesis in wheat (Triticum aestivum L.) induced by short periods of high temperature. *Ann. Bot.* 49, 835–846. doi: 10.1093/oxfordjournals.aob.a086310

Sakata, T., Oshino, T., Miura, S., Tomabechi, M., Tsunaga, Y., Higashitani, N., et al. (2010). Auxins reverse plant male sterility caused by high temperatures. *Proc. Natl. Acad. Sci.* 107, 8569–8574. doi: 10.1073/pnas.1000869107

Sakata, T., Takahashi, H., Nishiyama, I., and Higashitani, A. (2000). Effects of high temperature on the development of pollen mother cells and microspores in barley Hordeum vulgare L. *J. Plant Res.* 113:395. doi: 10.1007/pl00013947

Sato, S., Peet, M. M., and Thomas, J. F. (2002). Determining critical pre-and post-anthesis periods and physiological processes in Lycopersicon esculentum Mill. exposed to moderately elevated temperatures. *J. Exp. Bot.* 53, 1187–1195. doi: 10.1093/jexbot/53.371.1187

Schiessl, K., Lilley, J. L., Lee, T., Tamvakis, I., Kohlen, W., Bailey, P. C., et al. (2019). NODULE INCEPTION recruits the lateral root developmental program for symbiotic nodule organogenesis in Medicago truncatula. *Curr. Biol.* 29, 3657–3668. doi: 10.1016/j.cub.2019.09.005

Shimotohno, A., Aki, S. S., Takahashi, N., and Umeda, M. (2021). Regulation of the plant cell cycle in response to hormones and the environment. *Annu. Rev. Plant Biol.* 72, 273–296. doi: 10.1146/annurev-arplant-080720-103739

Simms, E. L., and Rausher, M. D. (1987). Costs and benefits of plant resistance to herbivory. *Am. Natural.* 130, 570–581. doi: 10.1086/284731

Snyman, M., and Cronjé, M. (2008). Modulation of heat shock factors accompanies salicylic acid-mediated potentiation of Hsp70 in tomato seedlings. *J. Exp. Bot.* 59, 2125–2132. doi: 10.1093/jxb/ern075

Song, G., Wang, M., Zeng, B., Zhang, J., Jiang, C., Hu, Q., et al. (2015). Anther response to high-temperature stress during development and pollen thermotolerance heterosis as revealed by pollen tube growth and in vitro pollen vigor analysis in upland cotton. *Planta* 241, 1271–1285. doi: 10.1007/s00425-015-2259-7

Suzuki, K., Tsukaguchi, T., Takeda, H., and Egawa, Y. (2001). Decrease of pollen stainability of green bean at high temperatures and relationship to heat tolerance. *J. Am. Soc. Horticult. Sci.* 126, 571–574. doi: 10.21273/jashs.126.5.571

Terceros, G. C., Resentini, F., Cucinotta, M., Manrique, S., Colombo, L., and Mendes, M. A. (2020). The importance of cytokinins during reproductive development in Arabidopsis and beyond. *Int. J. Mol. Sci.* 21:8161. doi: 10.3390/ijms21218161

Tian, X., Wang, F., Zhao, Y., Lan, T., Yu, K., Zhang, L., et al. (2020). Heat shock transcription factor A1b regulates heat tolerance in wheat and Arabidopsis through OPR3 and jasmonate signalling pathway. *Plant Biotechnol. J.* 18:1109. doi: 10.1111/pbi.13268

Verma, V., Ravindran, P., and Kumar, P. P. (2016). Plant hormone-mediated regulation of stress responses. *BMC Plant Biol.* 16:86. doi: 10.1186/s12870-016-0771-y

Wang, J., Gan, Y., Clarke, F., and McDonald, C. (2006). Response of chickpea yield to high temperature stress during reproductive development. *Crop Sci.* 46, 2171–2178. doi: 10.2135/cropsci2006.02.0092

Wu, C., Cui, K., Li, Q., Li, L., Wencheng, W., Hu, Q., et al. (2021). Estimating the yield stability of heat-tolerant rice genotypes under various heat conditions across reproductive stages: a 5-year case study. *Sci. Rep.* 11:13604. doi: 10.1038/s41598-021-93079-x

Xie, D.-X., Feys, B. F., James, S., Nieto-Rostro, M., and Turner, J. G. (1998). COI1: an Arabidopsis gene required for jasmonate-regulated defense and fertility. *Science* 280, 1091–1094. doi: 10.1126/science.280.5366.1091

Xiong, S. X., Lu, J. Y., Lou, Y., Teng, X. D., Gu, J. N., Zhang, C., et al. (2016). The transcription factors MS 188 and AMS form a complex to activate the expression of CYP 703A2 for sporopollenin biosynthesis in Arabidopsis thaliana. *Plant J.* 88, 936–946. doi: 10.1111/tpj.13284

Xu, J., Wolters-Arts, M., Mariani, C., Huber, H., and Rieu, I. (2017). Heat stress affects vegetative and reproductive performance and trait correlations in tomato (Solanum lycopersicum). *Euphytica* 213:156.

Xu, J., Yang, C., Yuan, Z., Zhang, D., Gondwe, M. Y., Ding, Z., et al. (2010). The ABORTED MICROSPORES regulatory network is required for postmeiotic male reproductive development in Arabidopsis thaliana. *Plant Cell* 22, 91–107. doi: 10.1105/tpc.109.071803

Yao, X., Tian, L., Yang, J., Zhao, Y.-N., Zhu, Y.-X., Dai, X., et al. (2018). Auxin production in diploid microsporocytes is necessary and sufficient for early stages of pollen development. *PLoS Genet.* 14:e1007397.doi: 10.1371/journal.pgen.1007397

Yu, C., Xu, X., Ge, J., Guo, Y., Dong, J., and Dong, Z. (2016). Premature breakdown of tapetum associated with reverse thermo-sensitive genic male-sterile line Huiyou50S in rapeseed (Brassica napus). *Acta Physiol. Plant.* 38:54.

Zhang, C., Feng, B., Chen, T., Zhang, X., Tao, L., and Fu, G. (2017). Sugars, antioxidant enzymes and IAA mediate salicylic acid to prevent rice spikelet degeneration caused by heat stress. *Plant Growth Regul.* 83, 313–323. doi: 10.1007/s10725-017-0296-x

Zhao, Q., Zhou, L., Liu, J., Cao, Z., Du, X., Huang, F., et al. (2018). Involvement of CAT in the detoxification of HT-induced ROS burst in rice anther and its relation to pollen fertility. *Plant Cell Rep.* 37, 741–757. doi: 10.1007/s00299-018-2264-y

Conflict of Interest: The authors declare that the research was conducted in the absence of any commercial or financial relationships that could be construed as a potential conflict of interest.

Publisher's Note: All claims expressed in this article are solely those of the authors and do not necessarily represent those of their affiliated organizations, or those of the publisher, the editors and the reviewers. Any product that may be evaluated in this article, or claim that may be made by its manufacturer, is not guaranteed or endorsed by the publisher.

frontiers | Frontiers in Plant Science

ORIGINAL RESEARCH
published: 02 June 2022
doi: 10.3389/fpls.2022.835380

Shade Delayed Flowering Phenology and Decreased Reproductive Growth of *Medicago sativa* L.

Fengfei Qin[1], Yixin Shen[1], Zhihua Li[1], Hui Qu[2], Jinxia Feng[1], Lingna Kong[1], Gele Teri[1], Haoming Luan[1] and Zhiling Cao[1]*

[1]College of Agro-grassland Science, Nanjing Agricultural University, Nanjing, China, [2]Institute of Grassland Research, Chinese Academy of Agricultural Sciences, Hohhot, China

Alfalfa (*Medicago sativa* L.) is an important forage in intercropping or rotation ecosystem, and shading is the principal limiting factor for its growth under the crop or forest. Agronomic studies showed that shading would systematically reduce the biomass of alfalfa. However, little is known about the reproduction of alfalfa under shading conditions. In order to study the effect of shading on the reproductive characteristics of alfalfa, two alfalfa cultivars ("Victoria" and "Eureka") were used to study the effect of shading levels (full light, 56.4% shade, and 78.7% shade) on alfalfa flowering phenology, pollen viability, stigma receptivity, and seed quality. Results showed that shading delayed flowering phenology, shortened the flowering stage, faded the flower colors, and significantly reduced pollen viability, stigma receptivity, the number of flowers, quantity, and quality of seeds. Under shading conditions, seed yield per plant was obviously positively correlated with germination potential, germination rate, pollen viability, and 1,000-seed weight. The number of flower buds, pollen viability, 1,000-seed weight, and germination rate had the greatest positive direct impact on seed yield per plant. Our findings suggested that delayed flowering and reducing reproduction growth were important strategies for alfalfa to cope with shading and pollen viability was the key bottleneck for the success of alfalfa reproduction under shading. However, given that alfalfa is a perennial vegetative-harvest forage, delaying flowering in a weak light environment was beneficial to maintain the high aboveground biomass of alfalfa. Therefore, this should be taken into account when breeding alfalfa cultivars suitable for intercropping. Future research should further reveal the genetic and molecular mechanism of delayed flowering regulating the accumulation and distribution of assimilates between vegetative and reproductive organs of alfalfa under shading, so as to provide a theoretical basis for breeding of shade-tolerant alfalfa cultivars.

Keywords: ***Medicago sativa* L., weak light, flowering phenology, pollen viability, stigma receptivity, fruiting**

OPEN ACCESS

Edited by:
Kevin Begcy,
University of Florida, United States

Reviewed by:
Mingya Wang,
Institute of Animal Sciences (CAAS), China
Ling Ling Chen,
Inner Mongolia University, China
Jiangqi Wen,
Oklahoma State University, United States

****Correspondence:***
Fengfei Qin
qinffei@njau.edu.cn

Specialty section:
This article was submitted to Plant Abiotic Stress, a section of the journal Frontiers in Plant Science

Received: *14 December 2021*
Accepted: *13 May 2022*
Published: *02 June 2022*

Citation:
Qin F, Shen Y, Li Z, Qu H, Feng J, Kong L, Teri G, Luan H and Cao Z (2022) Shade Delayed Flowering Phenology and Decreased Reproductive Growth of Medicago sativa L. Front. Plant Sci. 13:835380. doi: 10.3389/fpls.2022.835380

INTRODUCTION

Alfalfa (*Medicago sativa* L.) is a perennial forage with high quality and yield. As the most important legume forage in temperate regions, it is widely cultivated worldwide. Due to the rapid development of the dairy industry, China's demand for alfalfa has increased significantly; therefore, alfalfa cultivation requires new niches, especially in southern China, where the land

is mainly used for grain production and agriculture. The inter-row space of crops (such as maize and sorghum) or planted forests (such as orchard and poplar) provides opportunities for planting alfalfa. As a stress-resistant legume crop, alfalfa fixes a large amount of atmospheric nitrogen (approximately 135–605 kg ha^{-1} $year^{-1}$; Putnam et al., 2001), which enables alfalfa to grow in various soil types and provide nitrogen for interplanting or subsequent crops when alfalfa is planted in interplanting or rotation system. Previous studies have shown that alfalfa has a certain tolerance to slight shade (about 50% of full sunlight; Lin et al., 1999; Qin et al., 2010) and can maintain high biomass. Therefore, as an interplanting crop, alfalfa plays an important role in the intercropping ecosystem. However, when the light intensity of the intercropping system is lower than 50% of full sunlight, the photosynthetic efficiency and morphogenesis of alfalfa have adaptive change, including obvious top advantage, thinner stems and easy to fall off, thinner leaves, fewer branches and lower relative growth rate, and delayed growth (collectively termed as shade avoidance symptoms, SAS), which significantly reduce the aboveground biomass of alfalfa (Cooper and Qualls, 1967; Walgenbach and Marten, 1981; Lin et al., 1999; Qin et al., 2010). However, the above characteristics are based on the observations of alfalfa seedlings, little is known about the reproduction of alfalfa under weak light stress.

Light is a key environmental factor that regulates plant growth and development. It is involved in controlling multiple responses in the plant life cycle, including seed germination, seedling de-etiolation, phototropism, shade avoidance, circadian rhythms, and flowering time (Castillon et al., 2007). Plants often grow in shaded environments, mainly from the shade of adjacent plant branches and upper canopy groups. As plants grow fixedly, they cannot choose appropriate living conditions through free movement like animals. Therefore, plants have developed a strict and precise light signal regulation system to regulate plant internal growth and metabolic activities, and produced corresponding reproductive strategies to maintain the persistence of their population in the shade environments (Boardman, 1977).

So far, plants have responded to shading through two flowering strategies. *Arabidopsis thaliana* (Cerdán and Chory, 2003), *Lotus japonicus* (Ueoka-Nakanishi et al., 2011), and rice showed early flowering induction in shade avoidance syndrome, which was regarded as a seed setting strategy before serious resources constraints (Carriedo et al., 2016). However, plants such as grape, tomato, and sunflower, when photon flux density decreased to approximately 40% of the full sunlight, flower bud differentiation was delayed, which lead to decrease in its distribution of accumulated dry matter to reproductive organs. In addition, the number of photosynthetic organs increased to adapt to weak light environments (El-Aidy et al., 1983; Atlag, 1990; El-Gizawy et al., 1993; Li et al., 2002). However, this strategy reduced flower bud quality, flowering rate, sex cell concentration (Yi et al., 2006), pollen viability, and ovum quality, thus increased dropping blossoms and fruit (Ferree et al., 1998), and finally reducing weight and composition of grains (Echarte et al., 2012). No matter which flowering strategy is adopted, it is the most suitable way for plants to survive in weak light environments.

In order to fully understand the shade tolerance potential in alfalfa, it is necessary to comprehensively study the reproductive strategy of alfalfa under shading conditions. Therefore, the objective of this study was to investigate the effects of artificial shade on flowering phenology, floral transition, flower development, fruiting, seed yield, and quality of two alfalfa cultivars planted for two consecutive years. The results of this study will helpful to reveal the mechanism of shading induced reproductive changes in alfalfa and provide a theoretical basis for screening and breeding of shade-tolerant and high-yielding cultivars in intercropping ecosystem.

MATERIALS AND METHODS

Plant Materials and Growing and Shade Treatments

The experiment was conducted in three plastic greenhouses (4.5 m × 3 m × 2.5 m steel frame) from September 2017 to July 2018. Under natural photoperiod conditions (from winter 10 h/14 h to summer 14 h/10 h, day/night, during experiment period), there was no plastic cover within 50 cm from the ground, which was used for air circulation and free movements of pollinators (**Supplementary Figure 1**). The test site was located in Baima Teaching and Research Base of Nanjing Agricultural University (31°14′-32°37′N, 118°22′-119°14′E). The mean values of monthly day and night temperature outside the greenhouse during the flowering and fruiting period were shown in **Supplementary Figure 2**.

Two alfalfa cultivars Victoria (Fall Dormancy FD = 6) and Eureka (FD = 8) were selected for the experiment. The seeds of both cultivars were introduced from the United States. In September 2017, the seeds of each alfalfa cultivar were sowed in 24 separate pots (internal diameter 35 cm, height 27 cm) and filled with soil. The soil contained 90% humus soil and 10% pearlite (N + P + K > 4%, organic matter>30%), and 100 g organic fertilizer was applied in each pot. The seedlings grew continuously in three greenhouses, with eight pots in each greenhouse, and were thinned to five robust plants per pot when the seedlings were 4–5 cm (approximately 20 days after sowing).

In March 2018, after the alfalfa seedlings resumed growth from winter, two shading treatments and one full sunlight control treatment were set up. Two shading levels were created by using the neutral-density green shading net layer on the steel frame, and the light intensity (43.6 ± 1.3 and 21.3% ± 0.5% of full sunlight, marked as 56.4% shade and 78.7% shade, respectively) was measured by TES-1339 illuminance meter (Taiwan TES Electronic Industry Co., Ltd.). The experiment was conducted as completely random block design, with eight replicates for each treatment, and each pot was rotated to a new position every 14 days to reduce the influence of any position. Each pot was irrigated every 5 days to keep the soil moist. The shading treatment lasted for 5 months, covering the entire flowering, filling, and seed expansion season.

Measurements of Flowering, Fruiting, and Seed Trait

Flowering Phenology

Three plants were randomly marked in each treatment pot, and the first flowering date of each plant was record. The floral buds of marked plants were counted every 3 days, with 50% of floral buds in the bud initiation stage as the budding stage, the flowering stage of 10% of the alfalfa plants in flowering stage as the early flowering stage, and 80% of the alfalfa plants in the flowering stage as the full flowering stage (Mao, 2019). Under each shading treatment, the flowering stage was recorded from the first appearance of flower to the withering of the last flower.

Flowering Dynamics

Alfalfa is a cross-pollinated forage crop. In the experimental area, its flowering stage is from April to July, and the main pollinators are bees, especially *Megachile rotundata Fubricius*. During this period, at each light level, three plants per pot were randomly selected from each pot under shading treatment. The buds and flowers in three inflorescences of each plant were counted every day from the first appearance of the buds to the end of the flowering stage. The number of fallen flowers was estimated by counting the drop mark of the flowering peduncles. The following formula was used to calculate the flowering rates and fallen flower rates.

$$\text{Flowering rate}(\%) = \left(\frac{\text{Number of the flowering buds}}{\text{Number of buds}}\right) \times 100\% \quad (1)$$

$$\text{Fallen flower rate}(\%) = \left(\frac{\text{Number of the drop mark of peduncles}}{\text{Number of flowers}}\right) \times 100\% \quad (2)$$

Pollen Viability and Stigma Receptivity

Pollen fertility and stigma receptivity were tested by potassium iodide method and benzidine hydrogen peroxide method (Dafni and Maués, 1998), respectively. At each shading treatment, three plants were randomly selected from each pot. During the full flowering stage (May to June), three inflorescences of each plant at the same flowering stage were marked. In the morning, the pollen grains of five buds in each inflorescence were collected by gently peeling the keels in Petri plates and transferred to glass slides. The pollen grains were stained with 0.5% iodine and 1% potassium iodide solutions, and observed and counted under a microscope at ×10 magnification. The stigmas of the five flowers of each plant were immersed in the groove of concave glass slide with benzidine hydrogen peroxide (1% benzidine:3% hydrogen peroxide:H_2O = 4:11:22, volume ratio). More than two-thirds of the stigma turned blue, and when many bubbles formed around the stigmas, which indicated that the stigmas were receptive. The test lasted for 5 days, and the flowers were tagged at different days after flowering. The following formula was used to calculate pollen viability and stigma receptivity:

$$\text{Pollen viability}(\%) = \left(\frac{\text{Number of blue pollens}}{\text{Number of pollens}}\right) \times 100\% \quad (3)$$

$$\text{Stigma receptivity}(\%) = \left(\frac{\text{Number of blue stigmas}}{\text{Number of stigmas}}\right) \times 100\% \quad (4)$$

Seed Production and Quality

Three plants were randomly selected from each pot under shading treatment. The pods in the three inflorescences of marked plants were counted every day from the first appearance of the pods to the end of the seed production. The number of fallen pods was estimated by counting the drop marks of the pods every day. After collection, the total seed yield of each plant was determined and the seeds were air dried. The seeds produced by each plant were counted, and then, the 1,000-seed weight was determined in four replications. Germination study was conducted in a Petri plate, in which 100 seeds were placed on the top of a wet germination filter paper and stored in a germinator at 20°C ± 2°C. The first count on the 4th day, and the second count on the 10th day. The seedlings with roots longer than seed and at least one cotyledon connected to the root as germinating seeds.

The following formulas were used to calculate the pod setting rate, pod falling rate, germination potential, and germination rate:

$$\text{Pod setting rate}(\%) = \left(\frac{\text{Number of pods}}{\text{Number of flowering buds}}\right) \times 100\% \quad (5)$$

$$\text{Pod falling rate}(\%) = \left(\frac{\text{Number of the drop mark of pod}}{\text{Number of pods}}\right) \times 100\% \quad (6)$$

$$\text{Germination potential}(\%) = \left(\frac{\text{Number of germinated seeds on the 4th day}}{\text{Number of sampled seeds}}\right) \times 100\% \quad (7)$$

$$\text{Germination rate}(\%) = \left(\frac{\text{Number of germinated seeds on the 10th day}}{\text{Number of sampled seeds}}\right) \times 100\% \quad (8)$$

Statistical Analysis

The differences of plant morphological and physiological variables under shading treatment were determined by using one-way ANOVA followed by Duncan new multiple range test (95% CI), and the standard errors of the arithmetic means were provided. The correlation and path analysis of seed yield per plant and flowering and fruiting factors were carried out by

using Excel 2016 and SPSS 16.0. Pollen viability and average stigma receptivity within 5 days were used in the two analyses.

RESULTS

Flowering Phenology

Compared with alfalfa without shading treatment, alfalfa under shade entered budding stage, early flowering stage to full flowering stage later and had a shorter flowering stage. Under different shading levels, the flowering phenology and change trend of the two alfalfa cultivars were similar (**Table 1**). The budding stage of plants under 56.4% shade was delayed by 2–4 days, and the budding stage under 78.7% shade was delayed by 13–16 days. The early flowering stage of shaded plants delayed 2–4 days under 56.4% shade and 14–16 days under 78.7% shade, respectively. The full flowering stage of shaded plants delayed 5–8 days under 56.4% shade and 8–11 days under 78.7% shade. Moreover, the flowering stage of alfalfa was 115–120 days under full sunlight treatment, 67–69 days under 56.4% shade treatment, and 48–49 days under 78.7% shade treatment.

Flower Colors

The color of alfalfa plant under shading treatment was lighter, and there were fewer inflorescences and flowers per inflorescence (**Figure 1**). With the increase of shading, the flower color of the two alfalfa cultivars gradually faded, that is, the flower color of full sunlight treatment was dark purple, 56.4% shade was medium purple, and 78.7% shade was light purple.

Dynamics of Pollen Viability and Stigma Receptivity

The pollen viability of two alfalfa cultivars decreased significantly with increase of shade ($p < 0.05$), and the decline of Victoria was greater than that of Eureka (**Figure 2**).

TABLE 1 | Flowering phenology of two alfalfa cultivars under different shading levels.

Parameters	Treatment	Cultivar	
		Victoria	Eureka
Budding stage	Full light	April 18th	April 22th
	56.4% shade	April 22th	April 24th
	78.7% shade	May 3rd	May 4th
Early flowering stage	Full light	May 4th	May 6th
	56.4% shade	May 8th	May 8th
	78.7% shade	May 20th	May 20th
Full flowering stage	Full light	May 12th	May 17th
	56.4% shade	May 20th	May 22th
	78.7% shade	May 31st	May 30th
Flowering stage	Full light	April 18–August 17 (lasted 123 days)	April 22–August 17 (lasted 119 days)
	56.4% shade	April 22–July 1 (lasted 72 days)	April 24–July 1 (lasted 70 days)
	78.7% shade	May 3–June 21 (lasted 49 days)	May 4–June 23 (lasted 50 days)

Under full sunlight treatment, the stigma receptivity of the two cultivars was higher, from the first to the fourth day after flowering, but decreased significantly from the fifth day after flowering. Under 56.4% shade treatment, the stigma receptivity of the two cultivars was higher in the first 2 days after flowering, decreased gradually from the third day of flowering, and decreased significantly on the fifth day of flowering ($p < 0.05$). Under 78.7% shade treatment, the stigma receptivity of the two cultivars decreased significantly from the third days after flowering, but their response to shade was different in the first 2 days after flowering. The stigma receptivity of Eureka was not significantly different from that of full sunlight and 56.4% shading treatment, while that of Victoria was significantly lower than that of full sunlight and 56.4% shading treatment, which showed that shade had a great effect on pollen viability and sigma receptivity in Victoria (**Figures 3A,B**).

Flowering, Fruiting, and Seed Traits

Shade significantly inhibited the flowering and fruiting of two alfalfa cultivars. With the increase of shade, the number of flower bud, flowering rate, and pod setting rate decreased significantly ($p < 0.0001$; **Figures 4A,B,D**), while the rate of flower and pod falling rate increased significantly ($p < 0.0001$; **Figures 4C,E**). Seed germination potential, germination rate, 1,000-seed weight, and seed yield per plant decreased significantly with the increase of shade ($p < 0.0001$; **Figures 4F–I**).

Correlation Analysis Between Seed Yield per Plant and Flowering and Fruiting Factors

The seed yield per plant of Victoria was significantly positively correlated with germination potential, pollen viability, and 1,000-seed weight (**Table 2**). The seed yield per plant of Eureka was significantly positively correlated with the germination potential, germination rate, and pollen viability (**Table 3**).

Path Analysis Between Seed Yield per Plant and Flowering and Fruiting Factors

Path analysis results showed that there were differences in the effects of flowering and fruiting factors on seed yield per plant between the two alfalfa cultivars.

In terms of flowering factors, the direct path coefficient of Victoria flower bud number on seed yield per plant was the highest (0.905), while the direct path coefficient of average stigma receptivity on seed yield per plant was the lowest (−0.552). The direct path coefficient of pollen viability was very low (0.390), but it had higher indirect path coefficients with flower bud number (0.901) and flowering rate (0.460), which indirectly affected the seed yield per plant, so it had a significant positive correlation (0.999) with the seed yield per plant. The direct path coefficient of Eureka pollen viability on seed yield per plant was the highest (0.986), but the direct path coefficients of flowering rate, fallen flower rate, and average stigma receptivity on seed yield per plant were lower, which were −0.203, −0.171, and −0.075, respectively (**Table 4**).

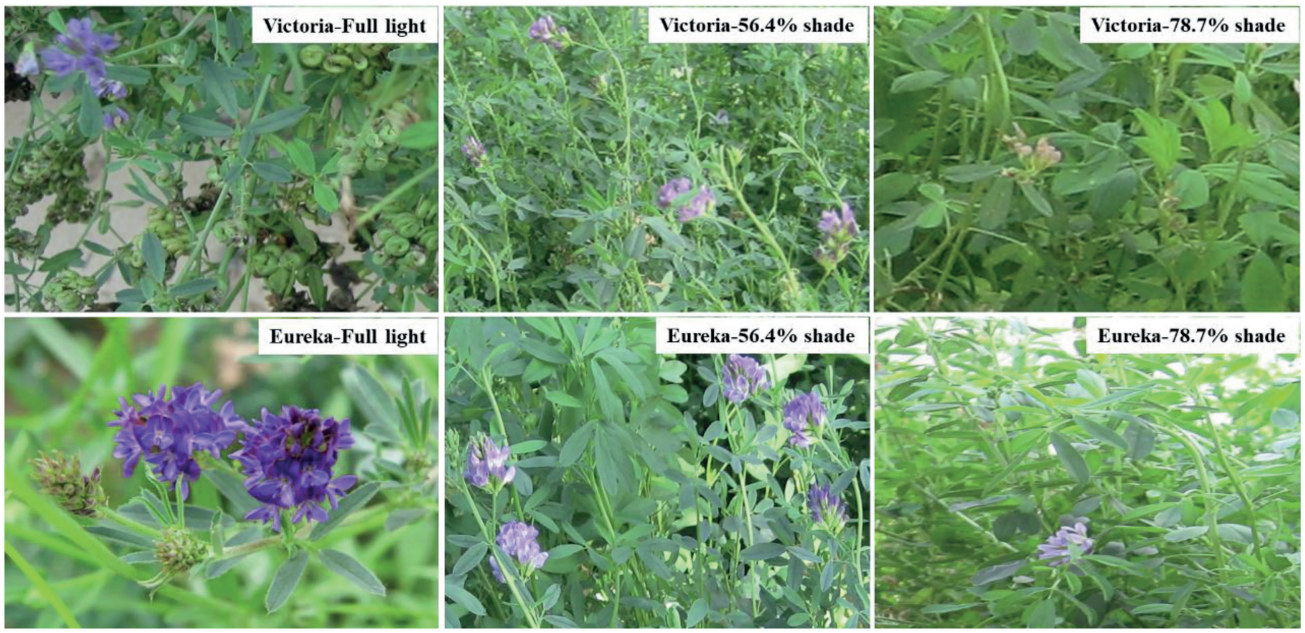

FIGURE 1 | Flower color of two alfalfa cultivars under different shading levels.

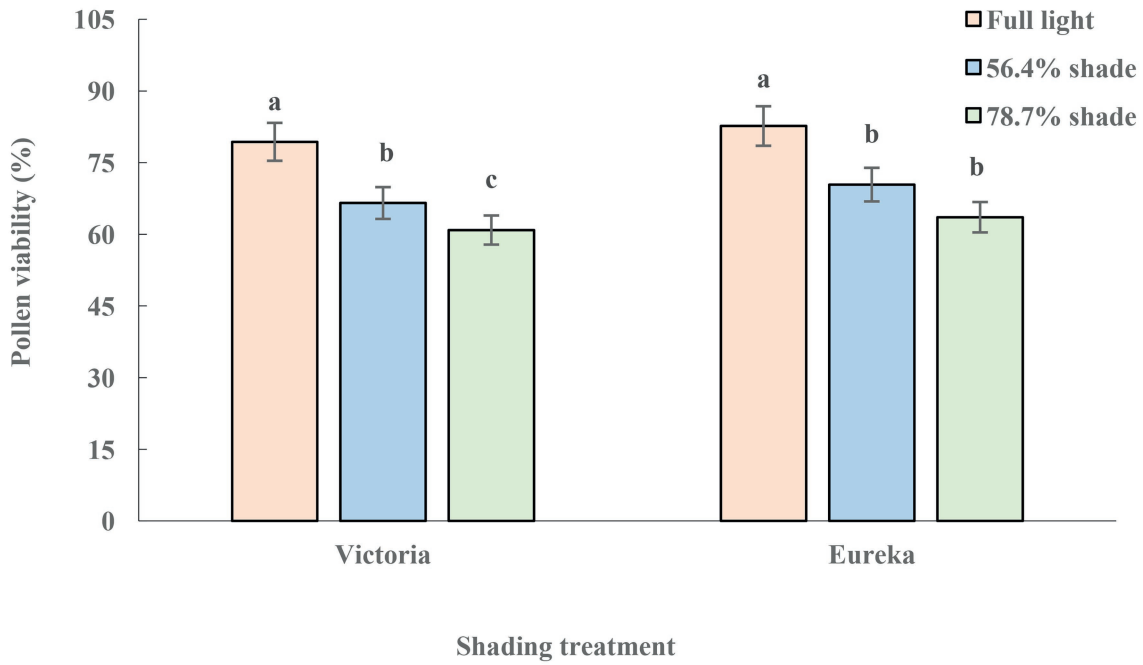

FIGURE 2 | Pollen viability of two alfalfa cultivars under different shading levels. Different letters indicate significant differences ($p < 0.05$).

In terms of fruiting factors, the direct path coefficient of Victoria 1,000-seed weight to seed yield per plant was the highest (0.669), and the direct path coefficient of pod setting rate was the lowest (−0.279). The direct path coefficient of germination potential on seed yield per plant was low (0.057), but it had a greater indirect effect (0.519), the indirect coefficient of 1,000-seed weight was higher (0.669), and there was a significant positive correlation with seed yield per plant (0.998). The direct path coefficient of Eureka germination rate on seed yield per plant was the highest (1.085), and the direct path

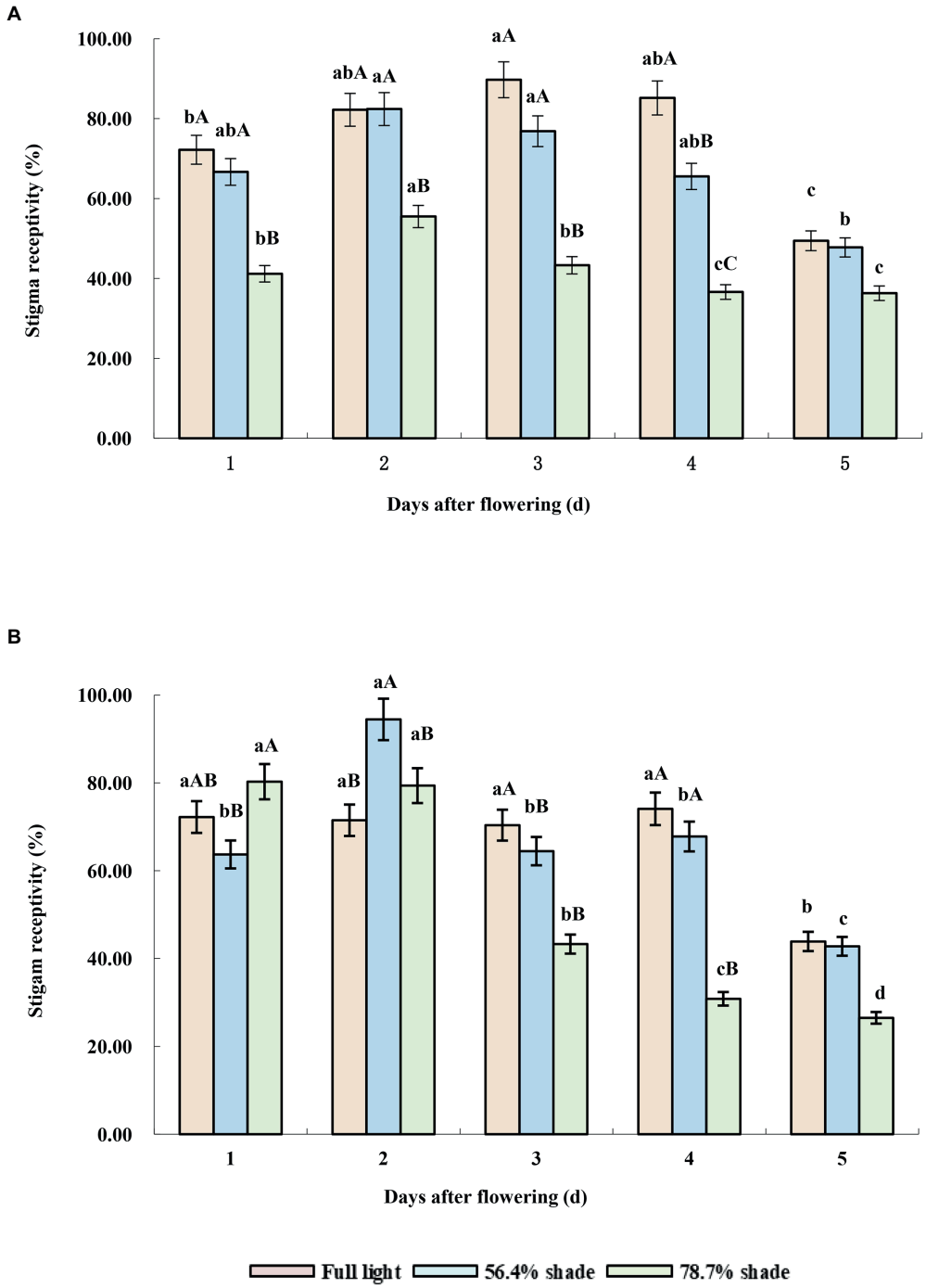

FIGURE 3 | Stigma receptivity of the two alfalfa cultivars under different shading levels. **(A)** Victoria, **(B)** Eureka. Different capital and lower case letters indicate significant difference under different shading levels and days after flowering at 0.05 level ($p < 0.05$), respectively.

coefficient of pod setting rate was the lowest (−1.145). The direct path coefficient of germination potential was lower, but the indirect coefficient with pod falling rate (0.357), germination rate (1.079), and 1,000-seed weight (0.767) was higher, which could have a great indirect effect on seed yield per plant, and had a very significant positive correlation (1.000) with seed yield per plant (**Table 5**).

DISCUSSION

As mentioned above, delayed flowering was one of important adaptive strategies of plant in response to shade. However, how plants adjust their flowering time to adapt to weak light has not been tested so far. Previous studies on *Antirrhinum majus* (Munir et al., 2004), bedding ornamentals (Faust et al.,

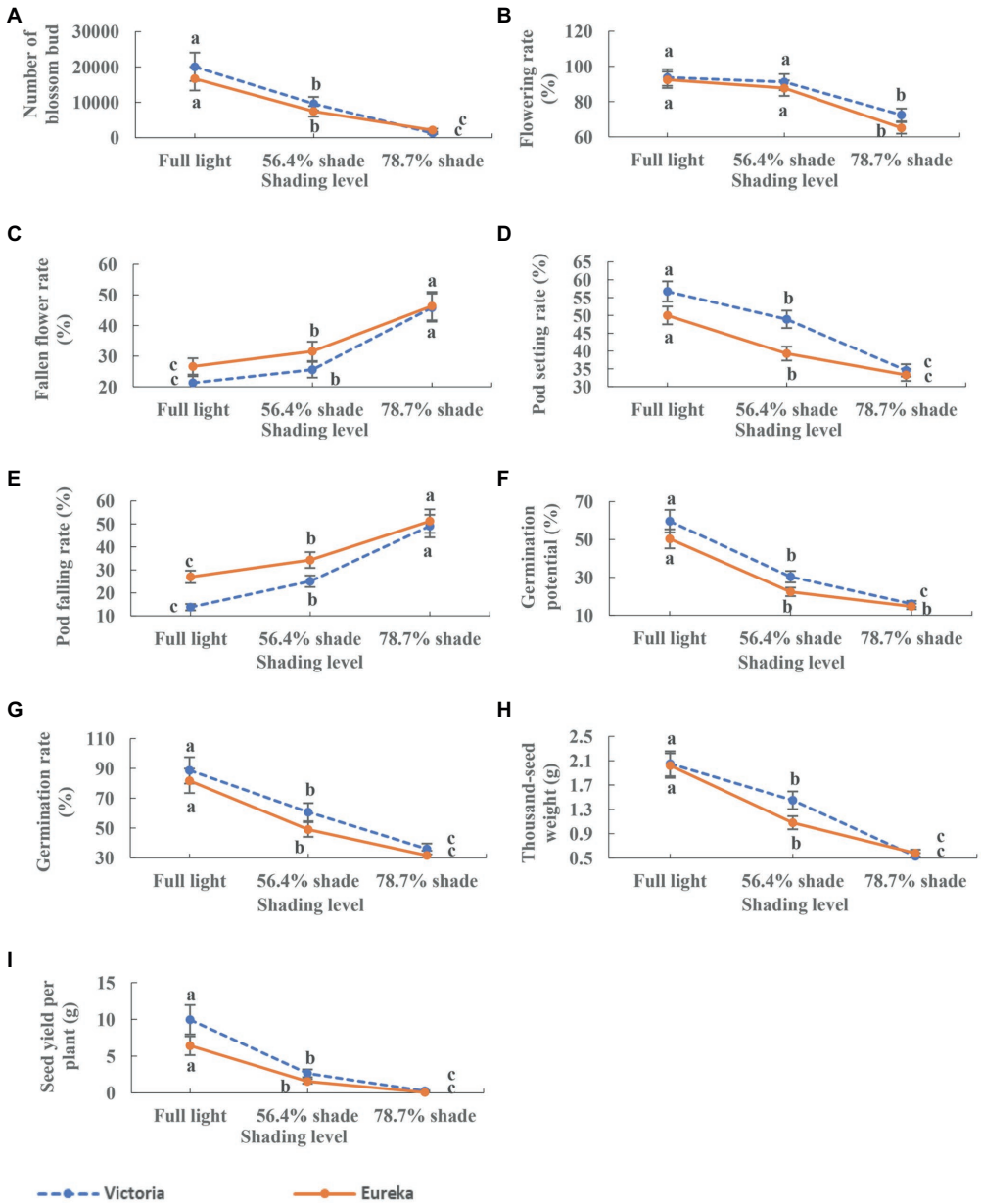

FIGURE 4 | Dynamics of flowering, fruiting, and seed traits of two alfalfa cultivars under different shading levels. **(A)** Number of flower bud, **(B)** flowering rate, **(C)** fallen flower rate, **(D)** pod setting rate, **(E)** pod falling rate, **(F)** germination potential, **(G)** germination rate, **(H)** 1,000-seed weight, and **(I)** seed yield per plant. Different low case letters indicate significant differences under different shading levels at 0.05 level ($p < 0.05$), respectively.

2005), *Swarnaprabha* rice (Panigrahy et al., 2019), and some soybean lines (Cober and Voldeng, 2001) showed that shading led to delayed flowering, and the reduction of carbohydrate availability under shading was partly responsible for the delayed flowering (Bernier et al., 1993). The addition of sucrose to flowering *Arabidopsis* grown in the dark proved that carbohydrate reserve can replace the current photosynthesis during floral induction (Roldan et al., 1999). Moreover, the weakening of photosynthesis, photosynthate accumulation, and reproductive growth in competition for photosynthetic products under shading delayed flower bud differentiation, reduced inflorescence and flowers, and shortened flowering time (Cober and Voldeng, 2001; Panigrahy et al., 2019). This was consistent with the results of alfalfa. Previous studies showed that compared with other cultivars, shade tolerant cultivar Victoria had less reduction in biomass (including leaf, stem and individual biomass), crown branch number and leaf anatomical structure (including parenchyma thickness, palisade cell width, mesophyll thickness and midvein thickness) under shading conditions (Qin et al., 2010, 2012, 2014). Moreover, recent finding showed the increased expression of miR156 reduced the transcription level of its targeted gene *msSPL*$_3$, thus prolonging the growth period of

TABLE 2 | Correlation between the seed yield per plant and flowering and fruiting factors of Victoria.

Trait	y	x1	x2	x3	x4	x5	x6	x7	x8	x9	x10
y	1										
x1	0.988	1									
x2	0.746	0.840	1								
x3	–0.779	–0.866	–0.999*	1							
x4	0.885	0.946	0.971	–0.982	1						
x5	–0.867	–0.933	–0.979	0.988	–0.999*	1					
x6	0.998*	0.996	0.791	–0.821	0.915	–0.920	1				
x7	0.989	1.000**	0.838	–0.864	0.944	–0.931	0.997*	1			
x8	0.999*	0.995	0.78	–0.811	0.908	–0.926	1.000**	0.995	1		
x9	0.805	0.887	0.996	–0.999*	0.989	–0.916	0.844	0.884	0.834	1	
x10	0.998*	0.996	0.787	0.818	0.913	–0.997*	1.000**	0.996	1.000**	0.841	1

*y, seed yield per plant; x1, number of flower bud; x2, flowering rate (%); x3, fallen flower rate (%); x4, pod setting rate (%); x5, pod falling rate (%); x6, germination potential (%); x7, germination rate (%); x8, pollen viability (%); x9, average stigma receptivity (%); and x10, 1,000-seed weight (g).*Respective correlation is significant at the 0.05 level. **Respective correlation is extremely significant at the 0.01 level (two tailed).*

TABLE 3 | Correlation between seed yield per plant and flowering and fruiting factors of Eureka.

Trait	y	x1	x2	x3	x4	x5	x6	x7	x8	x9	x10
y	1										
x1	0.990	1									
x2	0.791	0.870	1								
x3	–0.837	–0.907	–0.997*	1							
x4	0.991	0.997*	0.831	–0.873	1						
x5	–0.867	–0.929	–0.991	0.998*	–0.899	1					
x6	1.000**	0.987	0.778	–0.826	0.996	–0.856	1				
x7	0.997*	0.998*	0.836	–0.877	1.000**	–0.903	0.995	1			
x8	0.997*	0.998*	0.835	–0.876	1.000**	–0.902	0.995	1.000**	1		
x9	0.672	0.771	0.985	–0.968	0.721	–0.952-	0.656	0.727	0.726	1	
x10	0.992	1.000**	0.860	–0.898	0.999**	–0.921	0.990	0.999*	0.999*	0.757	1

y, seed yield per plant; x1, number of flower bud; x2, flowering rate (%); x3, fallen flower rate (%); x4, pod setting rate (%); x5, pod falling rate (%); x6, germination potential (%); x7, germination rate (%); x8, pollen viability (%); x9, average stigma receptivity (%); and x10, 1,000-seed weight (g).
**Respective correlation is significant at the 0.05 level. **Respective correlation is extremely significant at the 0.01 level (two tailed).*

TABLE 4 | Path analysis of seed yield per plant and flowering factors of two alfalfa cultivars.

Cultivar	Trait	Correlation coefficient	Direct effect	Indirect effect ($r_{ij} \rightarrow y$)				
				$x_{i1} \rightarrow y$	$x_{i2} \rightarrow y$	$x_{i3} \rightarrow y$	$x_{i4} \rightarrow y$	$x_{i5} \rightarrow y$
Victoria	x1	0.988	0.905		0.496	–0.311	0.388	–0.490
	x2	0.746	0.590	0.760		–0.358	0.304	–0.550
	x3	–0.779	0.359	–0.784	–0.590		–0.316	0.552
	x4	0.999	0.390	0.901	0.460	–0.291		–0.460
	x5	0.805	–0.552	0.803	0.588	–0.358	0.325	
Eureka	x1	0.990	0.086		–0.177	0.155	0.984	–0.058
	x2	0.791	–0.203	0.074		0.170	0.823	–0.074
	x3	–0.837	–0.171	–0.078	0.202		–0.864	0.073
	x4	0.997	0.986	0.085	–0.169	0.150		–0.055
	x5	0.672	–0.075	0.066	–0.200	0.165	0.716	

y, seed yield per plant; x1, number of flower bud; x2, flowering rate; x3, fallen flower rate; x4, pollen viability; and x5, average stigma receptivity.

vegetative stage and delaying the flowering time in alfalfa under shading (Aung et al., 2015; Lorenzo et al., 2019). It showed delayed flowering under weak light condition was conducive to the maintenance of aboveground biomass of alfalfa to a certain extent. However, as a perennial forage, the effect of delayed flowering on the accumulation, distribution of assimilates, and survival of alfalfa under shading needed to be monitored and researched.

Alfalfa is a monoecious, entomophilous, and cross-pollinated plant. When the flower bud develops to the fourth stage, the anther has burst and covered the stigma. At this time, almost all the mature pollen has been scattered on the stigma. However,

TABLE 5 | Path analysis of seed yield per plant and fruiting factors of two alfalfa cultivars.

Cultivar	Trait	Correlation coefficient	Direct effect	Indirect effect ($r_{ij} \rightarrow y$)				
				$x_{i6} \rightarrow y$	$x_{i7} \rightarrow y$	$x_{i8} \rightarrow y$	$x_{i9} \rightarrow y$	$x_{i10} \rightarrow y$
Victoria	x6	0.885	−0.279		0.005	0.052	0.492	0.611
	x7	−0.867	−0.005	0.279		−0.051	−0.485	−0.600
	x 8	0.998	0.057	−0.255	0.005		0.519	0.669
	x 9	0.989	0.521	−0.263	0.005	0.994		0.667
	x10	0.998	0.669	−0.255	0.005	0.057	0.519	
Eureka	x6	0.991	−1.145		−0.375	0.295	1.085	0.774
	x7	−0.867	−0.418	1.029		−0.254	−0.979	−0.714
	x 8	1.000	0.296	−1.140	0.357		1.079	0.767
	x 9	0.997	1.085	−1.145	0.377	0.295		0.774
	x10	0.992	0.775	−1.144	0.385	0.293	1.083	

y, seed yield per plant; x6, pod setting rate; x7, pod falling rate; x8, germination potential; x9, germination rate; and x10, 1,000-seed weight.

without insect pollination, the seed setting rate was still very low (Jiang et al., 2003). It was reported that the color and size of flowers were the primary factors to attract bees, bright colors can attract insects to spread pollen and promote plant reproduction, while faded or withered flowers reduced the access of bees, thus reducing seeds yield in a weak light environment (Clement, 1965). Anthocyanin is an important pigment in flower color and its biosynthesis, accumulation, and metabolic regulation were induced by light (Zhao et al., 2012). Under shading conditions, the insufficient supply of soluble sugars, such as sucrose, significantly decreased the content of anthocyanin in petals and inhibited the biosynthesis of anthocyanin in petals. In addition, molecular biology studies showed that the decline of anthocyanins in shade plants was the result of the joint action of all anthocyanin biosynthetic genes, especially the upstream *PlPAL* and *PlCHS*, whose expression decreased significantly under weak light and the upstream substrate inducing anthocyanin synthesis decreased significantly (Stein and Hensen, 2013). In order to clarify the effect of fading flower on seed setting rate of alfalfa, it is necessary to further study the visiting behave of insect in alfalfa under shade.

In the process of plant sexual reproduction, pollination begins with flower bud differentiation, anther dehiscence, and mature pollen release. Pollen grains carrying live male gametes or precursors must reach appropriate receptive stigmas for smooth fertilization (Yi et al., 2006). Therefore, pollen viability and stigma receptivity were the key steps for successful plant reproduction. Shading can inhibit the photosynthesis, lead to pistil atrophy, reduce the number of pollen, inhibit pollen germination and pollen tube growth, and increase ratio of abnormal pollen (Alice, 1996). These all led to the decline of alfalfa pollen vitality (**Figure 2**). It was worth mentioning that shading reduced the nutrient richness of pollen and nectar, which were the most attractive part of plants to insects. Nectar can absorb ultraviolet spectrum and can be accurately detected by insects. The pattern and spectral range of nectar reflected fluorescence provide pollinating insects with information on nectar existence and abundance (Jiang et al., 2003). Therefore, the decrease of energy, pollen, and nectar concentration may be an important factor affecting the successful pollination of alfalfa under shading conditions. The shortening of stigma receptivity duration under shading (**Figure 3**) may be due to the decrease of sex cells concentration (Yi et al., 2006) and stigma peroxidase (POD) activity, which was significantly positively correlated with light intensity (Sui et al., 2005). So far, there are few studies on the effects of shading on plant pollen viability and stigma receptivity, and its mechanism needs to be further studied.

The seed yield per plant of alfalfa depended on the number of flowers per branch, the number of florets per inflorescence, the number of ovules per floret, the number of pods per branch, the number of seeds per pod, and 1,000-seed weight, which all change with environmental conditions (Chen, 2001). Among the environmental factors, incident or intercepted solar radiation had proved to be the most influential (Izquierdo et al., 2008). Long-term shading reduced the flower bud yield, flowering rate, and pod setting rate of alfalfa, and increased fallen flower and fallen pod rates (**Figure 4**). These may be due to the insufficient supply of photo-assimilates and minerals. In the key early stage of development, the competition of stem growth for assimilates was better than that of fruit growth (Islam et al., 2005). This lead to a decline in pollen viability and fertilized eggs quality, as well as a decline in flowers and fruits under shading (Bepetel and Lakso, 1998). In this process, weak light reduced the production of flowering-related hormones, such as gibberellic acid, which can promote flower stem elongation and prevent fruit abscission, plays a key role (Folta and Maruhnich, 2007; Fukuda, 2013). From the beginning of seed filling to full maturity, weak light stress can lead to seed deterioration and reduce seed viability and vigor by changing seed components (Cockshull and Graves, 1992). It is reported that shading increases oil content, linoleic acid, and linolenic acid (Bellaloui et al., 2012), which limited C and N assimilation, thus reducing nitrate reductase activity, chlorophyll concentration, seed protein, and oil accumulation (Allen et al., 2009; Board et al., 2010). In this study, the effects of shading on alfalfa germination potential, germination rate, and 1,000-seed weight may have a similar mechanism. However, further research was needed to explain this possibility.

The 1,000-seed weight and germination rate of seeds indicated the size, plumpness, and vitality of seeds, which were determined

by the assimilates allocated to reproductive organs. In this study, the two factors that contributed the most to the seed yield per plant showed that the main reason for the decline of seed yield per plant was the reduction of assimilates allocated to seeds under weak light environments (**Table 5**). It should be noted that the pod setting rate had the greatest negative direct impact on the seed yield per plant and greatest negative indirect impact on germination potential, germination rate, and 1,000-seed weight (**Table 5**). The data available so far suggested that the weight and composition of seeds are the results of a complex process, among which vegetative organs (leaves) promote the supply of assimilates to the seeds, while reproductive structures (pods and seeds) may locally regulate seed metabolism (Bianculli et al., 2016). It is reported that compared with leaves, the soybean pods have contributed to the low-carbon economy under shading (Allen et al., 2009). In this work, it was difficult to assess whether this effect was due to the contribution of pods and leaves in transporting assimilates to seeds or to the competition of assimilates between pods and leaf synthesis. In order to clarify this point, it is necessary to further study the transport and allocation dynamics of the assimilates between alfalfa leaves and pods under weak light conditions.

Weak light had harmful to flowering, fruiting, and seed production of alfalfa. The extremely low seed yield per plant under shade showed that the reproductive growth of alfalfa was extremely dependent on light intensity, and it is a species with high light demand. Delayed flowering time, shortened flowering stage, decreased quantity and quality of flowers and fruits, decreased pollen viability and stigma receptivity, indicating that reducing the distribution of assimilates to reproduction growth was an important strategy for alfalfa to response to shading. However, because alfalfa is a perennial vegetative-harvest forage, this strategy may be beneficial to maintain the high aboveground biomass of alfalfa under weak light environment. Therefore, this strategy should be considered when breeding shade-tolerant cultivar under intercropping system. Future research should further reveal the genetic and molecular mechanism of delayed flowering regulating the accumulation and distribution of assimilates between vegetative and reproductive organs of alfalfa under shading, so as to provide a theoretical basis for breeding shade-tolerant alfalfa cultivars.

DATA AVAILABILITY STATEMENT

The raw data supporting the conclusions of this article will be made available by the authors, without undue reservation.

AUTHOR CONTRIBUTIONS

FQ and HQ conceived and designed the research. FQ, GT, HL, and ZC performed the experiments and data analysis. FQ and HQ analyzed the data and wrote the manuscript. ZL, YS, JF, and LK advised on the results and discussions. All authors discussed the results and implications, commented on the manuscript at all stages, and contributed to the article and approved the submitted version.

FUNDING

This work was financially supported by the National Key R&D Program of China, grant/award number: 2017YFC0506005; Open Innovation and Entrepreneurship Training Program of National Experimental Teaching Demonstration Center of Plant Production of Nanjing Agricultural University: ZKF202106; and SRT program of Nanjing Agricultural University: 202126XX04.

SUPPLEMENTARY MATERIAL

The Supplementary Material for this article can be found online at: https://www.frontiersin.org/articles/10.3389/fpls.2022.835380/full#supplementary-material

REFERENCES

Alice, Y. C. (1996). Pollen-pistil interactions during pollen-tube growth. *Trends Plant Sci.* 1, 45–51. doi: 10.1016/S1360-1385(96)80028-8

Allen, D. K., Ohlrogge, J. B., and Shachar-Hill, Y. (2009). The role of light in soybean seed filling metabolism. *Plant J.* 58, 220–234. doi: 10.1111/j.1365-313X.2008.03771.x

Atlag, J. (1990). Pollen fertility in some Helianthus L. species and their F1 hybrids with the cultivated sunflower. *Helia* 13, 47–54.

Aung, B., Gruber, M. Y., Amyot, L., Omari, K., Bertrand, A., and Hannoufa, A. (2015). Microrna156 as a promising tool for alfalfa improvement–aung. *Plant Biotechnol. J.* 13, 779–790. doi: 10.1111/pbi.12308

Bellaloui, N., Smith, J. R., Gillen, A. M., Fisher, D. K., and Mengistu, A. (2012). Effect of shade on seed protein, oil, fatty acids, and minerals in soybean lines varying in seed germinability in the early soybean production system. *Am. J. Plant Sci.* 03, 84–95. doi: 10.4236/ajps.2012.31008

Bepetel, M., and Lakso, A. N. (1998). Differential effects of shade on early-season fruit and shoot growth rates in empire apple. *HortSci.* 33, 823–825. doi: 10.21273/HORTSCI.33.5.823

Bernier, G., Havelange, A., Houssa, C., Petitjean, A., and Lejeune, P. (1993). Physiological signals that induce flowering. *Plant Cell* 5, 1147–1155. doi: 10.2307/3869768

Bianculli, M. L., Aguirrezábal, L. A. N., Pereyra Irujo, G. A., and Echarte, M. M. (2016). Contribution of incident solar radiation on leaves and pods to soybean seed weight and composition. *Eur. J. Agron.* 77, 1–9. doi: 10.1016/j.eja.2016.03.002

Board, J. E., Kumudini, S., Omielan, J., Prior, E., and Kahlon, C. S. (2010). Yield response of soybean to partial and total defoliation during the seed-filling period. *Crop Sci.* 50, 703–712. doi: 10.2135/cropsci2009.03.0128

Boardman, K. N. (1977). Comparative photosynthesis of sun and shade plants. *Annu. Rev. Plant Physiol.* 28, 355–377. doi: 10.1146/annurev.pp.28.060177.002035

Carriedo, L. G., Maloof, J. N., and Brady, S. M. (2016). Molecular control of crop shade avoidance. *Curr. Opin. Plant Biol.* 30, 151–158. doi: 10.1016/j.pbi.2016.03.005

Castillon, A., Shen, H., and Huq, E. (2007). Phytochrome interacting factors: central players in phytochrome-mediated light signaling networks. *Trends Plant Sci.* 12, 514–521. doi: 10.1016/j.tplants.2007.10.001

Cerdán, P. D., and Chory, J. (2003). Regulation of flowering time by light quality. *Nature* 423, 881–885. doi: 10.1038/nature01636

Chen, B. S. (2001). *Cultivation of grass and Forage crops*. Beijing: Press of China Agriculture.

Clement, W. M. (1965). Flower color, a factor in attractiveness of alfalfa clones for honeybees. *Crop Sci.* 5, 267–268. doi: 10.2135/cropsci1965.0011183X000500030023x

Cober, E. R., and Voldeng, H. D. (2001). Low R:FR light quality delays flowering of soybean lines. *Crop Sci.* 41, 1823–1826. doi: 10.2135/cropsci2001.1823

Cockshull, K. E., and Graves, C. J. (1992). Shading on yield of glasshouse tomatoes. *HortSci.* 67, 11–24.

Cooper, C. S., and Qualls, M. (1967). Morphology and chlorophyll content of shade and sun leaves of two legumes. *Crop Sci.* 7, 672–673. doi: 10.2135/cropsci1967.0011183X000700060036x

Dafni, A., and Maués, M. M. (1998). A rapid and simple procedure to determine stigma receptivity. *Sex. Plant Reprod.* 11, 177–180. doi: 10.1007/s004970050138

Echarte, M. M., Alberdi, I., and Aguirrezábal, L. A. N. (2012). Post-flowering assimilate availability regulates oil fatty acid composition in sunflower grains. *Crop Sci.* 52, 818–829. doi: 10.2135/cropsci2011.09.0477

El-Aidy, F., Moutafa, S., and El-Afry, M. (1983). Influence of shade on growth and yield of tomatoes cultivated during the summer season in Egypt. *Plasticulture* 47, 2–6.

El-Gizawy, M. A., Gomaa, M. H., El-Habbasha, M. K., and Mohamed, S. S. (1993). Effect of different shading levels on tomato plants 1. Growth, flowering and chemical composition. *Acta Hortic.* 323, 348–354. doi: 10.17660/ActaHortic.1993.323.31

Faust, J., Holcombe, V., Rajapakse, N. C., and Layne, D. R. (2005). The effect of daily light integral on bedding plant growth and flowering. *HortSci.* 40, 645–649. doi: 10.21273/HORTSCI.40.3.645

Ferree, D. C., Mcartney, S. J., and Scurlock, D. M. (1998). Influence of light on fruit set of French hybrid grapes. *HortSci.* 33, 510f–511f. doi: 10.21273/HORTSCI.33.3.510f

Folta, K. M., and Maruhnich, S. A. (2007). Green light: a signal to slow down or stop. *J. Exp. Bot.* 58, 3099–3111. doi: 10.1093/jxb/erm130

Fukuda, N. (2013). Advanced light control technologies in protected horticulture: a review of morphological and physiological responses in plants to light quality and its application. *J. Dev. Sustain. Agr.* 8, 32–40. doi: 10.11178/jdsa.8.32

Islam, N., Patil, G. G., and Gislerod, H. R. (2005). Effect of photoperiod and light integral on flowering and growth of *Eustoma grandiflorum* Raf Shinn. *Sci. Hortic.* 103, 441–451. doi: 10.1016/j.scienta.2004.06.018

Izquierdo, N. G., Dosio, G. A. A., Cantarero, M., Luján, J., and Aguirrezábal, L. A. N. (2008). Weight per grain, oil concentration, and solar radiation intercepted during grain filling in black hull and striped hull sunflower hybrids. *Crop Sci.* 48, 688–699. doi: 10.2135/cropsci2007.06.0339

Jiang, H., Bi, Y. F., He, C. G., and Zhang, J. (2003). A study on alfalfa pollinating mechanism and relationship of pollinating insects. *Pratacul. Sci.* 20, 1–6. doi: 10.3969/j.issn.10010629.2003.01.001

Li, X. Z., Liang, M. Z., Zhou, G. Q., and Chen, L. B. (2002). Effect of environment condition on pollen vigor and seed set during flowing time of rice. *Acta Agron. Sin.* 16, 53–70. doi: 10.1006/jfls.2001.0409

Lin, C. H., McGraw, R. L., George, M. F., and Garrett, H. E. (1999). Shade effects on forage crops with potential in temperate agroforestry practices. *Agrofor. Syst.* 44, 109–119. doi: 10.1023/a:1006205116354

Lorenzo, C. D., Iserte, J. A., Sanchez, L. M., Antonietti, M. S., Garcia, G. P., Hernando, C. E., et al. (2019). Shade delays flowering in *Medicago sativa*. *Plant J.* 99, 7–22. doi: 10.1111/tpj.14333

Mao, P. S. (2019). *Experiment and Practice Guidance of Grassland Science*. Beijing: China Agriculture Press.

Munir, M., Jamil, M., Baloch, J. U. D., and Khattak, K. R. (2004). Impact of light intensity on flowering time and plant quality of *Antirrhinum majus* L. cultivar chimes white. *J. Zhejiang Univ-SC. B* 5, 400–405. doi: 10.1631/jzus.2004.0400

Panigrahy, M., Ranga, A., Das, J., and Panigrahi, K. C. S. (2019). Shade tolerance in Swarnaprabha rice is associated with higher rate of panicle emergence and positively regulated by genes of ethylene and cytokinin pathway. *Sci. Rep.* 9, 1–17. doi: 10.1038/s41598-019-43096-8

Putnam, D., Russelle, M., Orloff, S., Kuhn, J., Fitzhugh, L., Godfrey, L., et al. (2001). *Alfalfa, Wildlife and the Environment–the Importance and Benefit of Alfalfa in the 21st Century*. California Alfalfa and Forage Association, Novato, CA.

Qin, F. F., Cui, Z. M., Wei, M., Tao, X., Jin, X. l., and Tang, H. Y. (2014). Effects of shading on growth characteristics of three alfalfa cultivars in summer. *Acta Agrestia. Sinica.* 22, 101–106. doi: 10.11733/j.issn.1007-0435.2014.01.016

Qin, F. F., Li, Q., Cui, Z. M., Li, H. P., and Yang, Z. R. (2012). Leaf anatomical structures and ecological adaptabilities to light of three alfalfa cultivars with different fall dormancies under shading during overwintering. *Chin. J. Plant Ecol.* 36, 333–345. doi: 10.3724/SP.J.1258.2012.00333

Qin, F. F., Shen, Y. X., Zhou, J. G., Wang, Q. S., Sun, Z. C., and Wang, B. (2010). Seedling morphology and growth responses of nine *Medicago sativa* varieties to shade conditions. *Acta Pratacul. Sin.* 25, 1263–1267. doi: 10.3724/SP.J.1077.2010.01263

Roldan, M., Gomez-Mena, C., Ruiz-Garcia, L., Salinas, J., and Martinez-Zapater, J. M. (1999). Sucrose availability on the aerial part of the plant promotes morphogenesis and flowering of Arabidopsis in the dark. *Plant J.* 20, 581–590. doi: 10.1046/j.1365-313X.1999.00632.x

Stein, K., and Hensen, I. (2013). The reproductive biology of two understory plants in the Atlantic rain forest. *Brazil. Ecol. Res.* 28, 593–602. doi: 10.1007/s11284-013-1050-0

Sui, Y. H., Zhu, S. D., Zhang, Z. X., Hu, D. P., and Shu, Y. J. (2005). Effects of environmental factors on key carbon-nitrogen metabolizing and antioxidizing enzyme activities of Amaranthus. *Chinese J. Ecol.* 24, 925–929. doi: 10.13292/j.1000-4890.2005.0070

Ueoka-Nakanishi, H., Hori, N., Ishida, K., Ono, N., Yamashino, T., Nakamichi, N., et al. (2011). Characterization of shade avoidance responses in lotus japonicus. *Biosci. Biotechnol. Biochem.* 75, 2148–2154. doi: 10.1271/bbb.110442

Walgenbach, R. P., and Marten, G. C. (1981). Release of soluble protein and nitrogen in alfalfa: III. Influence of shading. *Crop Sci.* 21, 859–862. doi: 10.2135/cropsci1981.001118

Yi, W. G., Law, S. E., McCoy, D., and Wetzstein, H. Y. (2006). Stigma development and receptivity in almond (*Prunus dulcis*). *Ann. Bot.* 97, 57–63. doi: 10.1093/aob/mcj0133x002100060015x

Zhao, D. Q., Hao, Z. J., and Tao, J. (2012). Effects of shade on plant growth and flower quality in the herbaceous peony. *Plant Physiol. Biochem.* 61, 187–196. doi: 10.1016/j.plaphy.2012.10.005

Conflict of Interest: The authors declare that the research was conducted in the absence of any commercial or financial relationships that could be construed as a potential conflict of interest.

Publisher's Note: All claims expressed in this article are solely those of the authors and do not necessarily represent those of their affiliated organizations, or those of the publisher, the editors and the reviewers. Any product that may be evaluated in this article, or claim that may be made by its manufacturer, is not guaranteed or endorsed by the publisher.

frontiers | Frontiers in Plant Science

ORIGINAL RESEARCH
published: 11 July 2022
doi: 10.3389/fpls.2022.925754

Long-Term Mild Heat Causes Post-Mitotic Pollen Abortion Through a Local Effect on Flowers

*Jiemeng Xu†, Stuart Y. Jansma, Mieke Wolters-Arts, Peter F. M. de Groot, Martijn J. Jansen and Ivo Rieu**

Department of Plant Systems Physiology, Radboud Institute for Biological and Environmental Sciences, Radboud University, Nijmegen, Netherlands

Crop reproductive success is significantly challenged by heatwaves, which are increasing in frequency and severity globally. Heat-induced male sterility is mainly due to aborted pollen development, but it is not clear whether this is through direct or systemic effects. Here, long-term mild heat (LTMH) treatment, mimicking a heatwave, was applied locally to tomato flowers or whole plants and followed up by cytological, transcriptomic, and biochemical analyses. By analyzing pollen viability, LTMH was shown to act directly on the flowers and not *via* effects on other plant tissue. The meiosis to early microspore stage of pollen development was the most sensitive to LTMH and 3 days of exposure around this period was sufficient to significantly reduce pollen viability at the flower anthesis stage. Extensive cytological analysis showed that abnormalities in pollen development could first be observed after pollen mitosis I, while no deviations in tapetum development were observed. Transcriptomic and biochemical analyses suggested that pollen development suffered from tapetal ER stress and that there was a limited role for oxidative stress. Our results provide the first evidence that heat acts directly on flowers to induce pollen sterility, and that the molecular-physiological responses of developing anthers to the LTMH are different from those to severe heat shock.

Keywords: long-term mild heat, oxidative stress, pollen development, tapetum development, tomato (Solanum lycopersicum)

OPEN ACCESS

Edited by:
Nobuhiro Suzuki,
Sophia University, Japan

Reviewed by:
Mohan B. Singh,
The University of Melbourne, Australia
Iris Aloisi,
University of Bologna, Italy

***Correspondence:**
Ivo Rieu
i.rieu@science.ru.nl

†Present address:
Jiemeng Xu,
Plant Science Department,
Rothamsted Research, Harpenden,
United Kingdom

Specialty section:
This article was submitted to Plant Abiotic Stress, a section of the journal Frontiers in Plant Science

Received: *21 April 2022*
Accepted: *26 May 2022*
Published: *11 July 2022*

Citation:
Xu J, Jansma SY, Wolters-Arts M, de Groot PFM, Jansen MJ and Rieu I (2022) Long-Term Mild Heat Causes Post-Mitotic Pollen Abortion Through a Local Effect on Flowers. Front. Plant Sci. 13:925754. doi: 10.3389/fpls.2022.925754

INTRODUCTION

The global surface temperature has risen significantly compared to the pre-industrial era and will continue to increase. As a result of this, heatwaves are occurring more frequently and becoming more severe, in terms of duration and temperature increment (IPCC, 2018). Temperatures higher than the ranges that plants are adapted to may result in heat stress, causing a decline in fitness and crop yield (Zhao et al., 2017). To maintain food security, there is an urgent demand to develop crop genotypes resilient to the warming climate (Ortiz-Bobea et al., 2021). While many biological processes in the plant are adversely affected by high temperatures, sexual reproduction and, in particular, pollen development are regarded as the most vulnerable in many species (Satake and Yoshida, 1978; Saini and Aspinall, 1982; Hedhly et al., 2009; Rieu et al., 2017; Begcy et al., 2019). This also applies to tomato, one of the main vegetable crops globally (Iwahori, 1965; Müller and Rieu, 2016).

Pollen development is a well-conserved process among flowering plants. In brief, during microsporogenesis, pollen mother cells (PMCs) differentiate and undergo meiosis to form tetrads of spores. Next, during microgametogenesis, microspores are released from the tetrads and undergo vacuolisation, nuclear polarization, and mitosis to form bicellular gametophytes. The gametophytes then mature and thereafter give rise to pollen grains ready for fertilization (McCormick, 2004). The developing pollen, in particular during the stages from meiosis to mitosis, receives nutrients, enzymes, and wall components from the surrounding sporophytic tissue layer, the tapetum (Lei and Liu, 2020).

A sudden heat shock and very high temperatures are well known to affect various processes during pollen development, depending on the timing of exposure. During meiosis, these types of heat stress affect recombination and cytokinesis (Ning et al., 2021). When experienced slightly later, it may result in abortion of tetrads and developing microspores, impair pollen wall deposition, and disturb tapetum development and function (Iwahori, 1965; Djanaguiraman et al., 2014; Song et al., 2015). Bicellular pollen can also be affected but are less sensitive (Frank et al., 2009; Jegadeesan et al., 2018). Anthers and pollen cells initiate a cytoplasmic heat shock response upon experiencing such high temperatures, suggesting the occurrence of stress from unfolding proteins (Frank et al., 2009; Giorno et al., 2010; Chaturvedi et al., 2015; Yang et al., 2015; Fragkostefanakis et al., 2016a; Mu et al., 2017). Indeed, an attenuated heat stress response (HSR) due to knockdown of *HSFA2* reduced tomato pollen tolerance to heat shock, while higher tolerance of male fertility to heat shock has been correlated to higher heat shock protein accumulation in some genotypes (Frank et al., 2009; Fragkostefanakis et al., 2016b; González-Schain et al., 2016; Pham et al., 2020). At the same time, the anthers and pollen suffer from oxidative stress, as evident from increases in reactive oxygen species (ROS) and ROS damage, as well as induction of antioxidants and the ROS scavenging machinery (Frank et al., 2009; Paupière et al., 2017; Djanaguiraman et al., 2018; Zhao et al., 2018).

Pollen development is also sensitive to heatwave-like temperature profiles, characterized by more mildly elevated temperatures, sustained for multiple days (long-term mild heat; LTMH). Several studies have found that LTMH exposure is most detrimental if it includes the time of meiosis/early microspore development (e.g., Ahmed et al., 1992; Sato et al., 2000; Porch and Jahn, 2001; Erickson and Markhart, 2002), suggesting some similarity to the effect of severe heat shock. However, it is not clear to what extent the cellular and physiological damage to anthers caused by the two types of heat is comparable, for example, whether cytoplasmic protein folding stress and ROS accumulation play a similar important role. Recent mild heat experiments in Arabidopsis suggest that the unfolded protein response (UPR) in the endoplasmic reticulum may be important in situations of milder heat (Deng et al., 2016; Feldeverd et al., 2020; Yamamoto et al., 2020). Transcriptomic analyses indicate a response to ROS upon LTMH exposure, but to what extent ROS contributes to cellular damage is not known (Bita et al., 2011). Regarding anther and pollen physiology, several studies indicate that LTMH exposure affects carbohydrate metabolism at the maturing pollen stage, although the reported effects on starch, sucrose, and hexose concentrations are not always the same, within and between species (Aloni et al., 2001; Pressman et al., 2002; Firon et al., 2006; Sato et al., 2006; Jain et al., 2007; Wang et al., 2020).

To be able to better understand the effects of LTMH on pollen development, detailed insight into the plant tissues and developmental stages that are affected is needed. Here, we used tomato, an important vegetable crop that increasingly often suffers from high-temperature stress, to investigate which plant tissue is affected by LTMH and which stage of pollen development is most sensitive to LTMH. We then determined the minimum period of LTMH exposure that reduces pollen viability at anthesis and compared the developmental progression of pollen and tapetum after control and a 4-day LTMH through thorough cytological and transcriptomic analysis. Finally, we evaluated the contribution of oxidative damage to pollen failure by analyzing lipid peroxidation levels, as well as ROS scavenging gene expression and enzyme activities.

MATERIALS AND METHODS

Plant Cultivation and Treatment

Solanum lycopersicum cultivar Micro-Tom (obtained from the National BioResource Project, Japan; accession TOMJPF00001) was used in this study, except for the temperature-controlled airbag experiment, which was performed with cultivar Money Maker. Seeds were sown on commercial soil (Lentse Potgrond number 4, Horticoop B.V., Katwijk, The Netherlands) and covered with a thin layer of vermiculite. Two weeks later, seedlings were transplanted into the same soil supplemented with 4 g L^{-1} fertilizer (Osmocote exact standard 3–4 M, Everris International B.V., Geldermalsen, The Netherlands). During germination and the seedling growth period, Micro-Tom plants were kept in cabinets under controlled temperature conditions (CT; 25 °C/19 °C day/night; 12 h/12 h photoperiod, ∼200 μmol s^{-1} m^{-2} provided by Philips Green Power LED DR/B/FR 120 lamps; 60% relative humidity). Upon flowering, approximately 1 month after sowing, plants were either maintained at CT or subjected to long-term mild heat (LTMH; 33 °C/27 °C, day/night). Similarly, Money Maker plants were grown in growth chambers, under control conditions (25 °C/19 °C day/night; 14 h/10 h photoperiod, ∼300 μmol s^{-1} m^{-2} provided by Philips D-Papillon daylight spectrum 340W lamps; 70/80% relative humidity) or LTMH (31 °C/25 °C). For the airbag experiment, single trusses were contained in near-airtight 1-L zip-lock bags, which were flushed with the help of an air pump (1 L min^{-1}). The air was derived directly from the room or first passed through a water bath to obtain a stable temperature of T+5 °C ("heated") or T-6 °C ("cooled") inside the bag.

Pollen Viability Assay

The viability of mature pollen collected from freshly open flowers was determined by an *in-vitro* germination assay. In brief, anthers from the flowers were cut into four slices and rehydrated in 1.5-ml Eppendorf tubes for 30 min. Afterwards,

pollen were incubated for 1.5 h in 0.5-ml germination medium (25% [w/v] PEG 4,000, 5% [w/v] sucrose, 1 mM KNO_3, 1 mM $Ca(NO_3)_2 \bullet 4H_2O$, 1.6 mM H_3BO_3, 0.8 mM $MgSO_4 \bullet 7H_2O$) under constant rotation. For every flower, 10 μL pollen suspension was loaded onto a haemocytometer for counting. Pollen with tubes longer than the pollen diameter were considered viable.

Cytological Analyses

For the cytological and ultrastructural analysis of the developing pollen and tapetum, 3.0 to 3.1 mm flower buds from plants that received a 4-day LTMH or control treatment during 13 to 10 days before anthesis (DBA) were labeled, and anthers were collected on consecutive days after the treatment (see sampling scheme in **Supplementary Figure S1A**) and fixed in 0.025 M phosphate buffer, pH 7.2, containing 2% glutaraldehyde and 4% paraformaldehyde, for 2 h at room temperature, followed by 2 h post-fixation with 1% osmium tetroxide in water. The samples were then dehydrated in a graded ethanol series and embedded in Spurr's resin. For light microscopy, sections of 1 μm in the median part of the anthers were cut and stained with 0.1% toluidine blue in 1% borax. Sections were viewed and photographed with a Leica DM2500 microscope (Leica Microsystems GmbH, Wetzlar, Germany), equipped with a Leica DFC 420C camera. For electron microscopy, 70 nm sections were cut, post-stained with uranyl acetate and lead citrate according to standard procedures and viewed with a JEOL JEM-1010 (JEOL Ltd., Tokyo, Japan), equipped with a Mega View III camera (Olympus, Soft Imaging System, Münster, Germany).

To describe the progression of pollen development, the number of cells per developmental stage (as described in **Supplementary Table S1**) was counted in each locule. Pollen was classified as with normal appearance, aberrant in shape and size, and plasmolysed or dead (i.e., no cytoplasm or only remnants of degenerated cytoplasm present). The tapetum development was also staged based on descriptions (**Supplementary Table S2**). Because tapetum cells of different stages were usually present in one locule simultaneously, the proportions of different stages were scored and the mean value was used. For each time point, the anthers from five to seven flowers were analyzed. In total, 770 locules containing 47,822 developing pollen from the control condition and 758 locules containing 45,016 developing pollen from the 4-day LTMH treatment were analyzed.

To determine the pollen size, fresh pollen at anthesis was viewed and photographed with a Leica DM2500 microscope and Leica DFC 420C camera after staining with 0.1% toluidine blue in 0.1% borax. In total, 2,260 pollen (from 11 flowers) and 1,874 pollen (from 9 flowers) from the control and 4-day LTMH treatments, respectively, were analyzed by using the image analysis software FIJI (https://imagej.nih.gov/ij/). The area of all pollen grains with a round shape was determined.

Microarray Analysis

On the day after a 4-day LTMH or control treatment, anther cones from 3.6 to 3.7 mm flower buds (corresponding to 9 DBA, see sampling scheme in **Supplementary Figure S1A**) were collected for total RNA isolation with Trizol reagent (Invitrogen, Thermo Fisher Scientific, Waltham, MA USA), followed by DNA digestion and purification with the RNeasy kit (Qiagen, Venlo, The Netherlands). RNA concentration and quality were checked with a Nanodrop 1000 (ThermoScientific, Thermo Fisher Scientific) and by 1.5% agarose gel electrophoresis. The cDNA was labeled with biotin using the Affymetrix GeneChip WT Terminal Labeling Kit (Affymetrix, Santa Clara, CA, USA) and hybridized to the Affymetrix EUTOM3 tomato exon arrays. The microarray signals were determined using MadMax microarray analysis software (hhtp://madmax.bioinformatics.nl). Robust Multiarray Averaging (RMA) was used for normalization. Original expression data were filtered for average absolute expression value $\geq$10 for at least one sample type and a log-based IQR $\geq$0.35, as determined according to (Chockalingam et al., 2016). All remaining transcript data were log-transformed before further analysis to correct for heterogeneity of variance. Principal components analysis was done using ClustVis (Metsalu and Vilo, 2015) with standard settings, that is, with row centring, row scaling with unit variance, and PCA method SVD with imputation. Ranked fold changes were used to determine enrichment of GO-Slim biological process annotations using Panther with false discovery rate correction (http://pantherdb.org/; version 16.0). Genes significantly differently expressed between treatments were identified using FDR $q \leq 0.05$ (Benjamini and Hochberg, 1995) and absolute fold change $\geq$1.5 as cut-offs. Over-representation of GO-slim biological process annotations among up- or downregulated genes was determined using Panther, using the whole tomato genome as a reference, Fisher's Exact test, and FDR correction. A hypergeometric test (http://nemates.org/MA/progs/overlap_stats.html) was applied to test whether the overlap between two subsets of genes was significantly different from expectation. A set of customized pollen and tapetum function associated genes in tomato was generated by fetching the orthologous genes (http://plants.ensembl.org/biomart/martview) to Arabidopsis genes with anther, pollen, and tapetum-related GO annotations, filtering for "all Arabidopsis paralogs are in the GO annotation list" and "two or fewer tomato paralogs", where applicable (**Supplementary Table S3**).

qPCR Analysis

For examination of UPR and tapetum regulatory genes, total RNA isolated for the microarray experiment was used. To examine the expression of reactive oxygen species (ROS) scavenging genes, flower buds received the 4-day LTMH at 13 to 10 days before anthesis (DBA) and control treatments were collected for anther samples at nine time points (**Supplementary Figure S1B**). Per plant, anthers of multiple flowers were pooled together. Four biological replicates (plants) were used per treatment per time point. Total RNA was extracted with trizol reagent (Invitrogen, Thermo Fisher Scientific). RNA concentration and quality were checked using a NanoDrop 1000 (ThermoScientific, Thermo Fisher Scientific) and the sample was treated with DNase I. Subsequently, cDNA was synthesized using the iScript cDNA synthesis kit (Bio-Rad, Hercules, CA, USA). Primers were designed with Primer3Plus software (primer3plus.com) or Beacon Designer

software (PREMIER Biosoft International, Palo Alto CA, USA) (**Supplementary Table S4**). Primers, SYBRGreen mix (Bio-Rad), and cDNA samples were mixed to a total volume of 25 μL. A 96-well thermocycler (Bio-Rad iCycler) was used for real-time RT-PCR reactions which followed a two-step protocol: 95 °C for 3 min and 40 cycles of 95 °C for 15 s, 60 °C for 45 s. LingRegPCR software (Ruijter et al., 2009) was used to calculate the average amplification efficiency per primer pair, which was combined with Cq values for computation of relative expression levels, which were then normalized against four reference genes, *CAC, SAND, LeEF1α,* and *RPL8*, using GeNorm (Vandesompele et al., 2002).

Lipid Peroxidation and ROS Scavenging Enzyme Activity Assays

For the lipid peroxidation assay, malondialdehyde (MDA) content was determined with thiobarbituric acid reactive substances assay. A similar set of samples as for qPCR (**Supplementary Figure S1B**) were ground into a fine powder and homogenized with 1 mL 80% ethanol. After centrifugation at 12,000 rpm for 10 min, 300 μL supernatant was mixed with an equal volume of 0.5% (w/v) 2-thiobarbituric acid in 20% trichloroacetic acid. The mixture was then incubated at 95 °C for 30 min. After cooling and centrifugation at 12,000 rpm for 5 min, the absorbance of the resulted supernatant was measured at 532 nm and 600 nm using a plate reader (SpectraMax 190, Molecular Devices, Sunnyvale, CA, USA). A calibration curve was generated by using 1,1,3,3-Tetraethoxypropane (T9889; Sigma-Aldrich) as a standard. For the ROS scavenging enzyme, samples (**Supplementary Figure S1B**) were homogenized in 150-μL 0.1 M potassium phosphate buffer (pH 7.0) with 1.0% polyvinylpolypyrrolidone. The extract was centrifuged at 18,000 g for 10 min and the resulting supernatant was stored at −80 °C. Protein concentration was determined as described by Bradford (1976) using bovine serum albumin as a standard. Catalase (CAT, EC 1.11.1.6) activity was determined using the Amplex®Red Catalase Assay Kit (Molecular Probes, Thermo Fisher Scientific) according to the manufacturer's instructions. Assays were performed with 5 μL protein extract and values were corrected for protein concentration. Ascorbate peroxidase (APX, EC 1.11.1.11) activity was determined as described by Nakano and Asada (1981), with minor modifications. A reaction mixture containing 30 μg of protein, 0.5 mL 1 mM ascorbate, and 0.5 mL 0.5 mM H_2O_2 was prepared, absorbance at 290 nm was determined after 30 and 240 s, and the difference was used for calculation of relative activity.

Statistical Analysis

For statistical analysis, pollen viability data were averaged for each plant and logit transformed using the formula PV' = ln((PV+1)/(101-PV)) and relative gene expression data were log transformed. One- or two-way ANOVA followed by Tukey's HSD or LSD *post-hoc* tests were applied to test for statistical significance of differences between treatments. All statistical analyses were performed with SPSS v20 (IBM, NY, USA).

RESULTS

Where and When Does LTMH Affect Pollen Development?

To determine whether exposure to long-term mild heat (LTMH) affects pollen development through a local effect on flowers or a systemic effect on the vegetative tissues, we heated single flower trusses of plants that were growing at control temperature (CT; 25/19 °C, day/night) by ∼5 °C and, vice versa, cooled flower trusses of plants growing in LTMH (31/25 °C) by ∼6 °C, for at least 10 days. In CT conditions, the viability of pollen from the flowers flushed with hot air was significantly lower than that of flowers from the same plant exposed to the ambient CT temperature; in LTMH, the viability of pollen from flowers flushed with cool air was significantly higher than that of flowers on the same plant exposed to the ambient warm LTMH temperature (**Figure 1A**). This indicates that the LTMH effect on developing pollen is local, at the level of the flower or below.

To determine which pollen developmental stages were sensitive to LTMH, tomato plants were subjected to 2 weeks of LTMH (33/27 °C, day/night), followed by a 2-week release at CT (25/19 °C). Under LTMH, pollen viability of freshly open flowers decreased if they were treated for 3 or more days before reaching anthesis, but a particularly strong reduction was observed when flowers were stressed for at least 9 days before they reached anthesis. When moved out of LTMH, a clear increment in pollen viability was observed in flowers that recovered in control temperature for at least 11 days (**Figure 1B**). To further determine what period of LTMH exposure was sufficient to induce the pollen damage, plants were exposed to LTMH for 2, 3, or 4 consecutive days only, starting at varying stages of flower development. Slight reductions in the viability of mature pollen were seen if plants were treated with 3- or 4-day MH when treatments ended at 4, 5, or 6 days before anthesis (DBA), while strong reductions were seen if these treatments ended at 8, 9, 10, or 11 DBA. The 2-day LTMH treatment did not significantly decrease pollen viability, irrespective of the flowering stage at which it was applied. Together, these results indicate that the 9-to-11 DBA stage of flower development is highly sensitive to LTMH and that pollen development is compromised if flowers experience at least 3 days of LTMH around this period.

Pollen Developmental Progression After 4-Day LTMH

The cytological consequences of a 4-day LTMH treatment ending at 10 DBA (meaning the plants were stressed at 13–10 DBA; **Supplementary Figure S1A**) on pollen development were determined by labeling flowers at 10 DBA (3.0–3.1 mm buds) and analyzing sectioned anthers on subsequent days. Pollen were mostly at the tetrad stage on the first day after the treatment (i.e., at 9 DBA; **Figure 2**). No large differences were detected in pollen developmental progression or cell death between the 4-day LTMH and CT treatments in the first 5 days after the treatment (i.e. until flowers were 5 days before anthesis; **Figure 2**). This included progression through mitosis I at 6 to 5 DBA in both treatment groups. Two days later, at 3 DBA, however, differences between the two treatments became

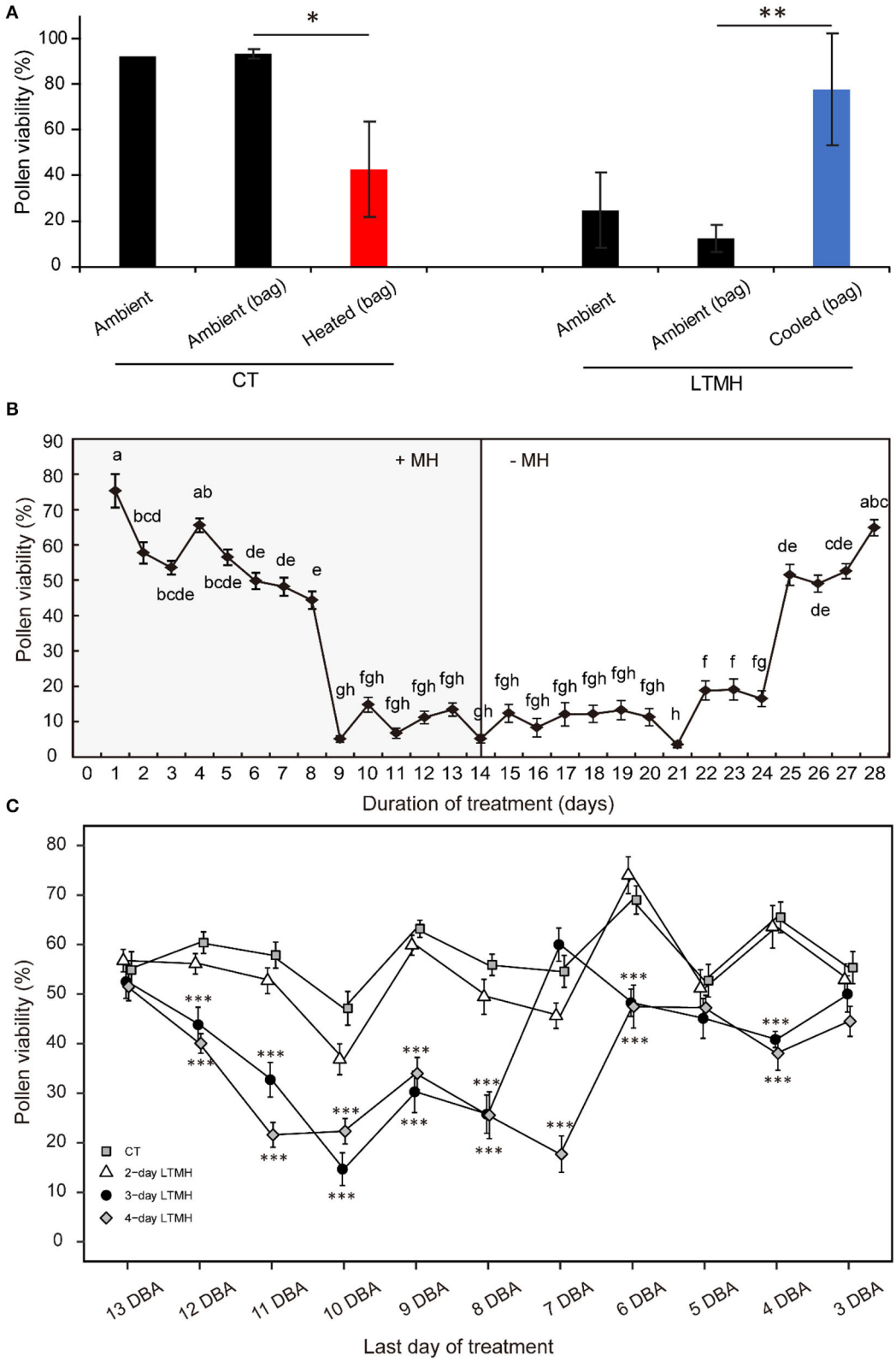

FIGURE 1 | The effects of long-term mild heat location, timing, and duration on viability of mature pollen. **(A)** Local temperature treatments: plants were grown in control (CT) or long-term mild heat (LTMH) conditions, and flower trusses were either exposed to the ambient temperature directly ("ambient"), to the ambient temperature by flushing ambient air through a bag around the truss ["ambient (bag)"], or reduced or increased temperature by flushing air of modified temperature

(Continued)

FIGURE 1 | through a bag around the truss ["cooled (bag)" or "heated (bag)"]. Viability of mature pollen (i.e., from freshly opened flowers) was measured 10 to 20 days after the onset of the treatment. Values indicate the mean ± SE (n = 2–3 plants, with pools of data from 1 to 3 days, each with at least three flowers per plant). *, significantly different from both controls, one-way ANOVA with LSD $P \leq 0.05$; **$P \leq 0.01$. **(B)** A 4-week stress-and-release experiment, with plants growing in LTMH for 2 weeks, followed by growth in CT for 2 weeks. Viability of mature pollen was determined daily. Values indicate the mean ± SE (n = 4 plants, with pools of 2 to 9 flowers analyzed per plant per sampling point). Different letter indicate significant differences between treatments, one-way ANOVA with Tukey $P \leq 0.05$. **(C)** Effect of LTMH treatments of variable durations and timing on viability of mature pollen. Samples are plotted according to their stage (expressed as days before anthesis; DBA) at the last day of the treatment. The 4-day LTMH treatment that ended at 10 DBA (i.e., flowers treated from 13 until 10 days before they would reach anthesis) was selected for subsequent cytological and gene expression experiments. Values indicate the mean ± SE (n = 5 plants, with pools of 2 to 3 flowers analyzed per plant per sampling point). *, significantly different from control at the same sampling point, one-way ANOVA with Tukey $P \leq 0.05$; **$P \leq 0.01$; ***$P \leq 0.001$.

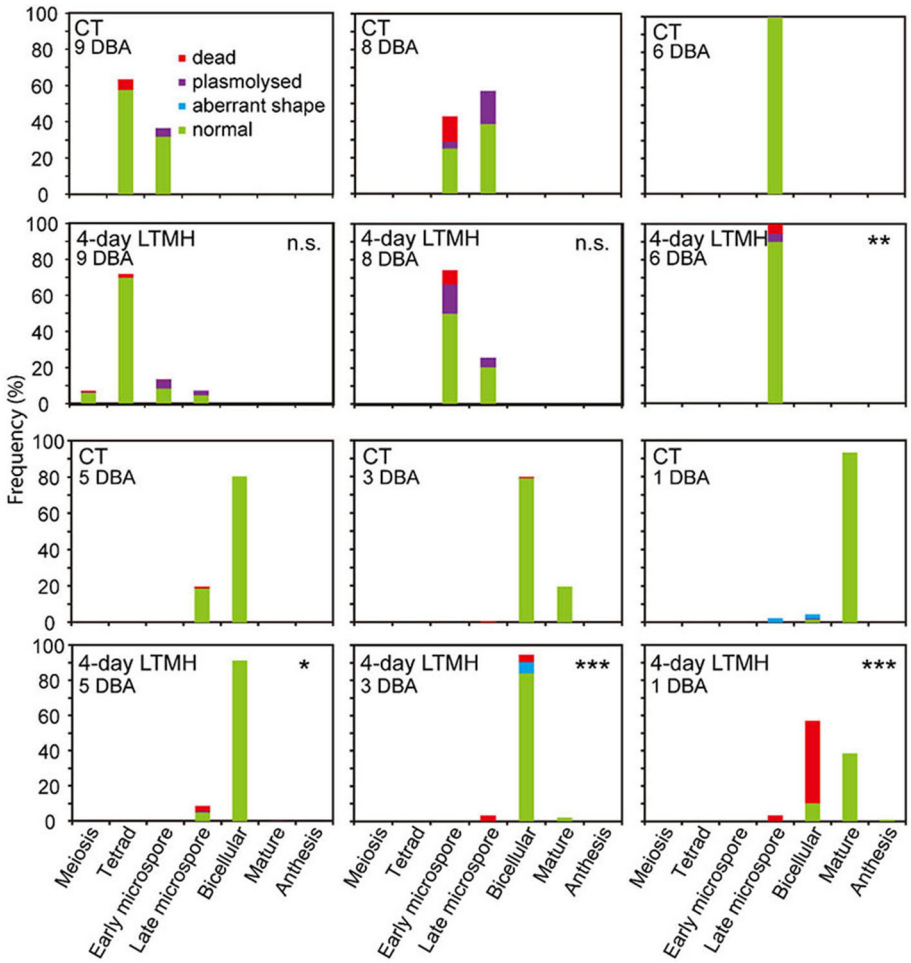

FIGURE 2 | Frequency analysis of pollen development in anthers from control and 4-day long-term mild heat treatment. Long-term mild heat (LTMH) or control temperature (CT) were applied for 4 days, and flowers that were at the 10-DBA stage on the last day of the treatment (i.e., they were treated from 13 DBA to 10 DBA) were labeled and then sampled on subsequent days (at stages of 9, 8, 6, 5, 3, and 1 DBA) for cytological analysis of pollen development (see **Supplementary Table S1**). For each flower stage per treatment, 100 to 140 locules were analyzed. Developing pollen were assigned to four categories: normal, aberrant shape, plasmolysed, or dead. *, Student's t-test, total percentage of normal, living pollen in LTMH treatment significantly less than in CT treatment on the same day $P < 0.05$; **$P < 0.01$; ***$P < 0.001$; n.s., not significant.

apparent and highly significant in terms of the proportion of normal, living pollen (**Figure 2**). The bicellular stage started with the accumulation of starch in both, the control and the 4-day LTMH treatment, but this process was more variable in the latter group, where pollen had fewer and smaller starch granules that tended to form clusters (**Figures 3A,B**, **4A,B**). This process was followed by the so-called second vacuolisation, in which the starch disappeared, a large vacuole formed and the size of the pollen gradually increased (**Figure 4C**). Altogether, pollen proceeded to the late bicellular stage in both treatment groups, but ∼10% of the bicellular pollen from the 4-day LTMH became aberrant (i.e., were oval-shaped or had less dense cytoplasm) or died, and few transited into the mature category (**Figure 2**). Differences were even more clear at 1 DBA and anthesis. With the increase in cytoplasm and disappearance of the large vacuole, numerous new starch granules were formed

toward the mature pollen stage. In the 4-day LTMH treatment group, pollen development was less synchronized and again part of the pollen produced fewer and smaller starch grains in comparison with the control (**Figures 3C,D**, **4D,E**). Notably, a large proportion of dead bicellular pollen was observed in the LTMH group at 1 DBA (**Figure 2**). At the anthesis stage, starch was not present anymore in either, control and the 4-day LTMH treated pollen. No or only small vacuoles were left in control pollen, while in the 4-day LTMH treated pollen, the size and number of vacuoles were more variable and many larger vacuoles were still observed (**Figures 4F,G**). In addition, anthesis stage pollen from 4-day LTMH were on average smaller than those from CT (**Figures 3E,F**, **4F,G**; **Supplementary Figure S2**). Contrasting to pollen development, no effect of the 4-day LTMH treatment was observed on the developmental progression of the tapetum relative to time and pollen development (**Figure 5**; **Supplementary Figure S3**).

Transcriptional Responses of Anthers to 4-Day LTMH

To get insight into the physiological damage of the 4-day LTMH on male reproductive tissue, developing anthers at the early microspore stage were collected for transcriptome analysis at 3 h into the day after the 4-day treatment (**Supplementary Figure S1A**; **Supplementary Table S5**). Principle component analysis showed clear differentiation between LTMH and control samples (**Supplementary Figure S4**). To obtain a broad overview of modified processes, an enrichment analysis for GO-slim 'biological process' annotations was done based on ranked fold changes (FC) of all analyzed genes (false discovery rate [FDR] $q<0.05$). There was a significant bias toward the downregulation of genes related to translation/ribosome assembly, DNA replication/mitosis, protein folding, endoplasmic reticulum unfolded protein response (UPR), and carbohydrate derivative biosynthetic processes (**Supplementary Table S6**). A slight bias toward upregulation was found for hormone-mediated signaling and flower development-related genes. Among the genes that were significantly differentially expressed between 4-day LTMH and control treatment ($|FC|>1.5$; $FDR<0.05$), 33 were found to be upregulated by LTMH and 59 downregulated (**Figure 6**). No overrepresented GO terms were found among the LTMH-upregulated genes, while, in line with the enrichment test, genes related to protein folding and the endoplasmic reticulum unfolded protein response (UPR) were strongly overrepresented among the LTMH-downregulated genes (**Supplementary Table S7**). The latter set contained orthologs of the major ER-stress gene BIP and genes related to glycosylation, COPII-coated vesicle budding, and signal peptide processing (see **Supplementary Table S8** for qPCR confirmation). A custom set of genes associated with tapetum and pollen development and function was also overrepresented among downregulated

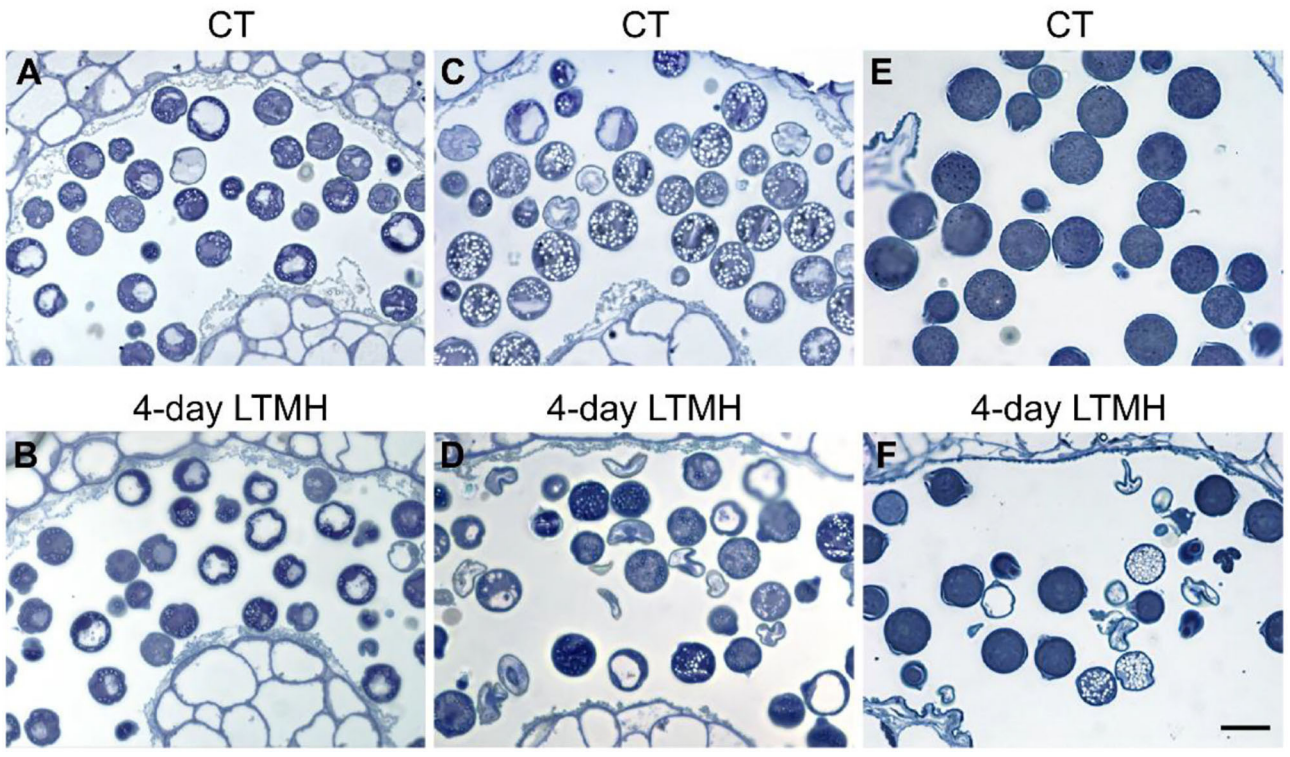

FIGURE 3 | Comparison of pollen cytology after control and 4-day long-term mild heat treatment by light microscopy. **(A,B)** Early bicellular pollen from control (CT) **(A)** and 4-day long-term mild heat treatment (LTMH) **(B)**. **(C,D)** Mature pollen from CT **(C)** and LTMH **(D)**. **(E,F)** Anthesis stage pollen from CT **(E)** and LTMH **(F)**. Bar = 20 μm.

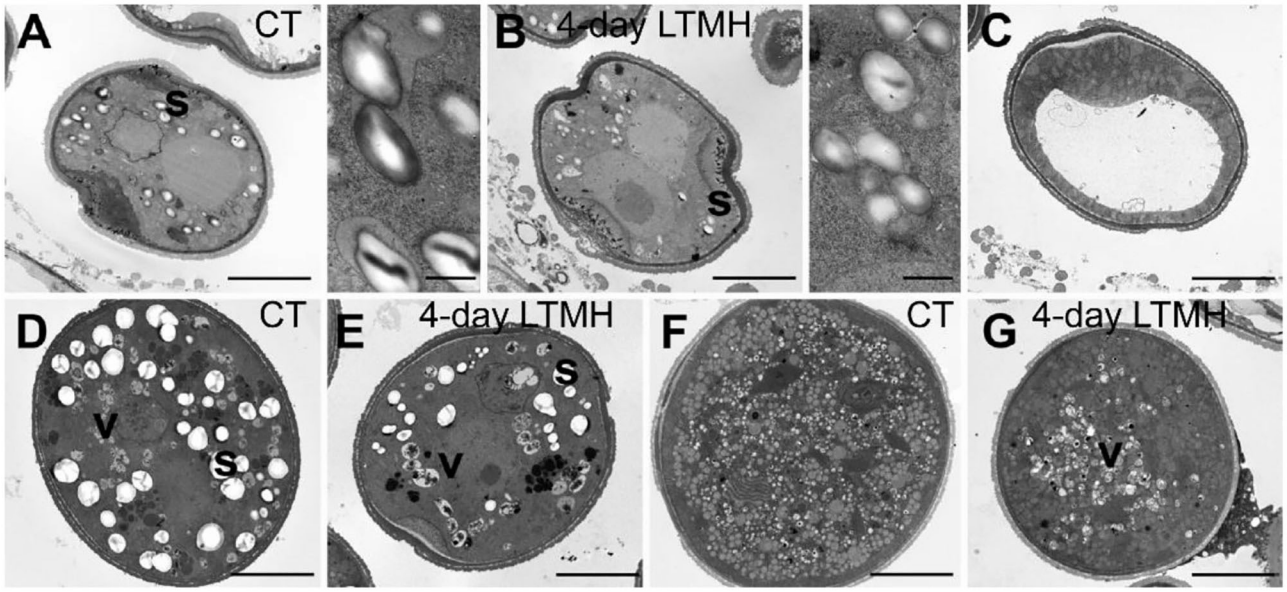

FIGURE 4 | Comparison of pollen ultrastructure between control and 4-day long-term mild heat treatment by electron microscopy. **(A,B)** Early bicellular from control temperature (CT) **(A)** and 4-day long-term mild heat treatment (LTMH) **(B)**, with close-ups of starch granules. **(C)** Second vacuolisation stage, characterized by absence of starch granules, from LTMH. No apparent differences were found relevant to control. **(D,E)** Mature pollen stage from control **(D)** and LTMH **(E)**. **(F,G)** Pollen at anthesis from control **(F)** and LTMH **(G)**. s, starch granule (large, white spherically shaped); v, vacuole (grayish, more or less spherically shaped, with dark debris visible inside). Bar = 5 μm.

genes (**Supplementary Table S6**; $P<0.001$). This included orthologs of genes coding for a DNA helicase, a SEC23/24 transport protein, two signal peptide peptidases (SPP), two UDP-galactose/glucose transmembrane transport proteins (UTR3), and tunicamycin-induced protein (TIN1). However, the major genes involved in the regulation of tapetum development were not differentially expressed between CT and the 4-day LTMH (see **Supplementary Table S9** for qPCR confirmation). Among the upregulated genes, multiple protease inhibitor genes were present, as well as two ROS-related genes, encoding catalase and vitamin C synthesis protein GDP-L-galactose phosphorylase. qPCR-based expression analysis of a set of ROS scavenging genes confirmed upregulation of *CAT1* during the last day of the 4-day LTMH treatment and several of the following days and showed that APX genes were upregulated during the heat (*APX3*) and several days after the 4-day LTMH treatment (*APX1*) (**Supplementary Figure S5**). These expression profiles were accompanied by higher catalase and ascorbate peroxidase enzyme activities, while overall lipid peroxidation damage in the anthers was not affected by LTMH (**Supplementary Figure S5**).

DISCUSSION

Heatwaves, which consist of multiple consecutive days of relatively high temperature during the warm season, are increasing in frequency and severity globally. In the present work, long-term mild heat (LTMH), as a proxy for heatwaves, negatively affected tomato pollen viability, in line with previous reports (Sato et al., 2000; Pressman et al., 2002; Xu et al., 2017b).

A General Stress-Sensitive Phase During Early Pollen Development

A stress-and-release experiment indicated that the period around 9 to 11 days before anthesis, covering the meiosis to early-microspore developmental stages, was most sensitive to LTMH, similar to what was reported before in tomato (Sato et al., 2002) and other species (Saini and Aspinall, 1982; Ahmed et al., 1992; Sakata et al., 2000; Porch and Jahn, 2001; Suzuki et al., 2001; Erickson and Markhart, 2002). Furthermore, we found that a short, 3- or 4-day LTMH treatment timed around this period was sufficient to lower pollen viability at anthesis. The same meiosis-to-microspore stage of pollen development was found to be the most susceptible to a short severe heat shock in various species (Iwahori, 1965; Draeger and Moore, 2017; Wang et al., 2017; Begcy et al., 2019), as well as to low temperature and drought in monocots (De Storme and Geelen, 2014). Thus, this early pollen developmental stage seems hypersensitive to physiological disturbance in general.

Early LTMH Exposure Has a Delayed Effect on Pollen Development

When tracking the development of pollen in flowers that were exposed to a short period of LTMH during the meiosis-to-microspore stage, cytological abnormalities were first detected several days later, during the formation and maturation of the bicellular pollen. Fewer and smaller starch grains were seen during the two successive peaks of starch accumulation, followed by a phase of pollen cell death. Surviving pollen were also smaller, on average, and vacuoles were not fully dissolved at anthesis. Seemingly normal pollen developmental progression

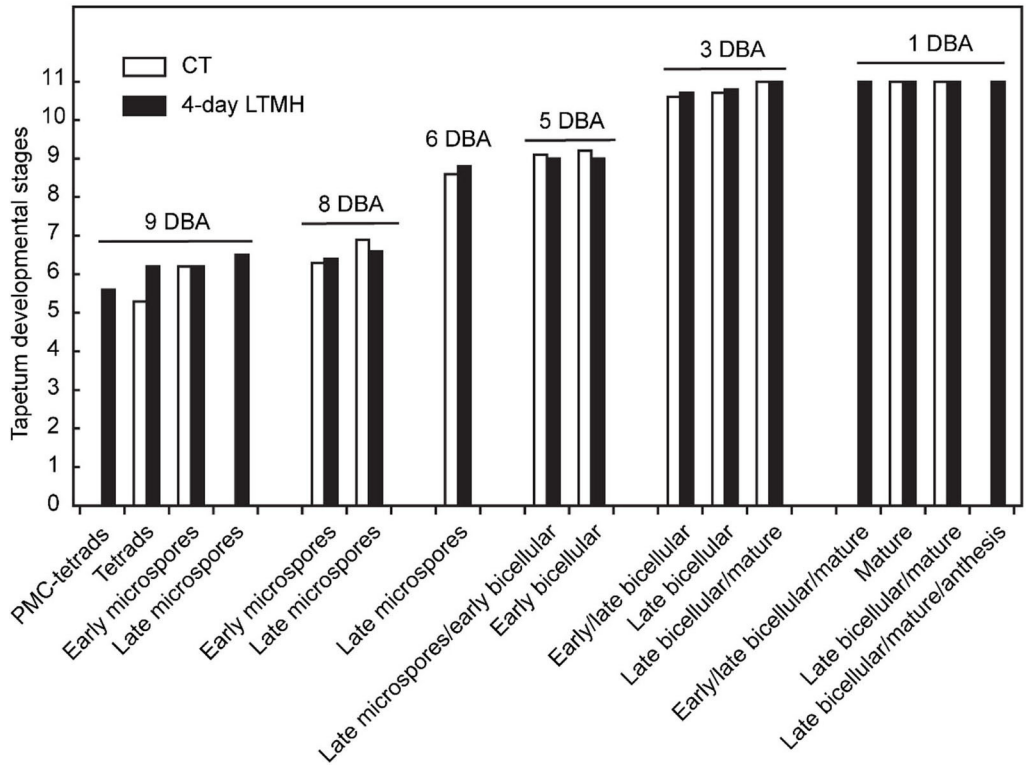

FIGURE 5 | Comparison of tapetum development between control and 4-day long-term mild heat treatment. Long-term mild heat (LTMH) or control temperature (CT) were applied for 4 days, and flowers that were at the 10-DBA stage on the last day of the treatment (i.e., they were treated from 13 DBA to 10 DBA) were labeled and then sampled on subsequent days (at stages of 9, 8, 6, 5, 3, and 1 DBA) for cytological analysis. For each flower stage, average tapetum developmental stage (see **Supplementary Table S2**) was plotted against pollen developmental stages of the samples (see **Supplementary Table S1**). For each stage per treatment, 100 to 140 locules were analyzed. pMC, pollen mother cell.

after early transient heat, until pollen mitosis or even beyond has also been seen in beans, wheat, and maize (Saini et al., 1984; Sakata et al., 2000; Suzuki et al., 2001; Begcy et al., 2019). This effect is markedly different from that of a short, severe heat shock or absolute high temperatures, which results in immediate defects to meiosis (Draeger and Moore, 2017; Wang et al., 2017; Ning et al., 2021) and abortion of early microspores (Iwahori, 1965; Harsant et al., 2013; Song et al., 2015). Pollen failure due to heat is frequently accompanied by, and ascribed to, mistiming of tapetum degeneration (Parish et al., 2012; De Storme and Geelen, 2014), often late ('persistent tapetum') in case of severe heat, and premature in case of mild heat (Saini et al., 1984; Ahmed et al., 1992; Sakata et al., 2000; Suzuki et al., 2001; Harsant et al., 2013). We did not detect abnormalities in cytology or persistence of the tapetum cells or mis-regulation of any of the major tapetum developmental regulator genes after early-stage exposure to 4-day LTMH. Endo et al. (2009) described a similar situation in rice under high temperature, with normal developmental progression of the tapetum and normal expression of known major tapetum regulators, while pollen viability was compromised. Also in *Brachypodium*, tapetal defects were not observed at milder heat (Harsant et al., 2013). However, it cannot be excluded that the treatment affected subcellular processes taking place in the tapetum. A role for tapetum in LTMH injury in tomato is suggested by our previous finding that a QTL for pollen LTMH tolerance behaved recessively, and thus acted in a sporophytic tissue (Xu et al., 2017a). Furthermore, we found here that pollen viability was equally affected by the non-overlapping 14–11 DBA and 10–7 DBA LTMH treatments (**Figure 1C**). Pollen quickly passes through a series of distinct developmental stages in this period, from pollen mother cells to tetrads to free microspores, meaning that either LTMH affects a process that is occurring constitutively in the developing pollen or that LTMH affects a non-pollen tissue that is less dynamic in this period. Indeed, the tapetum may be a more stable cell type in these early stages (**Figure 5**). In beans, the defects in the tapetum cells were specifically found in the morphology of the endoplasmic reticulum (Suzuki et al., 2001); much more subtle sub-cellular defects may have gone undetected in our analysis and warrant higher-resolution electron-microscopic analysis in the future.

Protein Folding Stress in the ER

An important question is what damage LTMH does to the young anthers to perturb subsequent pollen development. One of the hallmark effects of high temperature is incorrect folding of proteins, invoking the evolutionarily conserved cytoplasmic heat shock response (HSR) and endoplasmic reticulum stress response

FC	FDR q	ID	ITAG4.1 description
6.6	0.01	Solyc03g098790	cathepsin D inhibitor protein
5.7	0.00	Solyc09g084480	Protease inhibitor I (AHRD V3.3 *** Q07459_SOLTU)
3.7	0.04	Solyc02g090660	Patatin (AHRD V3.3 *** A0A218WXH7_PUNGR)
3.3	0.00	Solyc02g093180	HXXXD-type acyl-transferase family protein (AHRD V3.3 *** A0A2K3L8P7_TRIPR)
2.9	0.03	Solyc05g054090	induced stolen tip protein TUB8-like (AHRD V3.3 *** XP_004239829.1)
2.9	0.02	Solyc07g052490	MYB-like transcription factor ET.1
2.9	0.01	Solyc08g081620	#N/A
2.6	0.02	Solyc08g078960	Oxysterol-binding protein (AHRD V3.3 *** A0A200Q8D8_9MAGN)
2.4	0.01	Solyc12g094620	catalase
2.4	0.04	Solyc10g083470	E3 ubiquitin-protein ligase-like protein (AHRD V3.3 *** A0A1B1LUK2_VITPS)
2.3	0.03	Solyc01g010530	Sugar transporter protein 5
2.2	0.04	Solyc06g034200	Phosphate transporter (AHRD V3.3 *** Q9AYT3_TOBAC)
2.2	0.03	Solyc02g091750	LOW QUALITY PROTEIN: probable starch synthase 4, chloroplastic/amyloplastic (AHRD V3.3 *-* XP_025884911.1)
2.2	0.02	Solyc06g069880	protein PHYTOCHROME KINASE SUBSTRATE 3-like (AHRD V3.3 *** A0A2I4FQS5_9ROSI)
2.1	0.05	Solyc01g099810	Serine/arginine-rich-splicing factor SR34 (AHRD V3.3 *-* A0A0M9UMW1_NICAT)
2.1	0.05	Solyc09g009830	Alpha carbonic anhydrase (AHRD V3.3 *** A0A200QHP1_9MAGN)
2.0	0.02	Solyc09g083390	zinc knuckle (CCHC-type) family protein (AHRD V3.3 *-* AT5G43630.4)
2.0	0.04	Solyc12g056560	HSP20-like chaperones superfamily protein (AHRD V3.3 *-* Q9SRD6_ARATH)
1.9	0.05	Solyc03g097370	P-loop containing nucleoside triphosphate hydrolases superfamily protein (AHRD V3.3 *** A0A2U1LV77_ARTAN)
1.9	0.01	Solyc03g098780	Aspartic protease inhibitor.1
1.9	0.05	Solyc08g076800	RING/U-box superfamily protein (AHRD V3.3 *** A0A2U1QDA6_ARTAN)
1.9	0.04	Solyc07g007260	#N/A
1.8	0.04	Solyc07g040750	RNA helicase DEAD21
1.8	0.02	Solyc03g120390	auxin-regulated IAA15
1.8	0.02	Solyc07g061990	Solanesyl diphosphate synthase (AHRD V3.3 *** Q1W5D1_HEVBR)
1.7	0.04	Solyc01g110360	Fructose-bisphosphate aldolase (AHRD V3.3 *** Q9SXX5_NICPA)
1.6	0.01	Solyc10g005080	Late elongated hypocotyl (AHRD V3.3 *** J9PV71_NICAT)
1.6	0.03	Solyc10g075160	Ferredoxin (AHRD V3.3 *** K4D1V7_SOLLC)
1.6	0.04	Solyc08g008630	beta-carotene isomerase D27, chloroplastic (AHRD V3.3 *** A0A2I4EYC2_9ROSI)
1.6	0.02	Solyc01g096700	DnaJ domain-containing protein (AHRD V3.3 *-* A0A2U1QJS2_ARTAN)
1.5	0.01	Solyc03g115890	expansin 10
1.5	0.03	Solyc06g073320	GDP-L-galactose phosphorylase.1
1.5	0.02	Solyc01g100660	#N/A
-1.5	0.04	Solyc04g015620	DUF642 domain-containing protein (AHRD V3.3 *** A0A1Q3AUQ6_CEPFO)
-1.6	0.04	Solyc01g096900	DNA gyrase subunit A (AHRD V3.3 *** A0A2U1Q6G1_ARTAN)
-1.6	0.03	Solyc01g110130	DNA helicase (AHRD V3.3 *** A0A2G3BW33_CAPCH)
-1.6	0.04	Solyc03g080160	Nascent polypeptide-associated complex subunit alpha-like protein (AHRD V3.11 *** tr|A0A2K3M7R5|A0A2K3M7R5_TRIPR)
-1.6	0.02	Solyc10g085480	60S ribosomal protein L24 (AHRD V3.3 *** A0A2G2VU23_CAPBA)
-1.6	0.02	Solyc03g122090	25.3 kDa vesicle transport protein (AHRD V3.3 *** A0A1U8G1E9_CAPAN)
-1.6	0.05	Solyc08g044400	SacI homology domain-containing protein / WW domain-containing protein (AHRD V3.3 *** F4J9G0_ARATH)
-1.7	0.05	Solyc10g085550	Enolase (AHRD V3.3 *** A0A200Q2G1_9MAGN)
-1.7	0.05	Solyc01g009010	4-diphosphocytidyl-2-C-methyl-D-erythritol kinase
-1.8	0.04	Solyc04g082130	Pseudouridine synthase family protein (AHRD V3.11 *** tr|A0A2U1N9V5|A0A2U1N9V5_ARTAN)
-1.8	0.01	Solyc01g106470	Tunicamycin induced protein (AHRD V3.3 *** Q84JN2_ARATH)
-1.8	0.03	Solyc05g015530	Endoplasmic reticulum, stress-associated Ramp4 (AHRD V3.3 *** A0A2U1N8N8_ARTAN)
-1.8	0.04	Solyc12g056840	Phosphopantothenate-cysteine ligase-like protein (AHRD V3.3 *** A0A1P8BFH8_ARATH)
-1.9	0.01	Solyc04g071880	Pyrophosphate-energized membrane proton pump (AHRD V3.3 *** G5DWK6_SILLA)
-1.9	0.00	Solyc03g119210	Bifunctional inhibitor/plant lipid transfer protein/seed storage helical domain (AHRD V3.3 *** A0A200Q3B5_9MAGN)
-1.9	0.04	Solyc12g015880	Heat shock protein 90-1
-1.9	0.02	Solyc11g068500	Sec23/sec24 transport family protein (AHRD V3.3 *** G5DW78_SILLA)
-1.9	0.04	Solyc04g015360	GATA transcription factor (AHRD V3.3 *** K4BQ39_SOLLC)
-1.9	0.01	Solyc11g011220	transmembrane protein (Protein of unknown function DUF2359%2C transmembrane) (AHRD V3.3 *** AT1G23170.2)
-1.9	0.00	Solyc01g008820	signal peptide peptidase-like (AHRD V3.3 *** A0A2I4FPX2_9ROSI)
-1.9	0.02	Solyc03g113210	Mitochondrial outer membrane protein porin (AHRD V3.3 *** A0A2K3N5U3_TRIPR)
-2.0	0.00	Solyc07g049450	Protein disulfide-isomerase like 2-2 (AHRD V3.3 *** A0A2G3C063_CAPCH)
-2.0	0.00	Solyc11g064790	Signal peptide peptidase (AHRD V3.3 *** A0A2G2VN53_CAPBA)
-2.0	0.04	Solyc07g065760	Coiled-coil protein (AHRD V3.3 *** F4I1X8_ARATH)
-2.1	0.00	Solyc04g081570	Heat shock protein 90 (AHRD V3.3 *-* A0A0A7LYT2_ALBBR)
-2.1	0.01	Solyc12g013710	light dependent NADH:protochlorophyllide oxidoreductase 1
-2.1	0.04	Solyc02g084060	#N/A
-2.1	0.03	Solyc03g117020	Stromal cell-derived factor 2-like protein (AHRD V3.3 *** A0A2G3CZD1_CAPCH)
-2.1	0.01	Solyc04g076190	Eukaryotic aspartyl protease family protein (AHRD V3.3 *** F4K5B9_ARATH)
-2.2	0.00	Solyc06g010250	High-affinity nitrate transporter 2.2 (AHRD V3.3 *** NRT22_ORYSJ)
-2.3	0.05	Solyc05g053470	60 kDa chaperonin (AHRD V3.3 *** Q8H903_ORYSJ)
-2.3	0.00	Solyc01g100380	Calreticulin (AHRD V3.3 *** A0A2G3AWT5_CAPCH)
-2.3	0.04	Solyc03g044900	Calmodulin-like .1
-2.4	0.02	Solyc03g118040	calnexin
-2.4	0.04	Solyc03g115230	Solanum lycopersicum heat shock protein
-2.5	0.00	Solyc01g010650	UDP-galactose UDP-glucose transporter 3-like protein (AHRD V3.3 *** A0A2K3NS07_TRIPR)
-2.5	0.00	Solyc05g005000	Alpha/beta-Hydrolases superfamily protein (AHRD V3.3 *-* F4I5X3_ARATH)
-2.6	0.01	Solyc05g007150	UDP-galactose/UDP-glucose transporter 3 (AHRD V3.3 *** A0A2G2YDQ6_CAPAN)
-2.6	0.00	Solyc01g060130	TOMGTPASE Mill. GTPase
-2.6	0.00	Solyc03g120900	WD40 repeat (AHRD V3.3 *** A0A200QDT5_9MAGN)
-2.7	0.01	Solyc07g043560	Heat shock protein 70 kDa (AHRD V3.3 *** A0A2K3NQB8_TRIPR)
-2.7	0.01	Solyc09g075620	P-loop containing nucleoside triphosphate hydrolases superfamily protein (AHRD V3.3 *-* A0A1P8B4T0_ARATH)
-2.8	0.00	Solyc08g082820	TOMBIPGRBC Tomato BiP (binding protein)/grp78
-2.9	0.00	Solyc06g005940	Protein disulfide-isomerase (AHRD V3.3 *** A0A1U8GX36_CAPAN)
-3.0	0.04	Solyc06g075780	Zinc finger protein (AHRD V3.3 *** A0A200PZ96_9MAGN)
-3.2	0.01	Solyc04g072160	ripening regulated protein DDTFR8
-3.2	0.02	Solyc09g007630	P58IPK
-3.4	0.04	Solyc09g064380	Tetratricopeptide repeat (TPR)-like superfamily protein (AHRD V3.3 *** F4I456_ARATH)
-3.4	0.00	Solyc07g032250	nucleophosmin (AHRD V3.3 *** AT4G29520.1)
-3.5	0.00	Solyc05g050130	Acidic endochitinase (AHRD V3.11 *** sp|P29060|CHIA_TOBAC)
-3.6	0.00	Solyc08g078940	Bifunctional inhibitor/lipid-transfer protein/seed storage 2S albumin superfamily protein (AHRD V3.3 *** F4IC43_ARATH)
-3.7	0.00	Solyc03g082920	Heat shock protein 70 family (AHRD V3.3 *** A0A200QNK9_9MAGN)
-4.0	0.00	Solyc01g079610	DnaJ protein ERDJ3B (AHRD V3.3 *** A0A2G2Z6I0_CAPAN)
-4.0	0.00	Solyc06g069820	DUF674 family protein (AHRD V3.11 *** tr|A0A2K3NL09|A0A2K3NL09_TRIPR)
-4.2	0.01	Solyc09g011160	Regulator of chromosome condensation (RCC1) family protein (AHRD V3.3 *** A0A1I9LSN5_ARATH)
-5.2	0.05	Solyc09g064390	#N/A
-5.4	0.01	Solyc09g005120	DnaJ protein ERDJ3A (AHRD V3.3 *** A0A2G2VZ69_CAPBA)
-6.2	0.00	Solyc08g079870	subtilisin
-16.1	0.00	Solyc05g046340	Phosphomannomutase (AHRD V3.3 *** A0A2G3BTT3_CAPCH)

FIGURE 6 | Genes expressed significantly differently (FDR $\leq$ 0.05 and |fold change| $>$ 1.5) between 4-day long-term mild heat (LTMH) and control temperature (CT) treatments. The first, second, third, and fourth columns are fold change (FC), FDR q value, Solyc gene code, and functional description, respectively. Positive FC value (red label), expressed higher after LTMH than CT; negative FC value (blue label), expressed lower after LTMH than CT.

(unfolded protein response; UPR), which involve upregulation of the protein folding, modification, repair, and degradation pathways in various cellular compartments (Wang et al., 2004; Li and Howell, 2021). Interestingly, UPR genes constitute a large part of the genes downregulated on the day after the 4-day LTMH treatment, among others those encoding calreticulin, calnexin, BIP, HSP90-ER, protein disulfide-isomerase, and UDP-galactose transporter 3 proteins. Such a transcriptional response points to negative feedback, in which accumulated protective proteins repress the heat stress response, even to below control levels directly after the stress is released, as has been seen before (Bita et al., 2011; Liu et al., 2012; Bonnot and Nagel, 2021). So, while the earliest response of anthers to mild and severe heat mainly involves HSR-related genes (Bita et al., 2011; Fragkostefanakis et al., 2016b), the long-term response to LTMH seems to involve modulation of UPR-related gene expression. Interestingly, recent studies indicated that an intact UPR is essential for pollen development under very mildly elevated temperatures (Deng et al., 2016; Fragkostefanakis et al., 2016a; Feldeverd et al., 2020; Yamamoto et al., 2020; Lu et al., 2021). It has been suggested that the ER in the tapetum is under constitutive strain already under normal conditions, which could explain the high sensitivity of this tissue to additional stress (Singh et al., 2021). Therefore, it is worthwhile to further investigate the role of tapetum ER stress and its protection in heat-mediated pollen sterility.

Oxidative Stress

Reactive oxygen species (ROS) accumulation is considered secondary stress, often occurring as a result of exposure to a primary, external stress factor. ROS levels are finely tuned to maintain proper cellular homeostasis and are regulated in a developmental, stress, and feedback-dependent manner (Huang et al., 2019). During male reproductive development, deviations in ROS regulation lead to tapetal dysfunction and pollen abortion (Hu et al., 2011; Luo et al., 2013; Xie et al., 2014; Yi et al., 2016). In our study, the expression of *APX* genes was found to be induced during the LTMH treatment, in accordance with a previous report on early LTMH responses (Bita et al., 2011). Furthermore, *CAT1* and *APX3* expressions were still high in the following days. This pattern corresponded with increases in the respective enzyme activities. The upregulation is likely due to feedback regulation by elevated ROS levels (Rizhsky et al., 2004), but as no overall oxidative damage in the form of lipid peroxidation was detected, the increase in scavenger activity seems to have largely maintained ROS balance upon LTMH. This differentiates LTMH from severe heat, where oxidative damage is often detected, possibly because the activity of various scavengers is reduced at high absolute temperature (Panchuk et al., 2002; Djanaguiraman et al., 2014, 2018; Zhao et al., 2018). It is still possible that, under LTMH conditions, ROS caused damage in a specific subset of cells or tissues of the anther which remained undetected. In support of this notion, the tolerance of pollen development to LTMH was somewhat enhanced by overexpression of a glutaredoxin S17 (Müller et al., 2016) and by increasing endogenous flavonol levels (Rutley et al., 2021).

Carbohydrate Limitation and Partitioning

Developing microspores/pollen cells act as a sink and are thought to compete for limiting resources available in the anther locules, making them sensitive to disturbances in supply, use, and partitioning of nutrients (García et al., 2017). Starch and soluble sugar levels are finely regulated during pollen development: in plants grown under optimal conditions, starch accumulates after pollen mitosis I, followed by a break-down to form soluble sugars at the anthesis stage. These simple sugars then serve as the energy source for imminent pollen germination. In tomato, treatment with LTMH during the whole period of flower development significantly decreased the starch concentration in bicellular pollen and consequently, reduced soluble sugar content at anthesis (Pressman et al., 2002; Firon et al., 2006; Sato et al., 2006). We observed two distinct instances of starch accumulation in bicellular pollen, interrupted by the second vacuolisation and the 4-day LTMH treatment resulted in fewer and smaller starch granules in both instances. Reduced carbohydrate availability was also suggested by the significant bias toward the downregulation of the gene set associated with carbon derivative biosynthetic processes. As carbohydrates also act as osmolytes in dehydrating pollen (Firon et al., 2012), the LTMH-induced reduction of pollen volume at the final stage might well be the result of a low soluble sugar content. Questions remain as to the step in carbohydrate transport, partitioning, or metabolism affected by LTMH and whether the observed deviations are causal to pollen failure or rather a symptom thereof. The fact that the reduced pollen viability phenotype correlated to the direct surrounding temperature of the flower, and not to that of the rest of the plant, indicates that source activity and phloem loading are not limiting factors for pollen development under LTMH. Carbohydrate metabolism and transfer from the anther and tapetum to the developing pollen may be affected by LTMH. As we did not find downregulation of genes involved in these processes after LTMH, such as those for invertases and sucrose synthases (De Storme and Geelen, 2014), this would need to have occurred during the heat or involve post-transcriptional regulation. Alternatively, it has been hypothesized that carbohydrates are titrated away from developmental processes toward the mounting of an acclimating response (Rieu et al., 2017). Also, we found that several protease inhibitors were upregulated after LTMH, which may suggest extra investment in defense against pathogens and insects (Mosolov and Valueva, 2005).

In conclusion, our results show that LTMH affects male fertility through a direct, local effect on flowers and reveal fundamental differences between LTMH and severe heat-induced pollen failure, in terms of timing of pollen developmental deviations, severity of tapetum defects, and cellular damage. This suggests that multiple tolerance traits might be needed to improve plant reproductive performance in high-temperature conditions.

DATA AVAILABILITY STATEMENT

The raw microarray data generated in this study are available in the NCBI GEO repository under accession number GSE180168

and the processed data can be found in the supplemental datasets provided.

AUTHOR CONTRIBUTIONS

JX, SJ, and IR conceived and designed the study and wrote the manuscript. JX, SJ, MW-A, PG, and MJ performed the research. JX, SJ, MW-A, and IR analyzed and interpreted the data. All authors contributed to the article and approved the submitted version.

FUNDING

This work was supported by the China Scholarship Council (CSC Grant Number 201207565002, to JX), the Dutch Research Council (NWO Grant Number 867.15.011, to IR), and the Dutch Topsector Horticulture and Starting Materials (TKI TU grant number TU-2018-012, to IR).

ACKNOWLEDGMENTS

The authors would like to thank the staff of the Radboud University Experimental Garden and Genebank (Nijmegen, The Netherlands) for taking excellent care of the plants. We appreciate the help from Dr. Liesbeth Pierson with microscopy and image analysis.

SUPPLEMENTARY MATERIAL

The Supplementary Material for this article can be found online at: https://www.frontiersin.org/articles/10.3389/fpls.2022.925754/full#supplementary-material

REFERENCES

Ahmed, F. E., Hall, A. E., and DeMason, D. A. (1992). Heat Injury During Floral Development in Cowpea (Vigna unguiculata, Fabaceae). *Am. J. Bot.* 79, 784. doi: 10.1002/j.1537-2197.1992.tb13655.x

Aloni, B., Peet, M., Pharr, M., and Karni, L. (2001). The effect of high temperature and high atmospheric Co2 on carbohydrate changes in bell pepper (*Capsicum annuum*) pollen in relation to its germination. *Physiol. Plant.* 112, 505–512. doi: 10.1034/j.1399-3054.2001.1120407.x

Begcy, K., Nosenko, T., Zhou, L. Z., Fragner, L., Weckwerth, W., and Dresselhaus, T. (2019). Male sterility in maize after transient heat stress during the tetrad stage of pollen development. *Plant Physiol.* 181, 683–700. doi: 10.1104/pp.19.00707

Benjamini, Y., and Hochberg, Y. (1995). Controlling the false discovery rate: a practical and powerful approach to multiple testing. *J. R. Stat. Soc.* 57, 289–300. doi: 10.1111/j.2517-6161.1995.tb02031.x

Bita, C. E., Zenoni, S., Vriezen, W. H., Mariani, C., Pezzotti, M., and Gerats, T. (2011). Temperature stress differentially modulates transcription in meiotic anthers of heat-tolerant and heat-sensitive tomato plants. *BMC Genom.* 12, 384. doi: 10.1186/1471-2164-12-384

Bonnot, T., and Nagel, D. H. (2021). Time of day prioritizes the pool of translating mRNAs in response to heat stress. *Plant Cell.* 33, 2164–2182. doi: 10.1093/plcell/koab113

Bradford, M. M. (1976). A rapid and sensitive method for the quantitation of microgram quantities of protein utilizing the principle of protein-dye binding. *Anal. Biochem.* 72, 248–254. doi: 10.1006/abio.1976.9999

Chaturvedi, P., Doerfler, H., Jegadeesan, S., Ghatak, A., Pressman, E., Castillejo, M. A., et al. (2015). Heat-treatment-responsive proteins in different developmental stages of tomato pollen detected by targeted mass accuracy precursor alignment (tMAPA). *J. Proteome Res.* 14, 4463–4471. doi: 10.1021/pr501240n

Chockalingam, S., Aluru, M., and Aluru, S. (2016). Microarray Data Processing Techniques for Genome-Scale Network Inference from Large Public Repositories. *Microarrays* 5, 23. doi: 10.3390/microarrays5030023

De Storme, N., and Geelen, D. (2014). The impact of environmental stress on male reproductive development in plants: biological processes and molecular mechanisms. *Plant Cell Environ.* 37, 1–18. doi: 10.1111/pce.12142

Deng, Y., Srivastava, R., Quilichini, T. D., Dong, H., Bao, Y., Horner, H. T., et al. (2016). IRE1, a component of the unfolded protein response signaling pathway, protects pollen development in Arabidopsis from heat stress. *Plant J.* 88, 193–204. doi: 10.1111/tpj.13239

Djanaguiraman, M., Perumal, R., Ciampitti, I. A., Gupta, S. K., and Prasad, P. V. V. (2018). Quantifying pearl millet response to high temperature stress: thresholds, sensitive stages, genetic variability and relative sensitivity of pollen and pistil. *Plant Cell Environ.* 41, 993–1007. doi: 10.1111/pce.12931

Djanaguiraman, M., Vara Prasad, P. V., Murugan, M., Perumal, R., and Reddy, U. K. (2014). Physiological differences among sorghum (Sorghum bicolor L. Moench) genotypes under high temperature stress. *Environ. Exp. Bot.* 100, 43–54. doi: 10.1016/j.envexpbot.2013.11.013

Draeger, T., and Moore, G. (2017). Short periods of high temperature during meiosis prevent normal meiotic progression and reduce grain number in hexaploid wheat (Triticum aestivum L.). *Theor. Appl. Genet.* 130, 1785–1800. doi: 10.1007/s00122-017-2925-1

Endo, M., Tsuchiya, T., Hamada, K., Kawamura, S., Yano, K., Ohshima, M., et al. (2009). High temperatures cause male sterility in rice plants with transcriptional alterations during pollen development. *Plant Cell Physiol.* 50, 1911–1922. doi: 10.1093/pcp/pcp135

Erickson, A. N., and Markhart, A. H. (2002). Flower developmental stage and organ sensitivity of bell pepper (Capsicum annuum L.) to elevated temperature. *Plant Cell Environ.* 25, 123–130. doi: 10.1046/j.0016-8025.2001.00807.x

Feldeverd, E., Porter, B. W., Yuen, C. Y. L., Iwai, K., Carrillo, R., Smith, T., et al. (2020). The arabidopsis protein disulfide isomerase subfamily M isoform, PDI9, localizes to the endoplasmic reticulum and influences pollen viability and proper formation of the pollen exine during heat stress. *Front. Plant Sci.* 11, 2035. doi: 10.3389/fpls.2020.610052

Firon, N., Nepi, M., and Pacini, E. (2012). Water status and associated processes mark critical stages in pollen development and functioning. *Ann. Bot.* 109, 1201–1213. doi: 10.1093/aob/mcs070

Firon, N., Shaked, R., Peet, M. M., Pharr, D. M., Zamski, E., Rosenfeld, K., et al. (2006). Pollen grains of heat tolerant tomato cultivars retain higher carbohydrate concentration under heat stress conditions. *Sci. Hortic.* 109, 212–217. doi: 10.1016/j.scienta.2006.03.007

Fragkostefanakis, S., Mesihovic, A., Hu, Y., and Schleiff, E. (2016a). Unfolded protein response in pollen development and heat stress tolerance. *Plant Reprod.* 29, 81–91. doi: 10.1007/s00497-016-0276-8

Fragkostefanakis, S., Mesihovic, A., Simm, S., Paupière, M. J., Hu, Y., Paul, P., et al. (2016b). HsfA2 controls the activity of developmentally and stress-regulated heat stress protection mechanisms in tomato male reproductive tissues. *Plant Physiol.* 170, 2461–2477. doi: 10.1104/pp.15.01913

Frank, G., Pressman, E., Ophir, R., Althan, L., Shaked, R., Freedman, M., et al. (2009). Transcriptional profiling of maturing tomato (Solanum lycopersicum L.) microspores reveals the involvement of heat shock proteins, ROS scavengers, hormones, and sugars in the heat stress response. *J. Exp. Bot.* 60, 3891–3908. doi: 10.1093/jxb/erp234

García, C. C., Nepi, M., and Pacini, E. (2017). It is a matter of timing: asynchrony during pollen development and its consequences on pollen performance in angiosperms—a review. *Protoplasma.* 254, 57–73. doi: 10.1007/s00709-016-0950-6

Giorno, F., Wolters-Arts, M., Grillo, S., Scharf, K. D., Vriezen, W. H., and Mariani, C. (2010). Developmental and heat stress-regulated expression of HsfA2 and small heat shock proteins in tomato anthers. *J. Exp. Bot*. 61, 453–462. doi: 10.1093/jxb/erp316

González-Schain, N., Dreni, L., Lawas, L. M. F., Galbiati, M., Colombo, L., Heuer, S., et al. (2016). Genome-wide transcriptome analysis during anthesis reveals new insights into the molecular basis of heat stress responses in tolerant and sensitive rice varieties. *Plant Cell Physiol.* 57, 57–68. doi: 10.1093/pcp/pcv174

Harsant, J., Pavlovic, L., Chiu, G., Sultmanis, S., and Sage, T. L. (2013). High temperature stress and its effect on pollen development and morphological components of harvest index in the C3 model grass Brachypodium distachyon. *J. Exp. Bot*. 64, 2971–2983. doi: 10.1093/jxb/ert142

Hedhly, A., Hormaza, J. I., and Herrero, M. (2009). Global warming and sexual plant reproduction. *Trends Plant Sci.* 14, 30–36. doi: 10.1016/j.tplants.2008.11.001

Hu, L., Liang, W., Yin, C., Cui, X., Zong, J., Wang, X., et al. (2011). Rice MADS3 regulates ROS homeostasis during late anther development. *Plant Cell.* 23, 515–533. doi: 10.1105/tpc.110.074369

Huang, H., Ullah, F., Zhou, D.-X., Yi, M., and Zhao, Y. (2019). Mechanisms of ROS regulation of plant development and stress responses. *Front. Plant Sci*. 10, 800. doi: 10.3389/fpls.2019.00800

IPCC. (2018). "Summary for Policymakers." In: *Global Warming of 1.5°C. An IPCC Special Report on the impacts of global warming of 1.5°C above pre-industrial levels and related global greenhouse gas emission pathways, in the context of strengthening the global response to the threat of climate change*, Eds V. Masson-Delmotte, P. Zhai, H.-O. Pörtner, D. Roberts, J. Skea, R. Shukla, P, … T. Waterfield. Geneva, Switzerland, 1–32.

Iwahori, S. (1965). High temperature injuries in tomato. IV. Development of normal flower buds and morphological abnormalities of flower buds treated with high temperature. *J. Jpn. Soc. Hortic. Sci*. 34, 33–41. doi: 10.2503/jjshs.34.33

Jain, M., Prasad, P. V. V., Boote, K. J., Hartwell, A. L., and Chourey, P. S. (2007). Effects of season-long high temperature growth conditions on sugar-to-starch metabolism in developing microspores of grain sorghum (*Sorghum bicolor* L. Moench). *Planta.* 227, 67–79. doi: 10.1007/s00425-007-0595-y

Jegadeesan, S., Chaturvedi, P., Ghatak, A., Pressman, E., Meir, S., Faigenboim, A., et al. (2018). Proteomics of heat-stress and ethylene-mediated thermotolerance mechanisms in tomato pollen grains. *Front. Plant Sci*. 9, 1558. doi: 10.3389/fpls.2018.01558

Lei, X., and Liu, B. (2020). Tapetum-dependent male meiosis progression in plants: increasing evidence emerges. *Front. Plant Sci*. 10, 1667. doi: 10.3389/fpls.2019.01667

Li, Z., and Howell, S. H. (2021). Heat stress responses and thermotolerance in Maize. *Int. J. Mol. Sci*. 22, 948. doi: 10.3390/ijms22020948

Liu, G.-T., Wang, J.-F., Cramer, G., Dai, Z.-W., Duan, W., Xu, H.-G., et al. (2012). Transcriptomic analysis of grape (*Vitis vinifera* L.) leaves during and after recovery from heat stress. *BMC Plant Biol.* 12, 174. doi: 10.1186/1471-2229-12-174

Lu, S., Zhu, T., Wang, Z., Luo, L., Wang, S., Lu, M., et al. (2021). Arabidopsis immune-associated nucleotide-binding genes repress heat tolerance at the reproductive stage by inhibiting the unfolded protein response and promoting cell death. *Mol. Plant.* 14, 267–284. doi: 10.1016/j.molp.2020.11.010

Luo, D., Xu, H., Liu, Z., Guo, J., Li, H., Chen, L., et al. (2013). A detrimental mitochondrial-nuclear interaction causes cytoplasmic male sterility in rice. *Nat. Genet.* 45, 573–577. doi: 10.1038/ng.2570

McCormick, S. (2004). Control of male gametophyte development. *Plant Cell.* 16, S142–S153. doi: 10.1105/tpc.016659

Metsalu, T., and Vilo, J. (2015). ClustVis: a web tool for visualizing clustering of multivariate data using principal component analysis and heatmap. *Nucleic Acids Res*. 43, W566–W570. doi: 10.1093/nar/gkv468

Mosolov, V. V., and Valueva, T. A. (2005). Proteinase inhibitors and their function in plants: a review. *Appl. Biochem. Microbiol*. 41, 227–246. doi: 10.1007/s10438-005-0040-6

Mu, Q., Zhang, W., Zhang, Y., Yan, H., Liu, K., Matsui, T., et al. (2017). iTRAQ-based quantitative proteomics analysis on rice anther responding to high temperature. *Int. J. Mol. Sci*. 18, 1811. doi: 10.3390/ijms18091811

Müller, F., and Rieu, I. (2016). Acclimation to high temperature during pollen development. *Plant Reprod.* 29, 107–118. doi: 10.1007/s00497-016-0282-x

Müller, F., Xu, J., Kristensen, L., Wolters-Arts, M., De Groot, P. F. M., Jansma, S. Y., et al. (2016). High-temperature-induced defects in tomato (Solanum lycopersicum) anther and pollen development are associated with reduced expression of B-class floral patterning genes. *PLoS ONE* 11, e0167614. doi: 10.1371/journal.pone.0167614

Nakano, Y., and Asada, K. (1981). Hydrogen-peroxide is scavenged by ascorbate-specific peroxidase in Spinach-chloroplasts. *Plant Cell Physiol*. 22, 867–880. doi: 10.1093/oxfordjournals.pcp.a076232

Ning, Y., Liu, Q., Wang, C., Qin, E., Wu, Z., Wang, M., et al. (2021). Heat stress interferes with formation of double-strand breaks and homolog synapsis. *Plant Physiol.* 185, 1783–1797. doi: 10.1093/plphys/kiab012

Ortiz-Bobea, A., Ault, T. R., Carrillo, C. M., Chambers, R. G., and Lobell, D. B. (2021). Anthropogenic climate change has slowed global agricultural productivity growth. *Nat. Clim. Change.* 11, 306–312. doi: 10.1038/s41558-021-01000-1

Panchuk, I. I., Volkov, R. A., and Schöffl, F. (2002). Heat stress-and heat shock transcription factor-dependent expression and activity of ascorbate peroxidase in Arabidopsis. *Plant Physiol.* 129, 838–853. doi: 10.1104/pp.001362

Parish, R. W., Phan, H. A., Iacuone, S., and Li, S. F. (2012). Tapetal development and abiotic stress: a centre of vulnerability. *Funct. Plant Biol.* 39, 553–559. doi: 10.1071/FP12090

Paupière, M. J., Müller, F., Li, H., Rieu, I., Tikunov, Y. M., Visser, R. G. F., et al. (2017). Untargeted metabolomic analysis of tomato pollen development and heat stress response. *Plant Reprod*. 30, 81–94. doi: 10.1007/s00497-017-0301-6

Pham, D., Hoshikawa, K., Fujita, S., Fukumoto, S., Hirai, T., Shinozaki, Y., et al. (2020). A tomato heat-tolerant mutant shows improved pollen fertility and fruit-setting under long-term ambient high temperature. *Environ. Exp. Bot*. 178, 104150. doi: 10.1016/j.envexpbot.2020.104150

Porch, T. G., and Jahn, M. (2001). Effects of high-temperature stress on microsporogenesis in heat-sensitive and heat-tolerant genotypes of Phaseolus vulgaris. *Plant Cell Environ.* 24, 723–731. doi: 10.1046/j.1365-3040.2001.00716.x

Pressman, E., Peet, M. M., and Pharr, D. M. (2002). The effect of heat stress on tomato pollen characteristics is associated with changes in carbohydrate concentration in the developing anthers. *Ann. Bot*. 90, 631–636. doi: 10.1093/aob/mcf240

Rieu, I., Twell, D., and Firon, N. (2017). Pollen development at high temperature: from acclimation to collapse. *Plant Physiol.* 173, 1967–1976. doi: 10.1104/pp.16.01644

Rizhsky, L., Davletova, S., Liang, H., and Mittler, R. (2004). The zinc finger protein Zat12 is required for cytosolic ascorbate peroxidase 1 expression during oxidative stress in arabidopsis. *J. Biol. Chem*. 279, 11736–11743. doi: 10.1074/jbc.M313350200

Ruijter, J. M., Ramakers, C., Hoogaars, W. M. H., Karlen, Y., Bakker, O., van den Hoff, M. J. B., et al. (2009). Amplification efficiency: linking baseline and bias in the analysis of quantitative PCR data. *Nucleic Acids Res*. 37, e45. doi: 10.1093/nar/gkp045

Rutley, N., Miller, G., Wang, F., Harper, J. F., Miller, G., and Lieberman-Lazarovich, M. (2021). Enhanced reproductive thermotolerance of the tomato high pigment 2 mutant is associated with increased accumulation of flavonols in pollen. *Front. Plant Sci.* 12, 779. doi: 10.3389/fpls.2021.672368

Saini, H. S., and Aspinall, D. (1982). Abnormal sporogenesis in wheat (*Triticum aestivum* L.) induced by short periods of high temperature. *Ann. Bot*. 49, 835–846. doi: 10.1093/oxfordjournals.aob.a086310

Saini, H. S., Sedgley, M., and Aspinall, D. (1984). Development anatomy in wheat of male sterility induced by heat stress, water deficit or abscisic acid. *Funct. Plant Biol*. 11, 243–253. doi: 10.1071/PP9840243

Sakata, T., Takahashi, H., Nishiyama, I., and Higashitani, A. (2000). Effects of high temperature on the development of pollen mother cells and microspores in Barley Hordeum vulgare L. *J. Plant Res*. 113, 395–402. doi: 10.1007/PL00013947

Satake, T., and Yoshida, S. (1978). High temperature-induced sterility in indica rices at flowering. *Jpn. J. Crop Sci*. 47, 6–17. doi: 10.1626/jcs.47.6

Sato, S., Kamiyama, M., Iwata, T., Makita, N., Furukawa, H., and Ikeda, H. (2006). Moderate Increase of Mean Daily Temperature Adversely Affects Fruit Set of Lycopersicon esculentum by Disrupting Specific Physiological Processes in Male Reproductive Development. *Ann. Bot*. 97, 731–738. doi: 10.1093/aob/mcl037

Sato, S., Peet, M. M., and Thomas, J. F. (2000). Physiological factors limit fruit set of tomato (Lycopersicon esculentum Mill.) under chronic, mild heat stress. *Plant Cell Environ*. 23, 719–726. doi: 10.1046/j.1365-3040.2000.00589.x

Sato, S., Peet, M. M., and Thomas, J. F. (2002). Determining critical pre- and post-anthesis periods and physiological processes in Lycopersicon esculentum Mill. exposed to moderately elevated temperatures. *J. Exp. Bot*. 53, 1187–1195. doi: 10.1093/jexbot/53.371.1187

Singh, M. B., Lohani, N., and Bhalla, P. L. (2021). The role of endoplasmic reticulum stress response in pollen development and heat stress tolerance. *Front. Plant Sci.* 12, 568. doi: 10.3389/fpls.2021.661062

Song, G., Wang, M., Zeng, B., Zhang, J., Jiang, C., Hu, Q., et al. (2015). Anther response to high-temperature stress during development and pollen thermotolerance heterosis as revealed by pollen tube growth and *in vitro* pollen vigor analysis in upland cotton. *Planta.* 241, 1271–1285. doi: 10.1007/s00425-015-2259-7

Suzuki, K., Takeda, H., Tsukaguchi, T., and Egawa, Y. (2001). Ultrastructural study on degeneration of tapetum in anther of snap bean (Phaseolus vulgaris L.) under heat stress. *Sex. Plant Reprod.* 13, 293–299. doi: 10.1007/s004970100071

Vandesompele, J., De Preter, K., Pattyn, F., Poppe, B., Van Roy, N., De Paepe, A., et al. (2002). Accurate normalization of real-time quantitative RT-PCR data by geometric averaging of multiple internal control genes. *Genome Biol.* 3, research0034. doi: 10.1186/gb-2002-3-7-research0034

Wang, J., Li, D., Shang, F., and Kang, X. (2017). High temperature-induced production of unreduced pollen and its cytological effects in Populus. *Sci. Rep.* 7, 1–12. doi: 10.1038/s41598-017-05661-x

Wang, W., Vinocur, B., Shoseyov, O., and Altman, A. (2004). Role of plant heat-shock proteins and molecular chaperones in the abiotic stress response. *Trends Plant Sci.* 9, 244–252. doi: 10.1016/j.tplants.2004.03.006

Wang, Y., Tao, H., Zhang, P., Hou, X., Sheng, D., Tian, B., and …, Huang S (2020). Reduction in seed set upon exposure to high night temperature during flowering in maize. *Physiol. Plant.* 169, 73–82. doi: 10.1111/ppl.13049

Xie, H. T., Wan, Z. Y., Li, S., and Zhang, Y. (2014). Spatiotemporal production of reactive oxygen species by nadph oxidase is critical for tapetal programmed cell death and pollen development in Arabidopsis. *Plant Cell.* 26, 2007–2023. doi: 10.1105/tpc.114.125427

Xu, J., Driedonks, N., Rutten, M. J. M., Vriezen, W. H., de Boer, G.-J., and Rieu, I. (2017a). Mapping quantitative trait loci for heat tolerance of reproductive traits in tomato (Solanum lycopersicum). *Mol. Breed.* 37, 58. doi: 10.1007/s11032-017-0664-2

Xu, J., Wolters-Arts, M., Mariani, C., Huber, H., and Rieu, I. (2017b). Heat stress affects vegetative and reproductive performance and trait correlations in tomato (*Solanum lycopersicum*). *Euphytica* 213, 156. doi: 10.1007/s10681-017-1949-6

Yamamoto, M., Uji, S., Sugiyama, T., Sakamoto, T., Kimura, S., Endo, T., et al. (2020). ERdj3B-mediated quality control maintains anther development at high temperatures. *Plant Physiol.* 182, 1979–1990. doi: 10.1104/pp.19.01356

Yang, J., Chen, X., Zhu, C., Peng, X., He, X., Fu, J., et al. (2015). Using RNA-seq to profile gene expression of spikelet development in response to temperature and nitrogen during meiosis in rice (Oryza sativa L.). *PLoS ONE.* 10, e0145532. doi: 10.1371/journal.pone.0145532

Yi, J., Moon, S., Lee, Y.-S., Zhu, L., Liang, W., Zhang, D., et al. (2016). Defective tapetum cell death 1 (DTC1) regulates ROS levels by binding to metallothionein during tapetum degeneration. *Plant Physiol.* 170, 1611–1623. doi: 10.1104/pp.15.01561

Zhao, C., Liu, B., Piao, S., Wang, X., Lobell, D. B., Huang, Y., et al. (2017). Temperature increase reduces global yields of major crops in four independent estimates. *Proc. Natl. Acad. Sci. U. S. A.* 114, 9326–9331. doi: 10.1073/pnas.1701762114

Zhao, Q., Zhou, L., Liu, J., Du, X., Asad, M.-A.-U. A. U., Huang, F., et al. (2018). Relationship of ROS accumulation and superoxide dismutase isozymes in developing anther with floret fertility of rice under heat stress. *Plant Physiol. Biochem.* 122, 90–101. doi: 10.1016/j.plaphy.2017.11.009

Conflict of Interest: The authors declare that the research was conducted in the absence of any commercial or financial relationships that could be construed as a potential conflict of interest.

Publisher's Note: All claims expressed in this article are solely those of the authors and do not necessarily represent those of their affiliated organizations, or those of the publisher, the editors and the reviewers. Any product that may be evaluated in this article, or claim that may be made by its manufacturer, is not guaranteed or endorsed by the publisher.

frontiers | Frontiers in Plant Science

TYPE Original Research
PUBLISHED 15 August 2022
DOI 10.3389/fpls.2022.864892

OPEN ACCESS

EDITED BY
Marta Adelina Mendes,
University of Milan,
Italy

REVIEWED BY
Nieves Goicoechea,
University of Navarra,
Spain
John Paul Moore,
Stellenbosch University,
South Africa
Maurizio Di Marzo,
University of Milan,
Italy

*CORRESPONDENCE
Markus Keller
mkeller@wsu.edu

†PRESENT ADDRESSES
Regula Scheele-Baldinger,
Max Baldinger AG,
Rümikon, Switzerland
John C. Ferguson,
Environment and Natural Resources Institute, University of Alaska, Anchorage, AK, United States
Julie M. Tarara,
Ste. Michelle Wine Estates, Prosser, WA, United States

SPECIALTY SECTION
This article was submitted to Plant Abiotic Stress, a section of the journal Frontiers in Plant Science

RECEIVED 29 January 2022
ACCEPTED 26 July 2022
PUBLISHED 15 August 2022

CITATION
Keller M, Scheele-Baldinger R, Ferguson JC, Tarara JM and Mills LJ (2022) Inflorescence temperature influences fruit set, phenology, and sink strength of Cabernet Sauvignon grape berries. *Front. Plant Sci.* 13:864892. doi: 10.3389/fpls.2022.864892

Inflorescence temperature influences fruit set, phenology, and sink strength of Cabernet Sauvignon grape berries

Markus Keller[1]*, Regula Scheele-Baldinger[2†], John C. Ferguson[3†], Julie M. Tarara[3†] and Lynn J. Mills[1]

[1]Department of Horticulture, Irrigated Agriculture Research and Extension Center, Washington State University, Prosser, WA, United States, [2]Department of Agricultural and Food Sciences, Swiss Federal Institute of Technology, Zürich, Switzerland, [3]United States Department of Agriculture, Agricultural Research Service, Horticultural Crops Research Unit, Prosser, WA, United States

The temperature during the bloom period leading up to fruit set is a key determinant of reproductive success in plants and of harvest yield in crop plants. However, it is often unclear whether differences in yield components result from temperature effects on the whole plant or specifically on the flower or fruit sinks. We used a forced-convection, free-air cooling and heating system to manipulate the inflorescence temperature of field-grown Cabernet Sauvignon grapevines during the bloom period. Temperature regimes included cooling (ambient −7.5°C), heating (ambient +7.5°C), an ambient control, and a convective control. Cooling significantly retarded the time to fruit set and subsequent berry development, and heating shortened the time to fruit set and accelerated berry development relative to the two controls. Fruit set was decreased in cooled inflorescences, but although the cooling regime resulted in the lowest berry number per cluster, it also decreased seed and berry weight at harvest while not affecting seed number. Cooling inflorescences slightly decreased fruit soluble solids and pH, and increased titratable acidity, but did not affect color density. The inflorescence temperature did not impact leaf gas exchange and shoot growth, and shoot periderm formation occurred independently of the timing of fruit ripening. These results suggest that the temperature experienced by grape flowers during bloom time impacts fruit set and subsequent seed and berry development. Suboptimal temperatures not only reduce the proportion of flowers that set fruit but also limit the sink strength of the berries that do develop after fruit set. Shoot vigor and maturation, and leaf physiology, on the other hand, may be rather insensitive to temperature-induced changes in reproductive development.

KEYWORDS

grape (*Vitis* spp.), temperature manipulation, bloom, fruit set, sink strength, yield components

Introduction

Following pollination and fertilization, flowers, or more accurately ovaries, are transformed into fruit in a process known as fruit set. In fruit crops, adequate fruit set is key to attaining high yields for economically profitable production. However, the proportion of flowers that set fruit on a single inflorescence or on a whole plant varies widely. Fruit set in perennial crops such as grapevines can be reduced for many reasons including, for example, abnormal flower development, water or nutrient deficit or excess, pathogen infection, physical injury, insufficient sunlight, or temperatures outside the optimal range (May, 2004; Keller, 2020). Supply of photosynthates, either *de novo* assimilated in the leaves or remobilized from stored reserves in the perennial organs, is often thought to be limiting for fruit set (Vasconcelos et al., 2009; Ruan et al., 2012). In grape flowers, eggs that are not fertilized within 3–4 days after anthesis will degenerate (Kassemeyer and Staudt, 1981). Successful fertilization requires the sequential events of pollination, pollen germination, and pollen tube growth. In grapevines, pollen germination and pollen tube growth are maximal in the temperature range 25°C–30°C, and temperatures <10°C and >35°C inhibit germination, but even temperatures <15°C slow pollen tube growth too much to permit fertilization before eggs degenerate (Staudt, 1982). Excessively high temperatures also decrease pollen tube growth by reducing auxin production in the pistil (Zhu et al., 2021). Therefore, poor fruit set may result from slow pollen tube growth under both cool and hot conditions.

Earlier work on temperature effects on grapevine reproductive behavior was typically conducted under controlled-environment conditions, where whole plants were exposed to different temperature regimes. For example, in a growth chamber study conducted with small, fruiting cuttings, vines exposed to day/night temperatures of 14/9°C from 4 days after budbreak failed to fully differentiate their inflorescences and did not set fruit (Buttrose and Hale, 1973). Though the time to anthesis decreased as the temperature increased, fruit set was highest in vines exposed to 20/15°C and decreased at higher temperatures down to zero at 38/33°C. In a similar experiment, flowering was delayed and fruit set was lower in fruiting cuttings exposed to 12/9°C for 1 week during early bloom compared with vines held at 17/14°C or 25/20°C (Ebadi et al., 1995a). A more recent growth-chamber study with fruiting cuttings concluded that temperature did not influence bloom phenology, but temperatures of 37/31°C (day/night) and higher induced flower abortion (Merrill et al., 2020). Similarly, fruit set decreased in pot-grown grapevines as the growth chamber day temperature during the bloom period increased from 25°C to 40°C, with all night temperatures set at 20°C (Kliewer, 1977). Exposure of pot-grown vines in growth chambers to 40/25°C (day/night) for 4 days during bloom led to complete flower abortion, but the same treatment imposed at fruit set did not alter reproductive growth compared with the 25/15°C control (Greer and Weston, 2010). However, because the growth-chamber approach simultaneously manipulates both sink and source temperatures, it cannot answer the question whether any differences in fruit set or subsequent berry growth arise as a consequence of temperature-induced differences in sink strength of flowers or berries. Sink strength, defined as sink size × sink activity, describes the capacity of a plant organ to use imported resources for growth, metabolism, or storage (Yu et al., 2015).

Previously, we demonstrated that brief periods of shoot apex (i.e., sink) temperature differences during the budswell, budbreak, and early post-budbreak period of grapevines induce persistent, season-long differences in shoot growth and architecture, and reproductive growth (Keller et al., 2010; Keller and Tarara, 2010). At least some of the temperature-induced differences in shoot growth can be attributed to differences in vascular tissue differentiation in the emerging shoots (Galat Giorgi et al., 2020). Here we tested the effects of differences in inflorescence temperature during the bloom period leading up to fruit set. Our main goal was to determine whether differences in inflorescence temperature, rather than whole-plant temperature, were associated with differences in the degree of fruit set and other reproductive traits. We used a forced-convection, free-air cooling and heating system (Tarara et al., 2000) to manipulate the inflorescence temperature of field-grown grapevines without altering the temperature of nearby source leaves or other plant organs. We hypothesized that cooling an inflorescence would reduce its sink strength and heating an inflorescence would enhance its sink strength. Consequently, we expected the cooled inflorescences to show slower development and lower fruit set. But because lower fruit set results in fewer berries per cluster, it was unclear whether a temporary reduction in sink strength at the onset of berry growth would lead to smaller berries by the time of harvest, or whether there would be compensatory berry growth leading to larger berries. Compensatory berry growth was previously observed with the same grape cultivar grown in the same region in which this experiment was conducted, but that study did not test temperature-induced differences in berry numbers (Keller et al., 2008). In addition, sinks and sources are linked through feedback mechanisms, and a decrease in sink activity might result in sugar accumulation and thus lower photosynthesis in source leaves (Körner, 2003; Yu et al., 2015). Assuming that an alteration in the sink strength would lead to a modification in source activity, we also hypothesized that inflorescence cooling would result in a transient decrease in leaf photosynthesis or an increase in shoot growth. We worked with Cabernet Sauvignon (*Vitis vinifera* L.), which is the world's most widely planted wine grape cultivar, and its reproductive performance is thought not to be especially sensitive to unfavorable environmental conditions (May, 2004). We reasoned that if temperature effects were significant in this cultivar, they would likely also be significant in other, more responsive cultivars.

Materials and methods

Vineyard site and treatments

The experiment was conducted in 2004 in a vineyard block of own-rooted Cabernet Sauvignon grapevines planted in 1983 at the

Irrigated Agriculture Research and Extension Center near Prosser, WA, United States (46.25°N, 119.73°W, elevation 270 m a.s.l., annual precipitation ~200 mm). The soil is a > 4 m deep Warden fine sandy loam with volumetric water content (θ_v) of ~25% (v/v) at field capacity and ~8% at permanent wilting point (Evans et al., 1993). Vines were planted at 1.8 m within rows and 3 m between rows oriented north–south on a 3% southwest slope. They were trained to bilateral cordons at 1.2 m and winter-pruned to 35–40 buds per vine. A single inflorescence was retained on shoots that were included in the experiment, but no other canopy manipulations were carried out during the growing season. The vineyard was drip-irrigated using regulated deficit irrigation to limit shoot growth after fruit set as described previously (Keller et al., 2005, 2008).

The temperature of inflorescences was manipulated with a forced-convection, free-air cooling and heating system (Supplementary Figure 1). The system was described by Tarara et al. (2000) and modified as specified in Keller and Tarara (2010). It permits continuous control of target-tissue temperatures without altering solar radiation. Heated or chilled air was delivered directly to individual inflorescences. Four type-T thermocouples (copper-constantan, 0.13-mm diameter, 2-mm junctions), wired in parallel, were embedded in mock flowers made of silicon and wrapped within each inflorescence for temperature measurements (Figure 1A). Control of the cooling/heating system and data acquisition and storage followed the procedures described previously (Keller and Tarara, 2010). Three temperature regimes were applied during the bloom period: ambient, cool (7.5°C below ambient), and warm (7.5°C above ambient). In addition, a convective control (blower without heating or cooling) was included to account for possible effects due to air movement. To prevent heat or chilling injury, the device was programmed to pause at temperatures >40°C or <10°C. Treatments were randomly applied to eight pre-selected inflorescences ($n = 8$), each on a different shoot. Visually uniform (i.e., similar size and architecture) inflorescences were selected after the flowers were fully differentiated prior to the beginning of anthesis. Only inflorescences on the east side of the canopy were selected to minimize sunburn injury on the berries during their subsequent development. Treatments were applied from the beginning of anthesis or cap fall, determined visually as the time of loosening of the first calyptrae, until fruit set, determined visually as the time of initial berry enlargement (Coombe, 1995). While all treatments started on the same day, the duration of temperature control varied as a consequence of phenology-based termination of treatments.

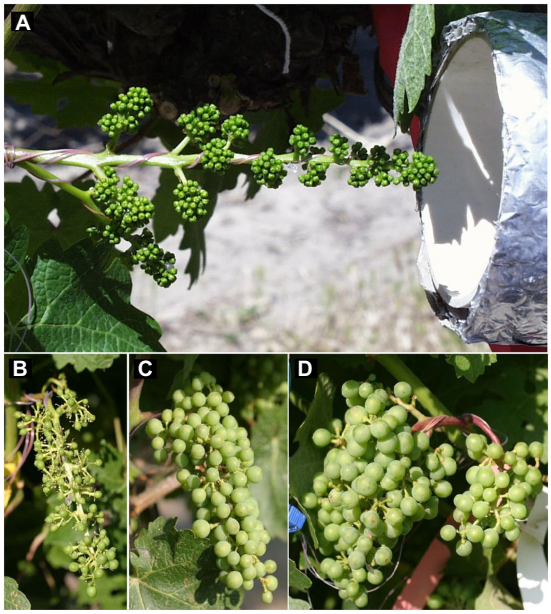

FIGURE 1
(A) Thermocouples embedded in silicon mock flowers and wrapped within an inflorescence, and outlet of cooling tube connected to free-air cooling/heating device used to manipulate inflorescence temperatures during the bloom period of field-grown grapevines. **(B)** Cabernet Sauvignon grape cluster after fruit set following cooling, **(C)** ambient conditions, or **(D)** heating of the inflorescence during the bloom period. Photos in **(B–D)** were taken on the same day immediately after the cooling treatment was terminated.

Environmental data and plant measurements

The θ_v under the vines was measured weekly using a neutron probe (503 DR Hydroprobe; CPN International, Pachero, CA, United States), with six PVC access tubes installed to a depth of 1.2 m both under drip emitters and equidistant between emitters. In addition to the temperature measurements collected by the cooling/heating system, air temperature within and above the canopy, and global irradiance above the canopy, were measured as described elsewhere (Keller et al., 2010; Keller and Tarara, 2010). Growing degree days during the bloom period were calculated from daily minimum and maximum temperatures, applying the standard base temperature for grapevines of 10°C (GDD_{10}; Keller, 2020), as well as a base temperature of 15°C (GDD_{15}) below which cap fall is thought to cease (May, 2004).

Phenological stages were monitored at least weekly according to the modified E-L system (Coombe, 1995). The length of each treatment shoot was measured weekly until shoot growth ceased, using a tape measure. Numbers of main leaves and of axillary (lateral) shoots and leaves were recorded every time shoot length was measured. Main shoot leaf area was estimated from measurements of midrib length (L, in cm) of each leaf, which were converted to leaf area (A_m, in cm^2) using a regression equation ($A_m = 3.44L + 0.91L^2$, $r = 0.96$, $p < 0.001$) developed from destructive measurements of 200 additional leaves, using a leaf area meter (model LI3100, LiCor, Lincoln, NE, United States). Lateral shoot leaf area (A_l, in cm^2) was estimated from lateral leaf number ($A_l = 31.23n + 2.49n^2$, $r = 0.94$, $p < 0.001$). The extent of shoot periderm formation was estimated as the number of brown internodes at the beginning of fruit ripening (termed veraison and

defined as 50% of berries having changed color from green to red or blue) and at harvest (Keller and Tarara, 2010).

The length of each treated fruit cluster from its tip to its attachment to the shoot was measured every time shoot length was measured. Flowers were counted using the bagging method, in which inflorescences are enclosed during the bloom period with a fine mesh bag to collect the abscised calyptrae (Kliewer, 1977; Keller et al., 2001; Dry et al., 2010). The abscised calyptrae were weighed and divided by flower counts as a proxy for average flower size (Keller et al., 2010). Some flowers were aborted before they opened and were counted separately. All treated clusters were harvested on the same day once the vineyard exceeded an overall total soluble solids (TSS) target of 24°Brix. The berries of each cluster were counted and weighed, and the flower and berry numbers were used to determine the percentage fruit set. Live green ovaries were excluded from the berry count as suggested by Dry et al. (2010). Additionally, 10 berries per cluster were weighed individually, and their seeds were counted and dried at 65°C for 48 h. The dry seeds were weighed and immersed in water to count "sinkers" and "floaters;" the latter look similar to fully developed seeds ("sinkers") but are hollow following abortion of their embryo and deterioration of the endosperm several weeks after fruit set (Ebadi et al., 1995a, 1996). Up to 100 berries were collected from each treated shoot to measure fruit TSS, titratable acidity (TA), pH, and color density (i.e., red color due to anthocyanins) as described elsewhere (Spayd et al., 2002). The amount of sugar per berry (sugar content) was estimated from berry weight and TSS.

Leaf gas exchange was measured weekly from the onset of the temperature treatments until 1 week after the cooling treatment was terminated for a total of six measurement dates. Measurements were taken under ambient conditions between 09:00 and 11:00 local standard time, using a CIRAS-2 infrared gas analyzer with a flow rate of 200 ml min^{-1} and a PLC6(U) broad-leaf cuvette (PP Systems, Hertfordshire, United Kingdom) on the leaf above the fruit cluster, which was fully exposed to sunlight (photosynthetic photon flux >1,000 µmol $m^{-2} s^{-1}$) but not to the temperature treatments. Leaf disks were collected 11 days into treatment application from the leaves that were used for gas exchange measurements. Six 0.283-cm^2 disks were collected from each leaf at sunset, frozen in liquid nitrogen, and stored at −80°C. Non-structural carbohydrates (soluble sugars and starch) were extracted and analyzed as described elsewhere (Halldorson and Keller, 2018).

Statistical analysis

Data were analyzed using Statistica version 14 (TIBCO Software, Palo Alto, CA, United States). Effects of temperature treatments and changes over time were analyzed by ANOVA; a repeated measures design was used for temporal changes. Duncan's new multiple range test was used for *post-hoc* means comparisons when treatment effects were significant. The pH values were converted to H^+ concentrations for data analysis and means were converted back to pH for presentation. Each treated cluster was considered a biological replicate ($n = 8$), and means of the 10-berry samples were used for analysis of the seed data. Results are reported as means ± standard error (SE) unless otherwise specified. Associations between key response variables were tested using Pearson product-moment correlation analysis. Where appropriate, actual p values rather than just significance levels are provided.

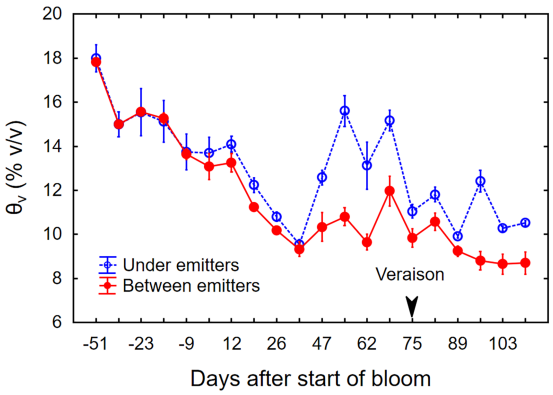

FIGURE 2
Changes in soil moisture (θ_v) from budbreak through harvest of field-grown, drip-irrigated Cabernet Sauvignon grapevines in southeastern Washington. Data represent the average (±SE) of three separate plants.

Results

Environment and phenology

At the beginning of the growing season, θ_v under the vines was ~18% (v/v) averaged over the top 90 cm of soil (Figure 2). The θ_v was maintained near 14% during bloom and then allowed to dry down to 9%–10% by mid-July, at which point the berries had reached about pea size and shoot growth slowed. Supplemental drip irrigation then maintained θ_v at 10%–12% between drip emitters and up to 16% beneath emitters through veraison, and near 9% between emitters during fruit ripening. During the experiment, the weather was mostly sunny; global irradiance varied between 0.9 and 1.1 kW m^{-2} at midday, and ambient temperatures ranged from 5°C during the coldest night to 35°C during the warmest day. The grapevine canopy intensified the diurnal temperature fluctuation. Daily minimum temperatures (T_{min}) inside the canopy were consistently 1°C–2°C lower, and daily maximum temperatures (T_{max}) were 1°C–2°C higher than ambient temperatures above the canopy (Supplementary Figure 2).

Temperature treatments were applied to inflorescences from the beginning of bloom through fruit set, a period that ranged from 10 days (heated) to 24 days (cooled). Thus heating shortened, and cooling lengthened, the bloom period relative to ambient conditions (Table 1). The treatments generated three distinct

TABLE 1 Effect of inflorescence temperature regimes generated using a free-air cooling/heating device during the bloom period on bloom duration, average daily maximum (T_{max}), minimum (T_{min}), and mean (T_{mean}) inflorescence temperatures, accumulated growing degree days with base 10°C (GDD_{10}) or 15°C (GDD_{15}), and time from either first bloom or fruit set to start of ripening (veraison) in field-grown Cabernet Sauvignon grapevines in southeastern Washington.

Treatment	Cooled	Ambient[b]	Blower	Heated	*p*
Bloom duration (d)	24 ± 2.2 a[a]	17 ± 1.1 b	16 ± 1.1 b	10 ± 0.5 c	<0.001
T_{max} (°C)	24.2 ± 1.5 c	30.3 ± 1.5 ab	28.7 ± 2.0 b	32.1 ± 2.3 a	<0.001
T_{min} (°C)	9.2 ± 0.7 c	10.9 ± 1.3 bc	12.8 ± 1.5 b	14.1 ± 2.0 a	<0.001
T_{mean} (°C)	16.0 ± 1.0 c	21.0 ± 1.2 b	20.2 ± 1.5 b	23.4 ± 1.5 a	<0.001
GDD_{10} (°C)	228 b	263 a	251 a	170 c	<0.001
GDD_{15} (°C)	58 c	133 a	121 a	105 b	<0.001
Bloom to veraison (d)	86 ± 1.1 a	73 ± 0.9 b	73 ± 0.8 b	69 ± 0.4 c	<0.001
Fruit set to veraison (d)	62 ± 1.6 a	56 ± 1.2 b	57 ± 0.8 b	59 ± 0.8 ab	0.009

[a]Means (±SE) within rows followed by different letters differ significantly ($p < 0.05$, $n = 8$) by Duncan's new multiple range test.
[b]Ambient temperatures were averaged for the entire 34-day treatment period (DOY 155–189) because ambient was used to calculate the set point temperatures for cooled and heated treatments.

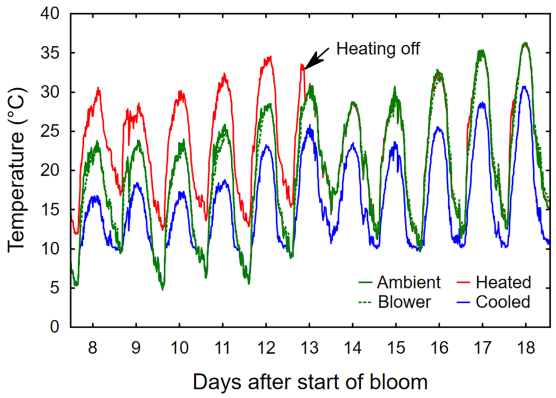

FIGURE 3
Representative example of temperature profiles of grape inflorescences whose temperature was manipulated, using a free-air cooling/heating device, during the bloom period in the field. Each line represents the average of eight independent inflorescences.

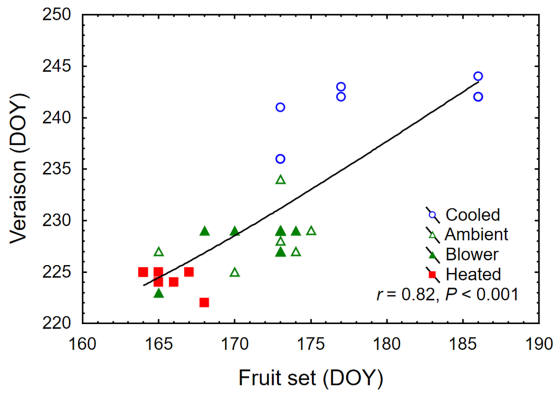

FIGURE 4
Association between day of year (DOY) of fruit set and veraison of grape clusters whose temperature was manipulated, using a free-air cooling/heating device, during the bloom period in the field. Each treatment was applied to eight independent inflorescences (n =32).

diurnal temperature ranges with a difference in average T_{min} of 4.9°C and T_{max} of 7.9°C between cooled and heated inflorescences (Table 1). During the 13-day heating period, the difference in T_{max} was close to the target 15°C, but that in T_{min} was lower due to the 10°C treatment cutoff point below which the cooled treatment tracked the ambient control (Figure 3). The temperature of inflorescences in the heating regime peaked at 39°C on 2 days, and the lowest absolute temperature reached in the ambient and cooling regimes was 4.5°C, also on two occasions. Because of generally warmer weather following termination of the heating treatment, the ambient inflorescences subsequently experienced similar temperatures as had the heated inflorescences, and the cooled inflorescences experienced similar temperatures as had the ambient inflorescences (Figure 3). The temperatures of the convective control (blower) were similar to ambient temperatures. During their respective treatment (i.e., bloom) period, heated inflorescences accumulated less GDD_{10} but more GDD_{15} than did cooled inflorescences, while ambient clusters accumulated the most GDD irrespective of the applied base temperature (Table 1). On a daily basis, cooled inflorescences accumulated 6.7 GDD_{10} and 1.7 GDD_{15} and heated inflorescences accumulated 13.1 GDD_{10} and 8.1 GDD_{15} per day ($p < 0.001$), while the two controls were intermediate at 9.5 GDD_{10} and 4.7 GDD_{15}. The differences in phenology that arose from the application of the temperature treatments during the bloom period persisted through veraison in mid-August. Compared with ambient and blower control clusters, inflorescence cooling delayed veraison by 13 days and heating advanced veraison by 4 days (Table 1). Moreover, cooling increased, and heating decreased, the variation in the time required to reach subsequent phenological stages. Across treatments, there was a linear relationship between the time of fruit set and the time of veraison (Figure 4).

TABLE 2 Effect of inflorescence temperature regimes generated using a free-air cooling/heating device during the bloom period on reproductive growth and harvest fruit composition of field-grown Cabernet Sauvignon grapevines in southeastern Washington.

Treatment	Cooled	Ambient	Blower	Heated	*p*
Flowers per inflorescence	470 ± 60	424 ± 60	417 ± 53	421 ± 48	0.89
Flower size (mg)[a]	0.39 ± 0.01	0.40 ± 0.02	0.37 ± 0.02	0.36 ± 0.01	0.21
Fruit set (%)	20 ± 3 b[b]	35 ± 5 a	34 ± 3 a	31 ± 2 a	0.02
Berries per cluster	81 ± 8 b	135 ± 16 a	136 ± 17 a	126 ± 14 a	0.04
Berry weight (g)	0.79 ± 0.04 b	0.91 ± 0.03 a	0.94 ± 0.06 a	0.96 ± 0.03 a	0.03
Seeds per berry	1.3 ± 0.05 b	1.4 ± 0.05 ab	1.4 ± 0.06 a	1.2 ± 0.04 b	0.03
Floating seeds (%)	34 ± 8	31 ± 5	35 ± 5	34 ± 4	0.96
Total seed weight (mg)	27.9 ± 1.6 b	33.7 ± 1.4 a	34.5 ± 2.0 a	30.3 ± 0.2 ab	0.01
Total soluble solids (°Brix)	23.6 ± 0.2	24.2 ± 0.5	24.3 ± 0.4	24.8 ± 0.3	0.19
Sugar per berry (mg)	185 ± 8 b[b]	221 ± 9 a	229 ± 15 a	237 ± 7 a	0.01
Titratable acidity ($g\,L^{-1}$)	7.1 ± 0.3 a	5.6 ± 0.3 ab	6.5 ± 0.7 ab	5.3 ± 0.1 b	0.03
pH	3.41 ± 0.02 b	3.58 ± 0.04 a	3.59 ± 0.07 a	3.63 ± 0.02 a	0.01
Color density ($AU\,ml^{-1}$)	14.7 ± 1.7	14.2 ± 1.4	13.3 ± 1.9	15.1 ± 1.1	0.81

Flowers were counted after bloom, all other data were collected at fruit harvest.

[a]Average dry weight of the flower calyptrae.

[b]Means (±SE) within rows followed by different letters differ significantly ($p < 0.05$, $n = 8$) by Duncan's new multiple range test; absence of letters indicates no significant effect.

Reproductive growth

The inflorescence temperature regimes significantly altered reproductive growth (Figures 1B–D). While the treatments did not affect the average calyptra weight (0.38 ± 0.07 mg; $p = 0.21$), the number of aborted unopened flowers (5.3 ± 1.6; $p = 0.59$) or their percentage (1.4 ± 0.5%; $p = 0.61$), and the number of flowers per inflorescence (433 ± 27; $p = 0.89$), cooling decreased fruit set percentage and the final berry number and weight (Table 2). Heating, however, did not impact these reproductive traits compared with ambient temperatures, which is consistent with the general warming trend during the experiment (Figure 3). On average, 71 ± 3% of the berries had a single seed, 28 ± 3% had two seeds, and 1 ± 1% had three seeds; we found no berries with four seeds and only a single seedless berry. Though there was no clear treatment effect on the number of seeds per berry and no effect on the proportions of sinker and floater seeds (66 vs. 34 ± 3%), inflorescence cooling resulted in the lowest seed weight per berry (Table 2). There also was a positive correlation between fruit set and seed weight (Figure 5A), as well as between seed weight and berry weight (Figure 5B) and between seed number and berry weight (Figure 5C). The latter association illustrates how inflorescence cooling decreased berry weight independently of seed number. Across treatments, fruit set decreased (Figure 6A), and both the number of berries per cluster (Figure 6B) and the rachis length at harvest (Figure 6C) increased as the number of flowers per inflorescence increased. Irrespective of the temperature manipulation treatment applied during bloom, an ~4.5-fold variation in flower number was associated with a 2-fold variation in rachis length. Unlike the flower number, however, the berry number per cluster did not correlate with rachis length ($r = 0.31$, $p = 0.08$), indicating that rachis length was determined before fruit set and that bigger clusters were more compact clusters.

Though there was no significant treatment effect on berry TSS (i.e., sugar concentration) and color density at harvest, cooling of inflorescences decreased the amount of sugar per berry (i.e., sugar content) and the pH (Table 2). The berries that formed on cooled inflorescences also had higher TA than the berries from heated inflorescences. From veraison to harvest, the berries from all treatments accumulated sugar at similar rates (3.3 ± 0.1 $mg\,d^{-1}$; $p = 0.08$), but the final sugar content correlated inversely with the date of veraison (Figure 7A). Also, there was a positive correlation between berry number per cluster and final sugar content (Figure 7B), and no correlation between the sugar accumulation rate and the leaf area per unit berry weight ($r = 0.07$, $p = 0.70$). The latter averaged 40 ± 4 $cm^2\,g^{-1}$ across temperature regimes but was higher in the cooling treatment (65 ± 11 $cm^2\ g^{-1}$) than in the other treatments (33 ± 3 $cm^2\,g^{-1}$; $p = 0.006$). Therefore, the lower sugar content of the berries from cooled inflorescences was mostly a result of their shorter ripening period due to delayed veraison, rather than of source limitation. Moreover, as the seed weight per berry increased, so did the sugar content (Figure 7C) but not the sugar concentration ($r = 0.20$, $p = 0.26$). There was a positive correlation between TSS and pH (Figure 8A) and negative correlations between TSS and TA (Figure 8B) and between TA and pH (Figure 8C), all of which were mostly driven by the impact of the temperature regimes applied during bloom (Table 2).

Vegetative growth

Over the first 4 weeks after bloom, i.e., before shoot growth became very slow due to the declining θ_v, the average shoot growth rate across treatments was 1.6 ± 0.1 $cm\,d^{-1}$ and the average shoot leaf area expansion rate was 66 ± 3 $cm^2\,d^{-1}$. Many shoot tips

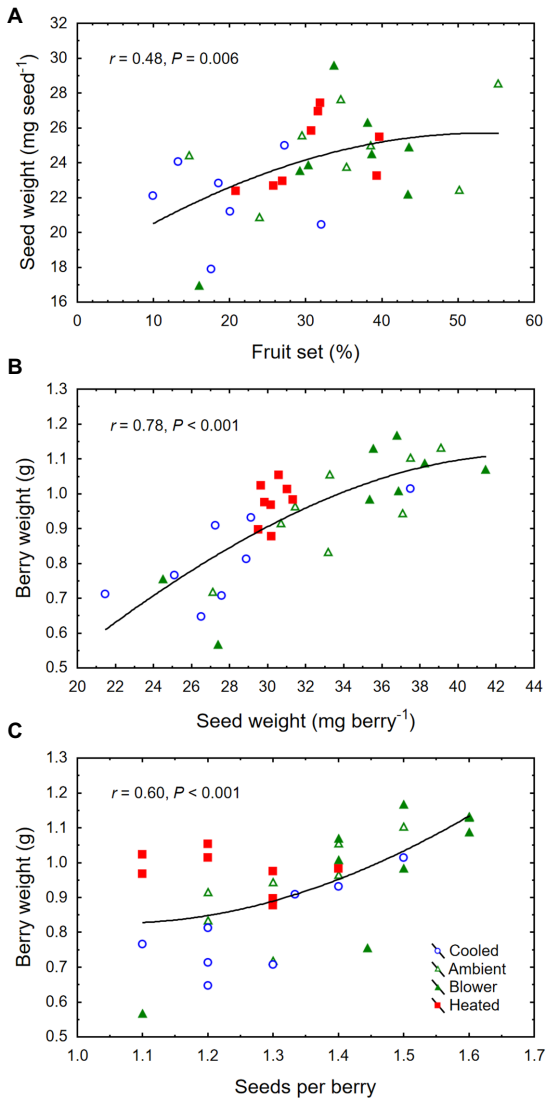

FIGURE 5
(A) Associations between fruit set and mean weight per seed, **(B)** seed weight per berry and berry weight, and **(C)** number of seeds per berry and berry weight at harvest of grape clusters whose temperature was manipulated, using a free-air cooling/heating device, during the bloom period in the field. Each treatment was applied to eight independent inflorescences (n =32).

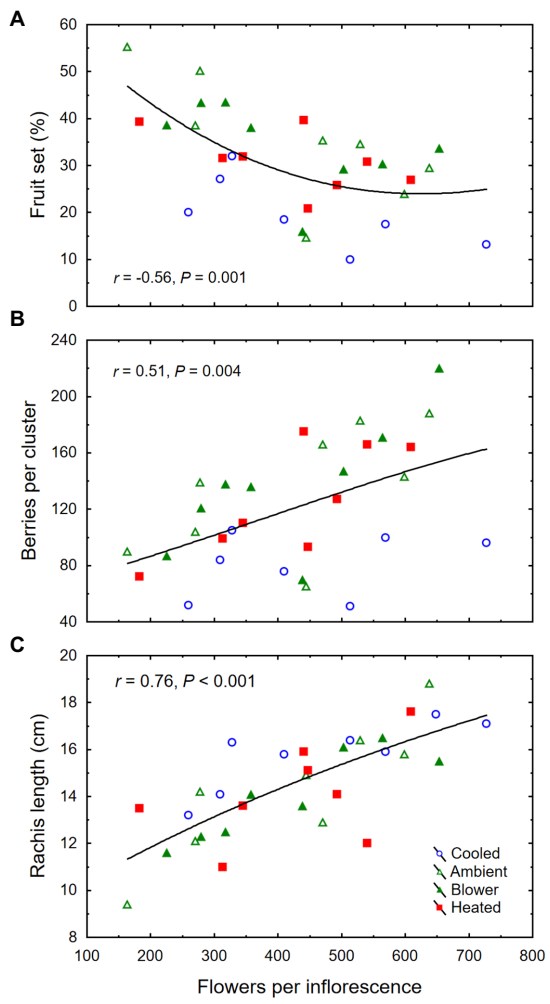

FIGURE 6
(A) Associations between number of flowers per inflorescence and fruit set, **(B)** number of berries per cluster, and **(C)** rachis length at harvest of grape clusters whose temperature was manipulated, using a free-air cooling/heating device, during the bloom period in the field. Each treatment was applied to eight independent inflorescences (n =32).

died by veraison, and virtually no shoot growth occurred during the berry ripening period. While the leaf area comprised by lateral leaves (i.e., leaves that formed on shoots growing from axillary or prompt buds) made up 23% of the total leaf area at bloom time, this proportion increased to 37% by veraison and remained constant thereafter. Although inflorescence cooling retarded, and heating accelerated, bloom time and berry development compared with ambient conditions, the inflorescence temperature regimes did not impact shoot growth and leaf expansion (Table 3). For instance, both the lateral leaf appearance rate and the shoot leaf area expansion rate were linear functions of the shoot growth rate (r=0.81 and r=0.90, respectively, p<0.001), but all measures of shoot vigor remained unaffected by the temperature regimes. The variation in vegetative growth was greater within than between temperature regimes. Indeed, both the lowest and the highest absolute values of shoot growth rate were found in the heating treatment. Furthermore, none of the reproductive traits correlated with any of the vegetative traits measured here.

At veraison, the shoots with cooled inflorescences had almost twice as many brown internodes as those from the other treatments (Table 3). Because the berries from cooled inflorescences took longer to reach veraison, their shoots had more time to form brown periderm, indicating that periderm formation occurred independently of berry ripening. By harvest, however, the other shoots had caught up and the difference in periderm formation disappeared. Pruning weight measurements in winter revealed no differences in dormant cane weight among

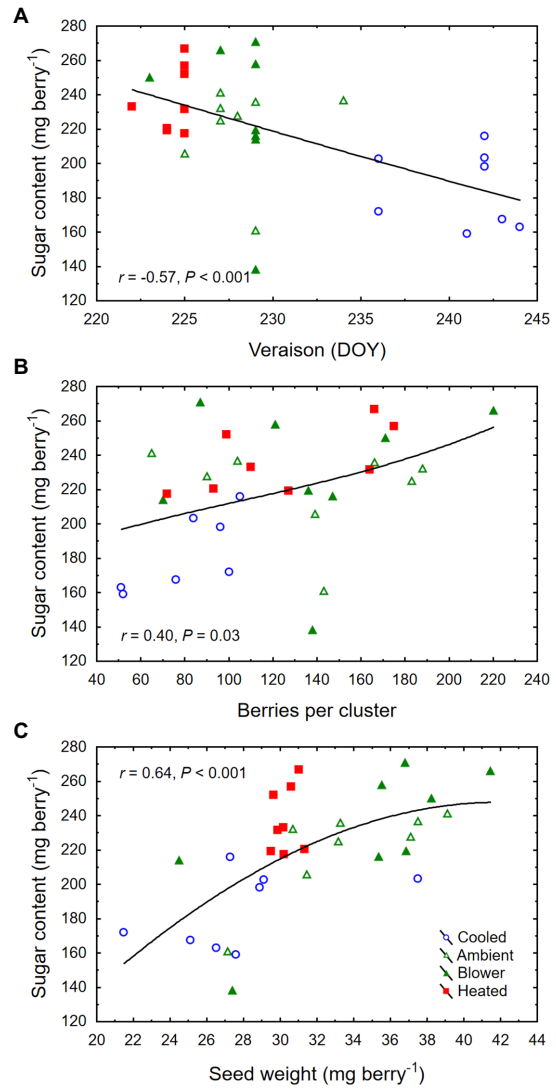

FIGURE 7
(A) Associations between day of year (DOY) of veraison and sugar content per berry, **(B)** number of berries per cluster and sugar content, and **(C)** seed weight per berry and sugar content at harvest of grape clusters whose temperature was manipulated, using a free-air cooling/heating device, during the bloom period in the field. Each treatment was applied to eight independent inflorescences (n =32).

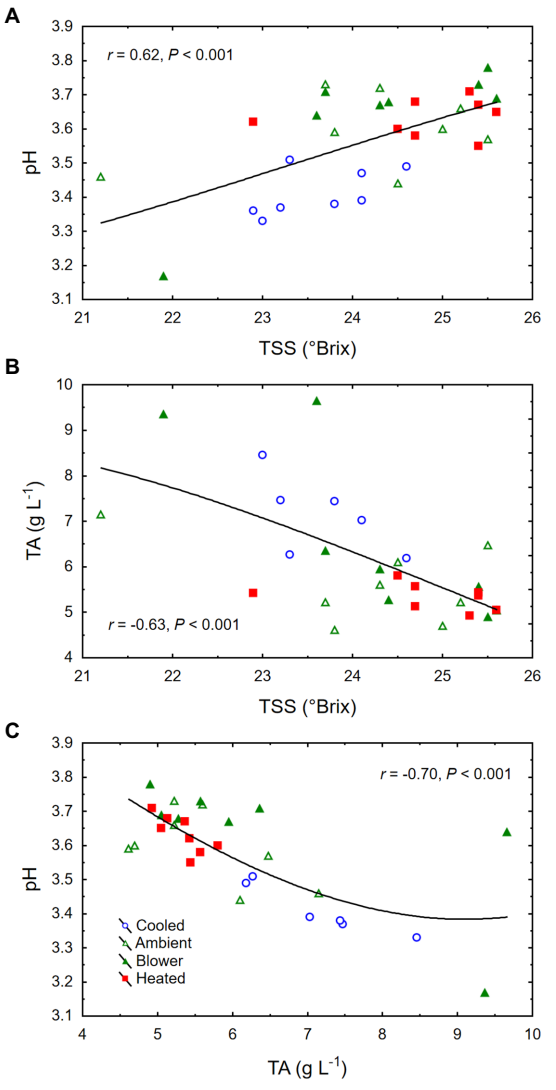

FIGURE 8
(A) Associations between berry total soluble solids (TSS) and pH, **(B)** TSS and titratable acidity (TA), and **(C)** TA and pH at harvest of grape clusters whose temperature was manipulated, using a free-air cooling/heating device, during the bloom period in the field. Each treatment was applied to eight independent inflorescences (n =32).

treatments (Table 3). The cane weight correlated strongly with the shoot length at veraison (r=0.92, p<0.001).

Leaf gas exchange and non-structural carbohydrates

We did not detect a consistent effect of the inflorescence temperature regimes on gas exchange of the leaf above the treated inflorescence. While the temperature treatments were being deployed, leaf stomatal conductance (g_s) tended to be higher in the heating regime than in the blower control (Figure 9A). This difference was not caused by changes in leaf temperatures (T_{leaf}) induced by the inflorescence treatments; T_{leaf} was similar across all temperature regimes (p=0.39; Figure 9B). Moreover, neither the heating treatment nor the blower control differed from the ambient control and the cooling regime, and although the overall temperature effect on g_s was significant (p=0.008), this did not apply to any individual day. Despite the differences in g_s, net photosynthesis (P_n) did not respond to the temperature regimes (p=0.49; Figure 9C). The treatments also did not affect transpiration rates (p=0.11; Figure 9D). No significant differences were found after the treatments were terminated, and g_s and P_n

TABLE 3 Effect of inflorescence temperature regimes generated using a free-air cooling/heating device during the bloom period on shoot growth and maturation (periderm formation), leaf area expansion, leaf non-structural carbohydrates (NSC), and dormant cane weight of field-grown Cabernet Sauvignon grapevines in southeastern Washington.

Treatment	Cooled	Ambient	Blower	Heated	*p*
Shoot growth rate (cm d^{-1})	1.7 ± 0.1	1.6 ± 0.2	1.4 ± 0.2	1.7 ± 0.3	0.79
Leaf area expansion rate (cm^2 d^{-1})	64 ± 6	65 ± 8	66 ± 5	69 ± 9	0.97
Leaf NSC (mg g^{-1} fresh weight)					
Starch	36.2 ± 3.1	35.4 ± 3.2	35.8 ± 1.6	31.0 ± 1.7	0.41
Soluble sugars	6.6 ± 0.7	4.8 ± 1.0	5.6 ± 1.0	7.1 ± 1.3	0.41
Shoot length (cm)[a]					
Bloom	84 ± 7	80 ± 4	72 ± 4	87 ± 7	0.32
Veraison	133 ± 10	128 ± 11	115 ± 10	143 ± 15	0.39
Main shoot leaf area (cm^2)					
Bloom	1,264 ± 126	1,157 ± 68	977 ± 39	1,250 ± 117	0.14
Veraison	2,408 ± 212	2,413 ± 202	2,109 ± 148	2,600 ± 313	0.50
Lateral shoot leaf area (cm^2)					
Bloom	398 ± 97	353 ± 59	275 ± 42	352 ± 46	0.61
Veraison	1,531 ± 209	1,336 ± 234	1,394 ± 188	1,345 ± 217	0.91
Periderm (brown internodes)					
Veraison	15 ± 0.8 a[b]	8 ± 1.2 b	8 ± 1.0 b	9 ± 0.2 b	<0.001
Harvest	17 ± 1.1	15 ± 1.6	15 ± 1.5	16 ± 1.7	0.79
Dormant cane weight (g)	47.8 ± 9.5	40.7 ± 7.7	37.2 ± 5.4	55.7 ± 13.6	0.54

[a]All changes over time were tested using a repeated measures design and were significant at $p < 0.001$; the treatment × time interaction was only significant for periderm ($p = 0.006$).
[b]Means (±SE) within rows followed by different letters differ significantly ($p < 0.05$, $n = 8$) by Duncan's new multiple range test; absence of letters indicates no significant effect.

decreased in response to the declining θ_v. Whereas E was closely correlated with g_s ($r = 0.83$, $p < 0.001$), the correlation between P_n and g_s, though significant, was quite low ($r = 0.23$, $p = 0.002$). Leaf non-structural carbohydrates at sunset were dominated by starch (79.7 ± 1.4%), followed by glucose (15.1 ± 0.5%), fructose (3.0 ± 0.2%), and sucrose (2.3 ± 0.4%). Neither starch nor soluble sugars differed among inflorescence temperature regimes (Table 3). There was no correlation between starch and sugar concentrations ($r = -0.03$, $p = 0.86$). There also was no correlation between P_n and either leaf starch ($r = -0.17$, $p = 0.37$) or soluble sugars ($r = 0.08$, $p = 0.67$).

Discussion

The present study, conducted in a vineyard in arid southeastern Washington, United States, found that the temperature of Cabernet Sauvignon inflorescences during the bloom period may alter flowering phenology, fruit set, and subsequent cluster development independently of the temperature of the canopy. Using targeted manipulation of inflorescence temperatures in canopies exposed to ambient temperatures, we found that warm microclimatic conditions were favorable for fruit set and seed development, which in turn advanced berry development and increased final berry weight. Flowers and berries on cooled inflorescences reached the subsequent phenological stages significantly later than those on heated inflorescences and produced smaller berries. Thus, manipulating the inflorescence temperature not only altered the duration of the bloom period (i.e., time to fruit set) but also had a lasting effect on berry development after fruit set. The time from fruit set to veraison varied relatively little among treatments, suggesting that differences in later phenology arose mostly from differences in the duration of bloom. By contrast, the temperature treatments had no effect on the number and size of the flowers, since the treatments were applied only after the flowers had been fully differentiated (Keller, 2020).

Cooling inflorescences to an average T_{max}/T_{min} of ~24/9°C not only lengthened the bloom period by 7 days but also reduced fruit set. However, despite the lower number of berries per cluster resulting from reduced fruit set, those clusters also had smaller berries with lighter seeds and lower sugar content at harvest, indicating that there was no compensatory increase in berry growth or sugar accumulation. In a growth chamber study, fruiting cuttings exposed to 14/9°C (day/night) failed to fully differentiate their inflorescences and did not set fruit (Buttrose and Hale, 1973). Fruit set in that study was highest in plantlets exposed to 20/15°C and decreased at higher temperatures down to zero at 38/33°C. Elsewhere, fruit set, seed number, and subsequent cell division and berry growth were highest when vines were held during bloom at 25/20°C, and decreased at higher temperatures (Kliewer, 1977). Another growth chamber study found no effect on fruit set but a reduction in seed number per berry in vines grown during bloom at 15/10°C compared with 25/10°C or 25/20°C (Ewart and Kliewer, 1977). In our study, inflorescence heating to an average T_{max}/T_{min} of ~32/14°C shortened the bloom period by 7 days but did not reduce fruit set. Except in the cooled inflorescences, fruit set in our study was

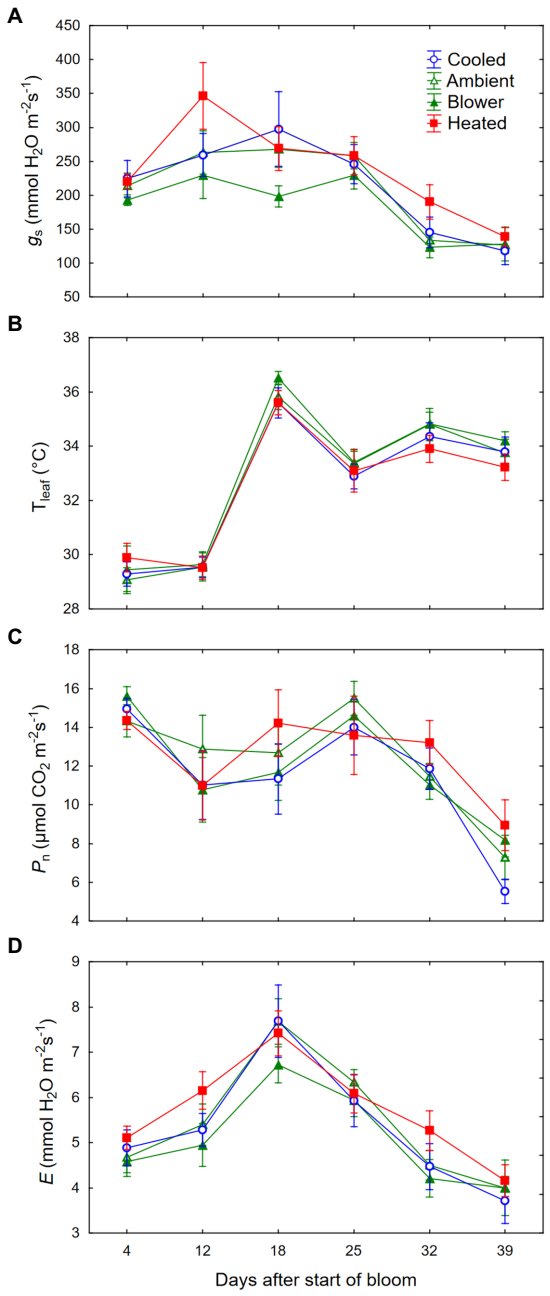

FIGURE 9
(A) Changes in leaf stomatal conductance (g_s), **(B)** leaf temperature (T_{leaf}), **(C)** photosynthesis (P_n), and **(D)** transpiration (E) of grapevine leaves above inflorescences whose temperature was manipulated, using a free-air cooling/heating device, during the bloom period in the field. Each treatment was applied to eight independent inflorescences.

similar to that observed previously for Cabernet Sauvignon in the same vineyard (Keller et al., 2010) and in different Australian wine regions but lower than in eight of the 10 cultivars tested in the Australian study (Dry et al., 2010). Differences in reproductive performance and environmental plasticity among grape cultivars is one possibility for differences among experiments. However, contrary to the cooling treatment, our heating treatment also decreased the variability in subsequent seed and berry development, suggesting that the high-temperature regime used here was close to the optimum for reproductive growth of Cabernet Sauvignon.

The fact that our experiment was conducted with a single grape cultivar in a single season limits the conclusions that can be drawn from our results. For example, this study could not identify an upper-temperature limit during bloom time, likely because the ambient T_{max} of inflorescences exceeded 35°C on only three consecutive days (peaking at 36.3°C) starting 4 days after the heating regime was terminated. A recent review of high-temperature effects on plant performance concluded that shortening the time to fruit set due to moderately high temperatures reduces seed and fruit weight (Zhu et al., 2021). Evidently, the temperature regime imposed by our heating treatment was not high enough to impair these reproductive traits. Despite shortening the bloom period, the moderately high temperatures applied in this study did not conclusively reduce seed weight and had no effect on final berry weight. The temperature response of Cabernet Sauvignon reproductive growth observed here resembles that of the subtropical crop tomato (*Solanum lycopersicum* L.) rather than that of the temperate (cereal) crops reviewed in Zhu et al. (2021). Even higher temperatures, however, may be detrimental to grapevine reproductive performance. For example, temperatures above 33/27°C (day/night) led to flower abortion and poor fruit set in growth chamber experiments (Buttrose and Hale, 1973; Greer and Weston, 2010; Merrill et al., 2020). Increasing the canopy temperature by 2°C–4°C above ambient during bloom in the field also reduced fruit set, and fruit set was lower in the warmer ($T_{max} \approx 33$°C) of the 2 years studied (Pagay and Collins, 2017). The diurnal temperature range reached under field conditions in our study (15°C–20°C) was greater than that imposed in earlier growth-chamber experiments (3°C or 5°C in Ebadi et al., 1995a,b, 5°C or 12.5°C in Buttrose and Hale, 1973; 6°C in Merrill et al., 2020; 10°C or 15°C in Greer and Weston, 2010) but similar to other field experiments (Pagay and Collins, 2017).

Our forced-convection, free-air cooling and heating system worked well in that the desired temperature patterns were achieved, set points were not exceeded, and differences between the ambient (i.e., non-treated) control and the convective (i.e., blower) control were insignificant. The system thus served as an effective tool to manipulate the inflorescence microclimate, just as it had previously been used to manipulate the cluster microclimate during fruit development and ripening (Spayd et al., 2002). Moreover, the temperature regimes applied to inflorescences did not alter shoot growth, leaf gas exchange, and leaf non-structural carbohydrates. Gas exchange and carbohydrate measurements were conducted on the leaf above each treated inflorescence, because during bloom time this leaf is a main source of photosynthates for the inflorescence below it, and is thus most likely to be influenced by source–sink feedback networks (Keller, 2020). Consequently, the manipulation of sink strength by our

temperature regimes did not modify the strength of nearby sources or the strength of other sinks (e.g., growing shoot tips). In addition, the reduction in fruit set, as well as seed and berry size following inflorescence cooling was not a result of limited photosynthate supply from the leaves but instead was a consequence of temperature acting on the flowers themselves. In growth chambers, low temperatures (12/9°C) just before and during bloom were found to impair embryo sac development in grape ovaries, possibly leading to an increase in floater seeds with aborted embryo and endosperm (Ebadi et al., 1995a,b). In our field experiment, however, there was no evidence that the number of seeds per berry or their viability was influenced by inflorescence temperature; the proportion of floater seeds was the same across all treatments. The proportion of floaters was similar to that reported for Chardonnay seeds by Ebadi et al. (1995a, 1996) but much higher than in a previous study with Cabernet Sauvignon, yet the seed number and seed weight were similar to that study (Hall et al., 2011). Both pollen germination on the stigma and the rate of pollen tube growth are also temperature-dependent; at <15°C these processes often become too slow for fertilization to occur (Staudt, 1982; Ebadi et al., 1995b). In some cases, pollen was sterile when inflorescences experienced temperatures <15°C at the beginning of bloom, even when photosynthate supply was abundant (Koblet, 1966). On the other hand, pollen tube growth is readily reactivated when warm temperatures follow a brief (e.g., 2 days) episode of cool temperatures (Staudt, 1982). In our experiment, the temperature of cooled inflorescences fluctuated on a diurnal and longer-term basis but was not consistently below 15°C, and thus, fruit set was reduced but not prevented entirely. In addition to the processes related to fruit set, inflorescence cooling likely also reduced cell division and cell expansion in the resulting berries, thus decreasing their final size. Both of these processes occur simultaneously during the first few weeks after anthesis (Harris et al., 1968), and both are limited by cold stress (<15°C) and heat stress (>35°C; Hale and Buttrose, 1974; Kliewer, 1977). We did not evaluate the number and size of mesocarp cells here, but because flowering occurs asynchronously across an inflorescence, the extended bloom period in the cooling treatment implies that berries resulting from early fruit set within a cooled inflorescence continued to be exposed to low temperatures after fruit set until the last flowers set fruit and cooling was terminated.

While the impact of inflorescence cooling on berry growth (i.e., cell division and cell expansion) decreased berry weight independently of berry number per cluster and seed number per berry, the final berry weight also correlated with both seed number and total seed weight across treatments. The correlation between seed number or weight and berry size is well established and is related to the seeds releasing growth-promoting auxin and gibberellin after fruit set (Winkler and Williams, 1935; Olmo, 1946; Keller, 2020). While only a single seed is required for a grape berry to develop, the total seed weight correlates strongly with the growth rate and final size (i.e., sink strength) of mesocarp cells and hence berries (Friend et al., 2009). Additionally, the correlation between final rachis length and flower but not berry number observed here supports the idea that developing flowers, much more so than berries, determine rachis growth and development (Theiler and Coombe, 1985; Gourieroux et al., 2016). Whether the connection between flower number and rachis growth is causally related to the occurrence of a ripening disorder named bunch-stem necrosis (BSN) remains unknown. An inverse correlation between the average bloom-time T_{max} and the incidence of late-season BSN has been reported for several grape cultivars (Theiler and Müller, 1987). However, although Cabernet Sauvignon is generally susceptible to BSN (Hall et al., 2011), we found no symptomatic clusters in the present study.

Differences in phenology, berry numbers, and berry size following inflorescence temperature manipulation did not alter shoot growth. Apparently, these shoots were not sink-limited. In earlier work with field-grown grapevines, reproductive growth was positively correlated with vegetative growth within shoots (Keller et al., 2015). Nonetheless, many wine industry members believe that late harvest or delayed fruit ripening will slow down shoot maturation and compromise the cold hardiness of overwintering buds. Our results do not support this assumption. Counting the number of brown internodes per shoot showed that the degree of periderm formation (often incorrectly termed "lignification") was independent of fruit development. The timing of veraison (i.e., of ripening initiation) did not coincide with the formation of periderm across treatments. The former was strongly altered by the temperature regimes applied during the bloom period, whereas the latter occurred simultaneously across treatments, which shows that ripening initiation and periderm formation are independent processes. This result is similar to the finding that veraison does not coincide with the transition of grapevine buds from paradormancy to endodormancy (Camargo-Alvarez et al., 2020). In both studies, the timing of veraison was highly responsive to temperature, whereas periderm formation and bud dormancy seemed to be driven mostly by photoperiod.

Grape growers have several options for influencing the microclimate of an inflorescence or cluster. Examples include the choice of training system, trunk height, vineyard floor management (e.g., control of weeds or cover crops), and canopy management (e.g., manipulation of the number of leaves around the clusters). Different training systems result in differences in canopy density and shoot orientation, which influences the microclimate around the clusters (Reynolds and Vanden Heuvel, 2009). Under the climatic conditions of the present study, a vertical temperature gradient of up to +4°C m^{-1} may exist upwards from the cooler trunk base (Peña Quiñones et al., 2019). An inflorescence that grows close to the ground is therefore likely to be exposed to cool air more often than is an inflorescence at a greater distance from the ground. Additionally, bare soil can be a source of heat transfer to the inflorescences by convection, especially during sunny days and when the soil surface is dry. Thus inflorescences are likely to be cooler in vineyards with a floor cover of weeds or cover crops. Removing leaves to expose clusters to solar radiation will also result in higher daytime (but somewhat lower nighttime) temperatures of inflorescences. However, leaf removal at or before

the time of bloom eliminates source area and generally reduces fruit set (Vander Weide et al., 2021). Shoot thinning (i.e., removal of entire shoots) early in the growing season also reduces the density of the canopy and thus probably contributes to a warmer microclimate around the clusters (Wang et al., 2019).

Conclusion

The forced-convection, free-air cooling and heating system is a useful research tool to investigate sink/source interactions and to study effects of organ temperature independently from those of light. By manipulating grape inflorescence temperatures, rather than whole-plant temperatures, we found that sink strength and hence fruit development is dependent on the temperature acting directly on the sinks themselves. Our results also showed that temperature differences perceived by flowering structures before fruit set can alter the subsequent phenological development of the fruit. Cooling inflorescences from the beginning of bloom lengthened, and heating inflorescences shortened, the bloom period, thus delaying (cooling) or accelerating (heating) the time to fruit set as well as the time to ripening onset. Among grapevine yield components, both berry number per cluster and final berry weight were reduced when the inflorescences experienced cool temperatures. At harvest, berries developing from cooled inflorescences also had lower total seed weight and sugar content, and higher acidity. Whereas daily average temperatures above 16°C appear to be necessary during the bloom period to maximize fruit set and subsequent berry development in Cabernet Sauvignon grapevines, no upper-temperature limit was found in this study. Though our highest temperature regime (daily average 23.4°C) did not modify fruit set and berry traits compared with the ambient regime (daily average 21°C), it did reduce the time to fruit set and veraison, and decreased the variability in subsequent berry development and seed weight, suggesting that this regime was close to the optimum for reproductive performance. The applicability of these results to other grape cultivars, especially cultivars that differ in their sensitivity to temperature variation, remains to be tested.

Data availability statement

The raw data supporting the conclusions of this article will be made available by the authors, without undue reservation.

Author contributions

MK conceived of the study, obtained the funding, and wrote the manuscript. JF and JT designed and operated the free-air cooling and heating system. RS-B, JF, and LM conducted the experiment. RS-B and MK analyzed the data. All authors contributed to the article and approved the submitted version.

Funding

This research was funded by the USDA Northwest Center for Small Fruits Research (grant number 5953582718), Washington State Grape and Wine Research Program, and Walter Hochstrasser Stiftung.

Acknowledgments

We thank Babette Grünwald, Maria Mireles, and Alan Kawakami for skilled technical assistance.

Conflict of interest

The authors declare that the research was conducted in the absence of any commercial or financial relationships that could be construed as a potential conflict of interest.

Publisher's note

Supplementary material

The Supplementary material for this article can be found online at: https://www.frontiersin.org/articles/10.3389/fpls.2022.864892/full#supplementary-material

References

Buttrose, M. S., and Hale, C. R. (1973). Effect of temperature on development of the grapevine inflorescence after bud burst. *Am. J. Enol. Vitic.* 24, 14–16.

Camargo-Alvarez, H., Salazar-Gutiérrez, M., Keller, M., and Hoogenboom, G. (2020). Modeling the effect of temperature on bud dormancy of grapevines. *Agric. For. Meteorol.* 280:107782. doi: 10.1016/j.agrformet.2019.107782

Coombe, B. G. (1995). Adoption of a system for identifying grapevine growth stages. *Aust. J. Grape Wine Res.* 1, 104–110. doi: 10.1111/j.1755-0238.1995.tb00086.x

Dry, P. R., Longbottom, M. L., McLoughlin, S., Johnson, T. E., and Collins, C. (2010). Classification of reproductive performance of ten winegrape varieties. *Aust. J. Grape Wine Res.* 16, 47–55. doi: 10.1111/j.1755-0238.2009.00085.x

Ebadi, A., Coombe, B. G., and May, P. (1995a). Fruit set on small chardonnay and shiraz vines grown under varying temperature regimes between budburst and flowering. *Aust. J. Grape Wine Res.* 1, 3–10. doi: 10.1111/j.1755-0238.1995.tb00071.x

Ebadi, A., May, P., Sedgley, M., and Coombe, B. G. (1995b). Effect of low temperature near flowering time on ovule development and pollen tube growth in

the grapevine (*Vitis vinifera* L.), cvs chardonnay and shiraz. *Aust. J. Grape Wine Res.* 1, 11–18. doi: 10.1111/j.1755-0238.1995.tb00072.x

Ebadi, A., Sedgley, M., May, P., and Coombe, B. G. (1996). Seed development and abortion in *Vitis vinifera* L., cv. chardonnay. *Int. J. Plant Sci.* 157, 703–712. doi: 10.1086/297392

Evans, R. G., Spayd, S. E., Wample, R. L., Kroeger, M. W., and Mahan, M. O. (1993). Water use of *Vitis vinifera* grapes in Washington. *Agric. Water Manag.* 23, 109–124. doi: 10.1016/0378-3774(93)90035-9

Ewart, A., and Kliewer, W. M. (1977). Effects of controlled day and night temperatures and nitrogen on fruit-set, ovule fertility, and fruit composition of several wine grape cultivars. *Am. J. Enol. Vitic.* 28, 88–95.

Friend, A. P., Trought, M. C. T., and Creasy, G. L. (2009). The influence of seed weight on the development and growth of berries and live green ovaries in *Vitis vinifera* L. cvs. Pinot noir and cabernet sauvignon. *Aust. J. Grape Wine Res.* 15, 166–174. doi: 10.1111/j.1755-0238.2009.00050.x

Galat Giorgi, E., Keller, M., Sadras, V., Roig, F. A., and Perez Peña, J. (2020). High temperature during the budswell phase of grapevines increases shoot water transport capacity. *Agric. For. Meteorol.* 295:108173. doi: 10.1016/j.agrformet.2020.108173

Gourieroux, A. M., McCully, M. E., Holzapfel, B. P., Scollary, G. R., and Rogiers, S. Y. (2016). Flowers regulate the growth and vascular development of the inflorescence rachis in *Vitis vinifera* L. *Plant Physiol. Biochem.* 108, 519–529. doi: 10.1016/j.plaphy.2016.08.016

Greer, D. H., and Weston, C. (2010). Heat stress affects flowering, berry growth, sugar accumulation and photosynthesis of *Vitis vinifera* cv. semillon grapevines grown in a controlled environment. *Funct. Plant Biol.* 37, 206–214. doi: 10.1071/FP09209

Hale, C. R., and Buttrose, M. S. (1974). Effect of temperature on ontogeny of berries of *Vitis vinifera* L. cv. cabernet sauvignon. *J. Am. Soc. Hortic. Sci.* 99, 390–394.

Hall, G. E., Bondada, B. R., and Keller, M. (2011). Loss of rachis cell viability is associated with ripening disorders in grapes. *J. Exp. Bot.* 62, 1145–1153. doi: 10.1093/jxb/erq355

Halldorson, M. M., and Keller, M. (2018). Grapevine leafroll disease alters leaf physiology but has little effect on plant cold hardiness. *Planta* 248, 1201–1211. doi: 10.1007/s00425-018-2967-x

Harris, J. M., Kriedemann, P. E., and Possingham, J. V. (1968). Anatomical aspects of grape berry development. *Vitis* 7, 106–119. doi: 10.5073/vitis.1968.7.106-119

Kassemeyer, H. H., and Staudt, G. (1981). Über die Entwicklung des Embryosacks und die Befruchtung der Reben. *Vitis* 20, 202–210. doi: 10.5073/vitis.1981.20.202-210

Keller, M. (2020). *The Science of Grapevines*. *3rd Ed.*, London: Elsevier Academic Press.

Keller, M., Deyermond, L. S., and Bondada, B. R. (2015). Plant hydraulic conductance adapts to shoot number but limits shoot vigour in grapevines. *Funct. Plant Biol.* 42, 366–375. doi: 10.1071/FP14206

Keller, M., Kummer, M., and Vasconcelos, M. C. (2001). Reproductive growth of grapevines in response to nitrogen supply and rootstock. *Aust. J. Grape Wine Res.* 7, 12–18. doi: 10.1111/j.1755-0238.2001.tb00188.x

Keller, M., Mills, L. J., Wample, R. L., and Spayd, S. E. (2005). Cluster thinning effects on three deficit-irrigated *Vitis vinifera* cultivars. *Am. J. Enol. Vitic.* 56, 91–103.

Keller, M., Smithyman, R. P., and Mills, L. J. (2008). Interactive effects of deficit irrigation and crop load on cabernet sauvignon in an arid climate. *Am. J. Enol. Vitic.* 59, 221–234.

Keller, M., and Tarara, J. M. (2010). Warm spring temperatures induce persistent season-long changes in shoot development in grapevines. *Ann. Bot.* 106, 131–141. doi: 10.1093/aob/mcq091

Keller, M., Tarara, J. M., and Mills, L. J. (2010). Spring temperatures alter reproductive development in grapevines. *Aust. J. Grape Wine Res.* 16, 445–454. doi: 10.1111/j.1755-0238.2010.00105.x

Kliewer, W. M. (1977). Effect of high temperatures during the bloom-set period on fruit-set, ovule fertility, and berry growth of several grape cultivars. *Am. J. Enol. Vitic.* 28, 215–222.

Koblet, W. (1966). Fruchtansatz bei Reben in Abhängigkeit von Triebbehandlung und Klimafaktoren. *Wein-Wiss.* 7, 297–379.

Körner, C. (2003). Carbon limitation in trees. *J. Ecol.* 91, 4–17. doi: 10.1046/j.1365-2745.2003.00742.x

May, P. (2004). *Flowering and Fruitset in Grapevines*. Adelaide: Phylloxera and Grape Industry Board of South Australia, Lythrum Press.

Merrill, N. K., García de Cortázar-Atauri, I., Parker, A. K., Walker, M. A., and Wolkovich, E. M. (2020). Exploring grapevine phenology and high temperatures response under controlled conditions. *Front. Envir. Sci.* 8:516527. doi: 10.3389/fenvs.2020.516527

Olmo, H. P. (1946). Correlations between seed and berry development in some seeded varieties of *Vitis vinifera*. *Proc. Am. Soc. Hort. Sci.* 48, 291–297.

Pagay, V., and Collins, C. (2017). Effects of timing and intensity of elevated temperatures on reproductive development of field-grown shiraz grapevines. *OENO One* 51, 409–421. doi: 10.20870/oeno-one.2017.51.4.1066

Peña Quiñones, A., Keller, M., Salazar Gutierrez, M. R., Khot, L., and Hoogenboom, G. (2019). Comparison between grapevine tissue temperature and air temperature. *Sci. Hort.* 247, 407–420. doi: 10.1016/j.scienta.2018.12.032

Reynolds, A. G., and Vanden Heuvel, J. E. (2009). Influence of grapevine training systems on vine growth and fruit composition: a review. *Am. J. Enol. Vitic.* 60, 251–268.

Ruan, Y. L., Patrick, J. W., Bouzayen, M., Osorio, S., and Fernie, A. R. (2012). Molecular regulation of seed and fruit set. *Trends Plant Sci.* 17, 656–665. doi: 10.1016/j.tplants.2012.06.005

Spayd, S. E., Tarara, J. M., Mee, D. L., and Ferguson, J. C. (2002). Separation of sunlight and temperature effects on the composition of *Vitis vinifera* cv. merlot berries. *Am. J. Enol. Vitic.* 53, 171–182.

Staudt, G. (1982). Pollenkeimung und Pollenschlauchwachstum *in vivo* bei *Vitis* und die Abhängigkeit von der Temperatur. *Vitis* 21, 205–216. doi: 10.5073/vitis.1982.21.205-216

Tarara, J. M., Ferguson, J. C., and Spayd, S. E. (2000). A chamber-free method of heating and cooling grape clusters in the vineyard. *Am. J. Enol. Vitic.* 51, 182–188.

Theiler, R., and Coombe, B. G. (1985). Influence of berry growth and growth regulators on the development of grape peduncles in *Vitis vinifera* L. *Vitis* 24, 1–11. doi: 10.5073/vitis.1985.24.1-11

Theiler, R., and Müller, H. (1987). Beziehung zwischen mittlerer Tagesmaximumtemperatur während der Blüteperiode und Stiellähmebefall für verschiedene Rebsorten und Standorte. *Mitt. Klosterneuburg* 37, 102–108.

Vander Weide, J., Gottschalk, C., Schultze, S. R., Nasrollahiazar, E., Poni, S., and Sabbatini, P. (2021). Impacts of pre-bloom leaf removal on wine grape production and quality parameters: a systematic review and meta-analysis. *Front. Plant Sci.* 11:621585. doi: 10.3389/fpls.2020.621585

Vasconcelos, M. C., Greven, M., Winefield, C. S., Trought, M. C. T., and Raw, V. (2009). The flowering process of *Vitis vinifera*: a review. *Am. J. Enol. Vitic.* 60, 411–434.

Wang, X., De Bei, R., Fuentes, S., and Collins, C. (2019). Influence of canopy management practices on canopy architecture and reproductive performance of Semillon and shiraz grapevines in a hot climate. *Am. J. Enol. Vitic.* 70, 360–372. doi: 10.5344/ajev.2019.19007

Winkler, A. J., and Williams, W. O. (1935). Effect of seed development on the growth of grapes. *Proc. Am. Soc. Hort. Sci.* 33, 430–434.

Yu, S. M., Lo, S. F., and Ho, T. H. D. (2015). Source-sink communication: regulated by hormone, nutrient, and stress cross-signaling. *Trends Plant Sci.* 20, 844–857. doi: 10.1016/j.tplants.2015.10.009

Zhu, T., Fonseca De Lima, C. F., and De Smet, I. (2021). The heat is on: how crop growth, development, and yield respond to high temperature. *J. Exp. Bot.* 72, 7359–7373. doi: 10.1093/jxb/erab308

frontiers | Frontiers in Plant Science

TYPE Original Research
PUBLISHED 03 February 2023
DOI 10.3389/fpls.2022.918730

OPEN ACCESS

EDITED BY
Marta Adelina Mendes,
University of Milan, Italy

REVIEWED BY
Umar Masood Quraishi,
Quaid-i-Azam University, Pakistan
Cara Griffiths,
Rothamsted Research,
United Kingdom
Sivakumar Sukumaran,
The University of Queensland,
Australia

*CORRESPONDENCE
Zoe A. Wilson
zoe.wilson@nottingham.ac.uk

SPECIALTY SECTION
This article was submitted to Plant Abiotic Stress, a section of the journal Frontiers in Plant Science

RECEIVED 12 April 2022
ACCEPTED 20 December 2022
PUBLISHED 03 February 2023

CITATION
Callens C, Fernandez-Goméz J, Tucker MR, Zhang D and Wilson ZA (2023) Heat stress responses vary during floret development in European spring barley cultivars.
Front. Plant Sci. 13:918730.
doi: 10.3389/fpls.2022.918730

Heat stress responses vary during floret development in European spring barley cultivars

Cindy Callens[1,2], José Fernandez-Goméz[1], Matthew R. Tucker[2], Dabing Zhang[2,3] and Zoe A. Wilson[1]*

[1]School of Biosciences, University of Nottingham, Loughborough, United Kingdom, [2]Waite Research Institute, School of Agriculture, Food and Wine, University of Adelaide, Urrbrae, SA, Australia, [3]Joint International Research Laboratory of Metabolic and Developmental Sciences, State Key Laboratory of Hybrid Rice, School of Life Sciences and Biotechnology, Shanghai Jiao Tong University, Shanghai, China

The Poaceae, or grasses, include many agriculturally important cereal crops such as rice (*Oryza sativa*), maize (*Zea mays*), barley (*Hordeum vulgare*) and bread wheat (*Triticum aestivum*). Barley is a widely grown cereal crop used for stock feed, malting and brewing. Abiotic stresses, particularly global warming, are the major causes of crop yield losses by affecting fertility and seed set. However, effects of heat stress on reproductive structures and fertility in barley have not been extensively investigated. In this study we examined three commercial European spring barley varieties under high temperature conditions to investigate the effects on floret development. Using a combination of fertility assays, X-ray micro computed tomography, 3-dimensional modelling, cytology and immunolabelling, we observed that male reproductive organs are severely impacted by increased temperature, while the female reproductive organs are less susceptible. Importantly, the timing of stress relative to reproductive development had a significant impact on fertility in a cultivar-dependent manner, this was most significant at pollen mitosis stage with fertility ranged from 31.6-56.0% depending on cultivar. This work provides insight into how heat stress, when applied during male pollen mother cell meiosis and pollen mitosis, affects barley fertility and seed set, and also describes complementary invasive and non-invasive techniques to investigate floret development. This information will be used to identify and study barley cultivars that are less susceptible to heat stress at specific stages of floral development.

KEYWORDS

barley, heat stress, floret development, meiosis, mitosis, pollen, male sterility, breeding

1 Introduction

The world is facing an exponentially increasing population with associated increased demands for food, and all major climate models predict a higher average temperature globally with larger temperature fluctuations and more frequent heat waves (Christidis et al., 2014; IPCC, 2014). Abiotic stresses are, individually or in combination, one of the major reasons for crop yield loss. These stresses cause morphological, physiological, biochemical and molecular changes that impair plant development (Bita and Gerats, 2013). Lesk et al. (2016) showed that extreme heat significantly reduced national cereal production globally by 9-10%. Of particular concern is that three of the five most important cereal crops worldwide (i.e. wheat, maize and barley) exhibit the strongest negative yield impacts due to the changing climate (David and Christopher, 2007). Jacott and Boden (2020) recently reviewed the consequences of high ambient temperatures on wheat and barley, summarizing negative impacts on inflorescence development, the transition to flowering, and fertility. The increased frequency of heat stress over the last 40 years has clearly led to a greater frequency of yield anomalies in wheat (Zampieri et al., 2017), which accounts for 21% of food production. This proportion could be challenged with an increase in temperature in regions where temperatures are currently optimal (Ortiz et al., 2008; Delphine et al., 2014). Experiments in rice also showed that heat stress has an adverse effect on important yield components especially fertile spikelets and 1000 grain weight, decreasing yield significantly (Aghamolki et al., 2016). Similarly in spring barley, an increase in ambient temperature from 20°C/16°C (day/night) to 28°C/24°C reduced floret number and grains per spike (Hemming et al., 2012; Ejaz and von Korff, 2017). This serves as a warning for future global food security.

Reproductive organs are significantly more vulnerable to high temperatures than other plant organs. Planting of crops is typically timed to minimise high temperature exposure during the later reproductive stages, however the fluctuations and extremes of temperature that are now occurring mean that there is an increasing probability that peaks of high temperature will overlap with the flowering period (Teixeira et al., 2013; Kupke et al., 2022). It is proposed that "stay green" traits that enable photosynthesis to be maintained for longer, particularly under environmental stress, may enable yield losses due to abiotic stress to be minimized (Barnabas et al., 2008). Seed set requires many developmental steps to be successfully completed; for example, pollen must first be produced, viable pollen grains must be released and the pollen tubes must grow correctly to ensure functional signalling mechanisms with the style and the ovule. Concurrently, the ovule must develop within the ovary to produce and nourish the embryo sac, producing a female gamete and a suitable environment for the downstream events of seed development (Wilkinson et al., 2018). Once fertilization is complete, the embryo and endosperm must then develop normally to ensure successful seed fill (Maestri et al., 2002; Barnabas et al., 2008; Wilson and Zhang, 2009). Nevertheless, these developmental processes show variable sensitivity to heat stress (Jacott and Boden, 2020).

Prior to fertilisation, Saini et al. (1983) reported that one third of ovaries in wheat that experienced heat stress during meiosis exhibited abnormal development. Pollen, by contrast, exhibits much higher levels of abortion after heat stress at the same stage. Indeed, male reproductive development has been shown to be one of the most heat-sensitive stages in cereals (Saini et al., 1983; Stone and Basra, 2001; Prasad et al., 2008). At the pre-meiotic stage, high temperatures caused development of short anthers possessing no pollen grains in barley, while heat stress during meiosis resulted in pollen grains that possessed exine, but showed little starch accumulation (Sakata et al., 2000). Draeger and Moore (2017) also showed that exposure of wheat to high temperatures affected the progression of Pollen Mother Cell (PMC) meiosis. Disruption of synapsis is one of the most commonly reported meiotic failures under high temperatures and this can lead to unpaired univalents that segregate randomly or are lost (Bomblies et al., 2015). Elevated temperatures have also been shown to compromise mitosis 1 and 2 in both wheat and barley pollen (Saini et al., 1984; Barnabas et al., 2008). This may be due to an inability to synthesize all required Heat Shock Proteins (HSPs) necessary to survive during heat stress conditions (Cooper et al., 1984; Mascarenhas and Crone, 1996; Barnabas et al., 2008), and is consistent with causal involvement of HSPs in thermotolerance in non-cereal species (Hong and Vierling, 2000). Genotypes that express HSPs are better able to withstand heat stress as they minimise heat-induced protein aggregation and thus during the recovery period, facilitate their refolding (Nguyen et al., 1994; Feder and Hofmann, 1999; Farooq et al., 2011). In many cases, expression of HSPs is developmentally regulated and they are thus present prior to heat stress (Maestri et al., 2002).

One challenge of studying the response of florets to heat stress in cereals is determining when and where defects appear, how this differs between cultivars with different phenology and architecture, and how this might be examined in a non-destructive manner. In this study we analysed the effects of heat stress during floret development in three European spring barley varieties under controlled environmental conditions. One of the varieties, RGT Planet, represents a variety of considerable promise for high yield and malt quality in diverse conditions, including dryland environments in Australia (SeedForce, 2017). Our overall aim was to generate baseline data that might be used to develop further screening strategies and targets for reproductive heat tolerance during floret development in barley. We found that after heat stress, anthers from all varieties showed abnormal development, whilst ovules were less severely affected. The three varieties tested showed differences in sterility, confirming their varying tolerance to heat stress. RGT Planet exhibited excellent yield under control conditions, but suffered significantly after heat stress. In contrast to

Moonshine and RGT Planet, Optic was the most severely affected by heat stress at pollen mitosis during floret development.

2 Materials and methods

2.1 Plant materials, growth and heat stress conditions

Seeds from three different spring barley varieties (*Hordeum vulgare*; Optic (derived from the cross Chad × (Corniche × Force), RAGT Moonshine and RGT Planet) were provided by the Wilson lab (University of Nottingham) and were sown in John Innes Potting Compost No.3 in 13cm diameter pots for germination and early plant establishment. All three are elite lines that have been on the AHDB Recommended List, although RAGT Moonshine and Optic were removed from the AHDB Recommended List in 2016 (AHDB, 2016). Optic is a variety created by Syngenta, while RAGT Moonshine and RGT Planet are varieties created by RAGT Seeds. RGT Planet is a relatively new variety that has been shown to be one of the highest yielding spring varieties on the AHDB Recommended List that is fully approved for brewing use (AHDB, 2017). All three are two-row varieties and are primarily grown in the United Kingdom, although RGT Planet is also popular in Australia. Temperatures of 15-20°C are considered optimal for growth and development of spring barley varieties (Kruszka et al., 2014).

After sowing, pots were placed in a controlled environment growth chamber with a continuous temperature of ~17°C and 16/8 -hour light/dark photoperiod and 80% relative humidity. After one week, the plants were transferred to CSNG (General Container Nursery Stock compost, Levington Advance) compost in 13cm diameter pots. Heat stress was applied to two stages of reproductive development (Pollen Mother Cell meiosis and pollen mitosis, Supplementary Figure S1). Staging of reproductive development was conducted according to the non-destructive staging described in Gómez and Wilson (2012), to ensure that all samples were at the appropriate and equivalent developmental stage. Pollen Mother Cell Meiosis corresponded to spike stage 4, spike one-quarter within previous last sheath; pollen mitosis corresponded to spike stage 13, spike half out (Gómez and Wilson, 2012). Stressed plants were compared to plants grown in control conditions to ensure there was a matching of the corresponding developmental stages. Male as well as female reproductive development were simultaneously targeted because the onset of the PMCs in anthers coincides approximately with meiosis in the megaspore mother cell (Saini et al., 1983).

Twelve plants of each variety were used for each condition: 1) Pollen Mother Cell (PMC) meiosis heat stress, 2) Pollen mitosis heat stress and 3) control. The periods of heat stress were carried out in a controlled environment growth room with a day/night temperature of 30/25°C, 80% relative humidity and a 16/8 -hour light/dark photoperiod to mimic rapid onset heat stress conditions. The temperatures were chosen to mimic heat waves occurring more frequently in Europe. Tillers were selected at the beginning of meiosis or mitosis, and were tagged for analysis before being submitted to heat stress. All pots were monitored daily and watered to avoid concurrent drought stress. Plants undergoing the PMC meiosis heat treatment were submitted to heat stress for two days, while plants undergoing the Pollen mitosis heat treatment remained in the heat stress conditions for five days to ensure completion of pollen mitosis I and II, before being transferred back to control conditions. Control plants were maintained at a constant 17°C, 80% relative humidity with a 16/8 -hour light/dark photoperiod.

2.2 Pollen viability assay

Pollen viability in control and heat stressed plants was assessed by analysis of starch levels in pollen grains using 0.2% (w/v) potassium iodide and 1% (w/v) iodine to determine their ability to germinate and fertilize (Chang et al., 2014). Normal mature pollen grains that contain starch granules stain black, whilst immature pollen grains or deformed pollen grains appear orange, or red. Pollen viability images were taken with a Nikon Eclipse 50i microscope and a Nikon DS-Fi1 camera.

2.3 Thin sectioning and cell wall immunolabelling

Florets were harvested from the tillers tagged for heat stress during pollen meiosis immediately before anthesis, fixed in 4% (w/v) paraformaldehyde in phosphate-buffered saline (PBS) with 0.1% (v/v) Triton X-100 and 0.1% (v/v) Tween 20 and embedded in paraffin. Floret sections (8µm) were mounted on slides at 42°C, the paraffin was removed from the sections using 100% Histoclear (v/v) and tissue was rehydrated by using an ethanol series (100%, 90%, 70% and 30% (v/v)) and water. Slides were washed with 1xPBS and treated subsequently with glycine to inactivate residual aldehyde groups. They were then washed with Incubation buffer (1% (w/v) bovine serum albumin (BSA)) in 1xPBS (Burton et al., 2011). Primary antibody was added to the sections and incubated in a humidity chamber for 1h: BG1 murine monoclonal antibodies raised against barley (1,3;1,4)-β-d-glucan (diluted 1:50; Biosupplies Australia, Parkville, Vic., Australia) and LM19 monoclonal antibodies raised against homogalacturonan (Meikle et al., 1994; Verhertbruggen et al., 2009; Burton et al., 2011). After three washes with Incubation buffer the slides were dried and the secondary antibodies added. Goat anti-mouse Alexa Fluor® 488 IgG (H+L) (diluted 1:200, Invitrogen, Australia) was used for BG1 and Dylight 550 Goat anti-rat IgM (diluted 1:200, Invitrogen, Australia) was used for

LM19. The slides were incubated for 2h and then washed with Incubation buffer. 0.1% (w/v) Calcofluor white was added and washed off before imaging with the Zeiss Axio Imager 2 as described in Aditya et al. (2015).

2.4 3D X-ray computed tomography imaging

The Phoenix Nanotom S, a nanofocus Computed Tomography (CT) system was used to scan barley florets of the three varieties at the Hounsfield Facility in Nottingham as previously described (Tracy et al. (2017). Control and heat stressed florets (heat stress applied during PMC meiosis) were scanned and the scans were segmented and analysed using VG Studio Max 2.2.

2.5 Reproductive organ phenotyping

Five different, randomly chosen florets were harvested immediately before anthesis after the heat treatments and in control conditions from all varieties and dissected to observe the morphology of the anthers. Images were taken with a Zeiss Stemi SV6 microscope and an Axiocam ERc Rev. 2.0 camera.

2.6 Evaluation of sterility

All tillers from control and heat stressed plants were harvested and the numbers of seeds per spike counted (Table 1) to determine the levels of fertility. For every spike the total number of spikelets and the number of spikelets that developed into seeds were counted. The reduction of fertility due to heat exposure was expressed as the percentage of sterility per tiller, by dividing the number of seeds formed by the total number of spikelets and multiplying by 100. Tagged heads from the plants were harvested and the percentage of sterility was determined on a tiller-by-tiller basis for each heat treatment and control conditions using a Kruskal-Wallis (one-way ANOVA) test to compare between treatments and varieties.

2.7 Phylogenetic analysis of heat shock proteins in barley

To determine orthologs of *AtHSP17.8* (AT1G07400.1) and *AtHSP70* (AT3G12580.1) a nucleotide BLAST search was carried out in NCBI, rice database and IPK Barlex database. Orthologs were identified for rice (*OsHSP17.8*, LOC_Os03g16030.1 and *OsHSP70*, LOC_Os11g47760.1) and barley (*HvHSP17.8*, AK368988.1 and *HvHSP70*, HORVU5Hr1G021300.3 and HORVU6Hr1G081460) and verified by multiple alignment through phylogenetic tree analysis (Supplementary Figure S2). The alignment was constructed using the Geneious alignment method and the Blosum62 cost matrix in Geneious (version 8.0 by Biomatters, available from http://www.geneious.com). These proteins were chosen to give an indication of differences between varieties in the response of heat shock proteins to heat stress. Due to the high similarity between the proteins in the cytosol subgroup of the HSP70 family, we focussed only on the closest orthologues in barley.

2.8 Quantitative reverse transcription (qRT) PCR

RNA was extracted with the RNeasy® Plant Mini Kit (Qiagen, UK) from at least five florets and pooled together.

TABLE 1 Average number of tillers per plant and seeds per spike, and number of tagged tillers for the three different varieties in control conditions, after PMC meiosis heat treatment or after pollen mitosis heat treatment ± standard deviation.

Variety	Treatment	Average number of tillers/plant	Number of tagged tillers	Average number of seeds/spike	Percentage fertility for each variety per spike compared to control
Optic	Control	7 ± 1.8		19 ± 2.8	100
	Meiosis	6 ± 0.7	8	14 ± 4.6	73.7
	Mitosis	5 ± 0.9	12	6 ± 3.8*	31.6
Moonshine	Control	7 ± 1		25 ± 2.0	100
	Meiosis	6 ± 0.7	5	16 ± 3.4*	64.0
	Mitosis	6 ± 1.1	16	14 ± 2.4*	56.0
RGT Planet	Control	6 ± 1.2		28 ± 2.8	100
	Meiosis	6 ± 1.6	12	12 ± 3.4*	42.9
	Mitosis	6 ± 1.3	13	13 ± 4.1*	46.4

Asterisks indicate a p-value <0.05 compared to the control.

cDNA was synthesised from total RNA using the SuperScript™ III reverse transcriptase (ThermoFisher Scientific, UK). qRT-PCR was performed with primers for *HvHSP17.8* (HvHSP17.8 Fw 5'GAGGTGGAGGACGGCAACA3' and HvHSP17.8 Rv 5'GATGGACTTGATCTCGGGTTT3') and *HvHSP70* (HvHSP70 Fw 5'ATCCTGAACGTGTCTGCTGA3' and HvHSP70 Rv 5'TGGTGTTGCGCATGTTGTAA 3') on three technical replicates and analysed using the LightCycler® 480 (Roche Life Science, UK). Expression values relative to the barley α-Tubulin gene (HvTubF 5'AGTGTCCTGTC CACCCACTC3' and HvTubR 5'AGCATGAAGTGGATCCT TGG3') were calculated.

3 Results

3.1 Anther morphology in barley varieties after heat stress

Anthers were dissected from at least three randomly selected florets for the different varieties (Optic, Moonshine and RGT Planet) that had been exposed to heat treatment at PMC meiosis and Pollen mitosis, and compared to those from the control conditions. Staging of anther development was conducted according to the non-destructive reproductive staging approach of Gómez and Wilson (2012), this ensured that heat stress was delivered at the appropriate developmental stage and that comparisons between samples were consistent based upon developmental stage. All of the heat-treated lines showed effects on anther morphology, with alterations in anther shape and a change in colour from yellow to white (Figure 1). In all three varieties, the effect on anther morphology was more severe after heat stress during PMC meiosis compared to Pollen mitosis, but both treatments showed impacts on anther shape and colour. In particular, Optic and RGT Planet showed a severe change in PMC meiosis heat stressed anthers (Figure 1). Anther morphology was investigated further using 3D images obtained from X-ray micro-CT scans of a representative floret from Optic and RGT Planet (Figure 2) and RAGT Moonshine (Supplementary Figure S3). Anther volume varied significantly; control non-stressed anthers were approximately 0.9mm^3 (4.33mm length, 1.98mm width, 1.43mm depth) in Optic and 1.1 mm3 (4.49 mm length. 2.83 mm width, 1.37 mm depth) in RGT Planet. Whereas the PMC meiosis heat stressed anthers were smaller: 0.29 mm^3 (3.91 mm length, 3.01 mm width, 1.82 mm depth) in Optic and 0.71 mm^3 (3.1 mm length, 2.35 mm width, 1.01 mm depth) in RGT Planet (Figure 2). The septum in the heat-stressed anthers could be observed as broken in the micro-CT scans, while this was not the case for the control anthers (Figure 2A).

Immunolabelling was subsequently used to observe sections of the anthers and highlight cell wall components such as 1,3;1,4-β-glucan, de-esterified homogalacturonan and cellulose to determine if the cell wall composition was impacted as a consequence of the heat stress (Figure 3; Supplementary Figures S4-6). Calcofluor white stained β-glycan polysaccharides in the outer layers of the anther, the filament vascular tissue and the pollen grains (Figure 3A). Some autofluorescence was detected in the pollen grains, particularly in the 1,3;1,4-β-glucan channel (Figure 3B), but positive controls confirmed 1,3;1,4-β-glucan and HG labelling (Figure 3C). The results clearly indicated that the meiosis heat-stressed anthers of all the lines were significantly impacted by the stress and labelling of HG in the anther walls appeared to be more intense compared to control anthers (Figures 3E, G, I). In Optic (Figures 3D, E), pollen was visible in the control anthers, but not in the PMC meiosis heat-stressed anthers. The epidermal cells of the anther wall were intact,

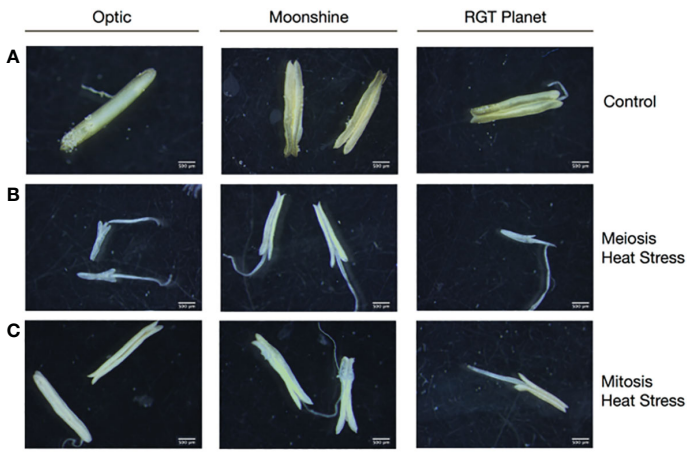

FIGURE 1
Anther development in barley cultivars Optic, Moonshine and RGT Planet. Representative anthers dissected from a minimum of three florets from Control **(A)** and heat stressed florets, **(B)** Heat Stress during Pollen Mother Cell meiosis and **(C)** Pollen Mitosis show differences in anther development under the different conditions.

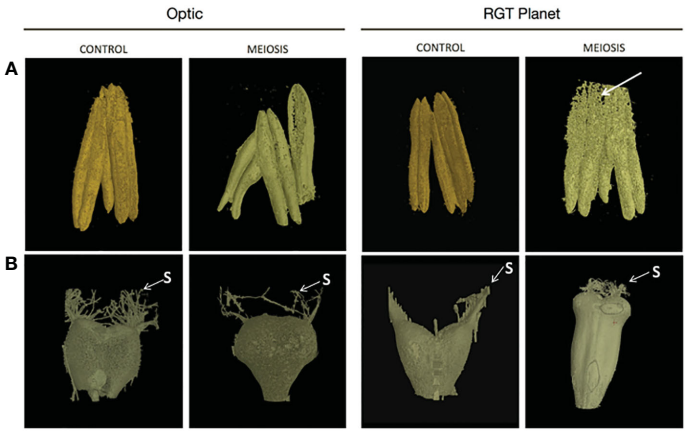

FIGURE 2
X-ray CT images of **(A)** anther and **(B)** carpel development from a representative floret from control and heat stress conditions for barley cultivars Optic and Planet. X-ray images of the anthers and carpels obtained by X-ray CT were compared for control environment and heat stress environment (heat stress during meiosis of pollen development) immediately before anthesis. Arrow indicates the broken septum in RGT Planet heat stressed anther.

but the endothecium had degraded. Both tissue layers were intact and visible in the Optic control anthers (Supplementary Figure S4). In Moonshine (Figures 3F, G), no pollen was visible in the PMC meiosis heat-stressed anthers despite it being observed in the micro-CT scanned images (Supplementary Figure S3). The epidermis was also intact, but the endothecium had degraded in the heat stressed anthers (Supplementary Figure S5). Similar to the other two varieties, while pollen grains were visible in the control anthers, none were visible in the heat stressed anthers in RGT Planet (Figures 3H, I). The anther wall in the heat stressed anthers seemed to have collapsed, which agrees with the observations from the micro-CT scan (Figure 2; Supplementary Figure S5).

3.2 Carpel morphology in barley varieties after heat stress

The 3D images of the carpels from Optic showed no significant changes in morphology between the PMC meiosis heat-stressed and control florets, but there was a difference in size (Figure 2; Supplementary Figure S4). The control carpel measured 1.31mm^3 (2.71mm length, 2.35mm width, 1.45mm depth), which is smaller than the heat stressed carpel, which measured 2.58mm^3 (2.86 length, 2.77mm width, 1.34 depth). The X-ray imaging also showed a significantly enlarged carpel in the RGT Planet heat-stressed floret with a volume of 4.46mm^3 (5.37mm length, 2.51mm width, 1.57mm depth) compared to the control which had a volume of 1.37mm^3 (2.42mm length, 2.22mm width, 1.13mm depth) (Figure 2).

The immunolabelling of ovule sections in Optic only showed slight differences between control and heat stressed florets (Figures 3J, K): the embryo sac was present in all cases, but there seemed to be less cell layers between the embryo sac and the integument, and nucellus cells appeared larger. This could be due to regional nucellar degeneration and/or faster development of heat-stressed ovules. Similarly, embryo sac morphology in the heat-stressed ovules of Moonshine did not show any significant difference compared to control ovules (Figures 3L, M). The ovules in the heat-stressed florets of RGT Planet seemed to be further developed than the controls (Figures 3N, O), but no obvious irregularities in the morphology of the embryo sacs could be identified.

3.3 Male fertility after heat stress

PMC meiosis and pollen mitosis stages are known to be vulnerable to heat stress during pollen development, therefore pollen viability was assessed using potassium iodide/iodine solution in anthers from all three varieties with and without heat treatment. Using this method, viable pollen stains black due to starch deposition whilst non-viable pollen stains orange-red. Despite the lack of pollen identified in thin sectioning, pollen was still present in anthers from some florets after heat stress at PMC meiosis and pollen mitosis, but there was a lack of starch staining indicating a high level of sterility (Supplementary Figure S1B). Pollen could be observed in the Optic and RGT Planet anthers, after both PMC meiosis and pollen mitosis heat stress, but was far less abundant than in the control plants, and poor staining suggested that little if any was viable. Moonshine was even more strongly affected with no pollen present after the PMC meiosis heat stress. After heat stress during pollen mitosis, viable pollen was observed in Moonshine but at a lower amount than in the control anthers. The impact of heat stress varied depending on developmental stage and cultivar, with increased sterility seen for heat stress during the pollen mitosis stage; with 26-57% sterility observed for heat stress at the

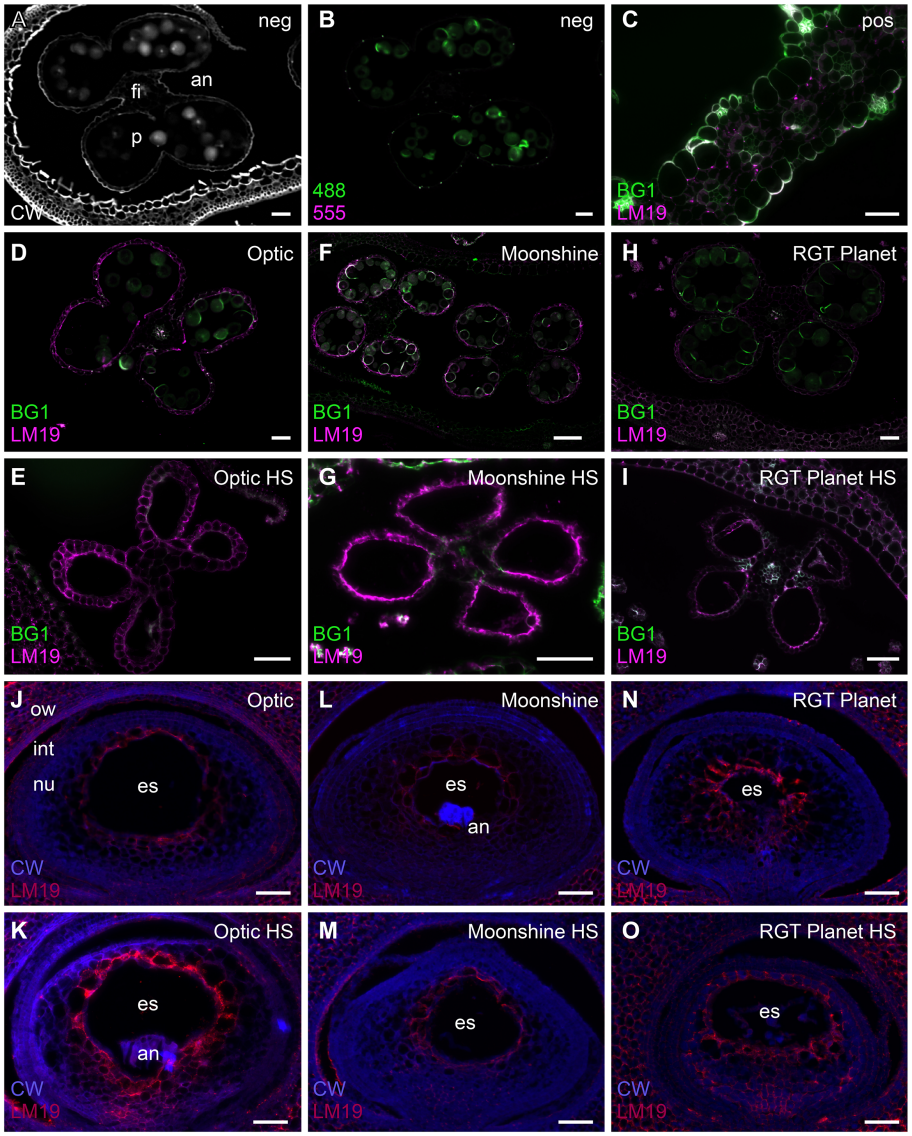

FIGURE 3
Immunolabelling of cell wall components in anthers and ovules in Optic, Moonshine and Planet. **(A)** Calcofluor white staining (CW, white colour) of a control anther (an). The filament (fi) and pollen (p) are indicated. **(B)** The same anther shown in A, showing autofluorescence (green) in the Alexafluor-488 channel. **(C)** A barley leaf sample showing positive labelling of (1,3;1,4)-β-glucan (BG1, green) and de-esterified pectin (LM19, magenta). **(D–O)** Comparison of control and heat stressed anthers and ovules in barley florets of the three varieties. Merged images of the antibody labelling patterns are shown. **(D)** Optic control anther. **(E)** Optic heat-stressed anther. **(F)** Moonshine control anther. **(G)** Moonshine heat-stressed anther. **(H)** Planet control anther. **(I)** Planet heat-stressed anther. **(J)** Optic control ovule. The ovary wall (ow), integuments (int), nucellus (nu) and embryo sac (es) are indicated. **(K)** Optic heat-stressed ovule. In this ovule the antipodals (an) are also evident. **(L)** Moonshine control ovule. **(M)** Moonshine heat-stressed ovule. **(N)** Planet control ovule. **(O)** Planet heat-stressed ovule. Bar = 50μm in all images. Images are representatives from at least 3 different florets per variety/heat stress treatment.

PMC meiosis stage, whilst 44-68% sterility was seen when heat stress occurred at pollen mitosis stage (Table 1).

3.4 Seed set after heat stress

The number of tillers and seeds per spike was assessed collectively for the three varieties after both treatments and in control conditions (Table 1). In Optic, there was no significant difference between the average number of seeds per spike after heat stress during PMC meiosis (~14 seeds) and the control (~19 seeds). However, there was a significant reduction of average seed number per spike after pollen mitosis heat stress compared to the control, from 19 to 6 seeds per spike. In Moonshine there was a significant decrease in seed set after both PMC meiosis and pollen mitosis heat treatments, from 25 in the control conditions

10.3389/fpls.2022.918730

to 16 and 14 respectively, after stress. The same could be observed in RGT Planet where a significant decrease was identified after both heat treatments (Table 1). In control conditions, there was an average of 28 seeds per spike, while after PMC meiosis heat stress this was reduced to 12 and after pollen mitosis heat stress to 13. These results contrasted with the lack of pollen and severe defects in pollen viability described above. However, it likely reflects variation in the response of different florets on each spike (depending on position) and different tillers depending on their developmental stage

To partially address this variability, all tagged heads from the plants were harvested and the percentage of sterility was determined on a tiller-by-tiller basis for each heat treatment and in control conditions for all varieties. A Kruskal-Wallis test was used to compare between treatments and between varieties (Figures 4, 5). Even though some spikes showed significant levels of sterility in Optic, consistent with the overall analysis, there was no significant difference in the percentage of sterility between PMC meiosis heat treatment and control conditions. There was however a difference between pollen mitosis heat treatment and control conditions, showing a significant increase in sterility (Figure 4A). In Moonshine there was no significant difference between both heat treatments and the control conditions, despite the majority of PMC meiosis heat treated tillers exhibiting 100% sterility. In this case, overall significance was likely confounded by a small sample size and a single tiller that showed relatively normal fertility (Figure 4B). In contrast, Moonshine did appear to be particularly tolerant to heat treatment at the pollen mitosis stage. In RGT Planet the sterility was significantly different between both heat treatments and the control (Figure 4C). Comparison between varieties showed that there was no significant difference after PMC meiosis heat stress (Figure 4B). After pollen mitosis heat treatment there was no significant difference between Moonshine and RGT Planet, but there was a significant difference between Moonshine or RGT Planet and Optic, the latter having increased sterility compared to the other two varieties. In control conditions Moonshine and Optic showed similar yields, while RGT Planet had a significantly higher yield.

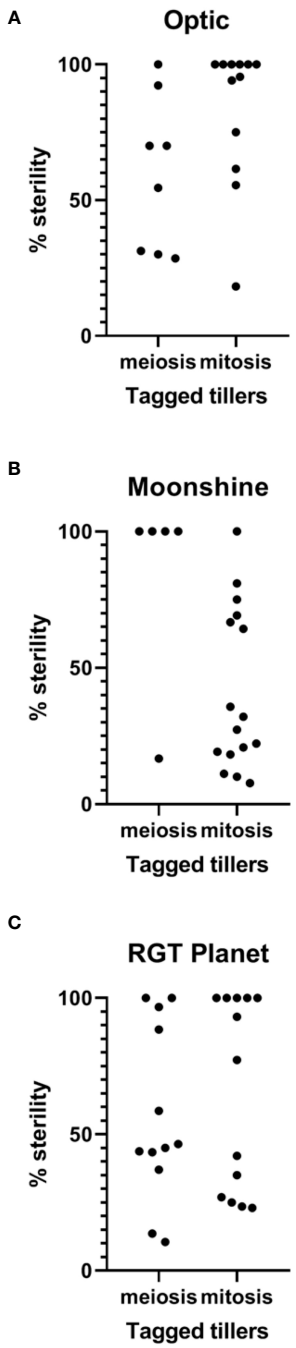

FIGURE 4
Sterility in heat stressed and control conditions in three European barley varieties. Percentage of sterility was calculated for all tillers for all three varieties after PMC meiosis and pollen mitosis heat treatments for **(A)** Optic **(B)** Moonshine and **(C)** RGT Planet. Kruskal-Wallis test was used to determine significance of difference between varieties and between treatments. All analysis was based upon based upon at least three biological replicates.

3.5 Genes encoding heat stress proteins, HvHSP17.8 and HvHSP70, are induced after heat stress applied during mitosis

To determine the impact of heat stress on gene expression, two well characterized Arabidopsis heat stress proteins were investigated in barley; *HvHSP17.8* is a small heat shock protein (sHSP) involved in protein stability, while *HvHSP70* is a chaperone involved in protein folding (Hartl, 1996; Wang et al., 2004). The putative barley orthologues of the two *Arabidopsis* heat stress genes [*HvHSP17.8* and *HvHSP70*, identified by BLAST and multiple alignment analysis (Supplementary Figure S2)] were analysed in florets as exemplars of gene expression changes after heat stress. The relative expression of *HvHSP17.8* and *HvHSP70* was examined

on the first and last day (day 5) of pollen mitosis heat stress for all three varieties and control plants (Figure 6). *HvHSP17.8* was significantly upregulated after one day of heat stress in Optic and RGT Planet, but not in Moonshine. Expression of *HvHSP17.8* had returned to the minimal background level after five days of heat stress. *HvHSP70* was upregulated in all three varieties after one day of heat stress, most significantly in RGT Planet. Although *HvHSP70* expression decreased after five days of heat stress, it was still upregulated in all three cultivars compared to the controls.

4 Discussion

Three elite barley varieties were assessed for their response to heat stress during floret development. In all cases, plants that experienced heat stress at two key stages (PMC meiosis and pollen mitosis) showed severe morphological deficiencies in anther development, and these are likely to be a leading cause of sterility due to high temperature stress. A short period of heat stress during early floret development resulted in significantly smaller and deformed anthers. Although the anthers were harvested at the same time from heat stressed and control plants, the septa in the heat stressed anthers had already broken, suggesting a more rapid developmental progression and/or a change in the physical properties of the anther walls. It has been suggested that thick locule walls and well-developed cavities in the septa may be responsible for heat tolerance in rice (Matsui et al., 2001). The cavities are hypothesised to enable easy rupture of the septa in response to the swelling of the pollen grains, while the thick locule walls promote the swelling of the pollen grains by retaining water in the locules (Matsui et al., 2001). In the anthers examined here, the locule walls and cavities seemed less developed in the heat stressed plants, which might be another reason why the pollen grains did not develop correctly.

Saini et al. (1984) described two types of anther defects after heat stress in wheat. Type 1 typically had premature tapetal degeneration which resulted in periplasmodial invasion of the locule at meiosis and ultimately led to sterility. Degeneration of the outer layers of the anther wall was also observed. The second type was characterised by microspores that completed pollen grain mitosis I (PGM1), but a proportion of which became disoriented from the tapetum and developed no further. The breakage of the septa identified in heat-stressed barley might also be attributed to the fragility of the anther walls, as we observed some degeneration of anther wall layers in the immunolabelled images from RGT Planet.

In addition to defects in anther morphology, pollen development was severely affected by heat stress during both PMC meiosis and pollen mitosis, with decreased viability, pollen count, and accumulation of starch. However, as shown by the X-ray micro CT images of Moonshine florets after PMC meiosis heat stress, and by the presence of viable pollen in Optic after meiosis heat stress, pollen is still formed in some heat-stressed florets and, based on KI staining and seed counts, some may be

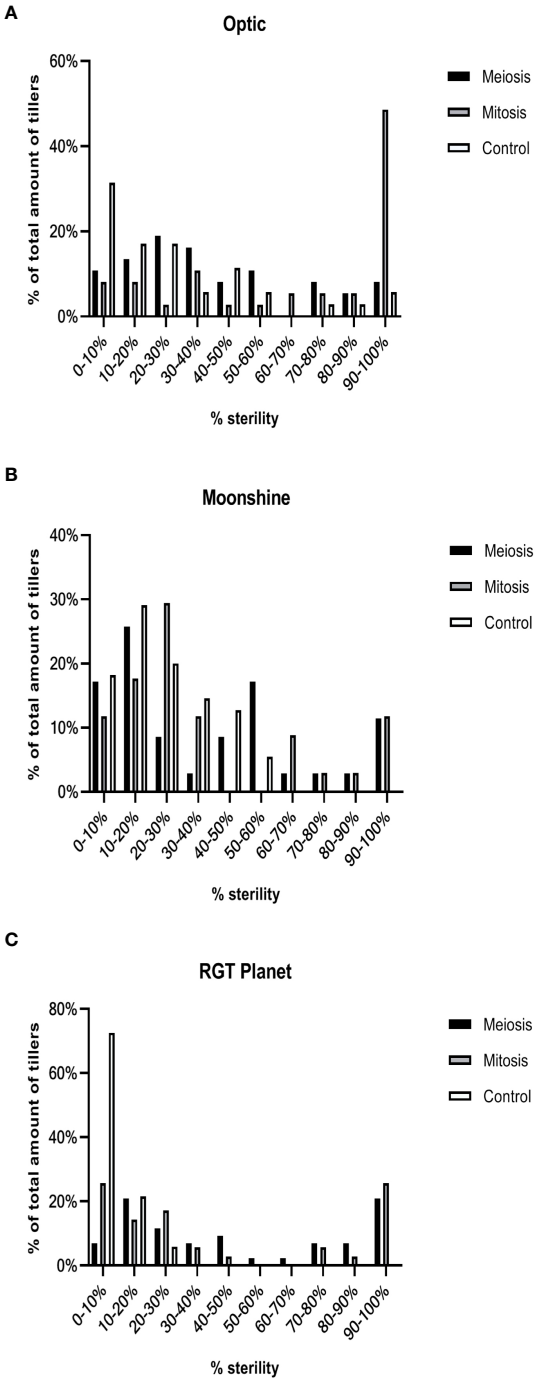

FIGURE 5
Frequency distribution of sterility in heat stressed and control conditions in three European barley varieties. The percentage sterility (florets that did not produce seed) was calculated for all three varieties in control conditions and after meiosis or mitosis I & II heat treatment for all pots **(A–C)**.

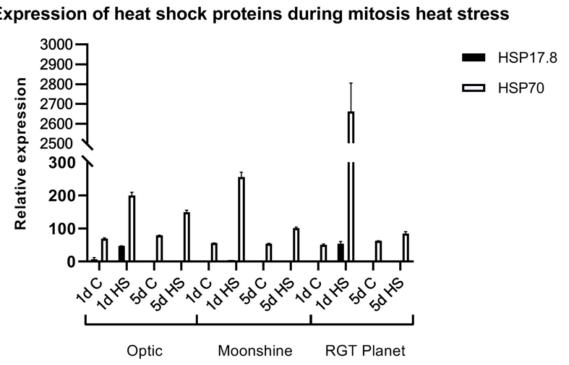

FIGURE 6
Expression of Heat Stress Proteins, HvHSP17.8 and HvHSP70, in florets of three European barley varieties, Optic, Moonshine and RGT Planet, during heat stress at the pollen mitosis I & II stages. C: control no heat stress; 1 and 5 days heat stress. Error bars indicate standard error, based upon at least three biological replicates.

viable. The absence of pollen detected in anthers during immunolabelling may be due to early anther rupture and loss of pollen during fixation and embedding. Alternatively, many florets may lack pollen entirely, and pollen is only released from some florets that avoid stress based on their position within the spike and their stage of development, which varies between the central and terminal regions. This highlights the importance of optimising non-destructive X-ray CT to assess anther development along the spike *in vivo* after heat stress.

Despite apparent contradictions between the immunolabelling experiments, KI staining assays, and CT data in regard to pollen grain number and viability after heat stress, seed set was used as a functional output of floret fertility. This varied between the treatments and cultivars. In Moonshine, overall seed set was significantly reduced across many tillers after heat treatment at PMC meiosis or pollen mitosis, but analysis of individual spikes suggested that Moonshine was more resilient against heat stress at the pollen mitosis stage. Optic, on the other hand, showed no significant response to heat stress at PMC meiosis, but was strongly sensitive at pollen mitosis. In contrast, RGT Planet was sensitive to heat stress at both PMC meiosis and mitosis stages of pollen development. These results potentially reveal different temporal sensitivities to heat stress in three elite barley cultivars.

The reduction in floret fertility and seed number may result from multiple defects in the pollen after heat stress. This includes reduced starch accumulation, which was observed in Optic pollen after heat stress at pollen mitosis. It has been suggested that stresses such as water stress can inhibit starch deposition in rice and wheat pollen, either by decreasing the availability of assimilates or by impairing the activities of enzymes involved in starch biosynthesis (Sheoran and Saini, 1996; Ji et al., 2010). Pressman et al. (2002) found that continuous high temperatures prevented the transient increase in starch concentration in tomato pollen grains which led to decreases in the concentrations of soluble sugars in the anther walls and the pollen. They concluded that this might contribute to decreased pollen viability in tomato after heat stress. This has been confirmed in other species, such as sorghum (Jain et al., 2007), and has been supported by evidence that barley grains from heat stressed plants accumulated less starch than grains from control plants due to reduced conversion of sucrose to starch (Wallwork et al., 1998). Heat stress has been reported to have a negative effect on the activities of enzymes involved in the sucrose-to-starch metabolism in cereals which might explain the reduction in starch content (Duke and Doehlert, 1996; Wilhelm et al., 1999; Hurkman et al., 2003).

The female reproductive organs did not show any significant differences in embryo sac phenotypes after heat stress. However, the carpels were bigger, possibly as a result of swelling of the unfertilized ovaries similar to that observed in wheat (Okada et al., 2018). Moreover, the carpels and ovules appeared to have developed faster than the controls. This suggests that in the three varieties under examination, the female reproductive organs are not as severely impacted by heat stress as anthers at the PMC meiotic and pollen mitotic stages of development, but advance more quickly through development. The broken septa in the anthers in the heat stressed plants also indicate that plants exposed to short pulse of heat stress around PMC meiosis might respond by speeding up reproductive organ development. A similar phenomenon was previously reported where heat stress hastened spike development and reduced spike number, thus impacting the number of grains per spike (Halse and Weir, 1974; Saini and Aspinall, 1982; Johnson and Kanemasu, 1983).

Several studies indicate that both pre- and post-fertilisation stages of ovary development are sensitive to stress, but this varies depending on the species and genotype (Sun et al., 2004; Zinn et al., 2010; Bac-Molenaar et al., 2015; Onyemaobi et al., 2017). In wheat, plants exposed to severe heat stress at the start of meiosis experienced disrupted nucellus and integument development, and complete ovule abortion at a frequency of 30% (Saini et al., 1983). In contrast, little is known about the effects of abiotic stress on cellular morphology and the regulatory network of the carpel and ovule in barley. The nucellar cells in all three barley cultivars examined here, particularly Optic, appeared to be disorganised and enlarged after heat stress relative to controls. However, in all cases, similar immunolabelling patterns for de-esterified homogalacturonan were observed around what appeared to be an intact embryo sac. Barley only has one ovule per floret and therefore needs to safeguard its one chance of survival. The multi-layered nucellus might be one of the reasons the developmental program of the ovule is more robust than that of the anther (Wilkinson et al., 2018).

The expression of two heat shock protein genes, *HvHSP17.8* and *HvHSP70*, were upregulated after heat stress. *HvHSP17.8* is a small heat shock protein (sHSP) that assists in preventing

aggregation and stabilizing proteins while *HvHSP70* is a chaperone that assists in protein folding processes (Hartl, 1996; Wang et al., 2004). Both genes have been shown to be upregulated under stress conditions and to confer heat stress tolerance (Sung et al., 2001; Guo et al., 2009; Montero-Barrientos et al., 2010). *HvHSP70* was upregulated in all three varieties after one day and also after five days of heat stress (Figure 6). *HvHSP70* expression showed a peak after one day of pollen mitosis heat stress in RGT Planet, with much higher expression than in the other two varieties. Optic showed the least amount of upregulation of *HvHSP70*, which correlated with the elevated level of sterility in this cultivar after pollen mitosis heat stress. In contrast, *HvHSP17.8* was upregulated in Optic and RGT Planet after one day of heat stress at the pollen mitosis stage, but levels were indistinguishable from controls after five days of heat stress. This might indicate that *HvHSP17.8* is involved in the early response to heat stress. Curiously, a significant increase in *HvHSP17.8* was not observed in Moonshine despite this cultivar appearing to be less susceptible to heat-stress at the pollen mitosis stage. One possibility is that the timing of *HvHSP17.8* induction differs in Moonshine; alternatively, other HSPs may be induced and contribute to the higher levels of stress tolerance observed in this cultivar.

5 Conclusions

A short period of heat stress during the reproductive phase in barley is detrimental for the development of the male reproductive organs, but less so for the female reproductive organs. Results indicate that after heat stress, floret development was generally hastened, which might reflect an overall stress response from the plant to ensure seed set, albeit with a smaller amount of seeds. Prolonged heat stress at a later stage in development (pollen mitosis) showed more severe effects in the male reproductive organs in Optic than in the other two varieties, with no viable pollen and significantly more sterility. The female reproductive organs of the three cultivars showed no severe effects after heat stress, at least in terms of embryo sac expansion. Overall, RGT Planet performed worst compared to the control conditions, whilst Moonshine performed best. However, there were less florets per spike in the heat stressed plants across all three varieties compared to control plants. Further investigation will be required to identify the traits that contribute to Moonshine being more heat tolerant than the other two varieties. The data provided here provides a basis for further studies into differential heat stress responses during key stages of barley reproductive development. Moreover, the use of X-ray imaging is a promising new method to visualise the morphology of floret organs without dissection and manipulation with chemicals, giving a more representative image and accurate volume measurements. Further work is needed to determine how the impact of the heat stress observed here equates to that under field conditions and the resultant potential consequences for yield loss. Nevertheless, significant yield reductions have been observed (Jacott and Boden, 2020), so it seems likely that equivalent impacts will be seen. The lines used here our elite cultivars that have not been particularly developed for heat stress resilience. However, the impact of the heat stress observed here can provide a basis for trait targeting for increasing future crop resilience.

Data availability statement

The original contributions presented in the study are included in the article/Supplementary Material. Further inquiries can be directed to the corresponding author.

Author contributions

CC, ZW, and DZ conceived the study. CC carried out the majority of experiments and data analysis. JFG assisted with plant maintenance and spike analysis. MT assisted with immunolabelling. All authors contributed to the article and approved the submitted version.

Funding

CC was supported by a Dual PhD scholarship from The University of Nottingham and University of Adelaide. This work was supported by the Australian Research Council (DZ, DP170103352; MT, FT140100780), an Australia-China Science and Research Fund Joint Research Centre grant ACSRF48187, the National Key Technologies Research and Development Program of China, Ministry of Science and Technology (grant no. 2016YFD 0100804; 2016YFE0101000), and the National Natural Science Foundation of China (NSFC) (31230051).

Acknowledgments

The authors wish to thank members of the Wilson, Zhang and Tucker laboratories for fruitful discussions and suggestions regarding experiments. In particular we thank Dr Laura Wilkinson for assisting with immunolabelling experiments.

Conflict of interest

The authors declare that the research was conducted in the absence of any commercial or financial relationships that could be construed as a potential conflict of interest.

Publisher's note

Supplementary material

The Supplementary Material for this article can be found online at: https://www.frontiersin.org/articles/10.3389/fpls.2022.918730/full#supplementary-material

SUPPLEMENTARY FIGURE 1
Schematic of heat stress treatments during pollen development for barley varieties and pollen viability in barley cultivars Optic, Moonshine and RGT Planet. **(A)** Two pots with four plants each of the three varieties were submitted to either meiosis heat stress during meiosis I and II of pollen development, or mitosis heat stress during mitosis I and II of pollen development. **(B)** Pollen viability is shown from a randomly selected floret right before anthesis from heat stressed plants and control plants. Black pollen is viable, while yellow/brown pollen is not viable; low numbers of pollen reflect the lack of pollen in the mature anthers.

SUPPLEMENTARY FIGURE 2
Phylogenetic analysis of rice, Arabidopsis and barley HSP17.8 **(A)** and HSP70 orthologs **(B)**. The alignments were constructed using the Geneious alignment method and the Blosum62 cost matrix in Geneious. **(C D)** Phylogenetic tree of Arabidopsis BLAST analysis HSP17.8 **(C)** and HSP70 **(D)**.

SUPPLEMENTARY FIGURE 3
X-ray CT images of anther and carpel development in control and heat stress conditions for Moonshine. X-ray images of the anthers and carpels obtained by X-ray CT are compared for control environment and heat stress environment (heat stress during meiosis of pollen development) right before anthesis.

SUPPLEMENTARY FIGURE 4
Immunolabelling of cell wall components in anthers and ovules in Optic. Comparison of control and heat stressed anthers and ovules in barley florets of the variety RGT Planet. Antibodies include BG1 (1,3;1,4-β-glucan, green) and LM19 (low methylesterified pectin, red). Calcofluor White counterstain was used to detect cellulose and mixed-linkage glucan (blue).

SUPPLEMENTARY FIGURE 5
Immunolabelling of cell wall components in anthers and ovules in Moonshine. Comparison of control and heat stressed anthers and ovules in barley florets of the variety RGT Planet. Antibodies include BG1 (1,3;1,4-β-glucan, green) and LM19 (low methylesterified pectin, red). Calcofluor White counterstain was used to detect cellulose and mixed-linkage glucan (blue).

SUPPLEMENTARY FIGURE 6
Immunolabelling of cell wall components in anthers and ovules in RGT Planet. Comparison of control and heat stressed anthers and ovules in barley florets of the variety RGT Planet. Antibodies include BG1 (1,3;1,4-β-glucan, green) and LM19 (low methylesterified pectin, red). Calcofluor White counterstain was used to detect cellulose and mixed-linkage glucan (blue).

References

Aditya, J., Lewis, J., Shirley, N., Tan, H.-T., Henderson, M., Fincher, G., et al (2015). The dynamics of cereal cyst nematode infection differ between susceptible and resistant barley cultivars and lead to changes in (1,3;1,4)-β-glucan levels and HvCslF gene transcript abundance. *New Phytol.* 207, 135–147. doi: 10.1111/nph.13349

Aghamolki, M. T. K., Yusop, M. K., Oad, F. C., Jaafar, H. Z., Khalatbari, A. M., Kharidah, S., et al. (2016). Impact of heat stress on growth and yield of rice (Oryza sativa l.) cultivars. *J. Food Agric. Environ.* 14, 111–116.

AHDB (2016). AHDB recommended lists 2016-2017. Available at: https://ahdb.org.uk/knowledge-library/recommended-lists-for-cereals-and-oilseeds-rl.

AHDB (2017). Spring barley harvest results 2017. Available at: https://ahdb.org.uk/knowledge-library/recommended-lists-for-cereals-and-oilseeds-rl.

Bac-Molenaar, J. A., Fradin, E. F., Becker, F. F. M., Rienstra, J. A., van der Schoot, J., Vreugdenhil, D., et al. (2015). Genome-wide association mapping of fertility reduction upon heat stress reveals developmental stage-specific QTLs in arabidopsis thaliana. *Plant Cell* 27, 1857–1874. doi: 10.1105/tpc.15.00248

Barnabas, B., Jager, K., and Feher, A. (2008). The effect of drought and heat stress on reproductive processes in cereals. *Plant Cell Environ.* 31, 11–38.

Bita, C. E., and Gerats, T. (2013). Plant tolerance to high temperature in a changing environment: scientific fundamentals and production of heat stress-tolerant crops. *Front. Plant Sci.* 4, 273. doi: 10.3389/fpls.2013.00273

Bomblies, K., Higgins, J. D., and Yant, L. (2015). Meiosis evolves: adaptation to external and internal environments. *New Phytol.* 208, 306–323. doi: 10.1111/nph.13499

Burton, R. A., Collins, H. M., Kibble, N. A., Smith, J. A., Shirley, N. J., Jobling, S. A., et al. (2011). Over-expression of specific HvCslF cellulose synthase-like genes in transgenic barley increases the levels of cell wall (1,3;1,4)-beta-d-glucans and alters their fine structure. *Plant Biotechnol. J.* 9, 117–135. doi: 10.1111/j.1467-7652.2010.00532.x

Chang, F., Zhang, Z., Jin, Y., and Ma, H. (2014). "Cell biological analyses of anther morphogenesis and pollen viability in arabidopsis and rice," in *Flower development: Methods and protocols*. Eds. J. L. Riechmann and F. Wellmer (New York, NY: Springer New York) 203–216.

Christidis, N., Jones, G. S., and Stott, P. A. (2014). Dramatically increasing chance of extremely hot summers since the 2003 European heatwave. *Nat. Climate Change* 5, 46.

Cooper, P., Ho, T.-H. D., and Hauptmann, R. M. (1984). Tissue specificity of the heat-shock response in maize. *Plant Physiol.* 75, 431. doi: 10.1104/pp.75.2.431

David, B. L., and Christopher, B. F. (2007). Global scale climate–crop yield relationships and the impacts of recent warming. *Environ. Res. Lett.* 2, 014002. doi: 10.1088/1748-9326/2/1/014002

Delphine, D., Declan, C., Navin, R., Jeff, P., and Rachel, W. (2014). Global crop yield response to extreme heat stress under multiple climate change futures. *Environ. Res. Lett.* 9, 034011. doi: 10.1088/1748-9326/9/3/034011

Draeger, T., and Moore, G. (2017). Short periods of high temperature during meiosis prevent normal meiotic progression and reduce grain number in hexaploid wheat (Triticum aestivum l.). *Theor. Appl. Genet.* 130, 1785–1800. doi: 10.1007/s00122-017-2925-1

Duke, E. R., and Doehlert, D. C. (1996). Effects of heat stress on enzyme activities and transcript levels in developing maize kernels grown in culture. *Environ. Exp. Bot.* 36, 199–208. doi: 10.1016/0098-8472(96)01004-0

Ejaz, M., and von Korff, M. (2017). The genetic control of reproductive development under high ambient temperature. *Plant Physiol.* 173, 294–306. doi: 10.1104/pp.16.01275

Farooq, M., Bramley, H., Palta, J. A., and Siddique, K. H. M. (2011). Heat stress in wheat during reproductive and grain-filling phases. *Crit. Rev. Plant Sci.* 30, 491–507. doi: 10.1080/07352689.2011.615687

Feder, M. E., and Hofmann, G. E. (1999). HEAT-SHOCK PROTEINS, MOLECULAR CHAPERONES, AND THE STRESS RESPONSE: Evolutionary and ecological physiology. *Annu. Rev. Physiol.* 61, 243–282. doi: 10.1146/annurev.physiol.61.1.243

Gómez, J. F., and Wilson, Z. A. (2012). Non-destructive staging of barley reproductive development for molecular analysis based upon external morphology. *J. Exp. Bot.* 63, 4085–4094. doi: 10.1093/jxb/ers092

Guo, P., Baum, M., Grando, S., Ceccarelli, S., Bai, G., Li, R., et al. (2009). Differentially expressed genes between drought-tolerant and drought-sensitive barley genotypes in response to drought stress during the reproductive stage. *J. Exp. Bot.* 60, 3531–3544. doi: 10.1093/jxb/erp194

Halse, N. J., and Weir, R. N. (1974). Effects of temperature on spikelet number of wheat. *Aust. J. Agric. Res.* 25, 687–695. doi: 10.1071/AR9740687

Hartl, F. U. (1996). Molecular chaperones in cellular protein folding. *Nature* 381, 571. doi: 10.1038/381571a0

Hemming, M. N., Walford, S. A., Fieg, S., Dennis, E. S., and Trevaskis, B. (2012). Identification of high-temperature-responsive genes in cereals. *Plant Physiol.* 158, 1439–1450. doi: 10.1104/pp.111.192013

Hong, S.-W., and Vierling, E. (2000). Mutants of arabidopsis thaliana defective in the acquisition of tolerance to high temperature stress. *Proc. Natl. Acad. Sci. United States America* 97, 4392–4397.

Hurkman, W. J., McCue, K. F., Altenbach, S. B., Korn, A., Tanaka, C. K., Kothari, K. M., et al. (2003). Effect of temperature on expression of genes encoding enzymes for starch biosynthesis in developing wheat endosperm. *Plant Sci.* 164, 873–881. doi: 10.1016/S0168-9452(03)00076-1

IPCC (2014). "Climate change 2014: Mitigation of climate change. contribution of working group III to the fifth assessment report of the intergovernmental panel on climate change,". Eds. O. Edenhofer, R. Pichs-Madruga, Y. Sokona, E. Farahani, S. Kadner, K. Seyboth, A. Adler, I. Baum, S. Brunner, P. Eickemeier, B. Kriemann, J. Savolainen, S. Schlömer, C. von Stechow, T. Zwickel and J. C. Minx (Cambridge, United Kingdom and New York, NY, USA: Cambridge University Press).

Jacott, C. N., and Boden, S. A. (2020). Feeling the heat: developmental and molecular responses of wheat and barley to high ambient temperatures. *J. Exp. Bot.* 71, 5740–5751. doi: 10.1093/jxb/eraa326

Jain, M., Prasad, P. V., Boote, K. J., Hartwell, A. L.Jr., and Chourey, P. S. (2007). Effects of season-long high temperature growth conditions on sugar-to-starch metabolism in developing microspores of grain sorghum (Sorghum bicolor l. moench). *Planta* 227, 67–79. doi: 10.1007/s00425-007-0595-y

Ji, X., Shiran, B., Wan, J., Lewis, D. C., Jenkins, C. L. D., Condon, A. G., et al. (2010). Importance of pre-anthesis anther sink strength for maintenance of grain number during reproductive stage water stress in wheat. *Plant Cell Environ.* 33, 926–942. doi: 10.1111/j.1365-3040.2010.02130.x

Johnson, R. C., and Kanemasu, E. T. (1983). Yield and development of winter wheat at elevated Temperatures1. *Agron. J.* 75, 561–565. doi: 10.2134/agronj1983.00021962007500030033x

Kruszka, K., Pacak, A., Swida-Barteczka, A., Nuc, P., Alaba, S., Wroblewska, Z., et al. (2014). Transcriptionally and post-transcriptionally regulated microRNAs in heat stress response in barley. *J. Exp. Bot.* 65, 6123–6135. doi: 10.1093/jxb/eru353

Kupke, B. M., Tucker, M. R., Able, J. A., and Porker, K. D. (2022). Manipulation of barley development and flowering time by exogenous application of plant growth regulators. *Front. Plant Sci.* 12, 694424. doi: 10.3389/fpls.2021.694424

Lesk, C., Rowhani, P., and Ramankutty, N. (2016). Influence of extreme weather disasters on global crop production. *Nature* 529, 84. doi: 10.1038/nature16467

Maestri, E., Klueva, N., Perrotta, C., Gulli, M., Nguyen, H. T., and Marmiroli, N. (2002). Molecular genetics of heat tolerance and heat shock proteins in cereals. *Plant Mol. Biol.* 48, 667–681. doi: 10.1023/A:1014826730024

Mascarenhas, J. P., and Crone, D. E. (1996). Pollen and the heat shock response. *Sexual Plant Reprod.* 9, 370–374. doi: 10.1007/BF02441959

Matsui, T., Omasa, K., and Horie, T. (2001). The difference in sterility due to high temperatures during the flowering period among japonica-rice varieties. *Plant Product. Sci.* 4, 90–93. doi: 10.1626/pps.4.90

Meikle, P. J., Hoogenraad, N. J., Bonig, I., Clarke, A. E., and Stone, B. A. (1994). A (1–>3,1–>4)-beta-glucan-specific monoclonal antibody and its use in the quantitation and immunocytochemical location of (1–>3,1–>4)-beta-glucans. *Plant J.* 5, 1–9. doi: 10.1046/j.1365-313X.1994.5010001.x

Montero-Barrientos, M., Hermosa, R., Cardoza, R. E., Gutiérrez, S., Nicolás, C., and Monte, E. (2010). Transgenic expression of the trichoderma harzianum hsp70 gene increases arabidopsis resistance to heat and other abiotic stresses. *J. Plant Physiol.* 167, 659–665. doi: 10.1016/j.jplph.2009.11.012

Nguyen, H. T., Joshi, C. P., Klueva, N., Weng, J., Hendershot, K. L., and Blum, A. (1994). The heat-shock response and expression of heat-shock proteins in wheat under diurnal heat stress and field conditions. *Funct. Plant Biol.* 21, 857–867. doi: 10.1071/PP9940857

Okada, T., Jayasinghe, JEARM, Nansamba, M., Baes, M., Warner, P., Kouidri, A., et al. (2018). Unfertilized ovary pushes wheat flower open for cross-pollination. *J. Exp. Bot.* 69, 399–412. doi: 10.1093/jxb/erx410

Onyemaobi, I., Liu, H., Siddique, K. H. M., and Yan, G. (2017). Both Male and female malfunction contributes to yield reduction under water stress during meiosis in bread wheat. *Front. Plant Sci.* 7. doi: 10.3389/fpls.2016.02071

Ortiz, R., Sayre, K. D., Govaerts, B., Gupta, R., Subbarao, G. V., Ban, T., et al. (2008). Climate change: Can wheat beat the heat? *Agricult. Ecosyst. Environ.* 126, 46–58. doi: 10.1016/j.agee.2008.01.019

Prasad, P. V. V., Pisipati, S. R., Mutava, R. N., and Tuinstra, M. R. (2008). Sensitivity of grain sorghum to high temperature stress during reproductive development. *Crop Sci.* 48, 1911–1917. doi: 10.2135/cropsci2008.01.0036

Pressman, E., Peet, M. M., and Pharr, D. M. (2002). The effect of heat stress on tomato pollen characteristics is associated with changes in carbohydrate concentration in the developing anthers. *Ann. Bot.* 90, 631–636. doi: 10.1093/aob/mcf240

Saini, H. S., and Aspinall, D. (1982). Abnormal sporogenesis in wheat (Triticum aestivum l.) induced by short periods of high temperature. *Ann. Bot.* 49, 835–846. doi: 10.1093/oxfordjournals.aob.a086310

Saini, H., Sedgley, M., and Aspinall, D. (1983). Effect of heat stress during floral development on pollen tube growth and ovary anatomy in wheat (<I>Triticum aestivum</I> l.). *Funct. Plant Biol.* 10, 137–144. doi: 10.1071/PP9830137

Saini, H. S., Sedgley, M., and Aspinall, D. (1984). Development anatomy in wheat of Male sterility induced by heat stress, water deficit or abscisic acid. *Funct. Plant Biol.* 11, 243–253. doi: 10.1071/PP9840243

Sakata, T., Takahashi, H., Nishiyama, I., and Higashitani, A. (2000). Effects of high temperature on the development of pollen mother cells and microspores in barley hordeum vulgare l. *J. Plant Res.* 113. doi: 10.1007/PL00013947

SeedForce (2017).

Sheoran, I. S., and Saini, H. S. (1996). Drought-induced male sterility in rice: Changes in carbohydrate levels and enzyme activities associated with the inhibition of starch accumulation in pollen. *Sexual Plant Reprod.* 9, 161–169. doi: 10.1007/BF02221396

Stone, P., and Basra, A. (2001). "The effects of heat stress on cereal yield and quality," in *Crop responses and adaptations to temperature stress* (Binghampton: NY Food Products Press), 179–187.

Sung, D. Y., Vierling, E., and Guy, C. L. (2001). Comprehensive expression profile analysis of the arabidopsis Hsp70 gene family. *Plant Physiol.* 126, 789–800. doi: 10.1104/pp.126.2.789

Sun, K., Hunt, K., and Hauser, B. A. (2004). Ovule abortion in arabidopsis triggered by stress. *Plant Physiol.* 135, 2358–2367. doi: 10.1104/pp.104.043091

Teixeira, E. I., Fischer, G., van Velthuizen, H., Walter, C., and Ewert, F. (2013). Global hot-spots of heat stress on agricultural crops due to climate change. *Agric. For. Meteorol.* 170, 206–215. doi: 10.1016/j.agrformet.2011.09.002

Tracy, S. R., Gómez, J. F., Sturrock, C. J., Wilson, Z. A., and Ferguson, A. C. (2017). Non-destructive determination of floral staging in cereals using X-ray micro computed tomography (μCT). *Plant Methods* 13, 9. doi: 10.1186/s13007-017-0162-x

Verhertbruggen, Y., Marcus, S. E., Haeger, A., Ordaz-Ortiz, J. J., and Knox, J. P. (2009). An extended set of monoclonal antibodies to pectic homogalacturonan. *Carbohydr. Res.* 344, 1858–1862. doi: 10.1016/j.carres.2008.11.010

Wallwork, M. A. B., Logue, S. J., MacLeod, L. C., and Jenner, C. F. (1998). Effect of high temperature during grain filling on starch synthesis in the developing barley grain. *Funct. Plant Biol.* 25, 173–181. doi: 10.1071/PP97084

Wang, W., Vinocur, B., Shoseyov, O., and Altman, A. (2004). Role of plant heat-shock proteins and molecular chaperones in the abiotic stress response. *Trends Plant Sci.* 9, 244–252. doi: 10.1016/j.tplants.2004.03.006

Wilhelm, E. P., Mullen, R. E., Keeling, P. L., and Singletary, G. W. (1999). Heat stress during grain filling in maize: Effects on kernel growth and metabolism. *Crop Sci.* 39, 1733–1741. doi: 10.2135/cropsci1999.3961733x

Wilkinson, L. G., Bird, D. C., and Tucker, M. R. (2018). Exploring the role of the ovule in cereal grain development and reproductive stress tolerance. *Annu. Plant Rev. online*. doi: 10.1002/9781119312994.apr0609

Wilson, Z. A., and Zhang, D.-B. (2009). From arabidopsis to rice: pathways in pollen development. *J. Exp. Bot.* 60, 1479–1492. doi: 10.1093/jxb/erp095

Zampieri, M., Ceglar, A., Dentener, F., and Toreti, A. (2017). Wheat yield loss attributable to heat waves, drought and water excess at the global, national and subnational scales. *Environ. Res. Lett.* 12, 064008. doi: 10.1088/1748-9326/aa723b

Zinn, K. E., Tunc-Ozdemir, M., and Harper, J. F. (2010). Temperature stress and plant sexual reproduction: uncovering the weakest links. *J. Exp. Bot.* 61, 1959–1968. doi: 10.1093/jxb/erq053

frontiers | Frontiers in Plant Science

TYPE Original Research
PUBLISHED 24 November 2023
DOI 10.3389/fpls.2023.1284573

OPEN ACCESS

EDITED BY
David Horvath,
Agricultural Research Service (USDA),
United States

REVIEWED BY
Federica Zanetti,
Università di Bologna, Italy
James Anderson,
Agricultural Research Service (USDA),
United States

*CORRESPONDENCE
Satya Swathi Nadakuduti
s.nadakuduti@ufl.edu

RECEIVED 28 August 2023
ACCEPTED 10 November 2023
PUBLISHED 24 November 2023

CITATION
Nadakuduti SS, Laforest LC, Tachev M, Decker AN, Egesa AO, Shirazi AS, Begcy K, Sarnoski PJ and Buell CR (2023) Heat stress during seed development leads to impaired physiological function and plasticity in seed oil accumulation in *Camelina sativa*.
Front. Plant Sci. 14:1284573.
doi: 10.3389/fpls.2023.1284573

Heat stress during seed development leads to impaired physiological function and plasticity in seed oil accumulation in *Camelina sativa*

Satya Swathi Nadakuduti[1,2,3]*, Larissa C. Laforest[2], Megan Tachev[1], Amanda N. Decker[1], Andrew Ogolla Egesa[1], Ashkon S. Shirazi[3], Kevin Begcy[1,2], Paul J. Sarnoski[4] and C. Robin Buell[5,6,7]

[1]Environmental Horticulture Department, University of Florida, Gainesville, FL, United States, [2]Plant Molecular and Cellular Biology Program, University of Florida, Gainesville, FL, United States, [3]The Student Science Training Program, Center for Precollegiate Education and Training, University of Florida, Gainesville, FL, United States, [4]Food Science and Human Nutrition Department, University of Florida, Gainesville, FL, United States, [5]Department of Crop and Soil Sciences, University of Georgia, Athens, GA, United States, [6]Center for Applied Genetic Technologies, University of Georgia, Athens, GA, United States, [7]Institute of Plant Breeding, Genetics and Genomics, University of Georgia, Athens, GA, United States

Camelina sativa, a member of the Brassicaceae, is a low-cost, renewable oilseed crop that produces seeds up to 40% oil by weight with high potential for use in food, feed, and biofuel applications. Camelina seeds contain high levels of the fatty acids α-linolenic acid (C18:3), linoleic acid (C18:2), oleic acid (C18:1), and gondoic acid (C20:1), which have high nutritional and industrial value. The impact of climate change, especially increased frequency and amplitude of heat waves, poses a serious threat to crop productivity. In this study, we evaluated the effect of elevated temperatures post-anthesis on the developing seeds of *C. sativa* and performed physiological, morphological, and chemical characterizations at 7, 14, 21, and 28 days post-anthesis (DPA), as well as at maturity. While the seed oil accumulation peaked at 21 DPA under control conditions, reaching 406mg/g dry weight, under heat stress it was only 186mg/g. Physiologically, transpiration rate (E) and internal CO_2 concentration (Ci) increased between 2 to 9 days post-stress imposition and overall net photosynthesis was impaired. Seed yield, seed weight, and oil content reduced by 84.5%, 38.5% and 54.1% respectively. We demonstrate that post-anthesis heat stress causes severe yield losses and developmental plasticity in fatty acid accumulation in oilseeds.

KEYWORDS

***Camelina sativa*, heat stress, seed oil, triacylglycerol, omega-3 fatty acid, photosynthesis, seed yield**

1 Introduction

Camelina sativa (L.) Crantz is an oil seed crop within the Brassicaceae family and produces seeds with up to 40% oil by weight (Rodríguez-Rodríguez et al., 2013; Berti et al., 2016). Camelina is a low-cost renewable crop with high potential for use as a biofuel, in addition to multiple uses in food, feed, and other biological applications. Not only does camelina have a short life cycle (85 to 100 days), it has the potential to expand crop production areas due to its ability to grow in semi-arid and drought prone areas with relatively infertile soils and minimal agricultural inputs (Vollmann and Eynck, 2015; Bansal and Durrett, 2016; Malik et al., 2018; Cappelli et al., 2019; Von Cossel et al., 2019; Zanetti et al., 2021). Due to its high yield, high seed oil levels with favorable fatty acid compositions, low production input costs, and amenability to genetic engineering, camelina is viewed as an optimal oilseed crop for biodiesel production (Stamenković et al., 2023). Seed development in oil seed crops especially in Brassicaceae has been characterized by three phases, I) growth phase, where rapid cell division occurs, II) accumulation phase, where seed oil and protein deposits are rapidly synthesized, and III) desiccation phase, where dehydration and seed maturation occurs (Gurr, 1980; Rodríguez-Rodríguez et al., 2013).

The major components of camelina seed oil are acyl lipids stored in the form of triacylglycerols (TAGs). TAGs are esters of glycerol, with each hydroxyl group esterified with a fatty acid (FA) at all three carbons. Due to their highly reduced state, TAGs represent compact molecules for carbon and energy storage in living organisms. *De novo* FA biosynthesis in plants occurs within the plastids, where acetyl CoA is used as the carbon precursor for the assembly of FAs. Acyl groups attached to acyl carrier proteins are elongated by sequential addition of 2 C units (Li-Beisson et al., 2013). The biosynthesis of TAGs occurs at the endoplasmic reticulum by sequential acylation and subsequent dephosphorylation of glycerol-3-phosphate (Li-Beisson et al., 2013). Diacylglycerol represents an important branch point between the synthesis of TAGs and membrane lipids. The last step in TAG synthesis involves the acylation of diacylglycerol using acyl CoAs or phosphatidylcholines as acyl donors (Li-Beisson et al., 2013; Mueller et al., 2017). Phosphatidylcholine is not only a major metabolic precursor for TAG synthesis but is also an abundant membrane lipid. The major flux in TAG synthesis (>95%) is associated with the diacylglycerol/phosphatidylcholine intermediate pool (Pollard and Shachar-Hill, 2022). Camelina TAGs have a high percent of polyunsaturated fatty acids (PUFAs) such as ω-3 FA, α-linolenic acid (C18:3, 19-43%) and ω-6 FA, linoleic acid (C18:2, 11-28%) (Vollmann and Eynck, 2015; Zanetti et al., 2017; Anderson et al., 2019; Hotton et al., 2020; Zanetti et al., 2021)) together constituting up to 50% of total fatty acids in camelina seed, followed by monounsaturated FAs (MUFAs).

Climate change is typically accompanied by an increase in the frequency, duration, and amplitude of droughts and heat waves (Zandalinas et al., 2021). Temperature is a major environmental factor that acts as an abiotic stressor; impacting plant growth and posing a major threat to crop productivity. High atmospheric temperatures have profound effects on the internal thermal environment of plants, altering the major physiological processes that dominate carbon fluxes, including photosynthesis, photorespiration, and respiration. In addition, a suite of stress-responsive organic compounds are formed under high temperatures, which consume substantial amounts of carbon (Dusenge et al., 2019). High temperatures have a detrimental effect on plant development, particularly on reproductive stages (Chen et al., 2016; Begcy et al., 2019b), impacting seed production and thus crop productivity. At the physiological level, high temperatures negatively affect the activity of photosynthetic enzymes (Jensen, 2000; Parrotta et al., 2020; Moore et al., 2021). Particularly, RUBISCO activity and its affinity for CO_2 decreases as temperature increases, affecting the overall plant photosynthetic capacity (Salvucci and Crafts-Brandner, 2004). Under heat stress (HS), an increased transpiration rate in response to high temperature works as an evaporative cooling mechanism to prevent thermal damage, a necessary trade-off with water conservation (Deva et al., 2020). However, excessive loss of water through elevated transpiration may surpass the plant's water uptake and transport, leading to wilting and closing of the stomata. The resulting decrease in CO_2 uptake has a clear effect on the net photosynthetic rate, and when accompanied by degradation of proteins and pigments due to heat damage, electron transport is impaired and photosystem I (PSI) and PSII are inactivated (Iqbal et al., 2021).

Plants have developed several adaptive responses to elevated and varying temperatures, including improved water use efficiency, decreased growth, early flowering, and modulation of plant membranes and storage lipids by triggering lipid-dependent signaling cascades (Zheng et al., 2011; Hou et al., 2016; Zhang and Sonnewald, 2017). As a result, investigating plant physiological responses to changing environmental factors, particularly from floral transition to seed set, is integral in adapting crop plants to combat for climate change. Specifically, high temperatures drastically affect plant reproductive stages impacting seed set, grain fill, and yield (Folsom et al., 2014; Lohani et al., 2022; Magno Massuia de Almeida et al., 2023) in addition to seed composition and quality (Elferjani and Soolanayakanahally, 2018; Alsajri et al., 2020; Brock et al., 2020; Ortiz et al., 2022). Although camelina has broad climatic adaptability, the resulting impact on seed oil yield and fatty acid profiles is key to its utility as a sustainable crop. Though limited agronomic studies have been performed in camelina, it is clear that temperature impacts oil yield and fatty acid composition of oil seeds (Vollmann and Eynck, 2015; Obour et al., 2017; Raziei et al., 2018; Krzyżaniak et al., 2019; Brock et al., 2020). Floral development and seed yield are strongly affected by temperature, with milder temperatures resulting in higher yields (Krzyżaniak et al., 2019; Zanetti et al., 2021). Furthermore, camelina accessions and cultivars grow in varying climatic niches throughout the globe, and temperature was found to elicit plasticity in seed oil in camelina (Brock et al., 2020) and other oil seed crops (Izquierdo et al., 2016; Xu et al., 2016; Alsajri et al., 2020; Nakagawa et al., 2020). *C. sativa* includes spring and winter biotypes, with spring biotypes being the most studied thus far since

winter biotypes required vernalization for flowering (Anderson et al., 2018; Malik et al., 2018). The majority of camelina accessions available and analyzed are spring biotypes (Hotton et al., 2020) and biochemical characterization of seed oil from multiple accessions indicated that the average FA profile has low levels of saturated FAs and higher levels of PUFAs (Rodríguez-Rodríguez et al., 2013; Hotton et al., 2020). Further, the predominant FAs and their proportions in total oil are consistent even among winter biotypes (Rodríguez-Rodríguez et al., 2013; Hotton et al., 2020). In the present study, we have chosen Suneson, a spring cultivar that is extensively used in biotechnology and genetic studies (Na et al., 2018; Ozseyhan et al., 2018; King et al., 2019; Na et al., 2019; Lhamo et al., 2020; Gomez-Cano et al., 2022; Bengtsson et al., 2023). We performed physiological, morphological, and chemical characterization of multiple camelina seed developmental stages to investigate the impact of post-anthesis HS on seed development and fatty acid accumulation.

2 Materials and methods

2.1 Plant material and growth conditions

Camelina sativa cv. Suneson plants were grown in a controlled environment growth chamber facility starting from seed at temperatures of 22/18°C (light/dark), 40% relative humidity with a photon flux density (PPFD) of 300 µmol m^{-2} s^{-1} under a 16h photoperiod. Flowers were marked at anthesis, and seeds were harvested for analysis at 7 days post anthesis (DPA), 14 DPA, 21 DPA, 28 DPA, and at full maturity directly into liquid nitrogen and stored at -80°C until processed. Mature seeds were collected when siliques dried out, and before seeds shed upon pod dehiscence. Anthesis was defined as a stage with fully opened flowers, with all four petals in bright yellow color. Anthesis was marked for a total of 55 plants in the CO growth chamber. When the plants developed at least 10-12 flowers at anthesis, half of the plants were either retained at the CO or moved to the HS growth chamber for seed development. The HS growth chamber was maintained at 34/24° C (light/dark) with all the other environmental conditions identical to the CO growth chamber. Five biological replicates for each stage were collected for all analyses. In the case of 7 DPA and 14 DPA, a combination of 3-5 plants were used to pool seeds as one replication due to small size of the seed with high water content.

2.2 Plant physiological measurements

The uppermost, completely expanded leaf of plants under CO and HS conditions was used to measure photosynthetic rate (A), transpiration rate (E), intracellular CO_2 concentration (Ci) and stomatal conductance (gws) using an infrared gas analyzer (Li-COR Li 6800, Lincoln, NE) as previously described (Begcy et al., 2019a). Measurements were taken at the beginning of flowering and extended over a period of 22 days, occurring at the following time points: 0, 2, 5, 9, 12, 17, and 22 days from flower initiation.

2.3 Analysis of seed fatty acid composition and quantification

Seeds were removed from the siliques stored at -80°C and lyophilized in a benchtop freeze-dryer (FreeZone, Labconco, Kansas City, MO, USA) for 24h at ~0.5mbar and -90°C. Seed lipids were quantified by converting their FAs to the corresponding fatty acid methyl esters (FAMEs) by transmethylation reaction based on (Li et al., 2006). Using a homogenizer, ~20 mg of lyophilized seeds were homogenized in 3ml toluene, combined with 1ml of 5% (v/v) concentrated sulfuric acid in methanol, 25µl 0.2% BHT (butylated hydroxytoluene in methanol), and 10µl of internal standard (IS) C17:0 TAG (5mg/ml) (Sigma# T2151). The mixture was vortexed for 30sec, then heated at 90-95°C for 1.5h and cooled to room temperature. 1.5ml of 0.9% NaCl (w/v) was added, and FAMEs were extracted 3x with 2 ml hexane. Pooled organic phases were then evaporated under N_2, and dried FAMEs were dissolved in 1ml of hexane. The FAMEs were analyzed by Gas Chromatography (GC 6890 Series, Agilent, Wilmington DE) using a DB-225MS column (30 m × 0.25 mm × 0.25 µm) at a flow rate of 0.8 mL/min. The GC conditions were as follows: initial temperature of 120°C, then ramp to 220°C at a rate of 4°C/min, and hold for 35 min. An external standard (Supelco® 37 Component FAME Mix, CRM47885, Sigma-Aldrich, St. Louis, MO) was used for peak identification and C17:0 IS was used for quantification.

2.4 Determination of plant growth parameters

Twelve plants were dedicated to determining plant growth parameters, thus, excluded from any destructive harvesting of developing seeds until the final harvest. Plants were grown in the CO growth chamber until the plants had at least 10 flowers at anthesis with multiple unopened flower buds. Half of the plants were transferred to the HS growth chamber described above while the rest remained under CO conditions. Six plants per treatment were exclusively utilized to determine various growth parameters, including total seed yield, 100 seed weight, above-ground biomass, and to collect plant physiological measurements under CO and HS conditions. Plants were harvested when siliques began to crack open, and seeds reached maturity. The seeds were cleaned and weighed for the total yield per plant. 100 seeds per plant were manually counted and weighed to determine 100-seed weight. For above-ground biomass measurements, upon reaching its final stages of senescence wherein the plant material is completely dry, with all seed pods dehisced, the whole plant above the soil surface was collected into paper bags, air dried until completely dry, and dry weight was measured per plant. Seeds from CO and HS treatments were sown, with six biological replications each; 30 seeds per replication were germinated in petri plates with moist filter paper and wrapped in aluminum foil. The plates were kept under CO conditions for a week and percentage germination was calculated as percentage of number of seeds germinated (with radicle emergence after one week) ÷ total number of seeds. A similar experiment with

two repetitions was conducted where 30 visibly heat damaged and regular HS seeds were germinated and percentage of germination was calculated.

2.5 Microscopic analysis of camelina siliques and seeds

Siliques and seeds harvested at 7, 14, 21, and 28 DPA of camelina plants grown under CO and HS conditions were imaged at 0.8-3X magnification on a Leica dissecting microscope (Wetzlar, Germany) using a microsystems CMS camera calibrated with Leica Application Suite X LAS X (3.7.4.23463).

2.6 Statistical analyses

Statistical analyses were performed either using JMP or R packages rstatix, ggplot, and ggsignif. Physiological and FAME composition data was subjected to a student's *t-test* to compare differences between plants grown under CO and HS conditions. Differences were considered significant at $P \leq 0.05$.

3 Results

3.1 Heat stress impairs physiological performance of *C. sativa* plants

To study the effect of increased temperature on the developing camelina siliques, we imposed a persistent HS environment for the duration of reproductive development post-anthesis. A parallel set of plants was maintained under optimal growth conditions and used as a control for all experiments. We quantified the physiological responses and observed that HS strongly impacts gas exchange parameters (Figure 1). Under CO (non-stressed) conditions, camelina plants did not show variations in photosynthetic rate (A), transpiration rate (E), intracellular CO_2 concentration (Ci), and stomatal conductance (gws) (Figure 1). Interestingly, a minor decline in photosynthesis was observed under CO conditions on and after day 17, likely due to typical senescence initiation (Figure 1A). In contrast, high temperatures decreased plant overall photosynthetic rate (A; Figure 1A). We observed a significant increase in transpiration rate (E) in response to high temperatures, effective from day one after HS induction ($P \leq 0.05$), peaking on the seventh day ($P \leq 0.001$), and declining thereafter (Figure 1B). A similar pattern was observed for internal CO_2 concentration (Ci) as well (Figure 1C). Additionally, a significant increase in stomatal conductance (gws) ($P \leq 0.001$) was detected under HS, which mirrored transpiration (E) under HS (Figure 1D). While CO plants had green leaves until four weeks following the start of temperature treatments, HS plants showed accelerated senescence, 10 days earlier than CO. At the end of reproductive development, HS camelina plants showed almost a 90% reduction in photosynthetic rate compared to CO plants. Taken together, our results show that increased temperature during reproductive development negatively affects the physiological status of camelina.

3.2 Morphological variation during *C. sativa* post-anthesis seed development under control and heat stress conditions

Under CO conditions, seed development of *C. sativa* progressed from anthesis to maturity in approximately 35 days. Silique and seed development occurred mainly during the first growth phase,

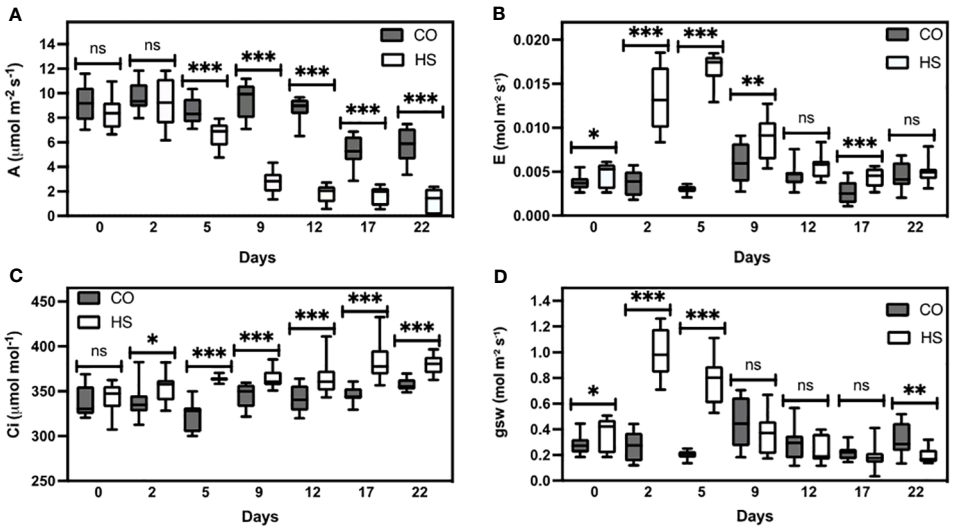

FIGURE 1
Gaseous exchange measurements of camelina under control and heat stress. **(A)** Photosynthesis (A), **(B)** transpiration rate (E), **(C)** intercellular CO_2 (Ci), and **(D)** stomatal conductance (gsw). CO-control, HS-Heat stress conditions. Measurements were performed using 300 Photosynthetic Photon Flux Density (PPFD) at ambient CO_2 (400 µmol mol^{-1}) and 40% relative humidity. ns $P > 0.05$; *$P \leq 0.05$, **$P \leq 0.01$, and ***$P \leq 0.001$. The error bars represent standard error of the mean.

10.3389/fpls.2023.1284573

which lasted up to 14 DPA, after which most siliques had sizes comparable to those at maturity (Figure 2A). The siliques remained green in color until 28 DPA, after which slight browning began. However, under HS conditions, silique development progressed more rapidly, with browning starting at 14 DPA (Figures 2A, B). While seed size between 14-21 DPA under CO is comparable to mature seed (Figure 2C), under HS several seeds per plant had visible heat damage at all stages, most prominently from 14 DPA onwards (Figure 2D). In addition to impaired seed development, the filling of siliques was also affected when developed under HS resulting in hollower siliques, whilst CO siliques were full of developing seeds (Figures 2A, B). Seed viability was evaluated for HS and CO seeds by germination experiments. Approximately 8% of HS seeds demonstrated visible heat damage with far darker coloration and a more shriveled appearance (Figure 2D). Although no significant overall differences in germination percentage was observed for undamaged HS seeds and CO seeds, visibly heat-damaged seeds (Figure 2D) had a 90% reduction in seed germination compared to visibly normal HS seeds.

3.3 High temperature negatively affects content and rate of fatty acid accumulation in developing *C. sativa* seed

To identify the effects of HS on seed oil profiles, we quantified FA accumulation throughout *C. sativa* seed development from 7 DPA, 14 DPA, 21 DPA, 28 DPA, and at maturity under CO and HS conditions. The total FA content at 7 DPA under CO and HS conditions was 64 mg/g seed and 49 mg/g seed, respectively (Table 1) and not significantly different in this early stage of development. However, the rate of FA accumulation varied throughout seed development under both CO and HS conditions. There was a continuous increase of FAs with no significant

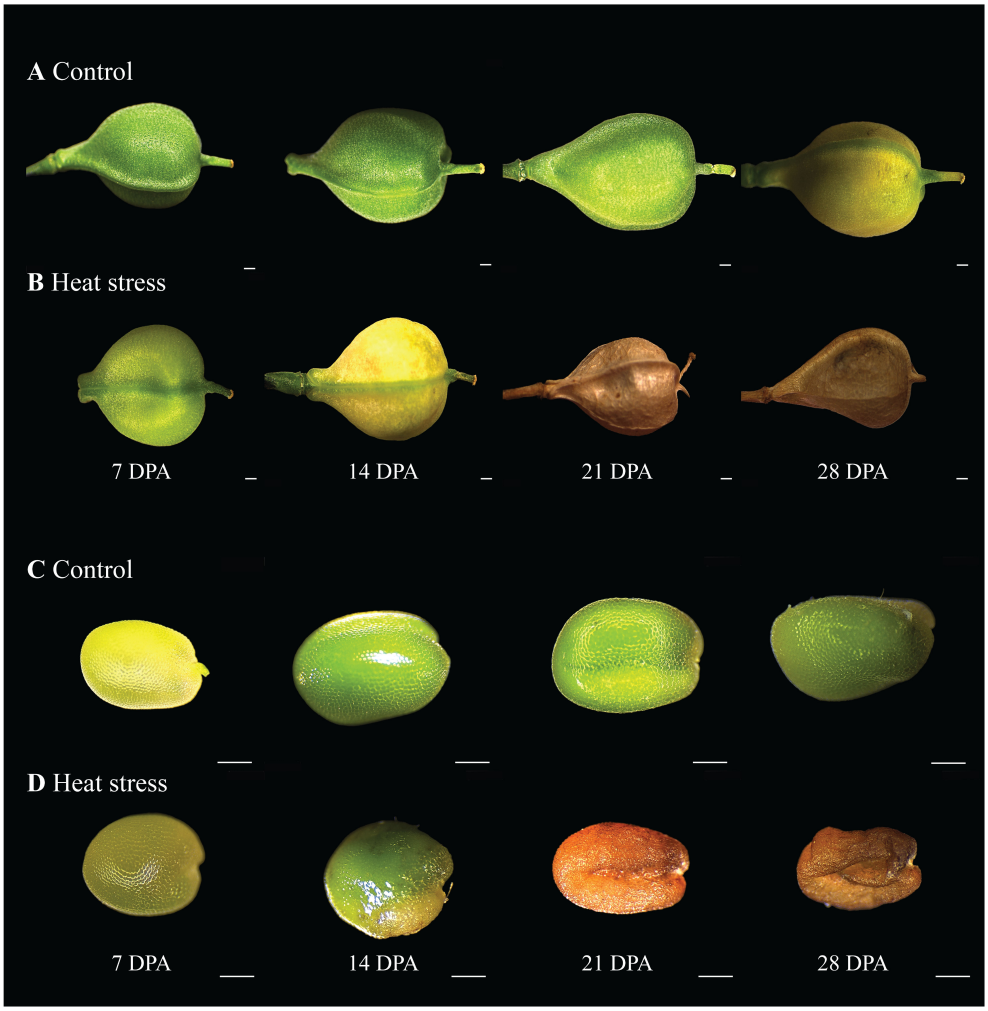

FIGURE 2
Morphological variation of post anthesis siliques and seed development. **(A)** Siliques under control conditions (CO) (22/18°C light/dark), **(B)** Siliques under heat stress (HS) (34/24°C light/dark), **(C)** CO seed, **(D)** HS seed. DPA, days post anthesis. Scale bar = 500μm.

TABLE 1 Fatty acid composition and quantification at various seed developmental stages in mg g^{-1} from *Camelina sativa* dry seed.

FA	7DPA			14DPA			21DPA			28DPA			Mature		
mg/g seed	CO	HS	SS	CO	HS	SS	CO	HS	SS	CO	HS	SS	CO	HS	SS
C14:0	0.27 ± 0.1	0.13 ± 0.02	ns	0.17 ± 0.07	0.26 ± 0.03	ns	0.26 ± 0.08	0.2 ± 0.01	ns	0.23 ± 0.04	0.26 ± 0.01	ns	0.25 ± 0.03	0.3 ± 0.02	ns
C16:0	10.41 ± 1.09	9.78 ± 0.58	ns	15.36 ± 4.77	20.28 ± 2.29	ns	27.83 ± 3.79	15.8 ± 0.33	*	24.01 ± 3.56	18.4 ± 0.33	ns	25.52 ± 3.2	25.04 ± 0.88	ns
C16:1	0.55 ± 0.09	0.19 ± 0.08	*	0.25 ± 0.07	0.55 ± 0.07	*	0.39 ± 0.06	0.57 ± 0.02	*	0.43 ± 0.06	0.7 ± 0.02	**	0.44 ± 0.05	0.77 ± 0.03	***
C18:0	3.95 ± 1.1	2.17 ± 0.25	ns	9.61 ± 3.17	7.73 ± 0.73	ns	15.49 ± 2.11	7.28 ± 0.2	**	12.28 ± 1.86	8.47 ± 0.29	ns	12.24 ± 1.6	11.74 ± 0.76	ns
$C18:1^{n9c}$	10.52 ± 4.74	8.77 ± 1.34	ns	29.4 ± 8.93	38.66 ± 4.66	ns	48.43 ± 6.35	38.45 ± 1.32	ns	38.53 ± 5.76	46.76 ± 1.43	ns	59.93 ± 9.81	53.01 ± 1.24	ns
$C18:2^{n6c}$	24.82 ± 4.72	20.05 ± 1.26	ns	46.31 ± 14.36	57.15 ± 8.36	ns	92.87 ± 11.45	55.56 ± 1.34	*	72.29 ± 10.81	65.28 ± 1.78	ns	79.93 ± 9.28	89.25 ± 2.39	ns
$C18:3^{n3}$	9.33 ± 1.99	6.24 ± 0.65	ns	24.73 ± 9.31	31.27 ± 6.21	ns	118.17 ± 19.56	27.64 ± 1.12	**	123.26 ± 17.06	33.64 ± 0.9	***	138.4 ± 15.17	62.86 ± 3.29	**
C20:0	1.36 ± 0.4	0.89 ± 0.18	ns	2.98 ± 1.33	6.58 ± 0.86	ns	10.47 ± 1.44	6.39 ± 0.19	*	8.87 ± 1.28	7.19 ± 0.25	ns	7.21 ± 0.76	9.17 ± 0.46	ns
C20:1	1.59 ± 1.42	0.21 ± 0.06	***	11.24 ± 6.53	23.99 ± 4.32	ns	59.16 ± 8.61	23.66 ± 1.01	**	51.11 ± 6.98	28.96 ± 0.95	*	62.74 ± 7.91	36.87 ± 1.06	*
C20:2	0.24 ± 0.08	0.23 ± 0.06	ns	1.25 ± 0.52	2.75 ± 0.6	ns	8.41 ± 1.31	2.65 ± 0.12	**	7.8 ± 1.11	3.24 ± 0.12	**	9.01 ± 0.95	4.77 ± 0.16	**
C20:3	0.85 ± 0.37	0.1 ± 0.04	ns	0.96 ± 0.29	0.82 ± 0.19	ns	4.7 ± 0.92	0.75 ± 0.04	**	5.5 ± 0.74	1.48 ± 0.59	**	6.01 ± 0.63	1.72 ± 0.11	***
C22:0	0.39 ± 0.09	0.37 ± 0.05	ns	0.74 ± 0.25	1.71 ± 0.2	*	2.35 ± 0.35	1.53 ± 0.04	*	2.08 ± 0.28	1.68 ± 0.05	ns	1.67 ± 0.2	2.47 ± 0.08	**
C22:1	0 ± 0	0 ± 0	ns	1.07 ± 0.96	3.95 ± 1.63	ns	14.65 ± 2.19	4.07 ± 1.03	**	13.75 ± 1.94	5.73 ± 0.23	**	12.18 ± 0.92	8.61 ± 0.34	**
C24:1	0 ± 0	0 ± 0	ns	0.57 ± 0.23	1.33 ± 0.32	ns	3.12 ± 0.54	1.83 ± 0.14	*	3.86 ± 0.55	1.99 ± 0.07	**	3.32 ± 0.24	2.89 ± 0.13	ns
Total FA	64.2 ± 12.7	49.1 ± 3.9	ns	144.6 ± 50.4	197 ± 29.9	ns	406.3 ± 57.4	186.4 ± 4.4	**	364 ± 51.6	223.8 ± 5.8	*	418.8 ± 49.9	309.5 ± 9.6	ns

DPA, Days Post Anthesis. The data represents the mean of n=5 ± SE. Asterisks denote statistically significant (SS) differences between the control (CO) and heat stress (HS) conditions at the same seed developmental stage (ns $P > 0.05$; *$P \leq 0.05$, **$P \leq 0.01$, and ***$P \leq 0.001$) as determined by Student's *t* tests. SE = standard error of the mean.

differences in seed FA content or composition under both treatments until 14 DPA. However, under HS, 14 DPA seeds had a slightly higher content of individual FAs detected when compared to CO (Figure 3) with a visible heat damage on the seeds (Figure 2D). FA accumulation in *C. sativa* seeds peaked at 21 DPA under CO conditions with 406 mg/g seed, and there was only a slight increase of total FA after this stage until maturity (Figure 3; Table 1). The impact of HS was most prominent at 21 DPA. Most FAs had significantly lower accumulation by 21 DPA under HS compared to CO, reducing the total seed FA content by 54% (Tables 1, S1). Unlike CO, where most of the FA accumulation occurred between 14 DPA and 21 DPA, there was a continued but low rate of FA accumulation throughout the seed development under HS after 14 DPA with the total FA content in HS matured seed reaching to 309.5 mg/g compared to 418.8 mg/g in CO seed (Figure 3; Table 1).

3.4 Qualitative and quantitative variation in *C. sativa* seed FA composition between developmental stages under control and heat stress conditions

In mature *C. sativa* seeds under CO conditions, we detected 33.3% α-linolenic acid, an ω-3 FA (C18:3) and 19.2% linoleic acid (C18:2), an ω-6 FA, together constituting slightly more than half (52.5%) of total FAs (Tables 1, S1). The next two major FAs, oleic acid (C18:1) and gondoic acid (C20:1) constituted 13.6% and 14.9% respectively. Altogether, in *C. sativa* mature seed, the four major FAs, C18:3, C18:2, C18:1 and C20:1 constituted 81% of seed oil, and their contents increased from 7 DPA to maturity. The FA composition in the early stages of seed development is distinct from mature seed even under CO conditions. For example, the percentage of saturated FAs detected is the highest at 7 DPA

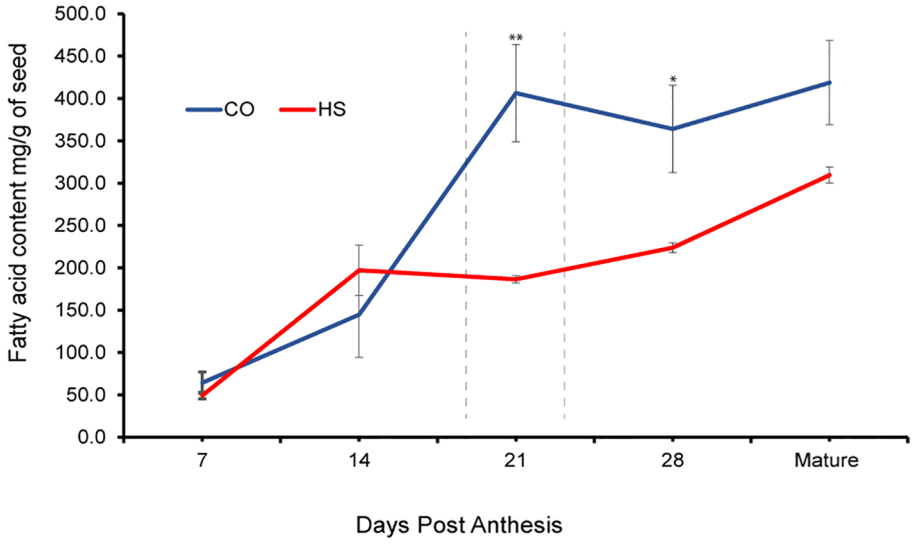

FIGURE 3
Fatty acid accumulation in developing seed of *C. sativa*. Under control (CO) and heat stress (HS) conditions at 7, 14, 21, 28 days post anthesis and at full maturity. The peak accumulation under CO conditions is designated with a dashed line. Asterisks denote statistically significant differences between the control (CO) and heat stress (HS) conditions at the same seed developmental stage (*$P \leq 0.05$, **$P \leq 0.01$, and ***$P \leq 0.001$) as determined by Student's *t* tests. The error bars represent standard error of the mean.

(27.2%) and subsequently decreased as the seeds developed, with the lowest levels detected at seed maturity (13.2%) (Table 1; Figure 4). The two major saturated FAs at 7 DPA include palmitic acid (C16:0, 17.4%) and stearic acid (C18:0, 6.02%), constituting up to 82% of saturated FAs. However, as the seed matured, reduction of saturated FAs and a corresponding increase in the unsaturated FAs was observed. As the seed FA accumulation peaked at 21 DPA under CO, the composition of FAs also varied with C18:3 and C20:1 FAs increased by five times, and C18:2 FAs doubled compared to 14 DPA (Table 1). On the other hand, the percentage of C18:1 FA in seeds dropped from 21.9% to 12.3% within the same period.

High temperature during seed development resulted in both qualitative and quantitative changes in FA accumulation. Some

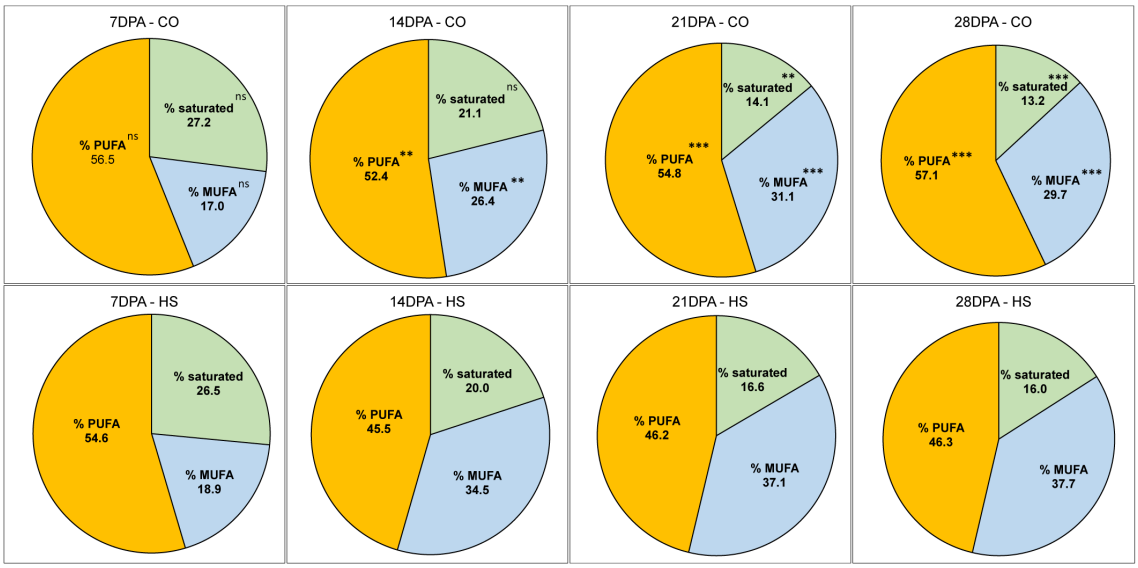

FIGURE 4
The percentage of Fatty acids (FAs) in developing seed of *C. sativa* categorized based on degree of saturation. Percentage of FAs categorized as saturated FAs, mono-unsaturated FAs (MUFAs), poly-unsaturated FAs (PUFAs) under control (CO) and heat stress (HS) conditions at 7, 14, 21, 28 days post anthesis and at full maturity. Percentage of Saturated FAs constituted sum of C14:0, C16:0, C18:0, C20:0, C22:0 FAs; % MUFAs constituted C16:1, C18:1, C20:1, C22:1, C24:1; % PUFAs constituted C18:2, C18:3, C20:2, C20:3, C20:2. Asterisks denote statistically significant (SS) differences between the control (CO) and heat stress (HS) conditions at the same seed developmental stage (ns $P > 0.05$; *$P \leq 0.05$, **$P \leq 0.01$, and ***$P \leq 0.001$) as determined by Student's *t* tests.

notable observations are a decrease in the percentage PUFAs and an increase in percentage MUFAs under HS compared to CO in most stages of *C. sativa* seed development. For example, at 21 DPA C18:3 FA is the major FA with 118.1mg/g in CO in contrast to 27.6mg/g under HS. Although there is a continued but low rate of FA accumulation under HS, we detected that C18:3 FA was significantly lower under HS at all stages of seed development until maturity, with C18:2 being the major FA in most stages instead. The ratio of ω-6 to ω-3 is therefore elevated under HS from 21 DPA (0.7, CO vs 2.0, HS) until maturity (0.57, CO vs 1.4, HS) (Table 1). Other PUFAs, including C20:2 and C20:3 FAs also showed a similar trend with reduced content under HS (Table 1). In contrast, the percentage of C18:1 FA remained higher under HS in all stages of seed development compared to CO. For example, percentage of C18:1 FA under HS at 21 DPA, 28 DPA and maturity are 20.6%, 20.8%, and 17.1% while under CO it is 12.2%, 10.8%, and 13.6% respectively.

3.5 Heat stress during seed development in *C. sativa* impacts yield

High temperatures during seed development impacted the overall growth of the camelina significantly (Figure 5A) with an 81.7% decrease in the above-ground biomass under HS compared to CO (Figure 5B). There was a substantial 84.5% reduction in seed yield in plants that continuously experienced heat during seed development (Figure 5C). Furthermore, the seed weight of camelina grown under HS had a 38.5% decrease in 100 seed weight (Figure 5D).

4 Discussion

4.1 Heat stress impairs physiological plant performance

Heat stress is one of the major environmental constraints for plant growth and agricultural crop productivity (Al-Khatib and Paulsen, 1990; Bita and Gerats, 2013). Photosynthesis is a heat-sensitive cellular process in plants since high temperatures cause damage to chloroplasts and mitochondria, inactivate RUBISCO, and reduce chlorophyll content and photosystem II (PSII) efficiency (Bernacchi et al., 2001; Bernacchi et al., 2003; Cen and Sage, 2005; Sharkey, 2005; Hu et al., 2020). One of the common strategies used by plants to tolerate HS conditions involves the adjustment between photosynthetic and transpiration rates through the regulation of stomata opening and closure. Stomata closure avoids water loss through evaporation but simultaneously reduces CO_2 intake and thus photosynthetic rate (Greer and Weedon, 2012; Shen et al., 2017). Some heat-tolerant plants, in contrast, can maintain their physiological status for longer periods and thus keep open their stomata and CO_2 uptake while cooling their leaf surface at elevated temperatures. This avoids, for instance, membrane and thylakoid damage. Thus, tight physiological regulation is required to balance the various effects caused by increased temperatures (Bita and Gerats, 2013; Rajendra Prasad et al., 2021). Compared with HS conditions, we observed that camelina plants grown under CO conditions have higher photosynthetic rates. Interestingly, after two days of heat treatment, higher transpiration (Figure 1B) and stomatal conductance (Figure 1D) were observed in HS camelina plants which indicates the initial reaction to open stomata to reduce the high leaf temperature and higher CO_2 uptake (Figure 1). Under HS, a steady decline of photosynthesis was observed after the fifth day and reaching almost non-detectable levels after day 15 (Figure 1A), this is also reflected in the rapid senescence of the pods and developing seeds (Figure 2).

Reproductive development is one of the most sensitive developmental stages to HS (Folsom et al., 2014; Begcy et al., 2019a). Elevated temperatures are detrimental to the formation of viable seeds due to the reduction of photo-assimilates, including starch and monomers of carbohydrates required during seed development as well as lipids used to form membranes (Zhuang et al., 2022). The photosynthetic capacity of camelina during reproductive development and seed filling stage greatly influenced the accumulation of dry matter in the plant, total seed yield and oil quality. Although physiological responses to increased temperatures are developmental stage-dependent, similar responses to high temperatures during seed development have been observed in tomato (*Solanum lycopersicum*) (Parrotta et al., 2020), rapeseed (*Brassica napus*) (Huang et al., 2019), and rice (*Oryza sativa*) (Sailaja et al., 2015).

4.2 Heat stress causes accelerated and altered seed development and quality

In this study we observed developmental changes in camelina seeds exposed to HS, as well as corresponding variations in lipid composition. Several aspects of plant reproduction are clearly affected by heat, such as a decreased seed set (Figure 5) and reduced seed size as shown by a significant decline in 100 seed weight. Previous studies have established that while *C. sativa* seed formation is completed by ~12 days after flowering, oil accumulation occurs most rapidly between 12-16 and 27-28 days after flowering and is mostly represented by the accumulation of C18:3 FA (Rodríguez-Rodríguez et al., 2013; Abdullah et al., 2016). Here, we show that seed growth under CO and HS, albeit to a lesser degree, was visible between 7 and 14 DPA. We observed browning of the CO siliques at 28 DPA, while under HS, browning was observed two weeks earlier. This clearly indicates that the period of seed development is reduced at high temperatures, thereby affecting seed weight and total yield. This accelerated but defective development is also reflected in the oil accumulation stage, which occurs between 14 DPA and 21 DPA under CO, but between 7 and 14 DPA under HS (Figure 3; Table 1). In line with our observations in *C. sativa*, decreased seed set, seed filling, and quality were also reported in oil seed crops such as *Brasicca napus*, soybean, and sunflower (Faraji et al., 2009; Izquierdo et al., 2016; Nakagawa et al., 2020; Staniak et al., 2021; Mácová et al., 2022).

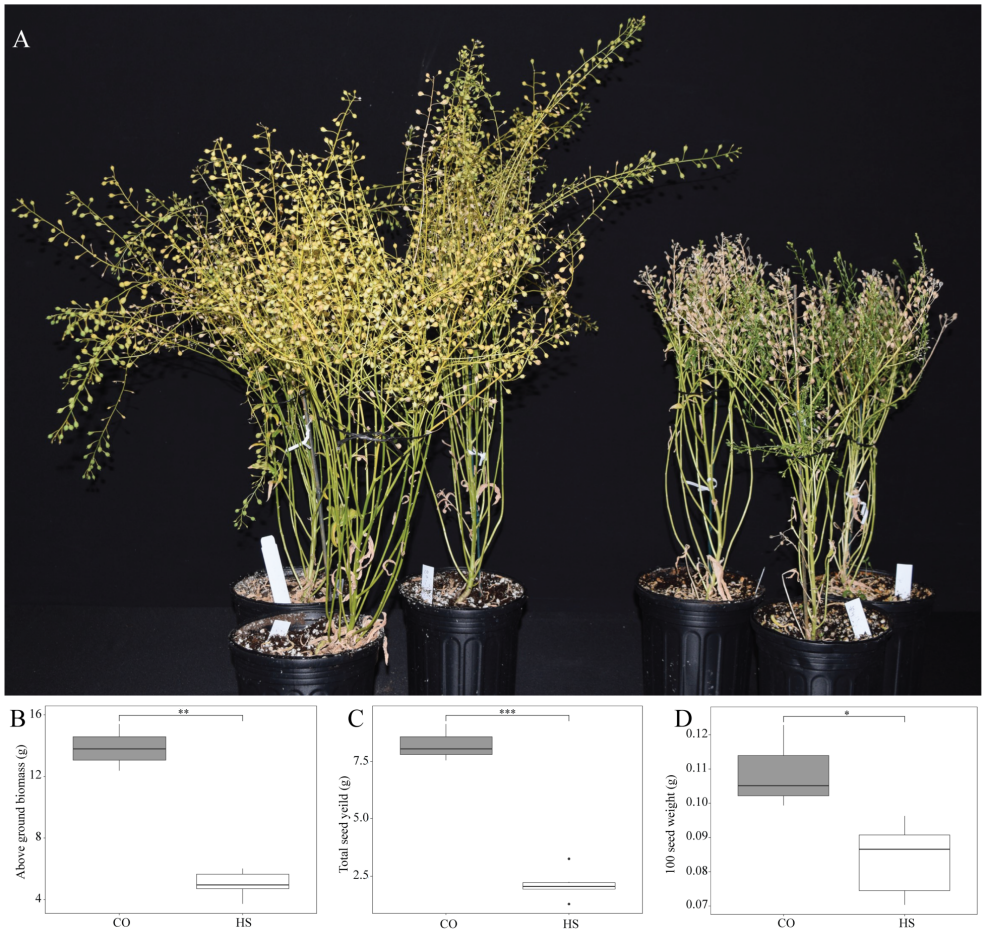

FIGURE 5
Effect of heat stress on plant growth and seed yield. **(A)** *Camelina sativa* cv. Suneson plants grown under control (CO) temperature of 22/18°C (light/dark) throughout their lifecycle compared to plants subjected to heat stress (HS) at 34/24°C during seed development phase. **(B)** 100-seed weight, **(C)** total seed yield, **(D)** Total above ground biomass. Asterisks denote statistically significant (SS) differences between the control (CO) and heat stress (HS) conditions at the same seed developmental stage (*$P \leq 0.05$, **$P \leq 0.01$, and ***$P \leq 0.001$) as determined by Student's *t* tests. The error bars represent standard deviations.

4.3 Camelina sativa seeds exhibit altered fatty acid composition under heat stress

FAs from C4:0 to C18:0 are produced *de novo* in plastids along with mono-unsaturated FAs with Oleic acid (C18:1) being the major product of plastidial fatty acid synthesis in many oilseed species (Li-Beisson et al., 2013). Oil composition has been shown to be influenced by abiotic stressors affecting the transport of fatty acids through various organelles. Particularly, export from plastids to the endoplasmic reticulum is affected, where oleic acid (C18:1) is converted into linoleic acids (C18:2), which is further desaturated to form linolenic acids (C18:3) (Ohlrogge and Browse, 1995). A decline in the level of polyunsaturated fatty acids (i.e., C18:3) is associated with heat tolerance in cultivars of soybean and peanut (Rustgi et al., 2021), and has been shown to lead to improved heat tolerance in tobacco cells (Zhang et al., 2005; Upchurch, 2008). In this study, the quantification of FAs was performed based on lyophilized seed dry mass for greater bio preservation of samples by eliminating exposure of seeds to air and heat, which can lead to oxidation of fatty acids and degradation of PUFA (Zhuang et al., 2022). Under CO conditions, FA profile exhibited a decrease in percentage of C18:1 and C18:2 from 14 DPA onwards (Table S1). Correspondingly, there is an increase in the C18:3, C20:1 and other longer chain FAs in later stages of seed development (Table 1). Interestingly, products of FA elongase activity on MUFAs, C20:1, C22:1, and C24:1 increase drastically from 14 DPA to 21 DPA, after which changes are minor as observed previously in camelina (Rodríguez-Rodríguez et al., 2013; Vollmann and Eynck, 2015; Abdullah et al., 2016; Brock et al., 2020).

Under HS conditions, we observed plasticity in seed FA accumulation with significant qualitative and quantitative differences in composition in addition to a decrease in overall FA yield. The composition of FA over development was reversed, with the HS FA profile being more represented by C18:1 and C18:2 FAs, with a decrease in trienoic FAs suggesting that further desaturation of FAs is not preferred under HS. This observation is supported by findings that FAD3 enzymes, involved in production of PUFAs, are regulated in response to temperature, with protein degradation occurring at higher temperatures (30°C) (O'Quin et al., 2010).

Similarly, the plastid C18:2 desaturase, FAD8, has been shown to undergo conformational destabilization at high temperatures of 27° C (Matsuda et al., 2005). Altogether, heat exposure can directly impact the accumulation of ω-3 FAs by impacting enzymatic activity. One factor to consider is the use of C18:3 FA in non-storage metabolic products in plants via a biosynthetic shift toward signaling. Besides being incorporated in TAGs for storage, linolenic acid is a precursor of the phytohormone jasmonic acid (JA), a biotic stress response signaling molecule which has also been shown to be involved in seed development and abiotic stress response in *Arabidopsis thaliana* (Mata-Perez et al., 2015; Balfagón et al., 2019). In fact, *fad3-2 fad7-2 fad8* Arabidopsis triple mutants exhibited male sterility, but wild type phenotype was restored by the application of JA (Wallis and Browse, 2002).

A decreased unsaturation index may be an advantageous response for several reasons. First, changes in metabolism toward stress tolerance could potentially occur via membrane modulation, whereby an increase in saturated FAs leads to a more rigid membrane. Reduction of trienoic fatty acids which are observed under HS in several plant species has been shown to confer HS tolerance to Arabidopsis double mutants *fad7fad8 (*plastidial C16:2 and C18:2 desaturases) (Murakami et al., 2000) and in *fad5* and *fad6* (plastidial C16:1 and C18:1 desaturases) (Wallis and Browse, 2002). The increase in MUFAs C16:1, C18:1, 20:1, and C22:1, especially at earlier developmental stages during seed formation, herein reported in *C. sativa* seeds under HS may be an adaptive response to HS, driven by changes in plastidial FA biosynthesis. Remodeling of membranes at this early developmental stage may aid the developing seed in surviving temperature stress, albeit at the cost of slower FA accumulation for energy storage. Interestingly, at 21 DPA, HS seeds appear to recover C18:3 accumulation, as the proportion of C18:2 FA decreases between 21 and 28 DPA, and both C18:1 and C18:2 proportion decrease between 28 DPA and maturity, while C18:3 FA accumulation is occurring between these stages. We may therefore infer that FA biosynthesis shifted to MUFA synthesis to protect cell function and embryo development by maintaining membrane stability and preventing FA oxidation, followed by a gradual return to PUFA biosynthesis. This temporary shift in lipid metabolism was also observed in the oil crop *Ricinus communis* (castor bean), which underwent a significant decrease in the polyunsaturation index of membrane lipids during HS, followed by a return to normal levels once HS was relieved (Zhuang et al., 2022). On the other hand, earlier sowing of camelina resulted in seeds with higher PUFA content due to lower temperatures during seed filling (Righini et al., 2019). Taken together, these findings support the phenotypic plasticity of camelina lipid metabolism in response to high temperature.

Here, we have described the impact of post anthesis heat on developmental FA accumulation in seeds in the biofuel crop *C. sativa* cv Suneson. The empirical evaluation of physiological performance of plants, and seed development under HS conditions compared to control aids in identification of the FA plasticity and time shift in peak FA accumulating phase in camelina due to high temperatures. Understanding the effects of temperature stress on production and quality of oil in a changing climate offer a pathway to crop improvement not only in camelina but may also be translated to other oil seed crops beyond Brassicaceae.

Data availability statement

The original contributions presented in the study are included in the article/Supplementary Material. Further inquiries can be directed to the corresponding author.

Author contributions

SN: Conceptualization, Data curation, Formal Analysis, Funding acquisition, Investigation, Methodology, Project administration, Resources, Supervision, Validation, Visualization, Writing – original draft, Writing – review & editing. LL: Formal Analysis, Investigation, Methodology, Software, Validation, Visualization, Writing – original draft, Writing – review & editing. MT: Data curation, Formal Analysis, Investigation, Methodology, Writing – review & editing. AD: Data curation, Investigation, Methodology, Software, Validation, Visualization, Writing – review & editing. AE: Data curation, Formal Analysis, Investigation, Methodology, Software, Visualization, Writing – review & editing. AS: Formal Analysis, Investigation, Methodology, Writing – review & editing. KB: Conceptualization, Formal Analysis, Funding acquisition, Investigation, Methodology, Software, Supervision, Validation, Visualization, Writing – original draft. PS: Investigation, Methodology, Validation, Writing – review & editing. CB: Conceptualization, Funding acquisition, Methodology, Writing – review & editing.

Funding

The author(s) declare financial support was received for the research, authorship, and/or publication of this article. Funding for SN was provided by the USDA-NIFA Hatch project FLA-ENH-006010. Funding for KB was provided by Hatch project FLA-ENH-005853. Funding for CB was provided by the Georgia Research Alliance, Georgia Seed Development, and University of Georgia.

Conflict of interest

The authors declare that the research was conducted in the absence of any commercial or financial relationships that could be construed as a potential conflict of interest.

Publisher's note

Supplementary material

The Supplementary Material for this article can be found online at: https://www.frontiersin.org/articles/10.3389/fpls.2023.1284573/full#supplementary-material

SUPPLEMENTARY TABLE 1
Percentage fatty acid (FA) composition from *Camelina sativa* seeds at various seed developmental stages calculated as % mean (n=5) of a FA ÷ sum of FAs ± SE. control (CO) and heat stress (HS). Asterisks denote statistically significant (SS) differences between the control (CO) and heat stress (HS) conditions at the same seed developmental stage (ns $P > 0.05$; *$P \leq 0.05$, **$P \leq 0.01$, and ***$P \leq 0.001$) as determined by Student's t tests. SE = standard error of the mean.

References

Abdullah, H. M., Akbari, P., Paulose, B., Schnell, D., Qi, W., Park, Y., et al. (2016). Transcriptome profiling of Camelina sativa to identify genes involved in triacylglycerol biosynthesis and accumulation in the developing seeds. *Biotechnol. Biofuels* 9, 136. doi: 10.1186/s13068-016-0555-5

Al-Khatib, K., and Paulsen, G. M. (1990). Photosynthesis and productivity during high-temperature stress of wheat genotypes from major world regions. *Crop Sci.* 30, 1127–1132. doi: 10.2135/cropsci1990.0011183x003000050034x

Alsajri, F. A., Wijewardana, C., Irby, J. T., Bellaloui, N., Krutz, L. J., Golden, B., et al. (2020). Developing functional relationships between temperature and soybean yield and seed quality. *Agron. J.* 112, 194–204. doi: 10.1002/AGJ2.20034

Anderson, J. V., Horvath, D. P., Doğramaci, M., Dorn, K. M., Chao, W. S., Watkin, E. E., et al. (2018). Expression of FLOWERING LOCUS C and a frameshift mutation of this gene on chromosome 20 differentiate a summer and winter annual biotype of Camelina sativa. *Plant Direct.* 2, 1–14. doi: 10.1002/pld3.60

Anderson, J. V., Wittenberg, A., Li, H., and Berti, M. T. (2019). High throughput phenotyping of Camelina sativa seeds for crude protein, total oil, and fatty acids profile by near infrared spectroscopy. *Ind. Crops Prod.* 137, 501–507. doi: 10.1016/j.indcrop.2019.04.075

Balfagón, D., Sengupta, S., Gómez-Cadenas, A., Fritschi, F. B., Azad, R. K., Mittler, R., et al. (2019). Jasmonic acid is required for plant acclimation to a combination of high light and heat stress. *Plant Physiol.* 181, 1668–1682. doi: 10.1104/PP.19.00956

Bansal, S., and Durrett, T. P. (2016). Camelina sativa: An ideal platform for the metabolic engineering and field production of industrial lipids. *Biochimie* 120, 9–16. doi: 10.1016/j.biochi.2015.06.009

Begcy, K., Mariano, E. D., Lembke, C. G., Zingaretti, S. M., Souza, G. M., Araújo, P., et al. (2019a). Overexpression of an evolutionarily conserved drought-responsive sugarcane gene enhances salinity and drought resilience. *Ann. Bot.* 124, 691–700. doi: 10.1093/aob/mcz044

Begcy, K., Nosenko, T., Zhou, L. Z., Fragner, L., Weckwerth, W., and Dresselhaus, T. (2019b). Male sterility in maize after transient heat stress during the tetrad stage of pollen development. *Plant Physiol.* 181, 683–700. doi: 10.1104/pp.19.00707

Bengtsson, J. D., Wallis, J. G., Bai, S., and Browse, J. (2023). The coexpression of two desaturases provides an optimized reduction of saturates in camelina oil. *Plant Biotechnol. J.* 21, 497–505. doi: 10.1111/pbi.13966

Bernacchi, C. J., Pimentel, C., and Long, S. P. (2003). *In vivo* temperature response functions of parameters required to model RuBP-limited photosynthesis. *Plant Cell Environ.* 26, 1419–1430. doi: 10.1046/j.0016-8025.2003.01050.x

Bernacchi, C. J., Singsaas, E. L., Pimentel, C., Portis, A. R., and Long, S. P. (2001). Improved temperature response functions for models of Rubisco-limited photosynthesis. *Plant Cell Environ.* 24, 253–259. doi: 10.1111/J.1365-3040.2001.00668.X

Berti, M., Gesch, R., Eynck, C., Anderson, J., and Cermak, S. (2016). Camelina uses, genetics, genomics, production, and management. *Ind. Crops Prod.* 94, 690–710. doi: 10.1016/j.indcrop.2016.09.034

Bita, C. E., and Gerats, T. (2013). Plant tolerance to high temperature in a changing environment: Scientific fundamentals and production of heat stress-tolerant crops. *Front. Plant Sci.* 4. doi: 10.3389/fpls.2013.00273

Brock, J. R., Scott, T., Lee, A. Y., Mosyakin, S. L., and Olsen, K. M. (2020). Interactions between genetics and environment shape Camelina seed oil composition. *BMC Plant Biol.* 20, 1–15. doi: 10.1186/s12870-020-02641-8

Cappelli, G., Zanetti, F., Ginaldi, F., Righini, D., Monti, A., and Bregaglio, S. (2019). Development of a process-based simulation model of camelina seed and oil production: A case study in Northern Italy. *Ind. Crops Prod.* 134, 234–243. doi: 10.1016/j.indcrop.2019.03.046

Cen, Y. P., and Sage, R. F. (2005). The regulation of Rubisco activity in response to variation in temperature and atmospheric CO2 partial pressure in sweet potato. *Plant Physiol.* 139, 979–990. doi: 10.1104/pp.105.066233

Chen, C., Begcy, K., Liu, K., Folsom, J. J., Wang, Z., Zhang, C., et al. (2016). Heat stress yields a unique MADS box transcription factor in determining seed size and thermal sensitivity. *Plant Physiol.* 171, 606–622. doi: 10.1104/pp.15.01992

Deva, C. R., Urban, M. O., Challinor, A. J., Falloon, P., and Svitákova, L. (2020). Enhanced leaf cooling is a pathway to heat tolerance in common bean. *Front. Plant Sci.* 11. doi: 10.3389/fpls.2020.00019

Dusenge, M. E., Duarte, A. G., and Way, D. A. (2019). Plant carbon metabolism and climate change: elevated CO2 and temperature impacts on photosynthesis, photorespiration and respiration. *New Phytol.* 221, 32–49. doi: 10.1111/nph.15283

Elferjani, R., and Soolanayakanahally, R. (2018). Canola responses to drought, heat, and combined stress: shared and specific effects on carbon assimilation, seed yield, and oil composition. *Front. Plant Sci.* 9. doi: 10.3389/fpls.2018.01224

Faraji, A., Latifi, N., Soltani, A., and Rad, A. H. S. (2009). Seed yield and water use efficiency of canola (Brassica napus L.) as affected by high temperature stress and supplemental irrigation. *Agric. Water Manage.* 96, 132–140. doi: 10.1016/j.agwat.2008.07.014

Folsom, J. J., Begcy, K., Hao, X., Wang, D., and Walia, H. (2014). Rice fertilization-independent Endosperm1 regulates seed size under heat stress by controlling early endosperm development. *Plant Physiol.* 165, 238–248. doi: 10.1104/pp.113.232413

Gomez-Cano, F., Chu, Y. H., Cruz-Gomez, M., Abdullah, H. M., Lee, Y. S., Schnell, D. J., et al. (2022). Exploring Camelina sativa lipid metabolism regulation by combining gene co-expression and DNA affinity purification analyses. *Plant J.* 110, 589–606. doi: 10.1111/tpj.15682

Greer, D. H., and Weedon, M. M. (2012). Modelling photosynthetic responses to temperature of grapevine (Vitis vinifera cv. Semillon) leaves on vines grown in a hot climate. *Plant Cell Environ.* 35, 1050–1064. doi: 10.1111/j.1365-3040.2011.02471.x

Gurr, M. I. (1980). "The biosynthesis of triacylglycerols," in *Lipids: Structure and Function*. Ed. P. K. Stumpf (Department of Biochemistry and Biophysics, University of California, Davis, California: Elsevier Inc.), 205–248.

Hotton, S. K., Kammerzell, M., Chan, R., Hernandez, B. T., Young, H. A., Tobias, C., et al. (2020). Phenotypic examination of camelina sativa (L.) crantz accessions from the USDA-ARS national genetics resource program. *Plants* 9, 1–28. doi: 10.3390/plants9050642

Hou, Q., Ufer, G., and Bartels, D. (2016). Lipid signalling in plant responses to abiotic stress. *Plant Cell Environ.* 39, 1029–1048. doi: 10.1111/pce.12666

Hu, S., Ding, Y., and Zhu, C. (2020). Sensitivity and responses of chloroplasts to heat stress in plants. *Front. Plant Sci.* 11. doi: 10.3389/fpls.2020.00375

Huang, R., Liu, Z., Xing, M., Yang, Y., Wu, X., Liu, H., et al. (2019). Heat stress suppresses brassica napus seed oil accumulation by inhibition of photosynthesis and bnWRI1 pathway. *Plant Cell Physiol.* 60, 1457–1470. doi: 10.1093/pcp/pcz052

Iqbal, W. A., Miller, I. G., Moore, R. L., Hope, I. J., Cowan-Turner, D., and Kapralov, M. V. (2021). Rubisco substitutions predicted to enhance crop performance through carbon uptake modelling. *J. Exp. Bot.* 72, 6066–6075. doi: 10.1093/jxb/erab278

Izquierdo, N. G., Martínez-Force, E., Garcés, R., Aguirrezábal, L. A., Zambelli, A., and Reid, R. (2016). Temperature effect on triacylglycerol species in seed oil from high stearic sunflower lines with different genetic backgrounds. *J. Sci. Food Agric.* 96, 4367–4376. doi: 10.1002/jsfa.7646

Jensen, R. G. (2000). Activation of Rubisco regulates photosynthesis at high temperature and CO2. *Proc. Natl. Acad. Sci. U.S.A.* 97, 12937–12938. doi: 10.1073/pnas.97.24.12937

King, K., Li, H., Kang, J., and Lu, C. (2019). Mapping quantitative trait loci for seed traits in Camelina sativa. *Theor. Appl. Genet.* 132, 2567–2577. doi: 10.1007/s00122-019-03371-8

Krzyżaniak, M., Stolarski, M. J., Tworkowski, J., Puttick, D., Eynck, C., Załuski, D., et al. (2019). Yield and seed composition of 10 spring camelina genotypes cultivated in the temperate climate of Central Europe. *Ind. Crops Prod.* 138, 111443. doi: 10.1016/j.indcrop.2019.06.006

Lhamo, D., Shao, Q., Tang, R., and Luan, S. (2020). Genome-wide analysis of the five phosphate transporter families in Camelina sativa and their expressions in response to low-P. *Int. J. Mol. Sci.* 21, 1–17. doi: 10.3390/ijms21218365

Li-Beisson, Y., Shorrosh, B., Beisson, F., Andersson, M. X., Arondel, V., Bates, P. D., et al. (2013). Acyl-lipid metabolism. *Arab B.* 11, e0161. doi: 10.1199/tab.0161

Li, Y., Beisson, F., Pollard, M., and Ohlrogge, J. (2006). Oil content of Arabidopsis seeds: The influence of seed anatomy, light and plant-to-plant variation. *Phytochemistry* 67, 904–915. doi: 10.1016/j.phytochem.2006.02.015

Lohani, N., Singh, M. B., and Bhalla, P. L. (2022). Short-term heat stress during flowering results in a decline in Canola seed productivity. *J. Agron. Crop Sci.* 208, 486–496. doi: 10.1111/JAC.12534

Mácová, K., Prabhullachandran, U., Štefková, M., Spyroglou, I., Pěnčík, A., Endlová, L., et al. (2022). Long-term high-temperature stress impacts on embryo and seed development in *Brassica napus*. *Front. Plant Sci.* 13. doi: 10.3389/fpls.2022.844292

Magno Massuia de Almeida, L., Coquemont-Guyot, M., Elie, N., Morvan-Bertrand, A., Avice, J. C., Mollier, A., et al. (2023). Repeated heat stress events during the reproductive phase impact the dynamic development of seeds in Brassica napus L. *Plant Sci.* 327, 111559. doi: 10.1016/J.PLANTSCI.2022.111559

Malik, M. R., Tang, J., Sharma, N., Burkitt, C., Ji, Y., Mykytyshyn, M., et al. (2018). Camelina sativa, an oilseed at the nexus between model system and commercial crop. *Plant Cell Rep.* 37, 1367–1381. doi: 10.1007/s00299-018-2308-3

Mata-Perez, C., Sanchez-Calvo, B., Begara-Morales, J. C., Luque, F., Jimenez-Ruiz, J., Padilla, M. N., et al. (2015). Transcriptomic profiling of linolenic acid-responsive genes in ROS signaling from RNA-seq data in arabidopsis. *Front. Plant Sci.* 6. doi: 10.3389/fpls.2015.00122

Matsuda, O., Sakamoto, H., Hashimoto, T., and Iba, K. (2005). A temperature-sensitive mechanism that regulates post-translational stability of a plastidial ω-3 fatty acid desaturase (FAD8) in Arabidopsis leaf tissues. *J. Biol. Chem.* 280, 3597–3604. doi: 10.1074/jbc.M407226200

Moore, C. E., Meacham-Hensold, K., Lemonnier, P., Slattery, R. A., Benjamin, C., Bernacchi, C. J., et al. (2021). The effect of increasing temperature on crop photosynthesis: From enzymes to ecosystems. *J. Exp. Bot.* 72, 2822–2844. doi: 10.1093/jxb/erab090

Mueller, S. P., Unger, M., Guender, L., Fekete, A., and Mueller, M. J. (2017). Phospholipid: Diacylglycerol acyltransferase-mediated triacylglyerol synthesis augments basal thermotolerance. *Plant Physiol.* 175, 486–497. doi: 10.1104/pp.17.00861

Murakami, Y., Tsuyama, M., Kobayashi, Y., Kodama, H., and Iba, K. (2000). Trienoic fatty acids and plant tolerance of high temperature. *Sci. (80-)* 287, 476–479. doi: 10.1126/SCIENCE.287.5452.476/ASSET/111CF504-0740-4C30-964F-EE436CB1DE28/ASSETS/GRAPHIC/SE0208212002.JPEG

Na, G., Aryal, N., Fatihi, A., Kang, J., and Lu, C. (2018). Seed-specific suppression of ADP-glucose pyrophosphorylase in Camelina sativa increases seed size and weight 06 Biological Sciences 0607 Plant Biology. *Biotechnol. Biofuels* 11, 330. doi: 10.1186/s13068-018-1334-2

Na, G. N., Mu, X., Grabowski, P., Schmutz, J., and Lu, C. (2019). Enhancing microRNA167A expression in seed decreases the α-linolenic acid content and increases seed size in Camelina sativa. *Plant J.* 98, 346–358. doi: 10.1111/tpj.14223

Nakagawa, A. C. S., Ario, N., Tomita, Y., Tanaka, S., Murayama, N., Mizuta, C., et al. (2020). High temperature during soybean seed development differentially alters lipid and protein metabolism. *Plant Prod. Sci.* 23, 504–512. doi: 10.1080/1343943X.2020.1742581

Obour, A. K., Obeng, E., Mohammed, Y. A., Ciampitti, I. A., Durrett, T. P., Aznar-Moreno, J. A., et al. (2017). Camelina seed yield and fatty acids as influenced by genotype and environment. *Agron. J.* 109, 947–956. doi: 10.2134/agronj2016.05.0256

Ohlrogge, J., and Browse, J. (1995). Lipid biosynthesis. *Plant Cell* 7, 957–970. doi: 10.1105/tpc.7.7.957

O'Quin, J. B., Bourassa, L., Zhang, D., Shockey, J. M., Gidda, S. K., Fosnot, S., et al. (2010). Temperature-sensitive post-translational regulation of plant omega-3 fatty-acid desaturases is mediated by the endoplasmic reticulum-associated degradation pathway. *J. Biol. Chem.* 285, 21781–21796. doi: 10.1074/jbc.M110.135236

Ortiz, A. C., De Smet, I., Sozzani, R., and Locke, A. M. (2022). Field-grown soybean shows genotypic variation in physiological and seed composition responses to heat stress during seed development. *Environ. Exp. Bot.* 195, 104768. doi: 10.1016/J.ENVEXPBOT.2021.104768

Ozseyhan, M. E., Kang, J., Mu, X., and Lu, C. (2018). Mutagenesis of the FAE1 genes significantly changes fatty acid composition in seeds of Camelina sativa. *Plant Physiol. Biochem.* 123, 1–7. doi: 10.1016/j.plaphy.2017.11.021

Parrotta, L., Aloisi, I., Faleri, C., Romi, M., Del Duca, S., and Cai, G. (2020). Chronic heat stress affects the photosynthetic apparatus of Solanum lycopersicum L. cv Micro-Tom. *Plant Physiol. Biochem.* 154, 463–475. doi: 10.1016/j.plaphy.2020.06.047

Pollard, M., and Shachar-Hill, Y. (2022). Kinetic complexities of triacylglycerol accumulation in developing embryos from Camelina sativa provide evidence for multiple biosynthetic systems. *J. Biol. Chem.* 298, 101396. doi: 10.1016/j.jbc.2021.101396

Rajendra Prasad, V. B., Govindaraj, M., Djanaguiraman, M., Djalovic, I., Shailani, A., Rawat, N., et al. (2021). Drought and high temperature stress in sorghum: Physiological, genetic, and molecular insights and breeding approaches. *Int. J. Mol. Sci.* 22 (18), 9826. doi: 10.3390/ijms22189826

Raziei, Z., Kahrizi, D., and Rostami-Ahmadvandi, H. (2018). Effects of climate on fatty acid profile in Camelina sativa. *Cell. Mol. Biol.* 64, 91–96. doi: 10.14715/cmb/2018.64.5.15

Righini, D., Zanetti, F., Martínez-Force, E., Mandrioli, M., Toschi, T. G., and Monti, A. (2019). Shifting sowing of camelina from spring to autumn enhances the oil quality for bio-based applications in response to temperature and seed carbon stock. *Ind. Crops Prod.* 137, 66–73. doi: 10.1016/J.INDCROP.2019.05.009

Rodríguez-Rodríguez, M. F., Sánchez-García, A., Salas, J. J., Garcés, R., and Martínez-Force, E. (2013). Characterization of the morphological changes and fatty acid profile of developing Camelina sativa seeds. *Ind. Crops Prod.* 50, 673–679. doi: 10.1016/j.indcrop.2013.07.042

Rustgi, S., Kakati, J. P., Jones, Z. T., Zoong Lwe, Z. S., and Narayanan, S. (2021). Heat tolerance as a function of membrane lipid remodeling in the major US oilseed crops (soybean and peanut). *J. Plant Biochem. Biotechnol.* 30, 652–667. doi: 10.1007/s13562-021-00729-2

Sailaja, B., Subrahmanyam, D., Neelamraju, S., Vishnukiran, T., Rao, Y. V., Vijayalakshmi, P., et al. (2015). Integrated physiological, biochemical, and molecular analysis identifies important traits and mechanisms associated with differential response of rice genotypes to elevated temperature. *Front. Plant Sci.* 6. doi: 10.3389/fpls.2015.01044

Salvucci, M. E., and Crafts-Brandner, S. J. (2004). Inhibition of photosynthesis by heat stress: The activation state of Rubisco as a limiting factor in photosynthesis. *Physiol. Plant* 120, 179–186. doi: 10.1111/j.0031-9317.2004.0173.x

Sharkey, T. D. (2005). Effects of moderate heat stress on photosynthesis: Importance of thylakoid reactions, rubisco deactivation, reactive oxygen species, and thermotolerance provided by isoprene. *Plant Cell Environ.* 28, 269–277. doi: 10.1111/j.1365-3040.2005.01324.x

Shen, H. F., Zhao, B., Xu, J. J., Liang, W., Huang, W. M., and Li, H. H. (2017). Effects of heat stress on changes in physiology and anatomy in two cultivars of Rhododendron. *South Afr. J. Bot.* 112, 338–345. doi: 10.1016/j.sajb.2017.06.018

Stamenković, O. S., Gautam, K., Singla-Pareek, S. L., Dhankher, O. P., Djalović, I. G., Kostić, M. D., et al. (2023). Biodiesel production from camelina oil: Present status and future perspectives. *Food Energy Secur.* 12, 1–25. doi: 10.1002/fes3.340

Staniak, M., Stępień-Warda, A., Czopek, K., Kocira, A., and Baca, E. (2021). Seeds quality and quantity of soybean [glycine max (L.) merr.] cultivars in response to cold stress. *Agronomy* 11, 1–13. doi: 10.3390/agronomy11030520

Upchurch, R. G. (2008). Fatty acid unsaturation, mobilization, and regulation in the response of plants to stress. *Biotechnol. Lett.* 30, 967–977. doi: 10.1007/s10529-008-9639-z

Vollmann, J., and Eynck, C. (2015). Camelina as a sustainable oilseed crop: Contributions of plant breeding and genetic engineering. *Biotechnol. J.* 10, 525–535. doi: 10.1002/biot.201400200

Von Cossel, M., Lewandowski, I., Elbersen, B., Staritsky, I., Van Eupen, M., Iqbal, Y., et al. (2019). Marginal agricultural land low-input systems for biomass production. *Energies* 12 (16), 3123. doi: 10.3390/en12163123

Wallis, J. G., and Browse, J. (2002) *Mutants of Arabidopsis reveal many roles for membrane lipids*. Available at: www.elsevier.com/locate/plipres.

Xu, G., Singh, S., Barnaby, J., Buyer, J., Reddy, V., and Sicher, R. (2016). Effects of growth temperature and carbon dioxide enrichment on soybean seed components at different stages of development. *Plant Physiol. Biochem.* 108, 313–322. doi: 10.1016/j.plaphy.2016.07.025

Zandalinas, S. I., Fritschi, F. B., and Mittler, R. (2021). Global warming, climate change, and environmental pollution: recipe for a multifactorial stress combination disaster. *Trends Plant Sci.* 26, 588–599. doi: 10.1016/j.tplants.2021.02.011

Zanetti, F., Alberghini, B., Marjanović Jeromela, A., Grahovac, N., Rajković, D., Kiprovski, B., et al. (2021). Camelina, an ancient oilseed crop actively contributing to the rural renaissance in Europe. A review. *Agron. sustain. Dev.* 41, 2. doi: 10.1007/s13593-020-00663-y

Zanetti, F., Eynck, C., Christou, M., Krzyżaniak, M., Righini, D., Alexopoulou, E., et al. (2017). Agronomic performance and seed quality attributes of Camelina (Camelina sativa L. crantz) in multi-environment trials across Europe and Canada. *Ind. Crops Prod.* 107, 602–608. doi: 10.1016/j.indcrop.2017.06.022

Zhang, M., Barg, R., Yin, M., Gueta-Dahan, Y., Leikin-Frenkel, A., Salts, Y., et al. (2005). Modulated fatty acid desaturation via overexpression of two distinct ω-3 desaturases differentially alters tolerance to various abiotic stresses in transgenic tobacco cells and plants. *Plant J.* 44, 361–371. doi: 10.1111/j.1365-313X.2005.02536.x

Zhang, H., and Sonnewald, U. (2017). Differences and commonalities of plant responses to single and combined stresses. *Plant J.* 90, 839–855. doi: 10.1111/tpj.13557

Zheng, G., Tian, B., Zhang, F., Tao, F., and Li, W. (2011). Plant adaptation to frequent alterations between high and low temperatures: remodelling of membrane lipids and maintenance of unsaturation levels. *Plant Cell Environ.* 34, 1431–1442. doi: 10.1111/J.1365-3040.2011.02341.X

Zhuang, Y., Dong, J., He, X., Wang, J., Li, C., Dong, L., et al. (2022). Impact of heating temperature and fatty acid type on the formation of lipid oxidation products during thermal processing. *Front. Nutr.* 9. doi: 10.3389/FNUT.2022.913297/BIBTEX

frontiers | Frontiers in Plant Science

TYPE Review
PUBLISHED 07 December 2023
DOI 10.3389/fpls.2023.1271644

OPEN ACCESS

EDITED BY
Junya Mizoi,
The University of Tokyo, Japan

REVIEWED BY
Naohiko Ohama,
The University of Tokyo, Japan
Attila Fábián,
Hungarian Research Network, Hungary

*CORRESPONDENCE
Marta A. Mendes
marta.mendes@unimi.it

†These authors have contribute equally to this work

RECEIVED 02 August 2023
ACCEPTED 13 November 2023
PUBLISHED 07 December 2023

CITATION
Resentini F, Orozco-Arroyo G, Cucinotta M and Mendes MA (2023) The impact of heat stress in plant reproduction.
Front. Plant Sci. 14:1271644.
doi: 10.3389/fpls.2023.1271644

The impact of heat stress in plant reproduction

Francesca Resentini†, Gregorio Orozco-Arroyo†, Mara Cucinotta and Marta A. Mendes*

Dipartimento di Bioscienze, Università degli Studi di Milano, Milano, Italy

The increment in global temperature reduces crop productivity, which in turn threatens food security. Currently, most of our food supply is produced by plants and the human population is estimated to reach 9 billion by 2050. Gaining insights into how plants navigate heat stress in their reproductive phase is essential for effectively overseeing the future of agricultural productivity. The reproductive success of numerous plant species can be jeopardized by just one exceptionally hot day. While the effects of heat stress on seedlings germination and root development have been extensively investigated, studies on reproduction are limited. The intricate processes of gamete development and fertilization unfold within a brief timeframe, largely concealed within the flower. Nonetheless, heat stress is known to have important effects on reproduction. Considering that heat stress typically affects both male and female reproductive structures concurrently, it remains crucial to identify cultivars with thermotolerance. In such cultivars, ovules and pollen can successfully undergo development despite the challenges posed by heat stress, enabling the completion of the fertilization process and resulting in a robust seed yield. Hereby, we review the current understanding of the molecular mechanisms underlying plant resistance to abiotic heat stress, focusing on the reproductive process in the model systems of *Arabidopsis and Oryza sativa*.

KEYWORDS

heat stress, plant reproduction, rice, *Arabidopsis*, calcium signaling, pollen development, ovule development

Introduction

Heat Stress (HS) causes substantial crop loss worldwide. The average global temperature is constantly increasing, and this change is expected to have deleterious effects on crop yield. A recent study showed that drought and, particularly, extreme heat episodes dramatically decreased cereal production by 9–10% between 1964 and 2007 (Lesk et al., 2016). Average temperatures are estimated to rise by 2–3°C over the next 30 to 50 years. Given the fact that the human population is estimated to reach 9 billion by 2050, genetic improvement of tolerance traits to abiotic stresses on stable crops is an immediate priority. Europe recently experienced several heat waves, in 2003 the heat-related death toll ran into tens of thousands. Another heat wave in 2012 impacted crop productivity and yield of several important food species with a decrease of up to 40%, as for sunflowers for example (Peng et al., 2004). Among

all the documented losses, it was estimated that rice grain production decreased by 10% for each 1°C increase, and it has also been predicted that every 1°C increase reduces wheat production by 3 - 4% (Xu J. et al., 2020; Wang et al., 2020). Similar deleterious effects have been shown for maize and barley, for which each day that the plants are exposed to a temperature over 30°C, yield is reduced by 1% (Rezaei et al., 2015). The year 2016 ranks as the warmest on record and the year 2018 was the fourth warmest since 1880 (Source: NASA/GISS) confirming a continuous trend towards warmer climates. Since extreme climatic events, such as heat waves, are increasingly common, agriculture will face extraordinary challenges to sustain productivity (Mulla et al., 2020).

Understanding how plants cope with HS during their reproductive phase is critical for managing the future of agricultural productivity, as most of our food supply is a product of plant reproduction. Even if the effect of temperature has been extensively studied using accessible plant tissues, such as leaves and roots, analysis on reproduction is often difficult because gametophyte development and fertilization are complex processes that occur during a narrow window of time and deep inside the flower. The effect of HS on plant reproduction is very wide affecting many reproductive tissues at the same time. HS leads to abnormalities in floral development, plants develop altered flower structures, with reduced flower size, or even the development of complete sterile flowers. These flower changes are translated into impaired pollination and fertilization processes that ultimately lead to reduced fruit and seed production. From the male side, HS impacts anther and pollen grain development leading to morphological abnormalities and displacement of the metabolic processes that impair pollen grain ability to germinate and to grow pollen tubes. From the female side, HS can disrupt gametogenesis, leading to abnormal development of the female gametophyte (embryo sac), this can affect the formation of essential components within the embryo sac, such as the gametes (egg cell). Impaired fertilization and embryo development are the ultimate consequences of HS which results in reduced and/or poor seed production (Barnabás et al., 2008; Prasad et al., 2008; Bita and Gerats, 2013) (Figure 1).

Many genes regulating responses and resistance to various biotic and abiotic stresses have been precisely identified. However, coordinated responses between roots and leaves at the whole plant level remain largely unknown. Roots and shoots communicate with each other to synchronize and optimize plant development and respond to environmental changes. Thus, the growth of these two structures is coordinated and this requires communication mediated by signal messengers that move between the aboveground and belowground structures (Ko and Helariutta, 2017). The vascular system serves as an effective long-distance communication system, with the phloem and xylem serving to input information relating to conditions (Lucas et al., 2013). An interesting observation is that a stress applied to systemic tissues is sensed by the inflorescence in a short timeframe (minutes or a few hours) (Choudhury et al., 2018), thus pointing to the existence of a fast communication pathway that most probably relies on (i) changes in electric potential, (ii) calcium ions (Ca^{2+}) and (iii) reactive oxygen species (ROS) (Iba, 2002; Liao et al., 2017; Jespersen, 2020).

For this reason, understanding how environmental cues are sensed and transmitted to systemic organs of plants such as the inflorescence and how this impacts the flower development therefore seeds' setting and plant reproduction in model species, such as *Arabidopsis*, could be relevant for the establishment of a baseline for crop improvement. Here we will provide an overview of the importance of molecular mechanisms underlying plant resistance to HS, focusing on the reproductive process in *Arabidopsis thaliana* and *Oryza sativa*, highlighting the role of Ca^{2+} as a link between the perception of environmental signal and a physiological response.

Pollen and ovule development response to HS in Arabidopsis

Flowering plants, i.e. angiosperms, alternate between a highly reduced gametophytic (haploid) and sporophytic (diploid) generations (Yadegari and Drews, 2004). The sporophyte is the multicellular diploid plant whereas the haploid structure

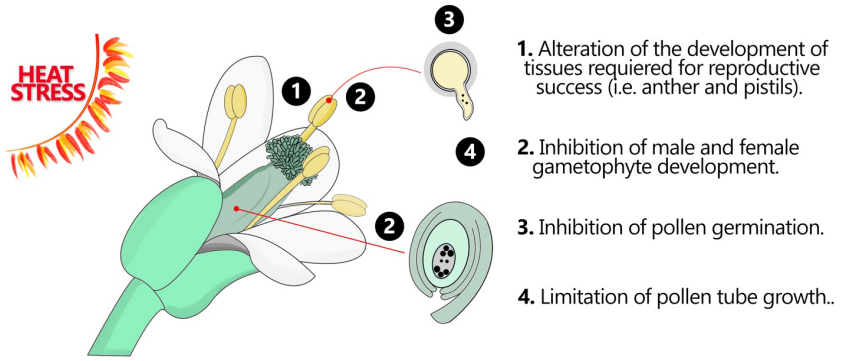

FIGURE 1
Flower organs and tissues in response HS. Heat stress can have significant impacts on various flower organs and tissues, leading to alterations in their development, structure, and function. These effects can disrupt normal floral development and ultimately impact reproductive success. This figure demonstrates how the fertile flower organs may respond to HS.

called gametophyte is generated by meiotic cell division within the male and female reproductive organs (Drews and Koltunow, 2011). In Arabidopsis, male gametophyte development occurs within stamens, composed of a filament and an anther. Within anthers, non-reproductive cells differentiate into specialized layers, including the tapetum, surrounding sporogenous cells (Scott et al., 2004). Two distinct phases, microsporogenesis and microgametogenesis, produce mature pollen. Microsporogenesis involves meiosis in pollen mother cells, generating haploid microspores. After callose wall degeneration, individual microspores are released (Borg et al., 2009). Subsequent mitotic divisions yield vegetative and generative cells. Asymmetric division in the first pollen mitosis determines unique gene expression profiles, defining structures and fates. A second mitosis produces twin sperm cells for double fertilization, leading to embryo and endosperm development (Twell et al., 1998). Abiotic stress in pollen development was comprehensively studied in the last years and reviews were produced where pollen defects in different species were reviewed (Chaturvedi et al., 2021).

In Arabidopsis was recently demonstrated that the male gametophyte (pollen) is particularly sensitive to heat fluctuations, causing defects in meiotic restitution (De Storme and Geelen, 2020). More in detail meiosis and in particular meiotic recombination are highly sensitive to elevated temperatures, meiotic microtubule cytoskeleton resulted in an irregular spindle orientation, and aberrant cytokinesis that consequently led to the production of aneuploid male gametes (De Storme and Geelen, 2020; Hedhly et al., 2020; De Jaeger-Braet et al., 2022). In Arabidopsis, the increase in crossover frequency at high temperatures was associated with elevated numbers of Type I interfering pathway crossover. Interestingly, the meiotic hyper-recombination observed in Arabidopsis resulted specific for HS, as plants subject to salt stress did not exhibit an increase in crossover frequency (Modliszewski et al., 2018). Precisely because of the HS effect on chromosome segregation, high-temperature treatment has been proposed as a tool in plant breeding to induce genome elimination and haploid induction. Indeed, if applied to haploid inducer mutants, such as mutant for the CENTROMERE-SPECIFIC HISTONE H3, short-term HS increases the efficiency of haploid induction by ten times (Ahmadli et al., 2023; Jin et al., 2023; Figure 2). Another aspect of male meiosis that is influenced by the HS is the duration of the different phases of meiosis. By performing live cell imaging on male meiocytes, De Jaeger-Braet et al. (2022) showed that the meiosis phase of meiocytes at a high temperature of 34°C is faster than at 21°C. By contrast, the pachytene/diakinesis phase gets prolonged at 34°C. The extension of this specific phase is recombination dependent since it was not detected in *ataxia telangiectasia mutated* (*atm*) mutant in which recombination is completely abolished.

Regarding the female part of development studies using the model plant Arabidopsis, HS reduced the total number of ovules and increased ovule abortion (Whittle et al., 2009). Furthermore, it has been described in Tomato that female pistils exposed to HS (32/26°C) and then crossed with pollen from plants grown in standard conditions (at 28/22°C) exhibited reduced fruit set and a reduced number of seeds per fruit compared with the control pistils of plants grown at 28/22°C (Peet et al., 1998). The seed set was even more reduced in the reciprocal experiment using maize plants when

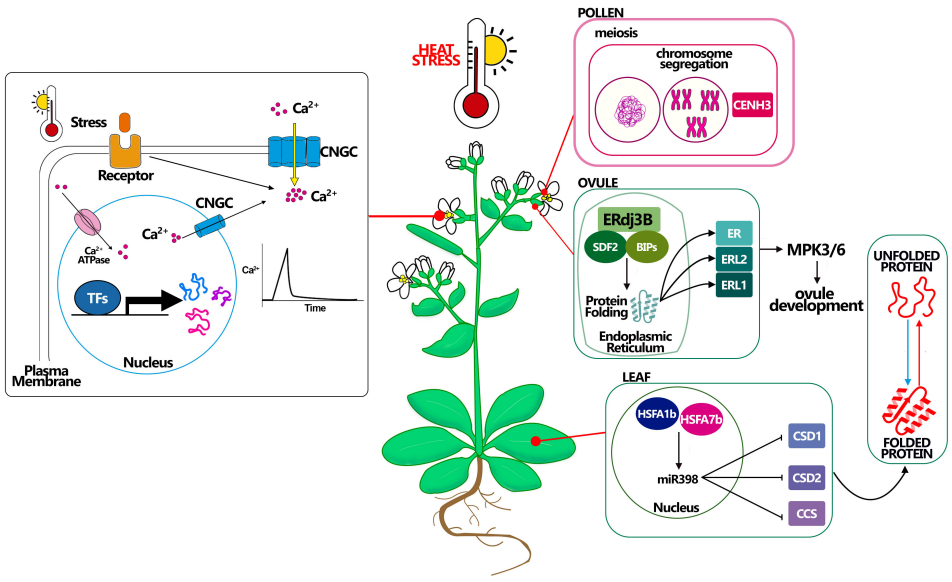

FIGURE 2
Molecular mechanisms connected with heat stress resistance in Arabidopsis. Heat affects plant Ca^{2+} channels, inducing a transient increase in cytosolic Ca^{2+} concentration. Stress sensors recognize environmental signals (i.e. heat) and activate plasma membrane-localized Ca^{2+} channels, allowing Ca^{2+} influx into the cytosol by the use of CNGCs channels. Cytosolic Ca^{2+} ion acts as a second messenger that triggers specific cellular responses. Pollen CENH3 mediates genome elimination during HS, this mechanism could be better studied to understand how to maintain meiosis under HS. Ovule complex ERdj3B acting in complex with SDF2 and BIPs in the endoplasmic reticulum control the protein folding, being essential to the plant tolerate the HS, probably via the ERL proteins. A good example in leaf development for thermotolerance is giving by miR398 which expression is controlled by HSFA proteins and that promotes the resistance to stress controlling the correct folding of the proteins.

transient HS was applied for three days on developing pollen that later was used to pollinate female flowers grown at optimal conditions (Begcy et al., 2019). These were the only studies that described some of the female defects caused by HS, which remained largely unstudied.

In Arabidopsis, the female germline initiates during the initial phase of ovule development. This process begins with the differentiation of a distal subepidermal cell known as the megaspore mother cell, which undergoes meiosis to give rise to four haploid megaspores, typically arranged in a linear tetrad. Among these four megaspores, only one survives to become the functional megaspore, while the remaining three undergo programmed cell death. Following megasporogenesis, the functional megaspore proceeds to undergo a Polygonum-type pattern of megagametogenesis, leading to the formation of the embryo sac and female gamete. Integument development in Arabidopsis is a simple two-cell layered structure that develops around the embryo sac and after fertilization protects the developing embryo developing the seed coat (Christensen et al., 2002; Yadegari and Drews, 2004, Mendes et al., 2016).

Arabidopsis endoplasmic reticulum-localized DnaJ family 3B (ERdj3B) was recently described as an important factor for the correct development of ovule integuments by controlling the translocation of the ERECTA-family receptor kinases in the ecotype Landsberg (Leng et al., 2022). ERdj3B is a component of the stromal cell-derived factor 2 (SDF2)–ERdj3B–binding immunoglobulin protein (BiP) chaperone complex, and has functions in protein folding, translocation, and quality control. ERdj3B was first described to be involved in thermotolerance during anther development (Yamamoto et al., 2020) and was also described now to have complex functions not only in ovule integument development but also in HS response from the female side. Leng and collaborators (Leng et al., 2022) further described that higher temperatures were shown to aggravate the defective phenotypes of erdj3b mutants, linking that the response to HS has more severe effects on ovule development when ERECTA-family receptor kinases are absent (Figure 2). A recent study also described the TCP transcription factors inhibit the homeotic conversion of ovules into carpelloid structures under HS, (Lan et al., 2023) reinforcing the fact that transcription factor complexes important for ovule identity can also be related to HS perception and could have significant implications for understanding the molecular mechanisms underlying the plant's response to HS and how it affects reproductive development.

HS proteins and HS transcription factors in Arabidopsis

For quite some time in cellular biology, HS proteins have been recognized as those whose levels significantly rise when cells are cultivated at elevated temperatures, providing a form of resilience. It is now understood that these proteins play a role in assisting newly synthesized proteins in proper folding and safeguarding proteins that may otherwise misfold and lose their intended functional conformation during stressful events. Importantly, these proteins are not solely associated with HS but also have connections to other biotic and/or abiotic stress conditions. HS proteins (HSPs) besides stress-responsive genes (Ul Haq et al., 2019), also are involved in plant growth and development under normal conditions, like the flowers, seeds, and fruits set development, in the tuberization (Agrawal et al., 2013) and nutrient uptake (Shekhar et al., 2016). Studies using Arabidopsis and crops (rice, maize, and wheat) showed that the basis of thermotolerance resides in the overexpression of HSP factors, which increase plant resistance to abiotic HS (Ul Haq et al., 2019). These studies have focused on the analysis of transgenic plants under a broad spectrum of induced HS treatments, which makes the data extremely variable and not suitable for comparison purposes (Yeh et al., 2012). The optimum scenario is to identify a stable accession or species that naturally overexpresses HSP factors that induce HS resistance. Furthermore, most of the thermotolerance studies are again based on seedling germination and root development, meanwhile, the reproductive phase is often not considered. Therefore, even though a plant can potentially tolerate HS at early phases of development, it might be HS susceptible at mature stages and hence sterile.

At the molecular level, the cellular response to HS is represented by the induction of HSP, a group of stress proteins that are classified as molecular chaperones and proteases. The molecular analysis of HSP promoters leads to the identification of the heat shock element (HSE), a stress-responsive promoter element essential for HS inducibility; this binding site is characterized by multiple adjacent 5`-nGAAn-3`. The position of HSEs in the genome is various and distances upstream of their transcription starting site. In vertebrates and plants, HSP transcription requires the transient binding of HS transcription factors (HSFs) to the HSEs present within their promoters (Wu, 1995; Morimoto, 1998; Kovács et al., 2022). Plant HSFs are divided in three classes A, B and C. Class A HSFs typically contain one or two acidic AHA motifs and function as transcriptional activators, as indicated by Döring et al. (2000). On the other hand, class B HSFs possess a B3 repressing domain, which has also been identified in 24 other transcription factors in Arabidopsis. Class C HSFs have not been thoroughly described (Czarnecka-Verner et al., 2004; Ikeda and Ohme-Takagi 2009; Guo et al., 2016). In contrast to the limited number of HSF members in vertebrates (4), Drosophila (1), *Caenorhabditis elegans* (1), and yeast (1), plant HSF families exhibit a considerable number of members derived from a complex, plant-specific superfamily, as highlighted by Wu (1995) and Morimoto (1998).

The large size of the plant HSFs family inevitably complicates the unraveling of their function under stress conditions (Scharf et al., 2012 and reviewed in Guo et al., 2016).

The identification of factors that allow plants to tolerate HS has been mainly performed in the model species Arabidopsis. Yet, research on economically relevant species has been performed (Ul Haq et al., 2019). In Arabidopsis during the vegetative phase, the constitutive expression of the HS transcription factors HSFA1a, b, d, and e are responsible for triggering the HS response (Yoshida et al., 2011). *HSF1abde* are responsible for basal thermotolerance and initiate the acquisition of thermotolerance. A second transcription factor from this family is HSFA2, the most highly heat-induced HSF. Remarkably, ectopic expression of *HSFA2* was

able to rescue the phenotype of the quadruple mutant *hsaf1abde* at reproductive stage (Liu and Charng, 2013). This is partly explained by the fact that HSFA2 can induce its own expression. HSFA3, HSFA7a, and HSFA7b are also induced by HSFA2 and/or HSFA1 after HS (Liu and Charng, 2013). Instead, the defective mutant *hsfa2* is only impaired in maintaining the acquired thermotolerance after long recovery (Charng et al., 2007). HSFs were extensively reviewed by Guo et al., 2016.

Manipulation on genes that have the potential to improve HS tolerance has focused mainly on genes involved in the synthesis of HSP. Yet, no clear evidence regarding the improvement to HS resistance of such mutants is available. One of the first studies that reported how a HSP manipulated can improve the tolerance to HS was made using the HSF SQUAMOSA promoter binding protein-like7 (SPL7, Yamanouchi et al., 2002). Mutant plants lacking the function of *spl7* develop more necrotic lesions on leaves under HS treatment (35°C for 24 hours followed by 42°C for 24 hours). *spl7* mutant lines complemented with wild-type SPL7 were more resistant to HS showing no occurrence of necrotic lesions during the growth period (Yamanouchi et al., 2002). Remarkably, a strong correlation between the inserted number of copies of the transgene and the reduction in the necrotic lesions was detected, suggesting that the "overexpression" of *SPL7* might be helpful to improving HS tolerance (Yamanouchi et al., 2002), any evidence in the reproductive part were studied. The sole HSF identified with a function in ovule development is HSFB2a. Plants with heterozygous mutations in HSFB2a display 50% sterile ovules and a significant decrease in both male and female transmission, suggesting that the gene's absence adversely affects the development of both male and female germ lines. Even if is not an HS related phenotype is it very interesting to notice that the homozygous mutant was already sterile, with block during female gametophyte (Wunderlich et al., 2014). A very interesting study demonstrated that heat-inducible miR398 that is directly activated by HSFA1b and HSFA7b is required for thermotolerance through the downregulation of its target genes CSD1, CSD2 and CCS which encode for copper chaperones. The corresponding mutations to *csd1*, *csd2* and *ccs* mutant plants are more heat-tolerant and the resistant transgenic plants expressing the miR398-resistant forms of CSD1, CSD2 or CCS were more sensitive to HS at 37°C (Guan et al., 2013, Figure 2). Studies involving miRNAs during reproductive tissues would be of outmost importance as in the last years were described to play several roles during reproduction (Petrella et al., 2021).

Calcium as a signal for HS in Arabidopsis

In plants, calcium ion (Ca^{2+}) plays an important role both as a structural component of plant cell walls and membranes and as an intracellular second messenger. As second messenger, Ca^{2+} is involved in an advanced network of signaling pathways taking part in various signaling processes generated in response to both biotic and abiotic stresses, as well as developmental stimuli (Kudla et al., 2018; Resentini et al., 2021; Ghosh et al., 2022). In nature, plants must cope with both seasonal and diurnal temperature changes. Particularly, temperature fluctuations that occur in a single day can be dangerous for plants since they can face temperature stress more rapidly as compared to other stresses such as drought or salinity (Larkindale and Knight, 2002; Ghosh et al., 2022). Therefore, like other organisms, plants have evolved defense mechanisms to efficiently cope with temperature stress and to prevent the disruption of multiple cellular processes, including protein folding, cytoskeletal organization, membrane stability, regulation of ROS and ion homeostasis (Weigand et al., 2021; Ghosh et al., 2022).

It has been shown that plants exposed to a heat shock show a transient increase of the cytosolic Ca^{2+} concentration (Gong et al., 1998; Wu and Jinn, 2010). Such an increase was shown to depend on the activity of some members of the CYCLIC NUCLEOTIDE-GATED channels (CNGCs) family (Finka et al., 2012; Cui et al., 2020). Interestingly, CNGCs have been implicated in diverse aspects of plant growth and development, such as pollen tube growth and fertility. Six CNGC members—CNGC7, 8, 9, 10, 16 and 18—have been reported as highly expressed in the pollen grain and pollen tube (Frietsch et al., 2007; Tunc-Ozdemir et al., 2013). Among them, genetic evidence identifies CNGC16 as a critical component in maintaining pollen fertility under conditions of heat and drought stress (Tunc-Ozdemir et al., 2013). The *cngc16* mutant, in fact, showed more than a 10-fold stress-dependent loss in pollen fitness as well as seed set under HS and drought stress. At the same time, *cngc16* mutant pollen exhibited attenuated expression of HS responsive genes (Tunc-Ozdemir et al., 2013). Nonetheless, there are scant pieces of evidence directly supporting a role for Ca^{2+} signals as an initial heat sensing response during plant reproduction (Ghosh et al., 2022) (Figure 2).

Weigand and colleagues in 2021 generated a reporter called CGf, a ratiometric, genetically encoded Ca^{2+} indicator with a mCherry domain fused to the intensiometric Ca^{2+} reporter GCaMP6f. By using this new tool, the authors showed that HS suppressed the tip-focused Ca^{2+} oscillations in growing pollen tubes with the consequent growth arrest and even pollen tube tip rupture (Weigand et al., 2021). This important result highlights the urgent need to better investigate the HS signaling in pollen tubes and better define the role of Ca^{2+} signaling components in this response. It is obvious that the temperature stress, by affecting pollen tube development will lead to decreased fertility and reduced seed production. A good knowledge of the specific role of Ca^{2+} signaling in a pollen tube, subjected to HS, will surely be instrumental to developing tailored strategies aimed at improving pollen resilience to HS. During fertilization process, synergids are an essential part of the female gametophyte. These cells are involved in guiding the pollen tube to the embryo sac and facilitating the entry of the male gamete, and commit programmed cell death upon pollen tube arrival (Mendes et al., 2016). Ca^{2+} spikes were detected in the reception and recognition of the pollen tube by the synergid cells and ultimately upon pollen tube burst and delivery of the male gametes and upon synergid cell death (Ngo et al., 2014). Studies understanding how Ca^{2+} spikes relationship with HS in the context of fertilization process is crucial for developing effective strategies to mitigate the negative impacts of HS on seed production and ensuring sustainable practices in the face of climate change.

HS effects in a crop of economic relevance, *Oryza sativa*

Rice, like several other cereal species, shows large adaptive phenotypic plasticity enabling yield stability across environments. However, high temperatures beyond the critical threshold of rice growth can cause severe reductions in grain yield and quality, particularly from the heading stage to the grain-filling stage. Generally, the process of male and female gametophyte formation in *Oryza sativa* is similar to what was described for Arabidopsis, is mainly divided into three stages: meiotic division of the spore mother cell, mitotic stage of functional spore cells, and mature stage of gametophyte (Itoh et al., 2005). Research focusing on rice ovule and pollen development are limited for several reasons, the main one is the fact that the gametophytes are deeply embedded in the inflorescences also called panicles, because of their conic shape (Li et al., 2023). Rice panicle comprises the main axis, a branch from the branch meristem, and a spikelet from the spikelet meristem. The spikelet meristem forms the sterile organs, glumes and lemmas that enclose the florets which on in its turn contains all the reproductive and fertile organs that give rise to seeds (grains) (Itoh et al., 2005). The flowering phase in rice is highly sensitive to high temperatures. Two days of HS conditions resulted in an increase in the number of spikelets with non-viable pollen, meanwhile, four or more days of HS led to complete male sterility and several morphological defects on panicle development in heat-sensitive variety Nipponbare (Figure 3) (Endo et al., 2009, Li et al., 2023). To gain insight into the molecular mechanism of heat-induced male sterility, Endo and collaborators analyzed transcriptional alteration in the anther under high-temperature conditions using DNA microarray. The identified high temperature-repressed genes, such as YY1 and YY2 were expressed predominantly in the tapetum at the uninucleate microspore stage. Among them two genes involved in lipid metabolism, a plant-specific cytochrome P450 and a GDSL type ligase were identified, suggesting that the composition of lipid derivatives in the pollen might be altered in anthers exposed to high temperatures (Endo et al., 2009). Another study (Zhang et al., 2012) evaluated transcriptomic changes accompanying HS in reproductive tissues, at early stages of development (pre- and during meiosis) from the heat-tolerant cultivar Indica-type 996, which exhibits better anther dehiscent, pollen fertility rate and final seed yield than heat-sensitive cultivar Indica-type 4628 (Luo et al., 2005; Zhang et al., 2008). The predominant transcription factor gene families responsive to HS were HSF, NAC, AP2/ERF, WRKY, MYB, and C2H2, showing time-dependent gene expression pattern under short/middle-term HS (from 20 minutes to 8 hours). Furthermore, the promoter analysis of HS early up-regulated genes showed the important role of some specific motifs, such as HSE, GCC box, ABRE and CE3 in response to HS (Zhang et al., 2012, Figure 3). It is widely known that the HSE motif can be recognized and bound by HSF to respond to heat shock (Yamamoto et al., 2005), while other motifs are linked to ethylene, ABA and Ca^{2+} signaling, suggesting the existence of a complex crosstalk between several hormones and stimuli during heat shock (Zhang et al., 2012). Recently another thermotolerant rice accession was described, T2-Jinxibai, that after 45°C for 24h, exhibited high resistance to HS and the seedlings exhibited a survival rate of 90.93% after heat treatment. Sixty transcription factors were differentially expressed in the thermotolerant accession including the members of the AP2/ERF, NAC, HSF, WRKY, and C2H2 families as seen for the thermotolerant Indica-type 996 cultivar (He et al., 2023, Figure 3).

Very interestingly, Jagadish et al. (2008) describes the heat tolerant cultivar *Oryza sativa* indica Nagina 22 (N22), which after a 6-hour high temperature treatment, still maintains a 71% of spikelet fertility. This is a positive significant value if compared with sensitive (Moroberekan - 18% fertility) or intermediate (IR64 - 48% fertility) cultivars (Jagadish et al., 2010). Conducting a proteomic examination of the anthers in the heat-tolerant cultivar N22 unveiled the distinct expression patterns of 13 proteins. Among these, seven proteins demonstrated sequence similarities to potential cold shock protein (CSP), an inorganic pyrophosphatase, a serine protease (AIR3), a dirigent-like protein, a ribosomal protein (S19), a small heat shock protein (sHSP), and an iron deficiency protein (IDS3). These proteins are presumed contributors to the observed heightened heat tolerance in the cultivar. Particularly interesting are the stress-responsive cold and heat shock proteins identified (Jagadish et al., 2010, Figure 3), which will require further analysis to determine their role in HS tolerance. Consequently, it has been proposed that heat shock proteins contribute to higher tolerance to HS in rice. Supporting this hypothesis, Sailaja et al. (2015) reported that the expression of several heat shock expression factors (HSFS - OsHSFA2a, OsHSFA2e, and OsHSFA7) were highly upregulated in N22 plants when they were under heat treatment (42°C for 24 hours), with respect to the heat susceptible cultivar Vandana. Only two HSFS (OsHSFA2e and OsHSFA7) were upregulated under the same heat treatment in the susceptible cultivar Vandana, although the increase on the level of expression was minimal when compared with N22.

N22 cultivar also presented an improvement in the photosynthetic rate and chlorophyll fluorescence, and reduced transpiration rate under HS. These traits may help this cultivar to show better performance on HS conditions and hence superior yield (Vivitha et al., 2018). The N22 cultivar was also used in another study to depict the global transcriptional response to HS in reproductive tissues, specifically during anthesis (González -Schain et al., 2016). It has been well documented that anthesis in rice is the stage most sensitive to high temperatures (Prasad et al., 2006; Jagadish et al., 2007), during which many physiological processes occur in less than one hour. Indeed, it was shown that reproductive tissue responds quickly, already after 30 minutes, to adjust their transcriptome to prevent damage produced by high temperature (38°C). Proper expression of protective chaperons in anthers at anthesis is needed to overcome stress damage and to ensure fertilization (González -Schain et al., 2016).

Similar to Arabidopsis, in the case of rice, there are relatively few instances where the impact of temperature stress on female reproductive processes has been explored. However, a more extensive body of knowledge exists regarding the effects of HS on male reproductive functions.This is because pollen is easily accessible compared to ovules coupled with the notion that pollen

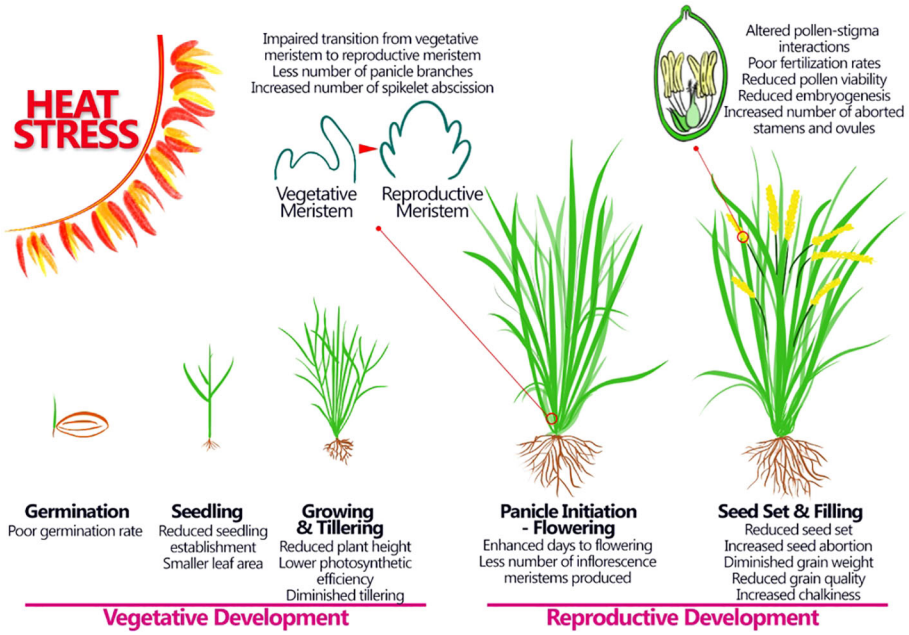

RICE THERMOTOLERANT ACCESIONS	DIFFERENTIALLY EXPRESSED GENES AND/OR FAMILIES
Indica-type 996	NAC, AP2/ERF, WRKY, MYB, C2H2
Nagina-22 (N22)	OsHSFA2a, OsHSFA2e, OsHSFA7, OsCSP Inorganic Pyrophosphatase, OsAIR3, dirigent-like protein, OsS19, OsSHSP, OsIDS3
T2 (Jinxibai)	MYB, WRKY, bZIP, C2H2, NAC, AP2/ERF, HSFs, HSPs
Sensitive accessions that acquire thermotolerance	OsRAB7, OsRBG1, OsHSP17.7, OsHSP101, mtHSP70, OsHSP18.6

FIGURE 3
Adverse impact of heat stress on morphological and physiological aspects of rice at different stages of development and possible genes and/or families involved in thermotolerance. Heat stress affects rice productivity by affecting both vegetative and reproductive stages, still major effects of heat stress are seen during the reproductive stage and can provoke alterations in the number of panicles produced in the latest stages, modifying the starch content and therefore the quality of the grain. Some thermotolerant accessions were studied and specific gene or families involved in the thermotolerance were discovered.

exhibits greater sensitivity to HS than female reproductive organs in different crop plants (Hedhly et al., 2009; Wang et al., 2021). However, recent studies revealed varying degrees of sensitivity of the pistil, ovaries, ovules, and gametophyte to the HS depending on rice varieties and developmental stages (Wang et al., 2021; Shi et al., 2022). Shi and colleagues (Shi et al., 2022) demonstrated the heat sensitivity of the pistil showing that HSed pistil pollinated with non-stressed pollen resulted in a significant reduction in spikelet fertility in the sensitive IR64 cultivar at 40°C. On the contrary, no sensitivity was observed in the N22 variety, indicating tolerance of N22 to HS also during pistil development. Interestingly, a significant proportion of ovules of IR64 variety subjected to HS were characterized by a non-corrected differentiation of megaspore mother cell or by the degeneration of all four megaspore cells instead of three after meiosis. All those effects resulted in a lesser proportion of viable embryo sacs, such as mature embryo sacs lacking the egg cell or the central cell (Shi et al., 2022). In addition to the effects on gametophyte, a previous study reported the effects of heat on the tissues of the pistil. In particular, about half of the spikelets observed at the SEM microscope developed pistil hyperplasia, i.e., proliferated female organs or tissues, including multiple stigmata and/or ovaries, and differentiation of trichomes from ovary epidermis (Takeoka et al., 1991). HS reduces the capacity of rice grain to assimilate supplies, such as starch and proteins, additionally also shortens grain-filling stage duration, leading to the reduction of grain weight and a chalky-appearing grains, greatly damaging their market value (Kobata and Uemuki, 2004; Peng et al., 2004). Given that starch constitutes the primary component of grains, its deficiency is a key factor contributing to the reduction in grain weight under high temperatures. Consequently, transcriptomic studies have demonstrated that HS suppresses the expression of genes involved in starch biosynthesis while promoting the expression of enzymes responsible for starch consumption (Yamakawa et al., 2007). For example, heightened temperatures led to increased expression levels of several α-amylase genes, namely *Amy1A, Amy1C, Amy3A, Amy3D, and Amy3E*, along with an elevation in enzyme activity. In contrast, the expression of starch biosynthetic genes such as granule-bound starch synthase I *(GBSSI)* and a starch branching enzyme *(BEIIb)* was reduced (Yamakawa et al., 2007). Subsequent research confirmed that the

expression of *Amy1A, Amy3C, and Amy3D* in the endosperm during seed ripening significantly contributes to the production of chalky grains in high-temperature conditions (Nakata et al., 2017). Furthermore, the downregulation of two key sucrose transporter genes, namely SUT1 and SUT2, under HS indicates a potential hindrance to the import of sucrose into the endosperm (Yamakawa and Hakata, 2010).Those results were supported by a parallel metabolomic analysis showing that sucrose and amino acids accumulated, and the level of sugar phosphates and organic acids decreased in HS-ripened caryopses (Yamakawa and Hakata, 2010). Thermotolerance in rice during both vegetative and reproductive growth without a yield penalty was recently identified by a natural quantitative trait locus (QTL), *TT2 -THERMOTOLERANCE 2.* TT2 encodes a Gγ subunit that codifies for a heterotrimeric GTP-binding proteins (G proteins), the thermotolerance was directly linked to the SCT1 (Sensing Ca^{2+} Transcription factor 1) - dependent alteration of wax biosynthesis. The calmodulin–SCT1 interaction was attenuated by reduced heat-triggered Ca^{2+} caused by disrupted TT2 (Kan et al., 2022).

Recently, the allele of the *TT1* gene coming from African rice (*O. glaberrima* - CG14), which encodes for a 26S proteasome α2 subunit protein, boost thermotolerance by enhancing the recycling and elimination of denatured ubiquitinated proteins consequence of HS. Remarkably, plants harbouring the *TT1*-CG14 allele greatly outperformed plants carrying the Asian rice (*TT1- O. sativa* spp. *japonica*) allele in grain per plant production after heat treatment (12h at 38°C/12h at 35°C for 5 days). Yield superiority conferred by the *TT1*-CG14 allele, was observed regardless if HS was applied during flowering or grain filling stages. These results validate the potential of the *TT1*-CG14 allele for breeding heat tolerant crops (Li et al., 2015).

Likewise, plants harbouring the TT3 QTL from CG14 presented higher survival rate at reproductive stage and improved grain yield after HS treatment (30 days at 38°C/34°C day/night) compared with plants carrying the Asian rice TT3-QTL (from *O. sativa* spp. *japonica*). TT3 quantitative trait loci contains the *TT3.1* and *TT3.2* genes, TT3.1 is a RING-type E3 ligase and TT3.2 is a chloroplast precursor protein (ubiquitinated by TT3.1). After HS, TT3.2 is accumulated in chloroplasts causing damages to the photosystem II complex, compromising the thylakoid stability. Consequently, the improved E3 ubiquitin ligase activity of TT3.1-CG14 ubiquitinating TT3.2 for its rapid vacuolar degradation, protect the thylakoids from HS, hence increasing the thermotolerance of the plants (Zhang et al., 2022).

El-Esawi and Alayafi (2019) demonstrated that the overexpression of OsRAB7 enhances not only HS tolerance but also increased grain yield. The RAB protein family is involved in multiple developmental processes and has been linked to tolerance to environmental stresses (reviewed in Tiwari et al., 2021). Transgenic plants overexpressing OsRAB7 presented an increment of nearly 40% in survival rate after a heat treatment (40°C day/32°C night, irrigated daily, for 10 days) with respect to the wild type individuals. Under HS conditions, both wild-type and overexpression lines presented diminishment in growth when compared to individuals growing in normal conditions. However, transgenic lines exhibited better growth performance when compared to the wild type under HS conditions. These findings suggest that the increased expression of OsRAB7 in transgenic rice plants positively influences their survival rate, growth, relative water content, and resilience against both drought and HSes. Given that OsRAB7 overexpression has been associated with improved salt tolerance in rice by enhancing stress signaling transduction through intracellular vesicle trafficking (Peng et al., 2014), it is highly likely that heightened HS tolerance is also achievable through enhanced intracellular vesicle trafficking (El-Esawi and Alayafi, 2019). The yield-related improved traits on the OsRAB7 overexpressing lines when compared with the wild type were: panicle length (+25%), number of spikelets per panicle (+11%), total number of spikelets per hill (+11%), number of filled grains per hill (+35%), filling rate (+21%), and total grain weight (+27%). It is important to notice that under normal conditions, the OsRAB7 overexpressing lines did not show any significant difference on yield traits compared to the wild type (El-Esawi and Alayafi, 2019). These data are extremely important because represent one of the few examples of reported transgenic lines that display a better yield performance under HS conditions. Indeed, most of the improved stress tolerance transgenic lines are focused on the survival rate of the plants but no data regarding the effect on yield is shown. Recently, Lo et al (2020) identified a novel *RICE BIG GRAIN 1 (RBG1)* gene that is involved in auxin homeostasis and enhances cell division. The overexpression of *RBG1* impacts several aspects of plant growth and development including a significant enhancement in the size of the panicle and seeds, when compared to wild-type plants. This positive yield effect, together with the fact that 31 members of the HSPs gene family resulted upregulated on *RBG1* overexpression lines when compared with wild type plants, led the researchers to evaluate the performance of these lines under several stress conditions including HS (4 days at 42°C). Notably, the RBG1 overexpression lines showed a higher survival rate after recovery (≈80%) than the wild-type plants (≈20%). However, if the positive effect on yield properties that confers the overexpression of RBG1 is still manifested under HS conditions remains unclear. Undoubtedly, OsRAB7 and OsRBG1 represent excellent candidates to be used in future breeding programs focused on dealing with climate change and raising the global temperature. Nonetheless, the performance under HS conditions of some other important yield-related traits such as plant height, number of panicles per plant, number of primary and secondary branches on the main panicle and thousand seeds weight, remain largely unexplored for these interesting transgenic lines (Lo et al., 2020).

Some natural allelic variations on *SLENDER GUY* 1 (*OsSLG1*), a cytosolic tRNA 2-thiolation protein, confer higher thermotolerance at both seedling and reproductive stages (Xu Y. et al., 2020). The loss of function of *SLG1* reduced more than 80% the survival rate of the seedlings after heat treatment. Interestingly, *slg1* plants at reproductive stage after heat treatment (40°C for 5 days) showed reduced seed-setting rate generated by a large reduction on the number of pollen grains on the surface of the stigma and consequently of growing pollen-tubes. The authors proposed that the SLG1 tRNA-modification activity positively impacts the translation efficiency of the cell, thus modulating the concentration of HSPs and reducing the proportion of mis-folded proteins (Xu Y. et al., 2020). In consequence, augmented translational

efficiency and fidelity resulted critically beneficial to tolerate high temperature stress.

HSPs along with HSFs are the most important players in heat response transcriptional regulatory networks. In 2003, Katiyar-Agarwal and colleagues demonstrated that overexpressing Arabidopsis HSP101 in rice under high-salinity conditions improved yield by enhancing pollen tube viability. Other studies involving HSPs demonstrated that the survival rate for rice plants overexpressing the sHSP17.7 after a 2-hour at 50°C treatment increased with respect to the control (Murakami et al., 2004). In a clear example of "cross-tolerance", rice lines overexpressing the sHSP17.7 protein were also capable of continuing to grow after a 6-day long drought period, while untransformed plants did not survive the treatment (Sato and Yokoya, 2008). The mitochondrial HS protein mtHSP70 is apparently involved in conferring heat tolerance resistance to rice protoplasts when overexpressed. Heat treatment (15 minutes at 48°C) on untransformed rice protoplasts resulted in around 27% survival rate, meanwhile protoplast overexpressing mtHSP70 presented a 60% survival rate (Qi et al., 2011, Li et al., 2023). These authors suggest that overexpression of mtHSP70 promotes increased HS tolerance on rice protoplasts by inhibiting programmed cell death triggered by high temperature through the maintenance of the mitochondrial membrane potential and preventing reactive oxygen species signal amplification (Qi et al., 2011). OsHSP18.6 is also capable of conferring enhanced HS tolerance when overexpressed. OsHSP18.6 overexpression lines displayed better root and shoot growth performance after a 3-week HS treatment (45°C/12h, 28°C/12h – Wang et al., 2015). Nonetheless, not all the HSPs increased HS tolerance when overexpressed. For example, overexpression of OsHsp17.0 and OsHsp23.7 did not improve HS tolerance with respect to wild type plants, but it enhanced salt stress and drought stress tolerances (Zou et al., 2012).

Future perspectives

In response to HS, plants employ several mechanisms to maintain homeostasis and normal cellular functions. Understanding how these processes occur in the reproductive tissues of model species such as *Arabidopsis* is relevant for the establishment of a platform for advanced studies in crop species. Interestingly, HSPs are present not only in *Arabidopsis* but also in mammals, drosophila, yeast and so on. The studies of molecular mechanisms underlying tolerance of HS could also be important for understanding similar mechanisms in other species. The knowledge of the molecular mechanism due to HS derived from the characterization of putative thermotolerant related genes and pathways in model species might have a direct impact on other species, specifically in species with more economic relevance for humankind. Most of the consequences of climate change for agricultural production are expected to be negative, making the implementation of mitigation strategies much needed to adapt crops to these new conditions. Special attention is directed towards crops that are essential parts of the human caloric intake: rice, wheat, and maize (FAO 2023).

A plant exhibiting HS tolerance can sustain its regular growth and uphold, or even boost, total yield production in elevated temperature conditions by modifying metabolic and/or structural characteristics (Wahid et al., 2007). The features associated with heat tolerance are influenced by multiple genes and are connected to the morphological and physiological adaptations in rice. However, there is a scarcity of information regarding stress avoidance and tolerance mechanisms specific to rice. Identification of the molecular basis of plant adaptation is fundamental to driving plant breeding into the development of novel varieties that can adapt to climate changes. In addition, genome editing tools could play a role in bolstering or hastening crop responses to climate change and/or biofortified crops to provide adequate nutritional quality to a growing population (Leisner, 2020). Rice, like several other cereal species, shows large adaptive phenotypic plasticity enabling yield stability across environments.

Author contributions

FR: Conceptualization, Writing – original draft. GO-A: Conceptualization, Writing – original draft. MC: Writing – original draft. MM: Writing – original draft, Conceptualization, Writing – review & editing.

Funding

The author(s) declare financial support was received for the research, authorship, and/or publication of this article. MM was supported by Linea 2 - PSR2021, Bioscience Department, University of Milan, and by MUR PRIN2022 (PRIN202223MMIRA_01). MC was supported by Linea 2 - PSR2021, Bioscience Department, University of Milan, and by CRISPit Project MSCA-2021-SE-01. FR was supported by MUR PRIN2017 (PRIN 2017ZBBYNC) and GO-A was supported by a PhD fellowship from the University of Milan.

Conflict of interest

The authors declare that the research was conducted in the absence of any commercial or financial relationships that could be construed as a potential conflict of interest.

Publisher's note

References

Agrawal, L., Narula, K., Basu, S., Shekhar, S., Ghosh, S., Datta, A., et al. (2013). Comparative proteomics reveals a role for seed storage protein AmA1 in cellular growth, development, and nutrient accumulation. *J. Proteome Res.* 12 (11), 4904–4930. doi: 10.1021/pr4007987

Ahmadli, U., Kalidass, M., Khaitova, L. C., Fuchs, J., Cuacos, M., Demidov, D., et al. (2023). High temperature increases centromere-mediated genome elimination frequency and enhances haploid induction in Arabidopsis. *Plant Commun.* 4 (3), 100507. doi: 10.1016/j.xplc.2022.100507

Barnabás, B., Jäger, K., and Fehér, A. (2008). The effect of drought and HS on reproductive processes in cereals. *Plant Cell Environ.* 31 (1), 11–38. doi: 10.1111/j.1365-3040.2007.01727.x

Begcy, K., Nosenko, T., Zhou, L. Z., Fragner, L., Weckwerth, W., and Dresselhaus, T. (2019). Male sterility in maize after transient HS during the tetrad stage of pollen development. *Plant Physiol.* 181 (2), 683–700. doi: 10.1104/pp.19.00707

Bita, C. E., and Gerats, T. (2013). Plant tolerance to high temperature in a changing environment: scientific fundamentals and production of HS-tolerant crops. *Front. Plant Sci.* 4, 273. doi: 10.3389/fpls.2013.00273

Borg, M., Brownfield, L., and Twell, D. (2009). Male gametophyte development: a molecular perspective. *J. Exp. Bot.* 60 (5), 1465–1478. doi: 10.1093/jxb/ern355

Charng, Y., Liu, H., Liu, N., Chi, W., Wang, C., Chang, S., et al. (2007). A heat-inducible transcription factor, HsfA2, is required for extension for acquired thermotolerance in Arabidopsis. *Plant Physiol.* 143, 251–262. doi: 10.1104/pp.106.091322

Chaturvedi, P., Wiese, A. J., Ghatak, A., Záveská Drábková, L., Weckwerth, W., and Honys, D. (2021). HS response mechanisms in pollen development. *New Phytol.* 231 (2), 571–585. doi: 10.1111/nph.17380

Choudhury, F. K., Devireddy, A. R., Azad, R. K., Shulaev, V., and Mittler, R. (2018). Local and systemic metabolic responses during light-induced rapid systemic signaling. *Plant Physiol.* 178 (4), 1461–1472. doi: 10.1104/pp.18.01031

Christensen, C. A., Gorsich, S. W., Brown, R. H., Jones, L. G., Brown, J., Shaw, J. M., et al. (2002). Mitochondrial GFA2 is required for synergid cell death in Arabidopsis. *The Plant Cell* 14(9), 2215–2232. doi: 10.1105/tpc.002170

Cui, Y., Lu, S., Li, Z., Cheng, J., Hu, P., Zhu, T., et al. (2020). CYCLIC NUCLEOTIDE-GATED ION CHANNELs 14 and 16 promote tolerance to heat and chilling in rice. *Plant Physiol.* 183 (4), 1794–1808. doi: 10.1104/pp.20.00591

Czarnecka-Verner, E., Pan, S., Salem, T., and Gurley, W. B. (2004). Plant class b HSFs inhibit transcription and exhibit affinity for TFIIB and TBP. *Plant Mol. Biol.* 56, 57–75. doi: 10.1007/s11103-004-2307-3

De Jaeger-Braet, J., Krause, L., Buchholz, A., and Schnittger, A. (2022). HS reveals a specialized variant of the pachytene checkpoint in meiosis of Arabidopsis thaliana. *Plant Cell.* 34 (1), 433–454. doi: 10.1093/plcell/koab257

De Storme, N., and Geelen, D. (2020). High temperatures alter cross-over distribution and induce male meiotic restitution in Arabidopsis thaliana. *Commun. Biol.* 3 (1), 187. doi: 10.1038/s42003-020-0897-1

Döring, P., Treuter, E., Kistner, C., Lyck, R., Chen, A., and Nover, L. (2000). The role of AHA motifs in the activator function of tomato HS transcription factors HsfA1 and HsfA2. *Plant Cell* 12 (2), 265–278. doi: 10.1105/tpc.12.2.265

Drews, G. N., and Koltunow, A. M. (2011). The female gametophyte. *Arabidopsis Book* 2011 (9). doi: 10.1199/tab.0155

El-Esawi, M. A., and Alayafi, A. A. (2019). Overexpression of rice Rab7 gene improves drought and heat tolerance and increases grain yield in rice (Oryza sativa L.). *Genes* 10 (1), 56. doi: 10.3390/genes10010056

Endo, M., Tsuchiya, T., Hamada, K., Kawamura, S., Yano, K., Ohshima, M., et al. (2009). High temperatures cause male sterility in rice plants with transcriptional alterations during pollen development. *Plant Cell Physiol.* 50 (11), 1911–1922. doi: 10.1093/pcp/pcp135

Finka, A., Cuendet, A. F. H., Maathuis, F. J., Saidi, Y., and Goloubinoff, P. (2012). Plasma membrane cyclic nucleotide gated calcium channels control land plant thermal sensing and acquired thermotolerance. *Plant Cell* 24 (8), 3333–3348. doi: 10.1105/tpc.112.095844

Frietsch, S., Wang, Y.-F., Sladek, C., Poulsen, L. R., Romanowsky, S. M., Schroeder., J. I., et al. (2007). A cyclic nucleotide-gated channel is essential for polarized tip growth of pollen. *Proc. Natl. Acad. Sci. U.S.A.* 104, 14531–14536. doi: 10.1073/pnas.0701781104

Ghosh, S., Bheri, M., Bisht, D., and Pandey, G. K. (2022). Calcium signaling and transport machinery: Potential for development of stress tolerance in plants. *Curr. Plant Biol.* 29, 100235. doi: 10.1016/j.cpb.2022.100235

Gong, M., van der Luit, A. H., Knight, M. R., and Trewavas, A. J. (1998). Heat-shock-induced changes in intracellular Ca2+ level in tobacco seedlings in relation to thermotolerance. *Plant Physiol.* 116 (1), 429–437. doi: 10.1104/pp.116.1.429

González-Schain, N., Dreni, L., Lawas, L. M., Galbiati, M., Colombo, L., Heuer, S., et al. (2016). Genome-wide transcriptome analysis during anthesis reveals new insights into the molecular basis of HS responses in tolerant and sensitive rice varieties. *Plant Cell Physiol.* 57 (1), 57–68. doi: 10.1093/pcp/pcv174

Guan, Q., Lu, X., Zeng, H., Zhang, Y., and Zhu, J. (2013). HS induction of mi r 398 triggers a regulatory loop that is critical for thermotolerance in a rabidopsis. *Plant J.* 74 (5), 840–851. doi: 10.1111/tpj.12169

Guo, M., Liu, J. H., Ma, X., Luo, D. X., Gong, Z. H., and Lu, M. H. (2016). The plant HS transcription factors (HSFs): structure, regulation, and function in response to abiotic stresses. *Front. Plant Sci.* 7. doi: 10.3389/fpls.2016.00114

He, Y., Guan, H., Li, B., Zhang, S., Xu, Y., Yao, Y., et al. (2023). Transcriptome analysis reveals the dynamic and rapid transcriptional reprogramming involved in HS and identification of heat response genes in rice. *Int. J. Mol. Sci.* 24 (19), 14802. doi: 10.3390/ijms241914802

Hedhly, A., Hormaza, J. I., and Herrero, M. (2009). Global warming and sexual plant reproduction. *Trends Plant Sci.* 14 (1), 30–36. doi: 10.1016/j.tplants.2008.11.001

Hedhly, A., Nestorova, A., Herrmann, A., and Grossniklaus, U. (2020). Acute HS during stamen development affects both the germline and sporophytic lineages in Arabidopsis thaliana (L.) Heynh. *Environ. Exp. Bot.* 173, 103992. doi: 10.1016/j.envexpbot.2020.103992

Iba, K. (2002). Acclimative response to temperature stress in higher plants: approaches of gene engineering for temperature tolerance. *Annu. Rev. Plant Biol.* 53 (1), 225–245. doi: 10.1146/annurev.arplant.53.100201.160729

Ikeda, M., and Ohme-Takagi, M. (2009). A novel group of transcriptional repressors in arabidopsis. *Plant Cell Physiol.* 50 (5), 970–975. doi: 10.1093/pcp/pcp048

Itoh, J. I., Nonomura, K. I., Ikeda, K., Yamaki, S., Inukai, Y., Yamagishi, H., et al. (2005). Rice plant development: from zygote to spikelet. *Plant Cell Physiol.* 46 (1), 23–47. doi: 10.1093/pcp/pci501

Jagadish, S. V., Craufurd, P. Q., and Wheeler, T. R. (2007). High temperature stress and spikelet fertility in rice (Oryza sativa L.). *J. Exp. Bot.* 58 (7), 1627–1635. doi: 10.1093/jxb/erm003

Jagadish, S. V. K., Craufurd, P. Q., and Wheeler, T. R. (2008). Phenotyping parents of mapping populations of rice for heat tolerance during anthesis. *Crop Sci.* 48 (3), 1140–1146. doi: 10.2135/cropsci2007.10.0559

Jagadish, S. V. K., Muthurajan, R., Oane, R., Wheeler, T. R., Heuer, S., Bennett, J., et al. (2010). Physiological and proteomic approaches to address heat tolerance during anthesis in rice (Oryza sativa L.). *J. Exp. Bot.* 61 (1), 143–156. doi: 10.1093/jxb/erp289

Jespersen, D. (2020). Heat shock induced stress tolerance in plants: Physiological, biochemical, and molecular mechanisms of acquired tolerance. In Priming-mediated stress and cross-stress tolerance in crop plants. *Acad. Press*, 161–174. doi: 10.1016/B978-0-12-817892-8.00010-6

Jin, C., Sun, L., Trinh, H. K., and Danny, G. (2023). HS promotes haploid formation during CENH3-mediated genome elimination in Arabidopsis. *Plant Reprod.* 36, 147–155. doi: 10.1007/s00497-023-00457-8

Kan, Y., Mu, X. R., Zhang, H., Gao, J., Shan, J. X., Ye, W. W., et al. (2022). *TT2* controls rice thermotolerance through SCT1-dependent alteration of wax biosynthesis. *Nat. Plants* 8, 53–67. doi: 10.1038/s41477-021-01039-0

Ko, D., and Helariutta, Y. (2017). Shoot–root communication in flowering plants. *Curr. Biol.* 27 (17), R973–R978. doi: 10.1016/j.cub.2017.06.054

Kobata, T., and Uemuki, N. (2004). High temperatures during the grain-filling period do not reduce the potential grain dry matter increase of rice. *Agron. J.* 96 (2), 406–414. doi: 10.2134/agronj2004.0406

Kovács, D., Kovács, M., Ahmed, S., and Barna, J. (2022). Functional diversification of heat shock factors. *Biol. futura* 73, 427–439. doi: 10.1007/s42977-022-00138-z

Kudla, J., Becker, D., Grill, E., Hedrich, R., Hippler, M., Kummer, U., et al. (2018). Advances and current challenges in calcium signaling. *New Phytol.* 218 (2), 414–431. doi: 10.1111/nph.14966

Lan, J., Wang, N., Wang, Y., Jiang, Y., Yu, H., Cao, X., et al. (2023). Arabidopsis TCP4 transcription factor inhibits high temperature-induced homeotic conversion of ovules. *Nat. Commun.* 14 (1), 5673. doi: 10.1038/s41467-023-41416-1

Larkindale, J., and Knight, M. R. (2002). Protection against HS-induced oxidative damage in Arabidopsis involves calcium, abscisic acid, ethylene, and salicylic acid. *Plant Physiol.* 128 (2), 682–695. doi: 10.1104/pp.010320

Leisner, C. P. (2020). Climate change impacts on food security-focus on perennial cropping systems and nutritional value. *Plant Sci.* 293, 110412. doi: 10.1016/j.plantsci.2020.110412

Leng, Y. J., Yao, Y. S., Yang, K. Z., Wu, P. X., Xia, Y. X., Zuo, C. R., et al. (2022). Arabidopsis ERdj3B coordinates with ERECTA-family receptor kinases to regulate ovule development and the HS response. *Plant Cell.* 34 (10), 3665–3684. doi: 10.1093/plcell/koac226

Lesk, C., Rowhani, P., and Ramankutty, N. (2016). Influence of extreme weather disasters on global crop production. *Nature* 529 (7584), 84–87. doi: 10.1038/nature16467

Li, X., Chao, D., Wu, Y., Huang, X., Chen, K., Cui, L., et al. (2015). Natural alleles of a proteasome α2 subunit gene contribute to thermotolerance and adaptation of African rice. *Nat. Genet.* 47 (7), 827–833. doi: 10.1038/ng.3305

Li, J. Y., Yang, C., Xu, J., Lu, H. P., and Liu, J. X. (2023). The hot science in rice research: How rice plants cope with HS. *Plant Cell Environ.* 46 (4), 1087–1103. doi: 10.1111/pce.14509

Liao, C., Zheng, Y., and Guo, Y. (2017). MYB30 transcription factor regulates oxidative and HS responses through ANNEXIN-mediated cytosolic calcium signaling in Arabidopsis. *New Phytol.* 216 (1), 163–177. doi: 10.1111/nph.14679

Liu, H. C., and Charng, Y. Y. (2013). Common and distinct functions of Arabidopsis class A1 and A2 heat shock factors in diverse abiotic stress responses and development. *Plant Physiol.* 163 (1), 276–290. doi: 10.1104/pp.113.221168

Lo, S. F., Cheng, M. L., Hsing, Y. I. C., Chen, Y. S., Lee, K. W., Hong, Y. F., et al. (2020). Rice Big Grain 1 promotes cell division to enhance organ development, stress tolerance and grain yield. *Plant Biotechnol. J.* 18 (9), 1969–1983. doi: 10.1111/pbi.13357

Lucas, W. J., Groover, A., Lichtenberger, R., Furuta, K., Yadav, S. R., Helariutta, Y., et al. (2013). The plant vascular system: evolution, development and functions F. *J. Integr. Plant Biol.* 55 (4), 294–388. doi: 10.1111/jipb.12041

Luo, L., Liu, G., Xiao, Y., Tang, W., and Chen, L. (2005). Influences of high-temperature stress on the fertility of pollen, spikelet and grain-weight in rice. *J. Hunan Agri Univ* 31, 593–596.

Mendes, M. A., Guerra, R. F., Castelnovo, B., Silva-Velazquez, Y., Morandini, P., Manrique, S., et al. (2016). Live and let die: a REM complex promotes fertilization through synergid cell death in Arabidopsis. *Development* 143(15), 2780–2790. doi: 10.1242/dev.134916

Modliszewski, J. L., Wang, H., Albright, A. R., Lewis, S. M., Bennett, A. R., Huang, J., et al. (2018). Elevated temperature increases meiotic crossover frequency via the interfering (Type I) pathway in Arabidopsis thaliana. *PloS Genet.* 14 (5), e1007384. doi: 10.1371/journal.pgen.1007384

Morimoto, R. I. (1998). Regulation of the heat shock transcriptional response: cross talk between a family of heat shock factors, molecular chaperones, and negative regulators. *Genes Dev.* 12 (24), 3788–3796. doi: 10.1101/gad.12.24.3788

Mulla, S., Singh, S. K., Singh, K. K., and Praveen, B. (2020). Climate change and agriculture: a review of crop models. *Global Climate Change Environ. policy: Agric. Perspect.*, 423–435. doi: 10.1007/978-981-13-9570-3_15

Murakami, T., Matsuba, S., Funatsuki,, Kawaguchi, K., Surayama, H., Tanida, M., et al. (2004). Over-expression of a small heat shock protein, sHSP17.7, confers both heat tolerance and UV-B resistance to rice plants. *Mol. Breed.* 13, 165–175. doi: 10.1023/B:MOLB.0000018764.30795.c1

Nakata, M., Fukamatsu, Y., Miyashita, T., Hakata, M., Kimura, R., Nakata, Y., et al. (2017). High temperature-induced expression of rice α-amylases in developing endosperm produces chalky grains. *Front. Plant Sci.* 8, 2089. doi: 10.3389/fpls.2017.02089

Ngo, Q. A., Vogler, H., Lituiev, D. S., Nestorova, A., and Grossniklaus, U. (2014). A calcium dialog mediated by the FERONIA signal transduction pathway controls plant sperm delivery. *Dev. Cell* 29(4), 491–500. doi: 10.1016/j.devcel.2014.04.008

Peet, M. M., Sato, S., and Gardner, R. G. (1998). Comparing HS effects on male-fertile and male-sterile tomatoes. *Plant Cell Environment* 21, 225–231. doi: 10.1046/j.1365-3040.1998.00281.x

Peng, X., Ding, X., Chang, T., Wang, Z., Liu, R., Zeng, X., et al. (2014). Overexpression of a vesicle trafficking gene, OsRab7, enhances salt tolerance in rice. *Sci. World J.* 2014, 483526. doi: 10.1155/2014/483526

Peng, S., Huang, J., Sheehy, J. E., Laza, R. C., Visperas, R. M., Zhong, X., et al. (2004). Rice yields decline with higher night temperature from global warming. *Proc. Natl. Acad. Sci.* 101 (27), 9971–9975. doi: 10.1073/pnas.0403720101

Petrella, R., Cucinotta, M., Mendes, M. A., Underwood, C. J., and Colombo, L. (2021). The emerging role of small RNAs in ovule development, a kind of magic. *Plant Reprod.* 34 (4), 335–335. doi: 10.1007/s00497-021-00421-4

Prasad, P. V. V., Boote, K. J., Allen, L. H., Sheehy, J. E., and Thomas, J. M. G. (2006). Species, ecotype and cultivar differences in spikelet fertility and harvest index of rice in response to high temperature stress. *Field Crops Res.* 95, (2–3), 398–411. doi: 10.1016/j.fcr.2005.04.008

Prasad, P. V. V., Staggenborg, S. A., and Ristic, Z. (2008). Impacts of drought and/or HS on physiological, developmental, growth, and yield processes of crop plants. *Response Crops to limited water: Understand model Water Stress effects Plant Growth processes* 1, 301–355. doi: 10.2134/advagricsystmodel1.c11

Qi, Y., Wang, H., Zou, Y., Liu, C., Liu, Y., Wang, Y., et al. (2011). Over-expression of mitochondrial heat shock protein 70 suppresses programmed cell death in rice. *FEBS Lett.* 585 (1), 231–239. doi: 10.1016/j.febslet.2010.11.051

Resentini, F., Ruberti, C., Grenzi, M., Bonza, M. C., and Costa, A. (2021). The signatures of organellar calcium. *Plant Physiol.* 187 (4), 1985–2004. doi: 10.1093/plphys/kiab189

Rezaei, E. E., Webber, H., Gaiser, T., Naab, J., and Ewert, F. (2015). HS in cereals: Mechanisms and modelling. *Eur. J. Agron.* 64, 98–113. doi: 10.1016/j.eja.2014.10.003

Sailaja, B., Subrahmanyam, D., Neelamraju, S., Vishnukiran, T., Rao, Y. V., Vijayalakshmi, P., et al. (2015). Integrated physiological, biochemical, and molecular analysis identifies important traits and mechanisms associated with differential response of rice genotypes to elevated temperature. *Front. Plant Sci.* 6, 1044. doi: 10.3389/fpls.2015.01044

Sato, Y., and Yokoya, S. (2008). Enhanced tolerance to drought stress in transgenic rice plants overexpressing a small heat-shock protein, sHSP17.7. *Plant Cell Rep.* 27 (2), 329–334. doi: 10.1007/s00299-007-0470-0

Scharf, K. D., Berberich, T., Ebersberger, I., and Nover, L. (2012). The plant HS transcription factor (Hsf) family: structure, function and evolution. *Biochim. Biophys. Acta (BBA)-Gene Regul. Mech.* 1819 (2), 104–119. doi: 10.1016/j.bbagrm.2011.10.002

Scott, R. J., Spielman, M., and Dickinson, H. (2004). Stamen structure and function. *Plant Cell* 16 (suppl_1), S46–S60. doi: 10.1105/tpc.017012

Shekhar, S., Mishra, D., Gayali, S., Buragohain, A. K., Chakraborty, S., and Chakraborty, N. (2016). Comparison of proteomic and metabolomic profiles of two contrasting ecotypes of sweetpotato (Ipomoea batata L.). *J. Proteomics* 143, 306–317. doi: 10.1016/j.jprot.2016.03.028

Shi, W., Yang, J., Kumar, R., Zhang, X., Impa, S. M., Xiao, G., et al. (2022). HS during gametogenesis irreversibly damages female reproductive organ in rice. *Rice* 5 (1), 32. doi: 10.1186/s12284-022-00578-0

Takeoka, Y., Hiroi, K., Kitano, H., and Wada, T. (1991). Pistil hyperplasia in rice spikelets as affected by HS. *Sexual Plant Reprod.* 4, 39–43. doi: 10.1007/BF00194570

The State of Food Security and Nutrition in the World (2023). *Urbanization, agrifood systems transformation and healthy diets across the rural–urban continuum* (Rome: FAO). doi: 10.4060/cc3017en

Tiwari, P., Srivastava, D., Chauhan, A. S., Indoliya, Y., Singh, P. K., Tiwari, S., et al. (2021). Root system architecture, physiological analysis and dynamic transcriptomics unravel the drought-responsive traits in rice genotypes. *Ecotoxicol Environ. Saf.* 207, 111252. doi: 10.1016/j.ecoenv.2020.111252

Tunc-Ozdemir, M., Tang, C., Ishka, M. R., Brown, E., Groves, N. R., Myers, C. T., et al. (2013). A cyclic nucleotide-gated channel (CNGC16) in pollen is critical for stress tolerance in pollen reproductive development. *Plant Physiol.* 161 (2), 1010–1020. doi: 10.1104/pp.112.206888

Twell, D., Park, S. K., and Lalanne, E. (1998). Asymmetric division and cell-fate determination in developing pollen. *Trends Plant Sci.* 3 (8), 305–310. doi: 10.1105/tpc.002170

Ul Haq, S., Khan, A., Ali, M., Khattak, A. M., Gai, W. X., Zhang, H. X., et al. (2019). Heat shock proteins: dynamic biomolecules to counter plant biotic and abiotic stresses. *Int. J. Mol. Sci.* 20 (21), 5321. doi: 10.3390/ijms20215321

Vivitha, P., Raveendran, M., Vijayalakshmi, C., and Vijayalakshmi, D. (2018). Genetic dissection of high temperature stress tolerance using photosynthesis parameters in QTL introgressed lines of rice cv. Improved White Ponni. *Indian J. Plant Physiol.* 23, 741–747. doi: 10.1007/s40502-018-0408-2

Wahid, A., Gelani, S., Ashraf, M., and Foolad, M. R. (2007). Heat tolerance in plants: an overview. *Environ. Exp. Bot.* 61 (3), 199–223. doi: 10.1016/j.envexpbot.2007.05.011

Wang, W., Cai, C., He, J., Gu, J., Zhu, G., Zhang, W., et al. (2020). Yield, dry matter distribution and photosynthetic characteristics of rice under elevated CO2 and increased temperature conditions. *Field Crops Res.* 248, 107605. doi: 10.1016/j.fcr.2019.107605

Wang, Y., Impa, S. M., Sunkar, R., and Jagadish, S. V. K. (2021). The neglected other half - role of the pistil in plant HS responses. *Plant Cell Environ.* 44 (7), 2200–2210. doi: 10.1111/pce.14067

Wang, A., Yu, X., Mao, Y., Liu, Y., Liu, G., Liu, Y., et al. (2015). Overexpression of a small heat-shock-protein gene enhances tolerance to abiotic stresses in rice. *Plant Breed.* 134 (4), 384–393. doi: 10.1111/pbr.12289

Weigand, C., Kim, S. H., Brown, E., Medina, E., Mares, M.III, Miller, G., et al. (2021). A ratiometric calcium reporter CGf reveals calcium dynamics both in the single cell and whole plant levels under HS. *Front. Plant Sci.* 12, 777975. doi: 10.3389/fpls.2021.777975

Whittle, C. A., Otto, S. P., Johnston, M. O., and Krochko, J. E. (2009). Adaptive epigenetic memory of ancestral temperature regime in Arabidopsis thaliana. *Botany* 87 (6), 650–657. doi: 10.1139/B09-030

Wu, C. (1995). Heat shock transcription factors: structure and regulation. *Annu. Rev. Cell Dev. Biol.* 11 (1), 441–469. doi: 10.1146/annurev.cb.11.110195.002301

Wu, H. C., and Jinn, T. L. (2010). Heat shock-triggered Ca2+ mobilization accompanied by pectin methylesterase activity and cytosolic Ca2+ oscillation are crucial for plant thermotolerance. *Plant Signaling Behav.* 5 (10), 1252–1256. doi: 10.4161/psb.5.10.12607

Wunderlich, M., Gross-Hardt, R., and Schöffl, F. (2014). Heat shock factor HSFB2a involved in gametophyte development of Arabidopsis thaliana and its expression is controlled by a heat-inducible long non-coding antisense RNA. *Plant Mol. Biol.* 85 (6), 541–550. doi: 10.1007/s11103-014-0202-0

Xu, J., Henry, A., and Sreenivasulu, N. (2020). Rice yield formation under high day and night temperatures—A prerequisite to ensure future food security. *Plant Cell Environ.* 43 (7), 1595–1608. doi: 10.1111/pce.13748

Xu, Y., Zhang, L., Ou, S., Wang, R., Wang, Y., Chu, C., et al. (2020). Natural variations of SLG1 confer high-temperature tolerance in indica rice. *Nat. Commun.* 11 (1), 5441. doi: 10.1038/s41467-020-19320-9

Yadegari, R., and Drews, G. N. (2004). Female gametophyte development. *Plant Cell* 16 (suppl_1), S133–S141. doi: 10.1105/tpc.018192

Yamakawa, H., and Hakata, M. (2010). Atlas of rice grain filling-related metabolism under high temperature: joint analysis of metabolome and transcriptome demonstrated inhibition of starch accumulation and induction of amino acid accumulation. *Plant Cell Physiol.* 51 (5), 795–809. doi: 10.1093/pcp/pcq034

Yamakawa, H., Hirose, T., Kuroda, M., and Yamaguchi, T. (2007). Comprehensive expression profiling of rice grain filling-related genes under high temperature using DNA microarray. *Plant Physiol.* 144 (1), 258–277. doi: 10.1104/pp.107.098665

Yamamoto, A., Mizukami, Y., and Sakurai, H. (2005). Identification of a novel class of target genes and a novel type of binding sequence of heat shock transcription factor in Saccharomyces cerevisiae. *J. Biol. Chem.* 280 (12), 11911–11919. doi: 10.1074/jbc.M411256200

Yamamoto, M., Uji, S., Sugiyama, T., Sakamoto, T., Kimura, S., Endo, T., et al. (2020). ERdj3B-mediated quality control maintains anther development at high temperatures. *Plant Physiol.* 182, 1979–1990. doi: 10.1104/pp.19.01356

Yamanouchi, U., Yano, M., Lin, H., Ashikari, M., and Yamada, K. (2002). A rice spotted leaf gene, Spl7, encodes a HS transcription factor protein. *Proc. Natl. Acad. Sci.* 99 (11), 7530–7535. doi: 10.1073/pnas.112209199

Yeh, C. H., Kaplinsky, N. J., Hu, C., and Charng, Y. Y. (2012). Some like it hot, some like it warm: phenotyping to explore thermotolerance diversity. *Plant Sci.* 195, 10–23. doi: 10.1016/j.plantsci.2012.06.004

Yoshida, T., Ohama, N., Nakajima, J., Kidokoro, S., Mizoi, J., Nakashima, K., et al. (2011). Arabidopsis HsfA1 transcription factors function as the main positive regulators in heat shock-responsive gene expression. *Mol. Genet. Genomics* 286, 321–332. doi: 10.1007/s00438-011-0647-7

Zhang, G., Chen, L., Zhang, S., Liu, G., Tang, W., Li, M. H., et al. (2008). Effects of high temperature stress on pollen characters and anther microstructure of rice. *Acta Ecol. Sin.* 28, 1089–1097. (In Chinese with English abstract)

Zhang, X., Li, J., Liu, A., Zou, J., Zhou, X., Xiang, J., et al. (2012). Expression profile in rice panicle: insights into heat response mechanism at reproductive stage. *PloS One* 7 (11), e49652. doi: 10.1371/journal.pone.0049652

Zhang, H., Zhou, J., Kan, Y., Shan, J., Ye, W., Dong, N., et al. (2022). A genetic module at one locus in rice protects chloroplasts to enhance thermotolerance. *Science* 376 (6599), 1293–1300. doi: 10.1126/science.abo5721

Zou, J., Liu, C., Liu, A., Zou, D., and Chen, X. (2012). Overexpression of OsHsp17. 0 and OsHsp23. 7 enhances drought and salt tolerance in rice. *J. Plant Physiol.* 169 (6), 628–635. doi: 10.1016/j.jplph.2011.12.014

Frontiers in Plant Science

Cultivates the science of plant biology and its applications

The most cited plant science journal, which advances our understanding of plant biology for sustainable food security, functional ecosystems and human health.

Discover the latest Research Topics

See more →

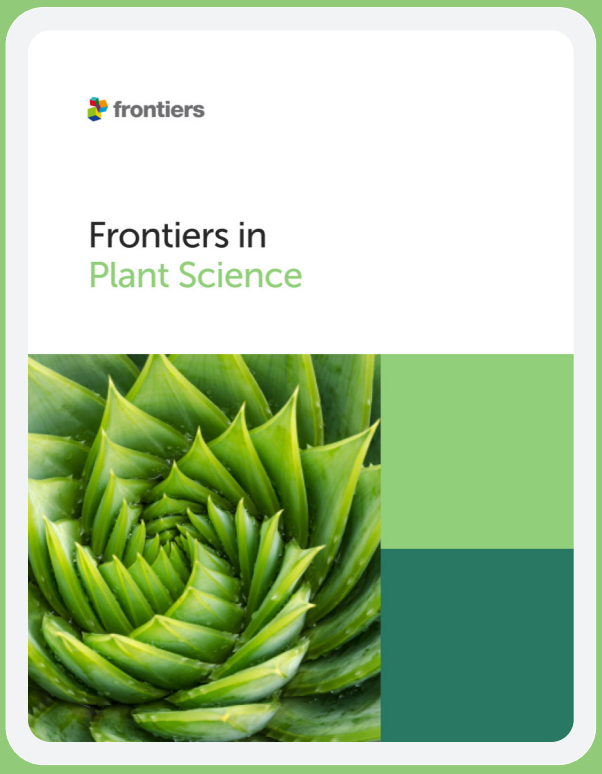

Frontiers

Avenue du Tribunal-Fédéral 34
1005 Lausanne, Switzerland
frontiersin.org

Contact us

+41 (0)21 510 17 00
frontiersin.org/about/contact